# Sedimentology and Reservoir Geology of the Middle-Upper Cretaceous Strata in Unity and Heglig Fields in SE Muglad Rift Basin, Sudan

Der **Fakultät für Geologie, Geotechnik und Bergbau**

der Technischen Universität Bergakademie Freiberg

eingereichte

## DISSERTATION

zur Erlangung des akademischen Grades

**Doctor rerum naturalium**
**Dr. rer. nat.**

vorgelegt

von **Herrn Ali Sayed Mohammed Ibrahim**

geboren am 01.01.1969 in Omdurman/Sudan

Freiberg, den 10.06.2003

# Table of contents

# Abstract

This study investigates the depositional environment, source area, sandstone composition, diagenetic properties, reservoir quality and palaeogeography of the Middle–Upper Cretaceous strata at the Unity and Heglig Fields in the SE Muglad Rift Basin, Sudan. In this study, the subsurface Cretaceous sediments were investigated essentially by seven sedimentological techniques. These included subsurface facies analysis, which was based on 1500 cutting samples and seven conventional cores description as well as on wire line logs and three seismic section analyses, petrographic analyses that included heavy mineral analysis, thin sections and scanning electron microscopic investigations, clay mineral as well as geochemical analyses.

The facies description and the analysis of conventional cores from the Bentiu, Aradeiba, and Zarga Formations in the Unity and Heglig Field revealed the presence of nine major lithofacies types, all of them are siliciclastic sediments. They can be interpreted as deposits of fluvial, deltaic and lacustrine environments. Moreover, based on wire line logs, cores and cutting sample descriptions and analyses and also on seismic section analyses, the Middle–Upper Cretaceous strata in Unity and Heglig Fields can be classified into three different units of first-order sequences, i.e. fluvial-dominated unit, lacustrine-dominated unit and deltaic-dominated unit. These depositional units most probably testify to environmental change in response to main tectonic pulses during the Turonian – Late Senonian second rifting phase. The seismic analysis revealed that the maximum thickness of the Cretaceous sediments in the study area reaches about 6000 m in the NW part of the Heglig Field. Moreover, the seismic interpretation has revealed three seismic facies reflection patterns: parallel and subparallel reflection patterns (uniform rates of deposition), divergent reflection pattern (differential subsidence rates) and hummocky clinoform pattern (clinoform lobes of delta).

The thin section investigations of the core samples revealed that feldspar accounts for 13.5 – 22 %, that of the quartz and the lithic fragments are ranging between 75.7 – 85.2 % and 0.0 7.3 % respectively. Consequently, the sandstones of the study area are classified as subarkoses. Moreover, the modal analysis of the sandstones revealed, that they stem generally

from a continental provenance, transitional between the stable interior of a craton and a basement uplift, which is a basement area of relatively high relief along rifts. This allows the detrital components to be recycled and transported for rather long distances and to be deposited in extensional and pull-apart basins. The reservoir quality of the Bentiu and Aradeiba Formations in general is better than that of the Zarga Formation. The porosity of the Bentiu and Aradeiba Formations ranges between 16.7 – 30.0 % and 18.6 – 25.3 %, respectively, whereas the porosity of the Zarga Formation ranges between 16.3 – 23.7 %. Moreover, the thin section investigations and the scanning electron microscope (SEM) analysis for the sandstones of the study area revealed that their reservoir quality was affected positively and negatively by several diagenetic processes. These processes include: mechanical compaction factors (grain slippage and crushing of the ductile grains), quartz overgrowths, precipitation of siderite and calcite, feldspar and clay mineral authigenesis, dissolution of carbonate and of the labile detrital grains and clay infiltration. Furthermore, the reservoir quality of the study intervals was not only affected by the above mentioned diagenetic processes, but also in a large-scale by the type of depositional environment.

The study of the heavy minerals revealed that the amounts of the heavy minerals kyanite and garnet supersede those of zircon, tourmaline and rutile. This indicates a metamorphic source rock of originally granitic and/or granodioritic composition for the sediments of the study area. Three heavy mineral assemblage zones with obvious lateral and vertical continuity were identified: a zircon-rutile zone (ZR), a sillimanite-epidote-hornblende zone (SEH) and a kyanite-staurolite-andalusite-garnet zone (KStAnG). On the basis of the ZTR (zircon-tourmaline-rutile) index as well as on the SEH (sillimanite-epidote-hornblende) index, four major maturation levels were constructed: immature, moderately mature, mature and overmature.

The clay mineral analysis allowed the subdivision of the Middle–Upper Cretaceous strata into three to two clay mineral zones, which reflect mainly different environmental and diagenetic conditions. The lower clay mineral zone consists of kaolinite, illite/smectite mixed layer, illite, smectite and chlorite. Whereas, the middle zone consists of kaolinite, smectite, illite/smectite mixed layer, illite and chlorite. The upper zone comprises kaolinite, illite, illite/smectite mixed layer, chlorite and smectite. The lower and the upper clay mineral zones contain higher values of kaolinite in comparison to the middle clay mineral zone, whereas the middle zone contains a higher value of smectite in comparison to the lower and the upper clay

mineral zones. The higher amount of the kaolinite in the lower and in the upper zones suggest most probably the intensity of chemical weathering and leaching processes under warm humid climate. The marked presence of smectite in the middle zone suggest that the warm humid climate was interrupted by dry seasons. Moreover, the lower clay mineral zone, which shows an increase of illite, chlorite, mixed layer illite/smectite and a higher illite crystallinity, indicates mixed and transitional influences from environmental/tectonic to burial diagenetic controls.

Geochemical investigations revealed preferential enrichment and depletion of certain chemical elements in the lacustrine/fluvial/deltaic environments. For instance, the less mobile elements Ti, Ga, Cr and Zr remained in higher amounts in the proximal facies (i.e. in the fluvial channel bar deposits and in the deltaic mouth bar deposits). In contrast, the more mobile elements Mg, Ca, K and Rb occur in higher concentrations in the distal facies (i.e. in the lacustrine deposits, deltaic distal bar deposits and floodplain sediment).

# 1 Introduction

## 1.1 Aim of the Study

The Republic of the Sudan is one of the developing countries in Africa, though it is rich in natural resources. One of those important resources, are the recently discovered hydrocarbon accumulations within the Central and Southern Sudan Interior Rift Basins. There are three major discoveries: Unity, Heglig, and Adar-Yale. These discoveries were made during the Chevron exploration activities in the 1970`s and 1980`s.

The present study is one of a series of integrated studies, which are currently carried out in the Department of Geology at the University of Khartoum. The overall objectives of these studies are oriented towards investigating the basin evolution and associated hydrocarbon resources of the Muglad Rift Basin. This study, in particular, deals with the subsurface facies sedimentology of the Middle – Upper Cretaceous sediments of upper Bentiu, Aradeiba and lower Zarga Formations within Unity and Heglig Fields at SE Muglad Rift Basin. Within this scope, the study is designed to highlight many important sedimentological aspects, which could further be integrated with other geological data to help in solving questions concerning the oil potential and to provide targets and leads for future exploration work.

The current research is concerned with the following:

(1)     To characterize the sedimentary facies and depositional paleoenvironments besides establishing a facies depositional model for Aradeiba Formation which can be used as a tool in directing the future exploration efforts.

(2)     To investigate the basin evolution, intensity of palaeo-weathering, sediment transportation processes, depositional history and source rock origin.

(3)     To infer the effect of the depositional regime and the diagenetic processes on reservoir and source rocks quality of the study intervals.

## 1.2 History of Petroleum Exploration in Sudan

The following history was summarized after Schull (1988) and Kaska (1989):

Exploration for petroleum in Sudan commenced early after the country´s independence from the Anglo-Egyptian administration. That was when the AGIP Company acquired a concession area along the Sudanese Red Sea coast in 1959. The extensive exploration efforts of AGIP resulted in no significant commercial discovery of oil or gas. The main target of AGIP was the Maghersum Formation beneath the Dungnab salt which is equivalent to the Egyptian Rudeis Formation (Lower Miocene), a known oil producing horizon.

During the world oil crisis of the early 1970´s when the oil prices raised sharply because of the Middle East political problem, the Sudanese Red Sea coast became the target of many oil companies such as Union Texas, Texas Eastern and Chevron.

The Chevron concession included the Khor Baraka delta within which the Suakin structure is located (Fig. 1.1). The structure is an anticlinal fold formed by a salt dome. Chevron tested the area with three exploratory wells. Two of them were associated with dry and condensate gas discoveries, the third was stopped due to technical problems of abnormal pressure and temperature. The three wells are Suakin-1, Bashayer-1 and South Suakin-1. The original reserve in the Suakin structure was not sufficiently attractive for the company. Consequently in the late 1970´s Chevron relinquished the Red Sea concession.

Until that date, petroleum exploration in Sudan has been concentrated along the Sudanese Red Sea coast for the following reasons:

(1)     The Egyptian Red Sea coast and the Gulf of Suez are well known areas of oil and gas production; so that a lateral extension to the south of these areas seemed to be a reasonable assumption.

(2)     The geology of the Red Sea area is relatively well known. Accordingly, the exploration risks were reduced as the targeted reservoirs and traps were well known.

(3)     The Sudan interior sedimentary basins were virgin areas. Thus, they were high risk zones to the petroleum companies.

(4)     All the earlier geological studies carried out in the Sudan interior suggested that the sedimentary cover above the Basement Complex is not more than one kilometre thick, which is not prospective for hydrocarbon exploration.

**Figure 1.1: Drainage and transportation map, with location of oil fields (McDonald, 2000)**

Despite of this, Chevron took the risk of exploring within the interior of Sudan and discovered what are now known as the Sudan Interior Basins.

In 1974, the Government of the Sudan Republic and Chevron signed a Production Sharing Agreement (PSA) offering Chevron the right to explore an area of approximately 516,000 square Kilometres in the interior of Sudan (Fig. 1.2). This area is big as 60% of the total area of the sedimentary cover of Sudan. Throughout the rest of 1974 and during the year 1975, aerial photography and Landsat images have been interpreted. By the end of 1975, airborne magnetometer and helicopter supported gravity surveys were completed. This work directed the seismic crews to enter the area. At the end of the year 1976, Baraka-1 well was drilled in the NW of the Muglad Basin Complex. This well is a dry well (plugged & abandoned) but it was very useful in directing the efforts of the exploration. During the first exploration efforts of the Chevron Company (1975 – 1980) which were concentrated in the Muglad Rift Basin, several oil discoveries were made, such as in Unity-I, Unity-2 and Abu Gabra-1 wells. Following several contractional relinquishments, Chevron was able to gain another 73,200 square kilometres in the Blue Nile and Baggara Basins in 1979 (Fig. 2.1). In 1981 nine wells were drilled. These included an additional oil discovery in Sharaf-1 well in NW Muglad Basin and several appraisal wells within the same basin in the Unity Field. In the same year the exploration was extended to include Talih-1 well oil discovery in the Unity Field as well as Adar-1 and Adar-2 wells in the Melut Basin. The exploration work was greatly speeded up during 1982. Eighteen wells were drilled in the Muglad and the Blue Nile Basins. By the end of 1983, a total of twenty four wells were drilled which included the first and the second oil discoveries in Heglig-2 and Toma-1 wells at Heglig Field in the Muglad Basin (Fig. 1.2). However, the activities of Chevron started to decline sharply in 1984. With fighting raging and the oil fields becoming a prime target of the rebels, for Chevron to remain in the country became too great a risk. During the 1990′s the Sudan Ministry of Energy and Mining drilled two wells in the Abu Gabra/Sharaf area in NW Muglad Basin with the intention of commercializing the oil discoveries in that area. In the year 1992, and for various speculations Chevron Company has relinquished the area, leaving behind a history which is full of many successes. In the meantime the Ex-Chevron concession was granted to the Greater Nile Petroleum Company.

Sun Oil Company began its exploration activity in the White Nile Basin (Fig. 2.3) in 1985 with the drilling of Hurriyah-1 near Kosti city. Two other wells (Khasseeb-1 & Narjis-1) were drilled near Bara city to the Southwest of Khartoum. Also another two wells (Al-Democratia-1 & Sudan-6) were drilled in the Khartoum Basin during the years 1987 and

1988. No successful oil discoveries have been made by Sun Oil Company, and the whole contractional area was relinquished in 1991.
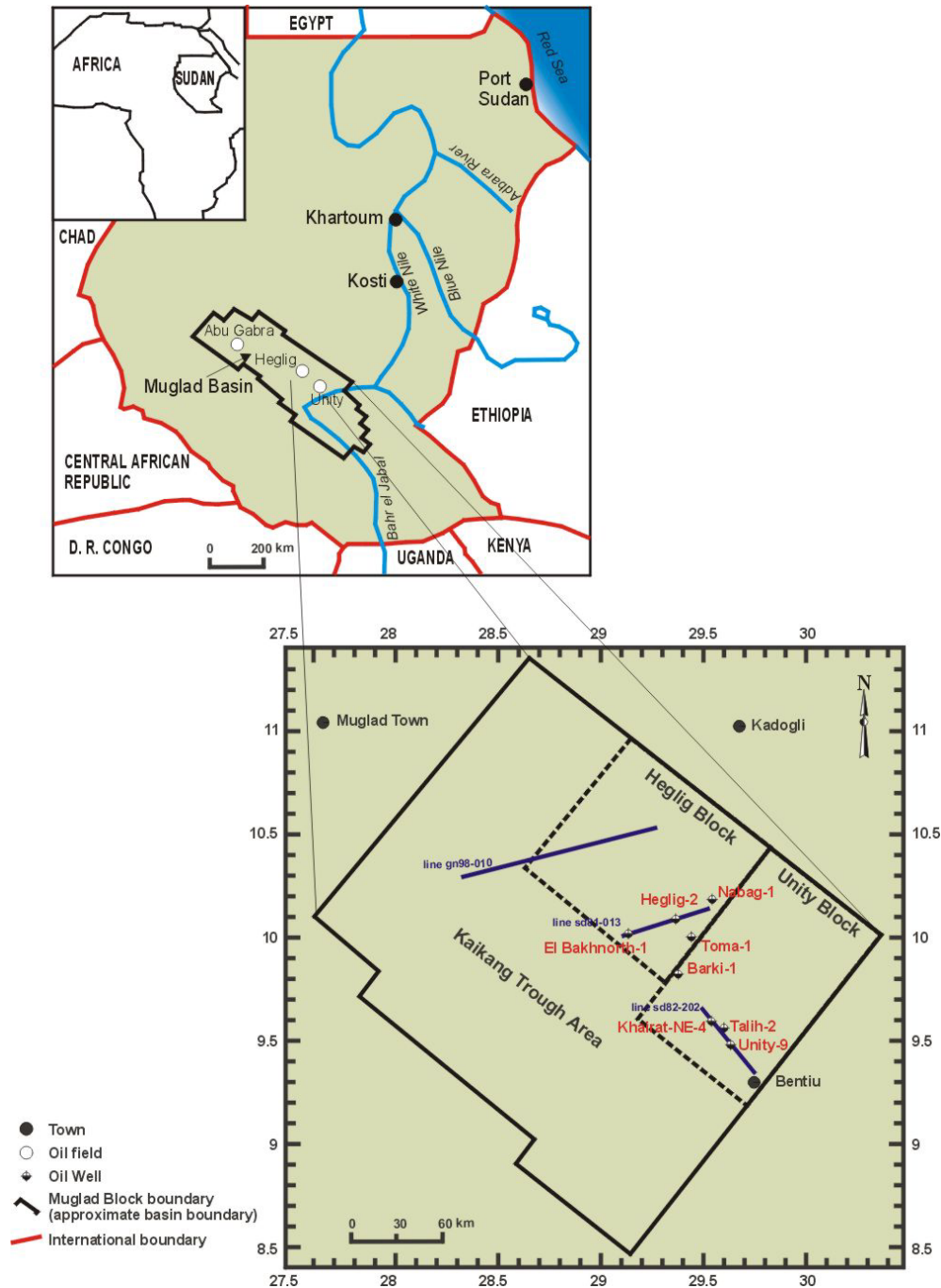


**Figure 1.2: Location map for the study area (from Mohammed et al., 1999).**

In April 1985, the Sudanese Government signed a three year technical assistance project with Robertson Research International PLC. The project involved many different geological activities such as geological surveying, geophysics, oil exploration etc.. The oil

exploration activities concentrated mainly on re-evaluating the main oil fields in the country which lie in the Muglad Basin.

Recently the Sudanese Ministry of Energy and Mining has held many agreements with different other companies including companies from China and from the home country which are now successfully exploring and pumping out oil from Muglad Basin. Subsequent attempts to get the oil industry up and running have been done. Moreover, in the 1990`s significant progress has been made, with the first wells brought on line, a 1,610 kilometer pipeline (the longest in Africa) built to get the oil to Port Sudan on the shore of the Red Sea (Fig. 1.1), and four refineries put up to meet domestic demand for petroleum products. In 1999, Sudan became an oil exporting country, it`s fortunes changed dramatically and now it is approaching a rosy future. In Heglig Field there are now three wells pumping out 200,000 barrels per day and other exploratory wells show promise of much oil under the ground. Sudan consumes 60,000 bpd domestically, leaving 140,000 bpd for export. The main player in the Sudan oil industry today is the Greater Nile Petroleum Company which is a consortium made up of China National Petroleum Company (CNPC), the Malaysian Petronas Company, Talisman of Canada, and the Sudanese Petroleum Company (Sudpet).

## 1.3 Location of the Study Area

The Muglad Basin Complex is the main petroliferous sedimentry basin in the Sudan and represents the western flank of its interior rift basins which are parts of the Central African rift system (Fig 2.1) (Fairhead, 1988). Two fields from this basin which are the largest oil fields in the country are investigated in the present study. These are Unity and Heglig Fields which occupy the southeastern part of this basin (Fig. 1.2). The Muglad Basin Complex, which is about 300 km wide and more than 1200 km long, is predominantly trending NW–SE. It extends from its northern part at the Southern Darfur Province, passes southwards through the Southern Kordofan, the Upper Nile and the Equatorial Provinces to link with the Anza Trough in northwestern Kenya (Fig 2.1). The northern end of the Muglad Basin terminates against the metamorphic and igneous complexes of the Darfur Dome, whereas the northwestern part ends at the Baggara Basin which is an E–W trending sedimentary basin, that formed synchronous with the Muglad Basin and the other Cretaceous sedimentary basins of West and Central Africa (Fig. 2.1). Geophysical studies indicate a sedimentary section up to 13,720 m (45276 ft) thick in the deepest part of the Muglad Basin, which is Kaikang

Trough. However, the maximum drilled thickness of sediments in the Muglad Basin does not exceed 15,000 ft, which consists mainly of lacustrine and fluvial sediments of Early Cretaceous to Tertiary age (Schull, 1988). This basin is bounded approximately by the longitudes 26° 00´ and 30° 00´ E and latitudes 8° 00´and 12° 00´ N (Fig. 1.2).

The area is linked with Khartoum by a railway line which passes through Sennar, Kosti, Er Rahad to Babanusa and then runs southward through the Muglad city to Wau (Fig. 1.1). Also from Babanusa a line runs westward via the NW Muglad Basin up to Nyala. A paved road runs from Khartoum to Kadugli through El Obeid, but from El Obeid many unpaved roads can be followed to different towns and villages in the area. These passage-ways cross thick forest and mountainous areas and are passable only during the dry season.

## 1.4 Physiography

### 1.4.1 Topography

Generally the Muglad Basin area is a flat plain of low relief surrounded by hilly metamorphic and igneous terrain of the Nuba mountains in the NE, isolated Basement and Nubian outcrops in the North and Basement Complex terrain in the SW, along the Sudanese and Central Africa Republic border (Fig. 2.4). With the exception of some isolated sandstone outcrops of Miocene to Pliocene age east of the Muglad town (El Shafie, 1975), the Muglad area is covered by stablized sand dunes locally veneered by silt or clay in the northern part. In the southern and southeastern parts, the surface sediments tend to be clayey and silty soils commonly referred to as black cotton soils. Moreover, alluvial and wadi sediments as well as swamp deposits of the White Nile tributaries border the eastern side of the area.

### 1.4.2 Drainage

The White Nile and its tributaries which are Bahr El Arab, Bahr El Gazal and Bahr El Zaraf are the major drainage in the area (Fig. 1.1). The White Nile is flowing across the southern and the eastern parts of the Muglad Basin. The southern part of the White Nile river is called Bahr El Jabal. The Kordofan and Darfur surface water drainage systems are mostly seasonal streams. The most significant drainage system of this kind in the area are Khor Abu Habel and Wadi Khadari. Some of the small spring-fed streams and of the ephemeral wadis and khors which carry run off, reach the White Nile or its perennial tributaries. The White Nile and its tributaries are largely affected by evaporation and infiltration.

### 1.4.3 Climate and the Plant Cover of the Area

The following is summarized after Smith (1949) and Harrison and Jackson (1958). The southern Central Sudan is generally considered to have Savannah-type climate where the average annual precipitation ranges between 120 and 800 mm. This Savannah-type climate shows a gradual change from the very humid southern equatorial climate to the semi-arid northern zone. The majority of the rainfall happens normally during July, August and September. The annual rainfall is irregular especially during the last decades when more dry seasons than expected occurred, causing a regional drought and desertification. The prevailing winter wind comes from the North while that during the rainy season comes from the Southwest. Wind velocities are usually less than 8 km/h. The average daytime temperature reaches approximately 38°C in May and September. In winter (December − March) the temperatures are lower, around 20° − 25°C. The mean humidity ranges from about 21% in the dry season to an average of 75% during the rainy season.

The natural vegetation ranges from a sparse cover of drought resistant grasses and shrubs in the arid north through a belt of open woods and grass land in the semi-arid central region, to thick forests in the well-watered south. Considerable parts of the area are covered by the genus Acacia such as Acacia verek (Hashab) which form one of the economic resources by producing Gum Arabic; Balanites aegyptiaca (Heglig); Borassus flabellifer (Daleib palm); Adansomia digita (Tebeldi or the Baobab tree); Tamarindus indica (Aradeib); as well as Acacia nilotica (Sunut); etc. In the flood plains, swamps and lagoons of the Sudd area a typical equatorial vegetation is prevalent.

## 1.5 Population

The population is sparse in the region. The area is inhabited by a diversity of ethnic groups, but most of them belong to the Baggara tribes like Misseriya, beside Dinka, Daju and Nuba (El Badi, 1995). In recent years, the drought in the northern Kordofan has forced other groups such as Kababish to migrate with their sheeps to the south. Ten percent of the population settle in the towns and villages, but the rest are nomads who migrate seasonally in search of water and pasture for their herds which are mainly of cattle, sheep and goats. The main activity of the population is animal breeding. However, some people grow sorghum (dura), millet, cotton, sesame, groundnut, gum arabic, besides some vegetables and fruits. All crops are grown depending on episodic rainfalls.

# 2  Geological Review

## 2.1 Introduction

The information available about the geology of the Sudan is fragmented. Our knowledge on the overall geological setting of the Sudan has improved after the beginning of the oil exploration activities in the 1970´s. Moreover, the contributions from the German Special Research Project (SFB 69), besides the publication in 1971 of Whiteman´s book on the geology of the Sudan, have greatly enhanced the geological data base of the Sudan and its adjacent countries.
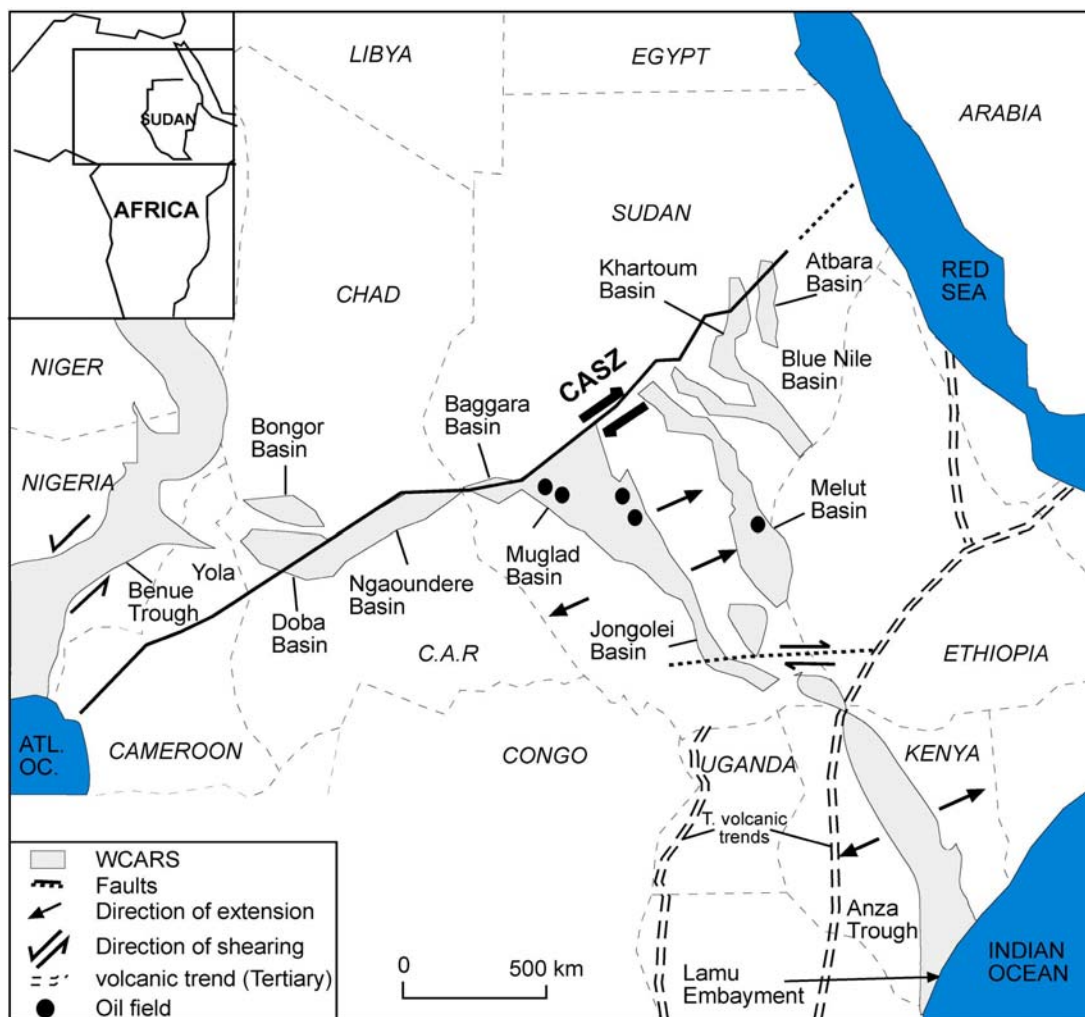


**Figure 2.1: Tectonic model of the West and Central African Rift System from Fairhead (1988).**

The main target of this chapter is to review some regional aspects of the structural, sedimentological, stratigraphical and palaeogeographical development of NE Africa. This is necessary because the development of the regional geological framework helps to understand the sedimentary evolution of the Sudan, particulary of the SE Muglad Basin. Sedimentary development in the Central and Southern Sudan rift basins seem to have been affected by both local and global geological events. A review of the major structural, igneous and sedimentary events is summarized in this chapter.

## 2.2 Geological Development of NE Africa

Many authors have discussed the various aspects of the geological development of NE Africa and their implications (Klitzsch 1983, 1984; Klitzsch and Lejal-Nicol 1984; Barazi 1985; Klitzsch 1986, 1989; Peterson 1986; Klitzsch and Wycisk 1987; Schandelmeier et al., 1987; Fairhead 1988; Schull 1988; Fairhead and Green 1989; Dualeh et al., 1990; Klitzsch and Squyres 1990; Schandelmeier et al., 1997). This includes the consolidation of the African craton and the formation of associated shear zones; the separation of East and West Gondwana; the opening of the Atlantic and the Indian Oceans besides the northward migration of the Africa continent. Moreover, on the African continent, rift basins have developed as a result of extensional tectonics related to differential opening of the Atlantic and Indian Oceans (Fairhead, 1988).

Concerning the geological events in the north of Africa, Van Houten (1980) concluded that the regional tectonics, the sea level changes and the sediments supply, all have controlled the development of the intracratonic basins. As an example, in the Sirte Basin (Gumati and Narin, 1991) demonstrated the interrelationship of the horst and graben development, marine transgressions and facies distribution. The NNW/SSE graben structures in Libya seem to have controlled the southward transgression of the Trans-Saharan sea way during the Turonian – Maastrichtian. In the south, the transgression reached northwards from the Gulf of Guinea, following the break up of Gondwana and the opening of the south Atlantic Ocean (Kogbe, 1980).

However, in East Africa, major geodynamic events have largely controlled the palaeogeography. The break up of east Gondwana during the Permo-Triassic has produced a number of intracratonic basins in Somalia, Ethiopia and Kenya. During the Carboniferous – Triassic, these were filled by Karroo sediments, followed by a series of marine transgressions

from Middle Jurassic to Tertiary resulting in the deposition of marine sediments. These sediments are intercalated with sequences of fluvial and lacustrine strata (Klitzsch and Lejal-Nicol 1984; Barazi 1985; Klitzsch and Wycisk 1987). Moreover, during the Late Cretaceous – Tertiary period volcanic eruptions were concentrated in NW Kenya and in Ethiopia and associated with the formation of the East African Rift (Getaneh 1981,1988; Peterson 1986; Beauchamp et al., 1990; Dualeh et al., 1990; Kogbe and Burollet 1990). A regional stratigraphic correlation across NE Africa is shown in Table (2.1).

In NW Sudan and SW Egypt the Paleozoic sediments consist mainly of fluvial strata intercalated with deltaic and shallow marine sequences (Klitzsch 1984; Klitzsch and Wycisk 1987). The Silurian sediments in NW Sudan are believed to consist of sandstones of fluvial to shallow marine origin. Moreover, recent studies have revealed that thick shale sequences occur within the Silurian sandstones (Abdullatif and Barazi, 1992). These Silurian shales probably represent the eastern extension of the graptolitic Silurian shales of the central Sahara (Klitzsch, 1983). The Permian, Triassic and Jurassic transgressions are confined to northern Egypt, and during that time deposition of continental sediments dominated in northern Sudan (Klitzsch and Wycisk, 1987). The Aptian transgression covered most of western Egypt and the border areas in the Sudan. However, the Late Cretaceous to Early Tertiary transgressions advanced further southward into northern Sudan resulting in interbedded fluvial and shallow marine deposits.

## 2.3 Tectonic and Structural Framework

The Central and Southern Sudan Interior Rift Basins are defined by extensive NW–SE, NNW–SSE, N–S, NE–SW, and E–W rifts that began to develop in the Late Jurassic ? to Early Cretaceous time (Schull 1988; Schandelmeier and Puddlo 1990). The development of these rift basins is thought to have been attributed to processes operated not only within the central areas of Africa but also along the eastern and western continental margins of Africa.

**Table 2.1: Stratigraphic correlation chart of NW, SW and Central Sudan, Central Ethiopia and Kenya.**

| ERA | PERIOD | CHRONOSTRATIGRAPHY | NUBIAN DESERT & NW SUDAN (1) | SUDAN (2) (S. Western) | SUDAN (3) (Central) | ETHIOPIA (4) (Central) | KENYA(5) (Coastal) |
|---|---|---|---|---|---|---|---|
| CENOZOIC | Quaternary | | | Zeraf Fm / Adok Fm / Tendi Fm / Nayil Fm | Gezira Fm | Shield Group | |
| | TERTIARY | Pliocene / Miocene / Oligocene / Eocene / Palaeocene | Hudi Chert / Gebel Abyad Fm. | Amal Fm | Hudi Chert | Trap Series (flood basalts & pyroclastics) | Marine Clastic |
| MESOZOIC | CRETACEOUS | Maastrichtian / Campanian / Santonian / Coniacian / Turonian / Cenomanian / Albian / Aptian / Barremian / Hauterivian / Valanginian / Berriasian | Kababish Fm / Wadi Howar Fm - Maghrabi Fm / Sabaya Fm / Selima Fm / Gilf Kebir Fm | Baraka Fm / Ghazal Fm / Zarga Fm / Aradeiba Fm / Bentiu Fm / Abu Gabra Fm / Sharaf Fm ? | Mansur Fm / Sawager Fm / Abu Gin Fm | Upper Sandstone Graua / Daghani / Antalo Limestone | Freretown Limestone / U. Jurassic Shale |
| | Jurassic | | | | El Azaza Fm | | |
| | Triassic | | Lakia Arabian Fm | | | Abbai Strata Adigrat Sanstone / Pre Adigrat Facies | Kambe Limestone / U+L Mariakani Sandstone / U+L Majaya Beds |
| PALAEOZOIC | Permian / Carboniferous / Devonian / Silurian / Ordovician / Cambrian | | Glacial Fm / Wadi Malik Fm / Tadrart Sandstone Fm / Umm Ras Fm / Karkur Talh Sandstone | | | | |
| PRECAMBRIAN | | | BASEMENT | BASEMENT | BASEMENT | BASEMENT | BASEMENT |

*(vertical label in SUDAN (2) column: KORDOFAN DARFUR; GROUP)*
*(vertical label at right side of KENYA column: KARROO)*

(1) Klitzsch and Lejal - Nicol (1984); Barazi (1985); Klitzsch and Wycisk (1987).
(2) Schull (1988).
(3) Sun Oil Company.
(4) Beauchamp et al. (1990); Bosellini et al. (2001).
(5) Peterson (1986); Kogbe and Burollet (1990).

U = Upper ,   L = Lower

The initiation of the African rift system is believed to have commenced in the Late Jurassic. According to RRI (1991), in Late Jurassic time a triple junction might have began to develop along the Kenya coastline, separating the Malagasy island from the African continent. The failed arm of this triple junction might have extended from the Lamu Embayment through the Anza Trough in northern Kenya and into the southern Sudan (Fig. 2.1). At the same time (Late Jurassic ?) and to the west, the African and South American cratons began to separate (Schull 1988; Schandelmeier and Puddlo 1990). As a consequence of these major events a shear reactivation along the Central African Shear Zone developed which has led to the development of parallel and subparallel half grabens of predominantly NW−SE orientation in the central and southern Sudan cratonic areas (Fig. 2.3).

**Table 2.2: Stratigraphic units of the Muglad rift basin, SW Sudan, their lithology and depositional environment (adapted from Schull 1988).**

| FORMATION | | LITHOLOGY AND ENVIRONMENTS | AGE | |
|---|---|---|---|---|
| **K O R D O F A N   G R O U P** | Zeraf Fm. | predominantly iron - stained sands and silts with minor claystones interbeds. braided streams / alluvial fans. | Recent - Middle Miocene | **T E R T I A R Y** |
| | Adok Fm. | | Oligocene - Late Ecocene | |
| | Tendi Fm. | predominantly claystone / shale interbedded with sandstones. fluvial / floodplain & lacustrine. | | |
| | Nayil Fm. | | | |
| | Amal Fm. | predominantly massive medium to coarse sandstones sequences. braided streams / alluvial fans. | Paleocene | |
| **D A R F U R   G R O U P** | Baraka Fm. | predominantly sandstones with minor shales and claystones interbeds. fluvial / alluvial fans. | Late Senonian Turonian | **C R E T A C E O U S** |
| | Ghazal Fm. | | | |
| | Zarga Fm. | predominantly sandstones, shales with interbeds of siltstones and sandstones. floodplain / lacustrine with fluvial / deltaic channel sands. | | |
| | Aradeiba Fm. | | | |
| Bentiu Fm. | | predominantly thick sandstones sequences. braided / meandering streams. | Cenomanian Late Albian | |
| Abu Gabra Fm. | | predominantly claystones and shales with fine sandstones and siltstones. lacustrine / deltaic. | Albian - Aption | |
| Sharaf Fm. | | claystones, shales with interbeds of fine sandstones and siltstones. lacustrine / fluvial - floodplain. | Barremian - Neocomian | |

▨ Source rocks     ▥ Reservoir rocks

According to Browne and Fairhead (1983), Schull (1988) and Fairhead (1988), the rift basins of Sudan belong to a much larger regional structural system, that extends across Central Africa to the west, to link up with the Atlantic coast via the Benue Trough in Nigeria and embraces the Red Sea-Gulf of Aden plate boundary to the east (Fig. 2.2). Within the

20

Sudan Republic, and from east to west, they include the Blue Nile Rift Basin, the White Nile Rift Basin, Melut Rift Basin, Muglad Rift Basin and Baggara Basin (Fig. 2.3). To the south the main branches of the Muglad and the White Nile Basins are linked to form the Melut Basin, which continues southward through Jonglei and Pibor Basins (Fig. 2.3), to link with the Anza Trough in northern Kenya (Fig. 2.1). This link was obscured later by the East African Rift System that has started to develop during Eocene – Oligocene time (Fig. 2.2). To the west, the Muglad Basin Complex is connected to the Atlantic coast via two main rifts. These are the E–W extending Baggara Rift, which is a possible eastward continuation of the Ngaoundere Rift, and the Benue Trough in Nigeria (Fig. 2.1). Both of the Muglad and the Ngaoundere Rift Basins are subsiding sediment filled troughs which have been possibly active since the Late Jurassic ?/ Early Cretaceous.
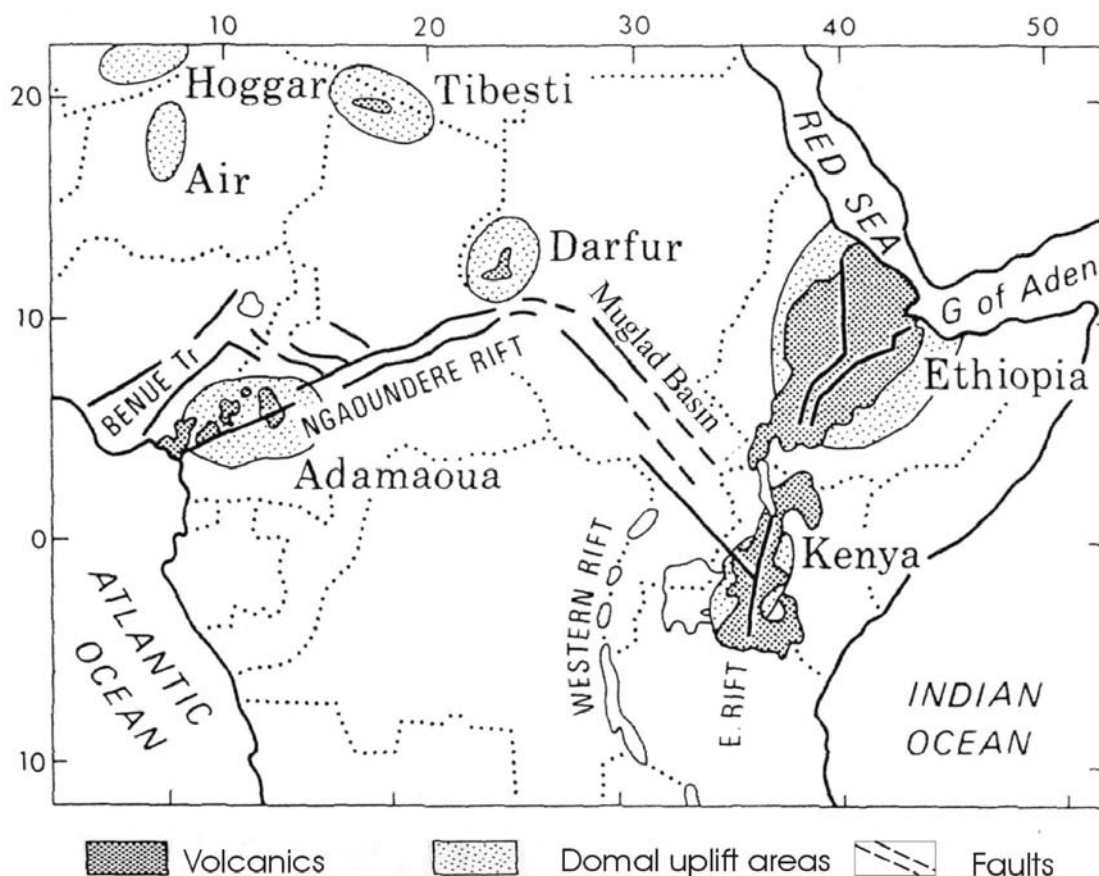


**Figure 2.2: Schematic map showing the main elements of the Western, Central and Eastern African Rift System from Browne and Fairhead (1983) and Robertson Research Int. (1991).**

To the Northeast the well known East African Rift is linked to the Red Sea and the Gulf of Aden plate boundaries in the Afar triple junction (Djibouti). This junction seems to

separate three distinct microplates: the Nubia, the Arabia and the Somalia plates. Southwards, the main branches of the East African Rift extend to meet the Indian Ocean at Beira in Mozambique. According to Lowell and Genik (1972), the Gulf of Aden is floored by oceanic crust, and most probably began opening 10 Ma ago in the Late Miocene. The Red Sea is also floored by oceanic crust. The magnetic anomaly pattern indicates spreading rate of two cm/year for the last three to four million years.

Parts of the West and East African Rift systems are associated with major domal uplifts, which have been focal points for alkaline volcanic activities. This Cenozoic intraplate alkaline volcanism is both mantle plume and rift related. It is located in Ethiopia, in Kenya and in Darfur (western Sudan). Other domal uplifts are situated at Tibesti (Chad), Jebel Haroudj (Libya), Hoggar (Algeria) and the Cameroon Line (Fig. 2.2)(Franz et al., 1994 a, 1997).

## 2.4 Rifting in Sudan

Rifting in Sudan began in the Late Jurassic and continued up to the Middle of the Miocene. Schull (1988) and Mc Hargue et al. (1992) have recognized three major episodes of rifting, concomitant subsidence and non-marine/nonvolcanic sedimentation. These three rifting periods (140 to 95 Ma (F1), 95 to 65 Ma (F2), and 65 to 30 Ma (F3)) resulted in the accumulation of 5400, 4200 and 5400 m of sediments in Muglad, Melut and Blue Nile rift basins, respectively. Fairhead (1988) attributes the Central Africa rift system to differential opening of the south, equatorial and central Atlantic Oceans. Furthermore, Fairhead (1988), Mbede (1987) and Reeves et al. (1987) suggested that the rift basins of southern Sudan are related to the Jurassic rifting of the Lamu Embayment and the Anza Trough in NW Kenya. This relationship is supported by geophysical, structural, palynological and sedimentological data (Schull 1988; Kaska 1989; Wycisk et al., 1990).

The differential opening of the Atlantic Ocean repeatedly activated shearing along the Central African Shear Zone (Fairhead 1988; Bosworth 1992). As a result, rifting occurs in Central Africa as well as in the Sudan. Furthermore, Schandelmeier et al. (1993) suggested that the Late Jurassic – Neocomian rifting in Sudan was an interactive process of mantle pluming and plate-boundary forces generated during sea-floor spreading activities in the proto-Indian Ocean. Moreover, Schandelmeier et al. (ibid.) came out with the following conclusion: First, the volcanic activity was probably related to a long lived Mesozoic mantle

plume, but magma emplacement was not accompanied by significant extensional strain in the Permo – Triassic, due to compressive plate boundary stresses. Secondly, the volume of magma increased and alkali-basaltic melts reached the surface after continental rifting was initiated by lithosphere tensional stresses in the Middle to Late Jurassic.

On the basis of geophysical data, well information and regional geology Schull (1988) divided the structural development of the Sudan into a pre-rifting phase, three rifting phases and a sag phase.

## 2.4.1 Pre-rifting Phase

By the end of the Pan-African orogeny (550 ±100 Ma), the region had become a consolidated platform. During the remainder of the Paleozoic and up to the Late Jurassic, this platform was the site of alkaline magmatism probably caused by a long lived mantle plume (Vail 1985; Schandelmeier et al., 1993). The general lack of lithic fragments in the oldest rift sediments further suggests that no significant amount of sedimentary section existed in the area prior to rifting (Schull, 1988).

## 2.4.2 Rifting Phases

Rifting is thought to have begun during Jurassic (?) to Early Cretaceous time (130 – 160 Ma). Three distinct periods of rifting have occurred in response to crustal extension, which provided the isostatic mechanism for subsidence. Subsidence was accomplished by normal faulting parallel and subparallel to the basinal axes and margins (Browne and Fairhead 1983; Schull 1988). These three rifting phases can be described as follows:

The primary rifting phase had begun in the Jurassic (?) – Early Cretaceous and continued until near the end of the Albian, simultaneously with the initial opening of the South Atlantic and the subsequent extension at the Benue Trough. Consequently, several African rifts and troughs such as Benue, East Niger, Ngaoundere and Anza began to develop (Fig. 2.1). Some basins developed within and in the immediate vicinity of the Cretaceous shear zones in the period from 120 – 90 Ma, due to shear movements. Moreover, Fairhead and Green (1989) suggested that the movements of the Central African Shear Zone were translated into the extensional basins of the Sudan interior. However, no volcanism is known to be associated with this early rifting phase in Sudan. The termination of the initial rifting is

stratigraphically marked by the basinwide deposition of thick sandstones of the Bentiu Formation (Schull 1988).

The second rifting phase occurred during the Turonian – Late Senonian. Stratigraphically, this phase is documented in the widespread deposition of lacustrine and floodplain claystones and siltstones, which abruptly terminated the deposition of the Bentiu Formation (Schull 1988). Furthermore, Fairhead (1988) concluded that changes in the opening of the Southern Atlantic account for the Late Cretaceous period of shear movement in the West and Central African Rift System. These tectonic effects came as compressional stresses at the Benue area and as a dextral reactivation along the Central African Fault Zone during the Late Cretaceous time, and hence, gave rise to the second rifting phase. In the ENE–WSW trending Baggara Basin, a continuation of CAFZ movement has been inferred from the compressional stresses in the seismic data, which is not proven in the adjacent NW Muglad Basin. Further to the SE, the trend appeared to have been terminated and replaced by the NW–SE trending basins, which are extensional in their development. In contrast to the primary rifting phase, this rifting phase was accompanied by minor volcanism. In wells, this phase is represented by a 300 ft (91 m) dolerite sill in the northwest Muglad Basin, dated (82 ±8 Ma) and a Senonian andesitic tuff in the central Melut Basin (Schull, 1988). These occurrences fit well with the approximate 90 Ma date cited as one of two periods of Mesozoic (?) igneous activity in central and northern Sudan (Vail, 1971). The end of this phase is marked by the deposition of an increasingly sand-rich sequence which ended with the Paleocene sandstone of the Amal Formation (Fig. 2.5) (Schull, 1988).

The final rifting phase began in the Late Eocene – Oligocene. The initiation of this phase was occurring simultaneously with the initial opening of the Red Sea (Lowell & Genik 1972). This final phase is reflected in the sediments by a thick sequence of lacustrine and floodplain claystones and siltstones. The only evidence of volcanism in wells is the occurrence of thin Eocene basalt flows in the southern Melut Basin near Ethiopia (Schull 1988). However, Vail (1971) pointed out that the age dating of the widely scattered volcanic outcrops in Sudan indicates occurrence of similar age volcanism. After this period of rifting throughout the Late Oligocene – Miocene, deposition became more sand-rich.
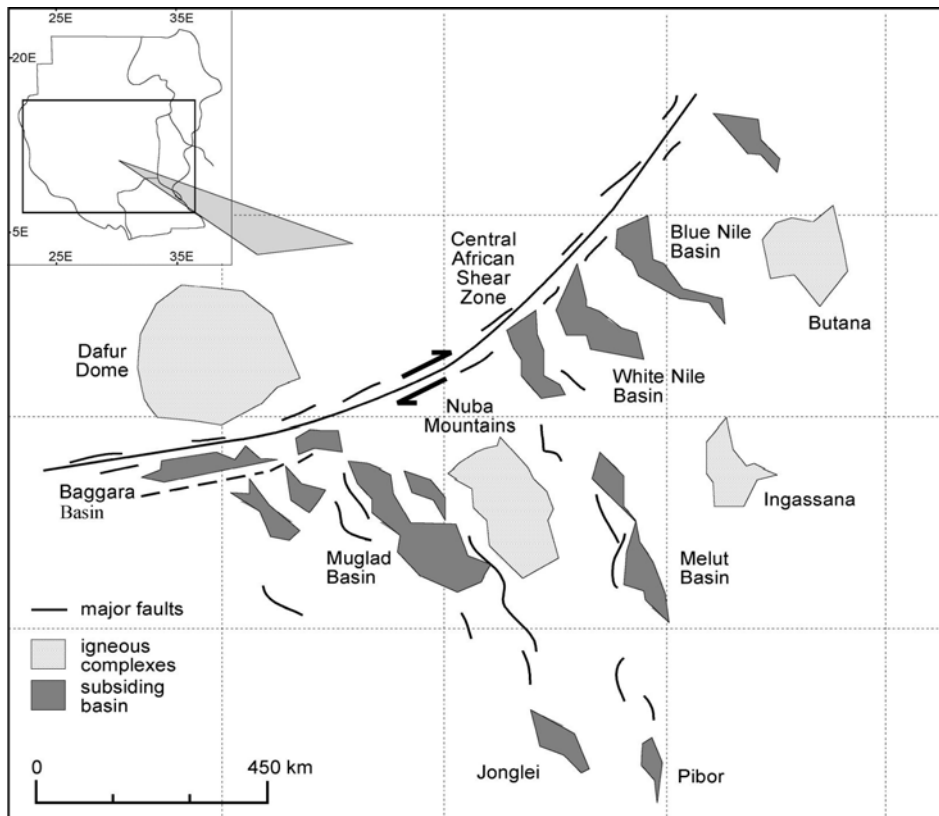
**Figure 2.3: Location of the principal basins of the Central and Southern Sudan in relation to the Central African Shear Zone (from Robertson Research Int. ,1991).**

### 2.4.3 The Sag Phase

The intracratonic sag phase was first identified by Schull (1988). In the Middle Miocene, the basinal areas entered an intracratonic sag phase of very gentle subsidence accompanied by little or no faulting. During that time the sedimentation in the Central and Southern Sudan Interior Rift Basins was essentially controlled by subsidence due to differential compaction of sediments. In Muglad and Melut Basins the Eocene - Oligocene sedimentation has continued across the Oligocene/Miocene boundary with the deposition of basinwide fluvial and floodplain sediments of the upper members of the Kordofan Group (Fig. 2.5). Also in northern Sudan, the basin evolution started with the formation of intracratonal rift basins and was followed by sag phase. In the sag phase, sedimentation was dominated by fluvial systems (Bussert, 2002 a).

However, the limited outcrops of the volcanic rocks in the area southeast of the Muglad Basin, which were been dated as 5.6 ±0.6 Ma and 2.7 ±0.8 Ma, indicate that minor volcanism occurred locally (Schull, 1988). However, during this time extensive volcanism did occur in adjoining areas to the north of the Muglad Basin (e.g., Marra Mountain and Meidob

Hills, Franz et al., 1997) as well as to the south and southeast of the Melut Basin in Kenya and Ethiopia (Fig. 2.2). Currently the area is tectionically stable with little earthquake and no volcanic activity (Browne et al., 1985).

## 2.5 The "Nubian Sandstone" in Sudan and NE Africa

There was confusion and controversy about the use of the term "Nubian Sandstone", its origin, stratigraphy and distribution. But recent studies in NW Sudan and NE Africa have concluded that the wide use of the term is "unjustified" from both sedimentological and stratigraphical point of view (Klitzsch and Squyres, 1990).

The term "Nubian Sandstone" was first introduced by Russeger (1837), who published a geological map in which this term was used to represent Late Cretaceous sandstone in the Nubian Desert of southern Egypt. Ever since, the term was widely used in northeastern and central Africa as well as in the Near East to characterize Paleozoic and Mesozoic strata. Moreover, the term "Nubian Sandstone" has been applied to the Cretaceous clastic strata in Ethiopia and Somalia (Beauchamp et al., 1990). Pomeyrol (1968) has discussed some problems associated with the term "Nubian Sandstone". Moreover, Omer (1983), provides a historical review of the use of the term "Nubian Sandstone". Early workers have felt the "dilemma" of using the term "Nubian Sandstone" and have suggested restriction or abandonment of the term (Sandford 1935; Desio 1935).

In the Sudan, Whiteman (1971) defined the term "Nubian Sandstone" as "the conglomerates, the sandstones and the argilites which lie unconformably on the Basement Complex and are overlain unconformably by the Hudi Chert Formation". However, this definition was slighty modified by Kheiralla (1966), who used the term "Nubian Sandstone Formation" for the sedimentary strata of variegated colours around the State of Khartoum. He divided the so called "Nubian Sandstone Formation" in Khartoum-Shendi area into five lithological units of which the Merkhiyat Sandstones unit (pebbly, well to poorly sorted, poorly cemented and cross stratified) is the dominant one. Based on paleoflora Omer (1983) suggested a lower to upper Cretaceous age to the "Nubian Sandstones" of central and eastern Sudan, whereas Prasad et al. (1986) suggested a Tertiary (Eocene – Miocene) age for the "Nubian Sandstones" at Mudaha Hill, west of Omdurman. However, the same sandstones of Mudaha Hill have been dated recently, as Albian – Cenomanian (Awad and Schrank 1990)

Furthermore, Klitzsch and Lejal-Nicol (1984), Barazi (1985), Peterson (1986), Klitzsch and Wycisk (1987), Beauchamp et al. (1990), Klitzsch and Squyres (1990), Kogbe and Burollet (1990) and Klitzsch (1990) carried out detailed sedimentological work in NE Africa (Table 2.1). Based on the structural and palaeogeographic development of NE Africa, the above authors have subdivided the "Nubian Sandstone" into three cycles and more than 20 formations ranging in age from Cambro – Ordovician to Tertiary. The depositional environments of these cycles range from fluvial, deltaic to shallow marine. The lower cycle consists of Paleozoic (Cambrian – Early Carboniferous) mainly marine sediments, whereas the middle cycle or the Karroo Cycle, which is of Late Carboniferous to Late Triassic age, consists of continental deposits. The upper cycle (Nubian Cycle) has Late Jurassic to Late Cretaceous age and consists of continental to marginal marine sediments. Moreover, Klitzsch and Wycisk (1987) attributed the confusion associated with the using of the term "Nubian Sandstone" in Africa to the following four reasons:

(1)     The first study at the Nubian area by Russeger (1837) had not been done in a wide regional scale.

(2)     The complexity of the facies; because the events were repeated several times and in different places during the earth history and this created strata with similar facies several times in different places. So it is easy to confuse near shore marine or fluvial-continental or deltaic sandstones of other ages.

(3)     In the older studies the use of fossils in dating sedimentary rocks was not fully considered.

(4)     The lack of financial resources besides the hostile desert environment.

Moreover, Klitzsch and Squyres (1990) suggest that the term "Nubian Sandstone" or similar terms have to be abolished as "stratigraphical terms". This is because the "terms were used for strata in other areas and other stratigraphic positions". The subdivision of the "Nubian Sandstones" indicates that a similar handling for other "terms" which are now used in Africa (e.g. Continental intercalaire (Kogbe & Burollet 1990)) should be done.

In relation to the subdivision of the "Nubian Sandstone", the sediments of the rift basins in Sudan were considered to represent the upper "Nubian" Cycle. Whereas, the sediments in the East African basins (in Somalia, Ethiopia and Kenya) were classified as belonging to the middle "Karroo" Cycle and to the upper "Nubian" Cycle.
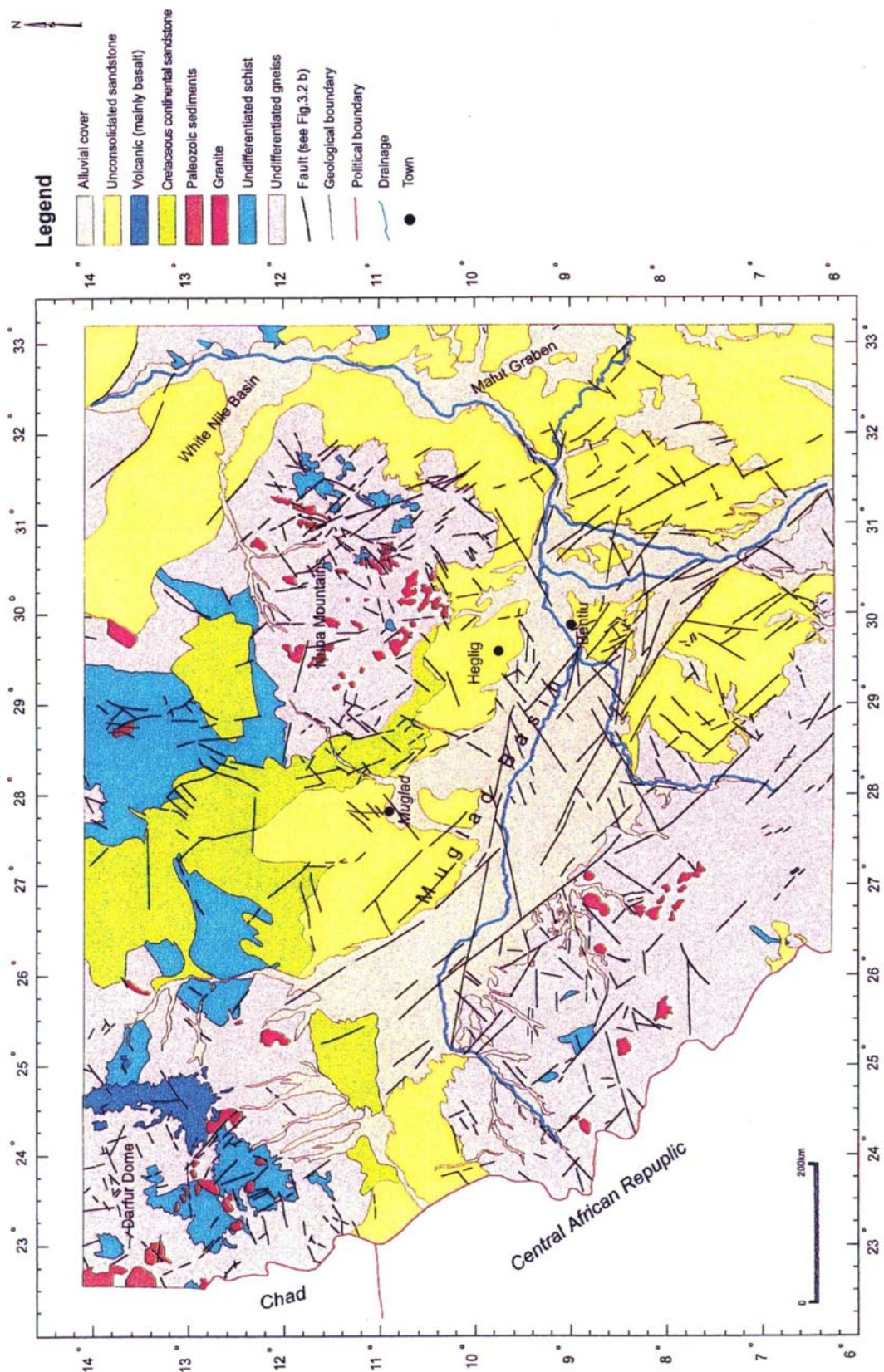
**Figure 2.4: Geological map of the southwestern part of Sudan (GRAS, 1981).**

## 2.6 Palaeogeographic and Palaeoclimatic Development

Different environmental and climatic conditions have been concluded from lithological, mineralogical and paleontological information. For example the Ordovician and Silurian ichnofossils, which have been found in the area between Uweinat Mountain (near the Sudanese/Libyian/Egyptian border) and Tageru Hill (at the northwestern corner of Kordofan) indicate that marine transgressions had reached the area. This area represents the eastern edge of a shallow basin, which was first entered by the Early Ordovician sea west of Uweinat Mountain, which reached the area west of Tageru Hill in Early or Middle Silurian time (Klitzsch and Wycisk, 1987). Also the onset of the Late Jurassic – Albian subsidence has allowed a limited marine incursion into the area of the Blue Nile Basin. As a result of this marine incursion, thick halite beds were deposited in the Blue Nile Bain in Tithonian (?) time (Bakr, 1995)
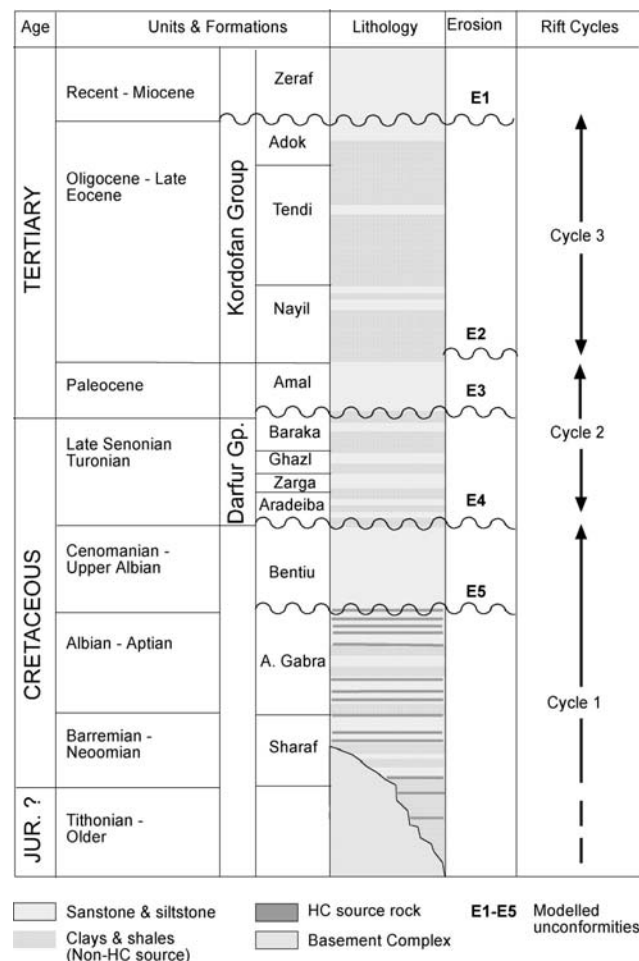


**Figure 2.5: A generalized stratigraphic column of the Muglad Basin (from Schull, 1988).**

Devonian Upper Tournaisian paleoflora in northern Sudan and Southern Egypt, indicate a dry and hot climate, which changed to a humid climate during the Visean. However, Wycisk et al. (1990) reported that during the Carboniferous time, local glaciation occurred in southwestern Egypt at the Gilf Kebir area (Northern Wadi Malik Formation). The only trace fossil found is a very frequently occurring double track (*Isopodichnus* sp.). Similar strata are present between the Darfur Mountains and the Gebel Kissu – Gebel Uweinat area, near El Fasher in the Darfur area as well as at Gebel Tageru (south of Wadi Howar). These sediments consist of diamictites similar to tillites. The climate became warm and wet during the Permian and the Triassic (Klitzsch and Wycisk, 1987). During the Jurassic and Cretaceous, it remained generally warm with humid and dry seasons (Lejal-Nicol, 1990) The Late Cretaceous to Tertiary paleoflora generally suggested a warm climate with dry and rainy seasons. In upper Egypt, Germann et al. (1987) suggested that the lateritic weathering products (kaolins, bauxite and oolitic ironstones) indicate a warm wet equatorial to sub-equatorial climate during the Late Cretaceous.

In central Sudan, Omer (1983) suggested that the climate during the Cretaceous was warm with longer dry periods and shorter rainy ones. Prasad (1970) stated that the paleoclimate of the "Nubian" sandstones in Shendi area (central Sudan) alternated between humid tropical to arid. This interpretation is based on the lateritic horizons observed within these sandstones. Beauchamp et al. (1990) concluded that the Cretaceous sedimentary strata in the eastern Sudan indicate a rather dry tropical climate. Furthermore, the wide spread silicified paleoflora in the central, eastern and NW Sudan also indicate a wet tropical condition with alternating dry and wet periods (Le Franc and Guiraud, 1990). Awad and Schrank (1990), based on macro- and microflora from the Albian/Cenomanian Omdurman Formation, suggested a tropical climate. Prasad et al. (1986) suggested a humid climate based on Tertiary (?) flora from Mudha Hill SW of Omdurman. Moreover, Germann et al. (1990) attributed the lateritic deposits within the Albian – Cenomanian Omdurman, Shendi and Wadi Milk Formation, to a hot humid climate. Furthermore, the iron crust or ferricrete which widely reported in the "Nubian" strata in central Sudan, suggest a wet tropical climate characterized by a long dry season (Nahon, 1986). Bussert (2002 b), reported that the major vertical changes in the "Nubian lithofacies" of the central northern Sudan, from more fine-grained to more coarse-grained fluvial deposits, were influenced by a shift from a more humid to a more arid paleoclimate. Lastly, the Cretaceous – Tertiary sand-rich fluvial systems

reported from outcrops and subsurface strata in the Muglad Basin also indicate that warm humid climatic conditions have prevailed (Ahmed 1983; Schull 1988).
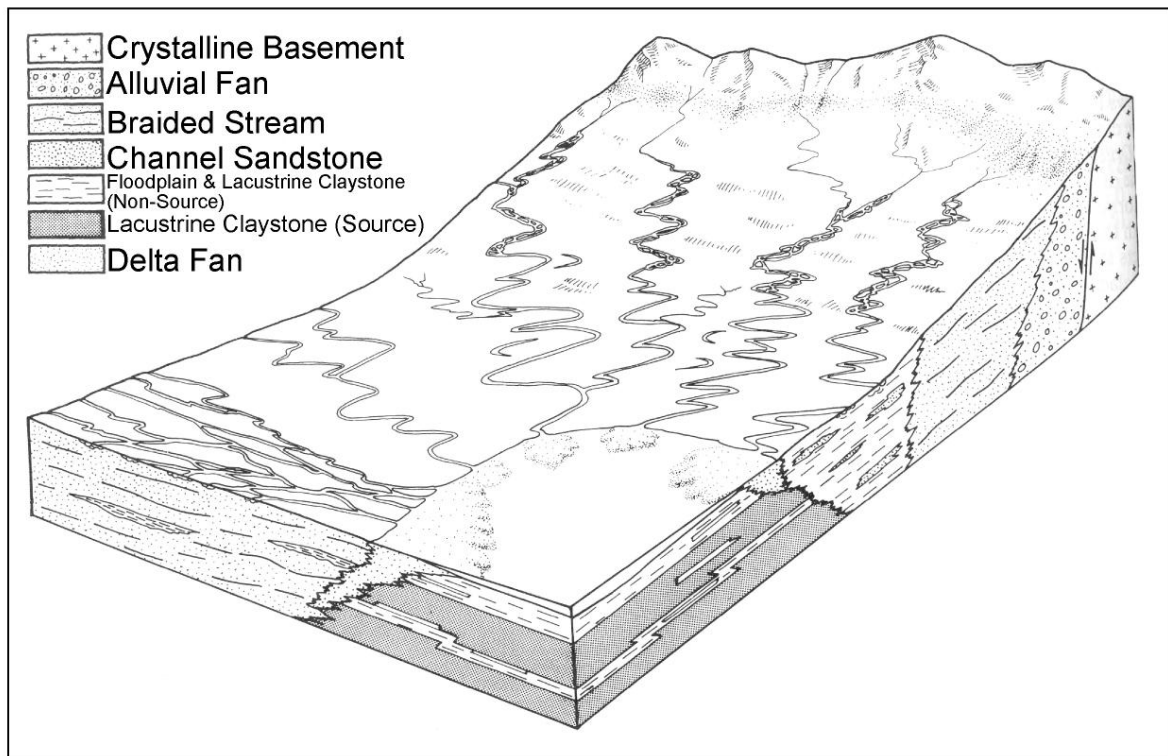


**Figure 2.6: Generalized depositional model depicting the environments operative during the filling of the southern Sudan Rift basin (from Schull, 1988).**

## 2.7 Sedimentology and Stratigraphy of the Muglad Basin

The advantages of the petroleum exploration activities within the Interior rift Basins of Sudan could be summarized in three important points:

(1) Recognition for the first time, of the presence of rift related sedimentary basins synchronous with the west, central and east African rift basins.

(2) Discovery of oil at Unity and Heglig Fields.

(3) Construction of the tectonic, the stratigraphic and the sedimentation framework, for the first time within the Sudan Interior.

The Muglad Basin is part of the Central African Rift System (Bermingham et al., 1983; Schull 1988; Fairhead 1988). Rifting resulted from crustal extension which was followed by subsidence and sedimentation. Several sub-basinal areas have been recognized,

but half-graben structures dominate the structural style. The maximum sediment thickness in the Muglad Basin, which was determined seismically, reaches about 15 km.

## 2.8 Lithostratigraphic Units of Muglad Basin

The main stratigraphic units in the Muglad area are (Table 2.2):

(1) The Precambrian Basement Complex.

(2) Late Jurassic (?)/ Early Cretaceous – Tertiary strata.

(3) The Tertiary – Quaternary sediments of Umm Rawaba Formation.

## 2.9 The Precambrian Basement Complex

The term Basement Complex is generally applied in the stratigraphy of the Sudan to include all the Precambrian and Cambrian crystalline rocks found in the country (Vail, 1978). The Basement Complex is cropping out at the SW, NW, and NE edges of the Muglad Basin (Fig. 2.4) The Basement Complex at the SW margin, in the Equatorial Province, consists of various types of gneisses, amphibolites, graphitic schists and marbles, whereas at the NW edge, in Southern Darfur, it consists of gneisses, schists and quartzites. In the NE and in the Nuba mountains it consists of granite and granodioritic gneisses, mica and graphitic schists and metavolcanics rocks (Vail, 1978). The Basement rocks were penetrated and cored in two wells within the NW Muglad area, in Baraka-1 and Adila-1 wells. At these localities granitic and granodioritic gneisses were encountered and have been dated as 540 ±40 Ma (Schull, 1988).

## 2.10 The Late Jurassic (?)/ Early Cretaceous – Tertiary Strata

The lower strata (Late Jurassic (?)/ Early Cretaceous to Tertiary) in the Muglad Basin are non-marine sediments deposited in lakes, deltas, alluvial fans and fluvial environments. Based on the cyclic subdivision of the "Nubian Sandstone" of NW Sudan, the sedimentary rocks of the Muglad Basin belong to the upper or the Nubian Cycle. The following accounts which are on the stratigraphy and sedimentology of the Late Jurassic (?)/ Early Cretaceous – Tertiary strata was summarized after Schull (1988) and Kaska (1989).

Kaska (1989) has established five spore/pollen zones for the Early Cretaceous to Tertiary non-marine sediments of the central Sudan on which age determination and correlations are made. These zones are: Early Cretaceous, Middle Cretaceous, Late Cretaceous, Early Paleocene and Oligocene/Late Eocene. The discovered flora are related to the Africa – South America (ASA) flora province. As a result to the repeated rifting, subsidence and sedimentation, three coarsening upward cycles have formed:

### 2.10.1 First Cycle Strata

The first cycle happened after the first rifting phase during Early Cretaceous to Albian time. The Sharaf Formation is early syn-rift sediments of this first cycle deposited during the Neocomian – Barremian. It consists mainly of claystones and shales deposited in lacustrine and floodplain environments. Within the Albian – Aptian time, the sedimentation was continued in lacustrine and deltaic fan environments resulting in the Abu Gabra Formation, which consists mainly of thick shales and claystones. This first cycle ends with the deposition of the Late Albian – Cenomanian Bentiu Formation, which consists predominantly of thick sandstone beds, deposits of braided and meandering streams, intercalated with thin claystone beds. The Bentiu Formation represents a change in the depositional style from an internal to an external drainage system (Figs. 2.5, 2.6 and Table 2.2).

### 2.10.2 Second Cycle Strata

This second cycle occurred during the Turonian – Late Senonian second rifting phase. It represents a coarsening-upward cycle and starts with the deposition of the Darfur Group (Fig. 2.5). The name Darfur Group was originally assigned by Chevron to include the differentiated Turonian – Senonian strata in the SE and NW Muglad Basin. Recently, RRI (1991) have assigned a Turonian to Lower Campanian age for this group. In the Muglad area the Darfur Group was subdivided into four formations. From bottom to top, these are Aradeiba, Zarga, Ghazal and Baraka Formations (Figs 2.5 and Table 2.2). The first three represent the principal reservoir intervals in the SE Muglad Basin.

Aradeiba Formation was first assigned by Chevron to include mainly the thick sandstone-clay strata which lie over the thick sandstone sequences of the Bentiu Formation and underlie the Zaraga Formation. In lithofacies criteria, the boundary between Aradeiba and Bentiu Formations is seen as an upward passage from a predominantly fluvial sandstone at the top of the Bentiu Formation to very thick mudstone – shale sequences at the base of the

Aradeiba Formation. The formation consists of mudstone, subfissile shale, siltstone and moderately thick interbeds of fine to medium grained sandstone (Figs. 2.5 and Table 2.2). The mudstones and the shales are dominantly grey in colour and locally grading into siltstones of the same colour. The thickness of this formation in Heglig and Unity areas ranges between 800 – 1270 feet. The upper boundary of this formation with the overlying Zarga Formation is hard to pick, because of the similarity between the upper part of Aradeiba and the lower part of Zarga Formation. In Unity and Heglig Fields, this formation acts as a major reservoir horizon and as a seal as well. Palynological studies by RRI (1991) suggest a lacustrine depositional environment with fluvial – deltaic channels and assigned a Turonian – Cretaceous age for this formation.

The Zarga Formation was originally identified by Chevron. Its Coniacian age was assigned by RRI (1991). The Zarga Formation overlies comformably the Aradeiba Formation. The upper boundary of this formation with the overlying Ghazal Formation is recognized by lithofacies criteria as an upward passage from the mudstone – shale intervals at the top of the formation, to a more arenaceous siltstone section at the base of Ghazal Formation. The formation consists of interbedded sequences of mudstone, sandstone and siltstone (Fig. 2.5 and Table 2.2). It is more argillaceous towards the basin centre. The sandstone as seen from the wells of Unity and Heglig Fields is coarse to fine-grained. The mudstone and the siltstone are yellow to brown in colour and slightly calcareous. This formation was identified in all wells of the SE Muglad Basin and particularly in the Unity and Heglig Fields with variable thicknesses ranging between ± 150 – 950 feet. Similar to the Aradeiba Formation, the Zarga Formation was deposited in a lacustrine environment with fluvial – deltaic channels (RRI, 1991).

The name of the Ghazal Formation was given by Chevron to describe the sediments of the uppermost reservoir horizon in Unity and Heglig Fields. Recently, RRI (1991) has assigned a Coniacian – Santonian age to this formation. This formation was identified in all wells of the SE Muglad Basin, and particularly in the Unity and Heglig Fields. However, in the NW Muglad Basin this formation is undifferentiated. The thickness of this formation in Unity and Heglig areas ranges between ± 390 – 1050 feet. The formation is lithologically similar to the underlying Zaraga Formation. It contains mudstone, shale, siltstone and sandstone (Fig. 2.5 and Table 2.2). The mudstone is yellow to brown in colour, slightly calcareous and occasionally grading into brown siltstone. The sandstone is mainly medium- to

coarse-grained. The upper boundary is identified by an upward passage from a section of equally interbedded mudstone, siltstone and sandstone sequences to predominantly arenaceous intervals at the base of the overlying Baraka Formation. On the basis of abundant microspores and freshwater algae, RRI (1991) proposed a fluvial and alluvial fan environment for this formation.

The Baraka Formation was originally identified by Chevron in the Muglad Basin as the topmost arenaceous strata of the Darfur Group. Unlike the other members of the Darfur Group, the Baraka Formation does not contribute to the reservoir zones in the Unity and Heglig Fields, this is because of the absence of adequate sealing (Fig. 2.5). The age (Lower Campanian) of the formation was assigned by RRI (1991) using palynological evidence. This formation was identified in all of the wells of the SE Muglad Basin. The thickness of this formation in the SE Muglad area ranges between 300 –1200 feet. The Baraka Formation consists mainly of sandstone interbedded with thin beds of green to grey mudstone. The sandstone is dominantly fine- to coarse- grained and occasionally very coarse. The presence of abundant microspores and freshwater algae (RRI, 1991), suggests that the formation was essentially deposited in fluvial to alluvial fan environment. However, the presence of minor evaporitic intercalations, may further suggest short periods of hypersalinity.

This second cycle ended with the deposition of Amal Formation which consists of thick massive sandstones deposited in alluvial fans and in braided streams (Figs. 2.5, 2.6 and Table 2.2).

## 2.10.3 Third Cycle Strata

The third rifting phase was created by the reactivation of extensional tectonism during Late Eocene – Oligocene time (Schull, 1988). The syn-rift sediments of this cycle consists of the Nayil and Tendi Formations which represent the middle part of the Kordofan Group (Fig. 2.5). These formations are dominated by claystones deposited in fluvial/ floodplain and lacustrine environments (Fig. 2.5 and Table 2.2). The third cycle ended the deposition of the Adok and Zeraf Formations, during Late Oligocene to Middle Miocene/ Recent. Sandstones and sands dominate in the Adok and Zeraf Formations, with only minor clay interbeds. Deposition happened mainly in braided stream environments (Figs. 2.5, 2.6 and Table 2.2).

## 2.11 The Tertiary - Quaternary Sediments of the Umm Ruwaba Formation

The Tertiary – Quaternary sediments of the Umm Ruwaba Formation represent the most widespread formation within the south central Sudan basins. It covers the surface area of the Muglad Basin,. and consists of unconsolidated to semi-consolidated gravels, sands, clayey sands and clays of fluvial and lacustrine environments, deposited during the Miocene – Pliocene (El Shafie, 1975). The sediments of the Umm Ruwaba Formation generally show rapid facies changes, which make the lateral correlation somewhat difficult (Ahmed, 1983).

## 2.12 Superficial Deposits

These are unconsolidated sands, clayey sands and black clays, which vary considerably in thickness. Black clays vary in thickness from a few centimetres to over 10 metres and conformably overlie the Umm Ruwaba Formation. Wind-blown sand deposits (Qoz), are widely spread in the northwestern part of the Muglad Basin. Fluvial deposits are found along the major drainage systems and are generally composed of sandy and clayey sediments, which sometimes form shallow aquifers. The weathering products along the western side of the Nuba Mountains form narrow bands of washed out debris deposits around the hills (Vail, 1978).

# 3 Methods of Investigation

## 3.1 Introduction

In this study, the subsurface Cretaceous sediments of Unity and Heglig Fields in the SE Muglad Rift Basin were investigated essentially by seven sedimentological techniques. These included subsurface facies analysis which was based on 1500 cutting samples and seven conventional cores descriptions as well as on wire line logs and three seismic section analyses, petrographic analyses that included heavy mineral analysis, thin sections and scanning electron microscopic investigations, clay mineral as well as geochemical analyses. The seven conventional core samples are from Bentiu, Aradeiba and Zarga Formations from four wells in the two fields. These wells are Unity-9 and Talih-2 in Unity Field as well as Heglig-2 and Toma-1 in Heglig Field. Moreover, the laboratorical works have involved 181 drill cutting samples and 21 core samples from the upper part of Bentiu, all Aradeiba and the lower part of Zarga Formations at six wells in the two fields. These wells are Unity-9, Talih-2, and Barki-1 (Unity Field) as well as Heglig-2, Toma-1 and Nabag-1 (Heglig Field). The location of these wells is shown in Fig. 1.2, whereas tables 3.1 & 3.2 provide a review of data, methods and techniques used in this study.

## 3.2 Wire Line Logs and Seismic Section Analyses

The interpretation of wire line logs and seismic sections as subsurface techniques is now widely used in sedimentology. Seismic techniques provide information on deep crustal structure and broad basin configuration before drilling. Moreover, a wide range of physical parameters can be measured using tools lowered down a petroleum exploration hole. These give information on lithology, porosity and oil and water saturation (Cant 1984; Allen and Allen 1990; Emery and Myers 1996). In this study the gamma-ray, sonic, spontaneous potential (SP), density, neutron and caliper wire line logs from the above mentioned wells at the two fields were interpreted to identify the lithologies and the lithofacies types along the wells profiles. Moreover, three seismic sections across Heglig and Unity Fields (Fig. 1.2 and Tables 3.1 & 3.2) were interpreted to assist in picking the lithostratigraphic boundaries, giving information about the stratigraphic sequences and to help in providing some lateral extended facies interpreted units in the study area. The interpretation of the wire line logs was

performed at the Geology Department, University of Khartoum, whereas that of the seismic sections was carried out in the Institute of Geology and Palaeontology in the Technical University of Freiberg (Tables 3.1 & 3.2).

**Table 3.1: Samples from the Unity field: data, methods and techniques used in this study.**

| Well | Formation | Drill Cutting & Core samples depth (ft.) | Heavy minerals | X-ray diffraction | X-ray fluorescence | Thin sections | Scanning electron microscope | Core description & analysis | Wire line log interpretation | Seismic section interpretation |
|---|---|---|---|---|---|---|---|---|---|---|
| | | | U. of K. | TU B | TU B | U. of K. | TU B | S.M.of E. | U. of K. | TUB F |
| Unity-9 | Zarga | 7241 | | | X | 7241 (ft) | 7241 (ft) | Core interval 7473-7457 ft | *Gamma-ray log | Sd 82-202 |
| | | 7253 | | X | | | | | | |
| | | 7310 | X | | | | | | | |
| | | 7380 | | X | | | | | | |
| | | 7400 | X | | | | | | | |
| | | 7463 | | X | | 7463 (ft) | 7463 (ft) | | | |
| | | 7470 | | | X | 7470 (ft) | 7470 (ft) | | | |
| | Aradeiba | 7590 | X | | | | | Core interval 8420-8393 ft | *SP log | |
| | | 7680 | X | | | | | | | |
| | | 7720 | | X | X | | | | | |
| | | 7780 | X | | | | | | | |
| | | 7820 | | X | | | | | *Sonic log | |
| | | 7880 | X | | | | | | | |
| | | 7900 | | | X | 7904 (ft) | 7904 (ft) | | *Density log | |
| | | 7970 | X | | | | | | | |
| | | 8050 | X | | | 8015 (ft) | 8015 (ft) | | | |
| | | 8070 | | | X | | | | | |
| | | 8120 | | X | | | | | *Neutron log | |
| | | 8130 | X | | | | | | | |
| | | 8220 | X | | | | | | | |
| | | 8250 | | | X | | | | | |
| | | 8310 | X | | | | | | *Caliper log | |
| | | 8330 | | X | | | | | | |
| | | 8390 | X | | | | | | | |
| | | 8393 | | | X | 8394 (ft) | 8394 (ft) | | | |
| | | 8414 | | X | | 8410 (ft) | 8410 (ft) | | | |
| | | 8417 | | | X | | | | | |
| | | 8480 | X | | | | | | | |
| | | 8590 | X | | | | | | | |
| | | 8650 | | | X | | | | | |
| | | 8730 | X | | | | | | | |
| | | 8780 | | X | X | | | | | |
| | Bentiu | 8871 | | | X | 8874 (ft) | 8874 (ft) | Core interval 8891-8861 ft | | |
| | | 8887 | | X | | 8887 (ft) | 8887 (ft) | | | |
| | | 8890 | X | | | 8889 (ft) | 8889 (ft) | | | |
| | | 9000 | X | | X | | | | | |
| | | 9050 | | X | | | | | | |
| Talih-2 | Zarga | 7490 | X | | | | | Core interval 7740-7699 ft | | |
| | | 7500 | | | X | | | | | |
| | | 7517 | | X | | | | | | |
| | | 7650 | X | | | | | | | |
| | | 7702 | | X | X | 7713 (ft) | 7713 (ft) | | | |
| | | 7733 | | X | | 7718 (ft) | 7718 (ft) | | | |
| | Ar. | 7800 | | | X | | | | | |

| Well | Formation | Depth | | | | | | | | |
|---|---|---|---|---|---|---|---|---|---|---|
| Talih-2 | Aradeiba | 7860 | X | | | | | | | |
| | | 7910 | | X | | | | | | |
| | | 7960 | X | | | | | | | |
| | | 8020 | | | X | | | | | |
| | | 8080 | X | | | | | | | |
| | | 8137 | | | X | | | Core interval 8346-8228 ft | | |
| | | 8155 | | X | | | | | | |
| | | 8160 | X | | | | | | | |
| | | 8174 | | X | | | | | | |
| | | 8230 | X | X | | 8231(ft) | 8231(ft) | | | |
| | | 8238 | | | | | | | | |
| | | 8239 | | | X | | | | | |
| | | 8260 | X | | | | | | | |
| | | 8310 | | X | | | | | | |
| | | 8350 | X | | | | | | | |
| | | 8440 | | X | X | | | | | |
| | | 8480 | X | | | | | | | |
| | | 8540 | X | | | | | | | |
| | | 8632 | | | X | 8634(ft) | 8634(ft) | | | |
| | | 8640 | | X | | | | | | |
| | | 8680 | X | | | | | | | |
| | | 8780 | X | | | | | | | |
| | | 8820 | | | X | | | | | |
| | | 8830 | | X | | | | | | |
| | | 8860 | X | | | | | | | |
| | Bentiu | 8890 | | | | | | | | |
| | | 9000 | | X | | | | | | |
| | | 9100 | X | | X | | | | | |
| | | 9210 | | X | | | | | | |
| Barki-1 | Zarga | 4100 | X | | | | | | | |
| | | 4120 | | | X | | | | | |
| | | 4150 | | X | | | | | | |
| | | 4250 | X | | | | | | | |
| | | 4280 | | | X | | | | | |
| | | 4310 | | X | | | | | | |
| | | 4400 | X | | | | | | | |
| | Aradeiba | 4430 | | | X | | | | | |
| | | 4520 | X | | | | | | | |
| | | 4600 | X | | | | | | | |
| | | 4660 | | X | X | | | | | |
| | | 4700 | X | | | | | | | |
| | | 4790 | | X | | | | | | |
| | | 4820 | X | | | | | | | |
| | | 4910 | | X | | | | | | |
| | | 4940 | X | | | | | | | |
| | | 5030 | X | | X | | | | | |
| | | 5120 | | X | | | | | | |
| | | 5150 | X | | | | | | | |
| | | 5360 | X | X | | | | | | |
| | | 5390 | | | X | | | | | |
| | Bentiu | 5427 | | X | | | | | | |
| | | 5500 | X | | X | | | | | |
| | | 5590 | | X | | | | | | |
| | | 5650 | X | | X | | | | | |

**Table 3.2: Samples from the Heglig field: data, methods and techniques used in this study.**

| Well | Formation | Drill Cutting & Core samples depth (ft.) | Heavy minerals | X-ray diffraction | X-ray fluorescence | Thin sections | Scanning electron microscope | Core description & analysis | Wire line log interpretation | Seismic section interpretation |
|---|---|---|---|---|---|---|---|---|---|---|
| | | | U. of K. | TU B | TU B | U. of K. | TU B | S.M.of E. | U. of K. | TUB F |
| Heglig-2 | Zarga | 4340 | | | X | | | Core interval 5557 – 5497 ft. | *Gamma-ray log | sd 81 - 013 |
| | | 4380 | X | X | | | | | | |
| | | 4500 | X | | | | | | | |
| | | 4520 | | | X | | | | | |
| | | 4590 | | X | | | | | | |
| | Aradeiba | 4620 | X | | | | | | | |
| | | 4680 | | | X | | | | *SP log | |
| | | 4700 | | X | | | | | | |
| | | 4740 | X | | | | | | | |
| | | 4820 | | X | | | | | | |
| | | 4840 | X | | | | | | | |
| | | 4860 | | | | | | | *Sonic log | |
| | | 4900 | | | X | | | | | |
| | | 4920 | | X | | | | | *Density log | |
| | | 4940 | X | | | | | | | |
| | | 5000 | | | X | | | | | |
| | | 5040 | | | X | | | | | |
| | | 5120 | X | | | | | | *Neutron log | |
| | | 5140 | | X | X | | | | | |
| | | 5220 | X | | | | | | | |
| | | 5230 | | X | | | | | | |
| | | 5240 | | | X | | | | | |
| | | 5300 | X | X | X | | | | *Caliper log | |
| | | 5380 | X | | | 5512 (ft) | 5512 (ft) | | | |
| | | 5400 | | X | | 5521 (ft) | 5521 (ft) | | | |
| | Bentiu | 5550 | X | | X | 5562 (ft) | 5562 (ft) | | | |
| | | 5660 | | X | | 5576 (ft) | 5576 (ft) | | | |
| | | 5723 | | | X | 5723 (ft) | 5723 (ft) | | | |
| | | 5750 | X | | | | | | | |
| | | 5850 | | X | | | | | | |
| Toma-1 | Zarga | 4110 | X | | | | | | | |
| | | 4160 | | | X | | | | | |
| | | 4180 | | X | | | | | | |
| | | 4340 | | X | | | | | | |
| | | 4400 | | | X | | | | | |
| | | 4440 | X | | | | | | | |
| | | 4460 | | X | | | | | | |
| | Aradeiba | 4520 | X | X | X | | | | | |
| | | 4580 | X | | | | | | | |
| | | 4640 | X | X | | | | | | |
| | | 4660 | | | X | | | | | |
| | | 4700 | | X | | | | | | |
| | | 4720 | | | X | | | | | |
| | | 4760 | X | | | | | | | |

| Well | Formation | Depth | | | | | | | Core interval 5338 – 5310 ft. | | gn 98 - 010 |
|---|---|---|---|---|---|---|---|---|---|---|---|
| Toma-1 | Aradeiba | 4800 | X | | | | | | | | |
| | | 4860 | X | | | | | | | | |
| | | 4900 | | X | | | | | | | |
| | | 4920 | | | X | | | | | | |
| | | 5040 | X | | | | | | | | |
| | | 5130 | X | | | | | | | | |
| | | 5150 | | | X | | | | | | |
| | | 5210 | X | | | | | | | | |
| | | 5230 | | X | | | | | | | |
| | | 5280 | X | | | | | | | | |
| | Bentiu | | | | X | X | 5313 (ft) | 5313 (ft) | | | |
| | | 5430 | X | | | | 5322 (ft) | 5322 (ft) | | | |
| | | 5560 | | X | | | | | | | |
| | | 5580 | | | X | | | | | | |
| | | 5600 | X | | | | | | | | |
| Nabag-1 | Zarga | 3810 | X | | | | | | | | |
| | | 3850 | | X | X | | | | | | |
| | | 3960 | X | | | | | | | | |
| | | 4100 | | X | X | | | | | | |
| | Aradeiba | 4200 | X | | | | | | | | |
| | | 4230 | | X | | | | | | | |
| | | 4295 | | | X | | | | | | |
| | | 4400 | X | X | | | | | | | |
| | | 4520 | | X | | | | | | | |
| | | 4580 | | | X | | | | | | |
| | | 4600 | X | | | | | | | | |
| | | 4630 | | X | | | | | | | |
| | | 4680 | | | X | | | | | | |
| | | 4820 | | X | | | | | | | |
| | | 4880 | X | | X | | | | | | |
| | | 5020 | | X | | | | | | | |
| | | 5050 | | | X | | | | | | |
| | Bentiu | 5200 | | X | | | | | | | |
| | | 5220 | X | | | | | | | | |
| | | 5250 | | | X | | | | | | |
| | | 5360 | | X | | | | | | | |
| | | 5450 | X | | X | | | | | | |

## 3.3 Conventional Core Analysis

The process of core analysis provides vital information unavailable from either wire line log measurements or drill cutting samples. The amonut of sedimentological information that can be obtained from a core is several orders of magnitude greater than is provided by wire line logs and cutting samples. These types of information include detailed lithology, macroscopic and microscopic definitions of the heterogeneities of the reservoir rocks as well as basic reservoir data. Core data is also used to calibrate the log responses (Miall, 1984). The type of cores analysed here in this study is conventional core. In this study seven cores from the above mentioned four wells were examined, described and photographed in the storehouses of the Sudanese Ministry of Energy and Mining, whereas further core analysis and 21 thin

sections from these cores were carried out at the Department of Geology, University of Khartoum (Tables 3.1 & 3.2).

## 3.4 Sample Selection and Treatment

The simple purpose of a good sampling selection is to get representative samples, which can provide reliable laboratory analysis results.

Thick sedimentary sequences of a similar time interval occur in the wells of the two fields. Therefore, using drill cutting samples can best suit the objectives of the heavy minerals analysis, to examine the heavy mineral changes within these sequences, both vertically and laterally. Drill cutting samles can provide better average composition of the interval strata, that is because of their homogeneity, than that provided by the side wall or conventional cores. Moreover, core samples might sometimes be heterogeneous due to the small local concentrations of minerals within the core sample itself (Eslinger and Pevear, 1988). However, the use of the drill cutting samples for clay minerals and geochemical analyses has the problems of mixing, cavings and drill mud contamination. Hence, to avoid such problems special provision have to be taken when using drill cutting samples.

To avoid the problems pointed out above, washed cutting samples were used in this study. Furthermore, the samples were checked with the daily drilling report and with the wire line logs (gamma, caliper etc.) to ensure that the samples were conforming with their respective lithological character as shown in the logs. In addition, poor borehole conditions were checked in the caliper logs to avoid mixing and caving. After the examination and description of the all samples under the binocular microscope, representive drill cutting samples were selected to cover the gap where there is no core to be taken for the analyses.

## 3.5 Heavy Mineral Analysis

Heavy minerals are defined as minerals having a specific gravity greater than 2.85 g/cm$^3$. They usually make up about 1 – 2 % of the total detrital grains in most sands and sandstones (Tucker, 1988).

Heavy mineral analysis, as a technique of sedimentology dates back to the year 1870. Recently it is widely used for diversified geological purposes, the ultimate objective of which

is often the determination of the source area of the sediments. In the present study the objectives behind studying the heavy minerals are fourfold:

(1)     To determine, characterize and indicate the source rocks of the Middle – Upper Cretaceous sediments in the Unity and Heglig Fields.

(2)     Heavy minerals are often used to give information about the conditions of weathering, transport, textural maturity and diagenesis.

(3)     To help, in conjunction with the clay minerals and the geochemical studies, in characterizing the palaeoclimatic and the palaeogeographic development of the Muglad Basin during the Cretaceous time.

(4)     To help in solving the dispute commonly arising with correlation, and establishing of some lithostratigraphic units.

### 3.5.1  Laboratory Procedures

Eighty unwashed representative drill cutting samples form the Middle – Upper Cretaceous facies strata at the six above mentioned wells in the two fields (Tables 3.1 & 3.2) were investigated for their heavy minerals contents. The heavy minerals analysis has been performed at the laboratories of the Geology Department, University of Khartoum. The laboratory analysis of the samples took place in several steps. These steps are: disaggregation, sieving, magnetic separation, heavy liquid separation, mounting of heavy grains, microscopic visual identification and counting.

All samples were submersed with distilled water for two days, using one litre plastic bottles, and then fixed to the sample shaker for 24 to 48 hours. Some samples were treated ultrasonically, so as to remove the iron staining and the kaolinitic coatings, which were expected to cover the surfaces of the mineral grains. This ultrasonic treatment may give way to some modifications in the surface texture of the grains (Hubert, 1971), hence for textural studies this kind of treatment must be carefully controlled.

The aim of wet sieving is to obtain an appropriate size fraction. The selection of the heavy mineral size fraction depends on the nature and the objectives behind the study. Krumbein et al. (1941) in their study of the source error in heavy minerals, found that the size fraction of 0.175 – 0.247 mm is most suitable. However, Barazi (1985) used the fraction of 0.045 – 0.25 mm for his sedimentological study of the Cretaceous sediments in northern

Sudan. Moreover, Mansour (1990) used the fraction range of 0.063 – 0.355 mm in his study of the Palaeozoic – Mesozoic sedimentary rocks of southern Egypt and northern Sudan.

In this study the heavy minerals fraction range of 0.045 – 0.25 mm is used. This is due to the fact that almost all of the heavy minerals lie within this range. Moreover, few grains of garnet are larger than 0.25 mm, whereas fractions smaller than 0.045 mm yield misleading high tourmaline concentrations (Hubert, 1971). The clean and disintegrated samples were then sieved using a agitating wet sieve (DIN 4188). The products were then dried in an oven under a temperature of 60° C. Throughout the disaggregation and the wet sieving no chemical treatment has been carried out so as to avoid mineral alterations caused by chemical reagents.

The choosen sand fraction has been subjected to two magnetic separation methods. Firstly, the ferro-magnetic grains (e.g. Magnetite) were separated from the fraction by using a horse-shoe magnet. Secondly, the remaining grains were then treated by an isodynamic separator. This step had separated the sample into magnetic and non-magnetic portions, depending on the magnetic susceptibility of each individual mineral. The process of separation was repeated several times to ensure complete separation of the electromagnetic particles. The non-magnetic heavy and light minerals concentrate in the non-magnetic portion.

The heavy liquid separation of a sample into heavy and light portions depends on the variation in the densities of the liquid and the minerals. The separation can be achieved by several high density liquids such as tribrommethane (bromoform), tetrabromethane and methylene iodide. All these liquids are toxic and must be handled with care. A newly invented heavy liquid known as sodium polytungstate is currently used. It is a non-toxic, high density inorganic salt having an adjustable bulk density up to $3.1 \, \text{g/cm}^3$. In the present work, bromoform (density = $2.89 \, \text{g/cm}^3$) was used in a fume chamber. Two techniques of bromoform separation are commonly used, gravity settling and centrifuging. The former was selected. However, the loss of the bromoform by evaporation during the acetone washing is a great disadvantage of this technique. When a sample is poured in a standard 250 ml separating funnel filled with bromoform, those grains with densities higher than the bromoform ($2.85 \, \text{g/cm}^3$) will eventually settle down the funnel, while those of lighter densities such as quartz and feldspars shall remain in suspension or float. The residual obtained, was then washed by acetone. Finally this resultant separated fraction was left to dry and then mounted on glass slides using Canda balsam.

The identification and counting of the heavy minerals were made using a polarizing microscope. Their identification is based on the optical properties of these heavy minerals such as colour, cleavage, form, relief, pleochroism, extinction angle and birefringence.

Counting of the heavy minerals for quantitative analysis have been done along ribbon traverses already drawn on the slide to facilitate the counting process. In this study the slides are often composed of 600 – 700 grains. All of the heavy mineral grains in each slide were counted and the percentage of each mineral was calculated. Hubert (1971) and Morton (1985) prefered to count only 400 – 500 grains, since the examination of 1000 grains will consume time and will not improve the final results. However, counting less than 100 grains will actually affect the quality of the results.

## 3.6 Clay Minerals Analysis

According to Chamley (1989), Tucker (1991) and Moore & Reynolds (1997), clay minerals are hydrous aluminosilicates with layered structures that constitute a large part of the phyllosilicate family. Folk (1974) proposed three definitions for clay, based on particle size, chemical composition and petrographic features. Brindley and Brown (1984) considered the clays as natural, fine-grained (< 2μm) and earthy materials, which are sensitive to pressure and temperature conditions and to variations in the chemical environment (sensitivity expressed as crystallographical and mineralogical changes). Weaver (1989) suggested the term physil (phyllosilicate) to be applied to all sheet silicate minerals. He believed that the term has no size connotation. Clay minerals are formed directly or indirectly from the hydrolytic decomposition of primary aluminosilicates and constitute a major part of claystones, mudstones, shales and argillites.

### 3.6.1 Objectives

According to Selley (1985), the study of clay minerals gives information not only about the depositional environment, but also about parent rocks, hydrothermal alteration, diagenesis and metamorphism.

In the present study the aims behind the study of clay minerals are:

> (a)    To characterize the clay minerals assemblages of the lacustrine/fluvial facies of the Middle – Upper Cretaceous strata.

(b)     To infer information about the sedimentary evolution in term of palaeo-weathering, diagenetic processes, depositional environments, source area and palaeoclimate.

Accordingly, 64 samples have been chosen for analysis by X-ray diffraction. The samples were chosen from the previous mentioned six wells at the two fields in order to cover the stratigraphic sequences of the upper part of Bentiu, all Aradeiba and the lower part of Zarga Formations (Tables 3.1 & 3.2). The analysis for the clay mineralogy took place in two main steps. These are the separation of the less than 2 microns size fraction and the XRD analysis. Separation of the clay fraction was carried out in the laboratories of the Department of Geology, University of Khartoum, whereas further XRD investigation was performed at the laboratories of the Institute of Applied Geosciences of the Technical University of Berlin.

## 3.6.2  Separation of the Clay Fraction

In order to extract the fraction of the sediments < 2μm from the samples, the following preparation methods were performed:

(1)     Initially all samples were carefully washed with distilled water to remove the remains of the drilling mud.

(2)     The wet samples were put in plastic bottles, submersed with distilled water and then fixed to the samples shaker for disintegration. Ultrasonic treatment was sometimes used for highly indurated samples.

(3)     Distilled water was added to the samples till a hydraulic conductivity of about < 50 – 60 μS (microsiemens) was reached.

(4)     The suspension was then centrifuged for two minutes with a speed of 2000 rounds/minute. The finer silt particles will eventually settle, while the less than 2μm size fraction will still remain in suspension.

(5)     The suspension was filtered through ceramic filters to get rid of the water and to gather the clay particles. The filtration product was collected in dishes, kept in an oven at 50° C.

(6)     For the analytical purposes, from the wet clay fraction (< 2μm) oriented mounts were prepared on glass slides to obtain the basal reflection orientation.

(7)    The prepared glass slides were kept in a desiccator for 24 hours to dry and then to be taken for air-dried measurements.

### 3.6.3  X-ray Diffraction

X-ray diffraction analysis was carried out in order to identify and semi-quantitatively deduce the percentages of the different clay minerals present in the strata of the Aradeiba Formation as well as in the strata of the upper part and the lower part of Bentiu and Zarga Formations, respectively.

Zussman (1977) and Moore & Reynolds (1997) gave comprehensive treatment of the theoretical and practical aspects of the XRD technique. Whereas, Tucker (1988) provided a concise summary about the application and interpretation aspects.

The XRD analyses were carried out using the Siemens 1710/1729 X-ray Diffractometer under the following conditions:

(a) Generator Settings : 50 KV and 30 mA.

(b) Cu Kα 1,2 wave length : 1.54060, 1.54439 Å

(c) Step size, sample time : 0.02 deg, 0.805, 40.0/deg.

(d) Primary Monochromatic filter used.

(e) Divergence slit : automatic (Specimen length 12.5 mm).

(f) Angle range from 3° to 30°.

The clay minerals were identified from their basal reflections determined from the XRD pattern, after (1) air drying (normal), (2) glycolation for 48 hours under 50° C, (3) heating to 350° C for one hour and lastly (4) heating to 550° C for 4 hours. Then the four runs were subjected to several analytical steps through two computer programmes which are Philips X´ Pert Organiser and X´Pert Plus. The net areas of the peaks of the basal reflection (001) of the clay minerals were calculated above the background and considered as the proportion of each mineral in the mixture. The total association was taken to be equal to 100 %. Then the relative proportions were deduced semi-quantitatively by using the factors cited in Schwertmann and Niederbudde (1993).

## 3.7 Geochemical Analysis

Early work on the geochemistry of sediments was largely confined to studies of the distribution of one or a limited number of elements through the sedimentary sequences, in order to obtain some geological relationships.

During the last decades there has been an increasing interest in the study of trace elements in sedimentary rocks. One of the goals of the study of trace elements is to decipher the environment of deposition of ancient sedimentary rocks. The most promising method is the use of trace elements as guides to water salinity and hence depositional environment (Degens et al., 1957). Moreover, differentiating marine and fresh water sediments on the basis of trace elements was done by Walters et al. (1987). Accordingly, a number of investigations established a definite relationship between the concentration of certain trace elements and the environment of deposition. As a result the trace elements can be subdivided into two groups; marine and non-marine indicators. However, the use of the trace elements in differentiating marine and fresh water sediments has many connotations. This is because the distribution of the trace elements is controlled by many factors, that interact with each other. Moreover, the two categories may represent widely varying source areas, climates, tectonic conditions and rates of sedimentation.

Generally, the concentration and distribution of elements within a sedimentary cycle provide information about the composition of the source rock, weathering processes, depositional environment and diagenetic processes (Krauskopf, 1979). Hence, in this study, the geochemistry is used for the recognition of the petrographic province of the Middle – Upper Cretaceous strata in the SE Muglad Basin and to throw light on the palaeo-weathering, depositional environments and on the diagenetic processes that had been operating during and after the deposition of the Middle – Upper Cretaceous strata.

### 3.7.1  X-ray Fluorescence (XRF)

X-ray Fluorescence is adopted in the present study for the inorganic geochemical analysis. Fifty eight samples have been chosen to cover the upper part of Bentiu, all Aradeiba as well as the lower part of Zarga Formations (Tables 3.1 & 3.2). The whole rock was analysed. The analyses were carried out in the laboratory of the Institute of Applied Geosciences, Technical University of Berlin. The fully automatic wavelength dispressive X-ray spectrometer, Philip

PW 1404/10 was used. The machine is associated with a PW 1500/15 automatic sample changer with 72 positions, and a digital "Microvax" computer unit.

Zussman (1977) provides basic theoretical and practical treatment of the (XRF) technique. Teggart et al. (1987) outline the principle, instrumentation, sample preparation and the precision of the technique. According to them, the major advantage of this technique is the simplicity of the spectra and the ease of analysis of elements heavier than Ca. It is inherent in XRF that higher abundances of all elements can be accurately determined and in general accuracy and precision increase with higher abundances. The Fused Pellets Method which, is summarized below after the above authors was used in this study:

(1)     Twenty grams from each sample were crushed and grinded to very fine powder (< 50 µm) using a Agate crusher machine. The crusher machine was cleaned after each sample crushing to prevent contamination.

(2)     Fused glass discs have been prepared from the samples powder as follow:

    (a)     0.6 grams from the sample powder were mixed with 3.6 grams from the Li – borate ($LiBo_3$ + $Li (Bo_2)_4$).

    (b)     The mixture was ignited to melt at 1200° C in a Pt-crucible inside an induction oven for six minutes.

    (c)     The melt was poured in a Pt-mould and quenched to form a glass tablet (disc).

The advantage of the glass disc method is that there is no matrix or textural effect due to the homogeneity of the disc. However, the disadvantages of this method are: The method is time consuming besides the limitation of detecting some elements such as Lithium.

### 3.7.2 Loss on Ignition (LOI)

For every geochemically analyzed sample the loss on ignition (LOI) was calculated. The loss on ignition is the decrease in weight of a rock sample on heating at high temperatures, due to the expulsion of volatile components like $H_2O$, OH, F, $SO_2$, and $CO_2$. It is determined as follows:

(1) 2 grams of sample powder is accurately weighed in a Pt-crucible.

(2) Heating for 1 hour at 1000° C in an oven.

(3) Cooling the heated sample in a desiccator, at least for 2 hours.

(4) Reweighting the sample after cooling to room temperature.

(5) Calculation of the loss on ignition according to the following relationship:

$$LOI \ [\%] = \frac{(W_1 - W_2)}{W_1} \times 100 \ ,$$

where $W_1$ is the weight of sample before heating and $W_2$ is the weight of sample after heating.

## 3.8 Scanning Electron Microscopic (SEM) Analysis

Since the nineteenth century, thin-section analysis of rocks using a polarizing or petrographic microscope has been a traditional tool of the geologist. With the petrographic microscope, geologists are able to examine a two-dimensional cross section through a rock, estimate the bulk mineral composition, and make important observations regarding grain fabric and texture. However, the actual three-dimensional grain relationships and details of the intergranular pore structure were always beyond reach (Joann, 1984).

With the introduction of the SEM, geologists are now able to go one step beyond thin section analysis, which is to look into the pore space, identify the minute minerals and to examine the distribution of authigenic minerals within the pores. Other advantages of the SEM over optical petrography are ease of sample preparation, greater depth of field and resolution, and a significantly higher magnification range. In addition less training is required to interpret an SEM micrograph.

This is not to say that the SEM replaces thin section analysis; instead, the SEM complements thin section analysis by providing a different type of information which when used in combination with other techniques provides important new information to help in characterizing the rocks (Joann, 1984).

In the present study, the objectives behind the SEM analysis are to:

(a)     Define more precisely the detailed mineralogical textures of the minerals within the pores.

(b)     Infer information about the evolution in term of depositional environments, diagenetic processess and palaeoclimate.

### 3.8.1 Sample Preparation

In order to prepare the samples for the SEM analysis, the following preparation steps were adopted after Joann (1984):

(1)     Fresh and uncontaminated sample surface was obtained by gently breaking the core plug with a small rock-chopper.

(2)     Any fine debris on the surface was dislodged with a Freon duster.

(3)     The samples were handled with disposable gloves, tongs, tweezers, etc., because skin oil from fingers will outgas in the SEM vacuum system.

(4)     The cut sample was attached to a SEM specimen plug with epoxy and was dried overnight in a low temperature drying oven .

(5)     A thin line of Silpaint is added to provide an electrical ground from the sample to the plug.

(6)     The sample is then coated with a conductive material such as carbon, gold or palladium. This coating is required to obtain a clear image of an insulating material such as a rock sample.

(7)     The coated SEM sample was placed in the chamber and was evacuated to high vacuum (approximately $2 \times 10^{-6}$ torr).

A total of 51 SEM micrographs have been done from 21 core samples from Bentiu, Aradeiba and Zarga Formations at the studied wells (Tables 3.1 & 3.2), using the scanning electron microscope Hitachi S- 2700 in the SEM Department at Technical University of Berlin.

# 4 Subsurface Facies Analysis

## 4.1 Introduction

Although it has long been recognized that oil can be generated from source rocks of non-marine origin, the global importance of hydrocarbons of this origin has only recently become apparent. Two factors in particular are responsible for this development. The first is the great increase in information available from Chinese oil fields, bringing with it the realization that most oil production in China comes from non-marine basins. The second has been the discovery of a succession of major oil fields in the Mesozoic continental rift basins within the African continent and along the South Atlantic margins of Africa and South America. These new data, plus previously known occurrences in North America, Europe and Australia, demonstrate that non-marine oil comes mainly from organic-rich lacustrine sediments (Wanli, 1985). In the Sudan, the Muglad Basin is considered as the most potential basin in which lacustrine and fluvial sediments have accumulated (Schull, 1988).

This chapter deals with the subsurface sedimentary facies of the Middle − Upper Cretaceous strata in the SE Muglad Basin. The purposes of this chapter are to characterize the facies associations, and to identify the depositional environment, palaeoclimate, palaeogeographic setting and to clarify the basin development, which will help to provide leeds and targets for future oil exploration.

The establishment of a complete lithofacies classification for the study area is based mainly on the full description and analysis of seven conventional cores which have been obtained from the Bentiu, Aradeiba and Zarga Formations at Unity-9, Talih-2, Heglig-2 and Toma-1 wells, as well as on investigations of 1500 cutting samples and wire line logs from Unity-9, Talih-2, Barki-1, Heglig-2, Toma-1 and Nabag-1 wells. Furthermore, this study includes three seismic lines. Two of them, which are gn 98-010 and sd 81-013, trend NE-SW, whereas the third one, which is sd 82-202, trends NW-SE (Tables 3.1, 3.2 and Figs. 1.2, 4.18, 4.20 & 4.22).

## 4.2 Facies Description and Analysis of Conventional Cores

From the lithofacies analysis of the conventional cores, 9 different major lithofacies types have been recognized.

### 4.2.1  Trough Cross-bedded Sandstone

This facies is dominant in the studied cores from the Bentiu Formation reaching a total thickness of 16.4 m. In the Aradeiba and Zarga Formations, the thickness of this facies is 3 m and 0.9 m respectively (Table 4.1) (Figs. 4.2, 4.3, 4.4, 4.6 and 4.7). The colour of this facies ranges from grey to white with reddish stain. The grain size ranges from medium to coarse, pebbly in some places. The grains are rounded to well rounded in shape and are moderately to well sorted. The observed porosity is high. However, some siliceous, carbonate and iron oxide cements have been observed. Carbonate has been confirmed by a acid test. Kaolinite represents the dominant matrix material. Oil shows have also observed (Plates 4.1, 4.2 & 4.3). This facies could be classified as "St" type according to Miall (1978) and could be interpreted as the deposits of migrating 3-D dunes in fluvial channels or in delta distributary channels.

### 4.2.2  Planar Cross-bedded Sandstone

The total thickness of this facies in the studied cores is about 0.8 m in Bentiu Formation, 3.3 m in Aradeiba Formation and 1 m in Zarga Formation (Table 4.1) (Figs. 4.3, 4.4, 4.5 & 4.7). Its colour ranges from light grey, dark grey to brown. Grain-size ranges from fine to coarse grained. The grains are rounded to well rounded and well sorted. Kaolinite is the dominant matrix material. Silica besides some iron oxides as well as some traces of carbonate are present as cements. However, the observed porosity is medium to high. The dominant sedimentary structure of this facies is planar tabular cross-bedding. This facies resembles the "Sp" facies type of the Miall (1978) classification (Plates 4.1, 4.2 & 4.3) and could be interpreted as a result of deposition in linguoid and transverse bars of fluvial channels or as delta mouth bars.

### 4.2.3  Low Angle Cross-bedded Sandstone

The total thickness of this facies is about 1.8 m in Bentiu, 3.6 m in Aradeiba and 1.5 m in Zarga Formations.(Table 4.1) (Figs. 4.2, 4.3, 4.4, 4.5, 4.6, 4.7 & 4.8). It´s colour ranges from white, light grey to grey. Grain-size ranges from very fine, fine, medium to coarse. The grains of this facies are rounded and well sorted in most of the studied cores. A kaolinitic matrix was observed. Moreover, some iron oxides and traces of carbonates were observed as cement. Oil shows are present as scattered spots. Porosity is high. It is similar to the "Sl" facies type of Miall´s (1978) facies classification (Plates 4.1, 4.2 & 4.3) and can be interpreted as deposits

of scour fills, washout dunes or antidunes, that formed in fluvial channels or in delta distributary channels.

### 4.2.4  Ripple Laminated Sandstone

The total thickness of this facies is about 0.8 m in Bentiu, 1.8 m in Aradeiba and 1.5 m in Zarga Formations (Tables 4.1) (Figs. 4.2, 4.3, 4.5, 4.6, 4.7 & 4.8). It´s colour varies from white, light grey to grey. The grain-size is ranging from very fine to medium; the grains are subrounded to rounded and are moderately sorted. A kaolinitic matrix is dominant. Moreover, some iron oxides, some quartz and traces of carbonate occur as cements. This facies resembles the "Sr" facies type in Miall´s (1978) classification (Plates 4.1, 4.2 & 4.3) and can be explained as ripples, that were deposited on the top of fluvial bars, on the top of deltaic mouth bars, on the floodplain or as natural levee deposits.

### 4.2.5  Massive Sandstone

This facies type was only observed in cores from the Bentiu and Aradeiba Formations, with a total thickness of 0.6 m and 0.3 m repectively (Table 4.1) (Figs. 4.2 & 4.6). Its colour ranges from white, light grey to dark grey. Grain size ranges from very fine to medium, with a gradual fining upward. The grains are subrounded to rounded and moderately sorted. Some iron oxides, quartz and traces of carbonate are occurring as cements. Kaolinite dissemination is dominant. Oil shows were also observed. Locally the massive-looking beds have faint bedding planes, which are not easy to recognize in the conventional cores. This massive sedimentary facies, which resembles the "Sm" facies type in Miall´s (1978) classification (Plates 4.1 & 4.2), was formed by very rapid sedimentation, probably by high-discharge events such as sheet-floods.

### 4.2.6  Horizontally Bedded Sandstone

This facies is present in the Bentiu, Aradeiba and Zarga Formations with total thicknesses of 0.9 m, 0.5 and 0.6 m, respectively (Table 4.1) (Figs. 4.2, 4.5 & 4.7). Colour varies from white to grey. Grain-size ranges from very fine, fine to medium. The grains are subrounded to well rounded in shape and are moderately to well sorted. Kaolinite is the dominant matrix material. Mud clasts and some traces of carbonates are also present. This facies resembles the "Sh" facies type in Miall´s (1978) facies classification (Plates 4.1, 4.2 & 4.3). The deposition of this facies may have taken place in fluvial channel or in delta mouth bar.

### 4.2.7 Fine Laminated Sandy Siltstone, Siltstone and Mudstone

This facies has total thickness of about 0.2 m in the Bentiu Formation and 4.8 m in the Aradeiba Formation, which is less than that of the Zarga Formation,. Which is 7.8 m (Table 4.1; Figs. 4.3, 4.4, 4.5, 4.6, 4.7 & 4.8). Its colour varies from light grey to dark grey. However, in few cases it is red to brown. Few carbonates cements were observed within this facies. The typical sedimentary structure in the sandy siltstone is plane parallel to low angle lamination with or without very small ripple marks. In the siltstones the dominant sedimentary structure is mainly fine lamination with very small ripple marks. The mudstones are finely laminated with some root casts. This facies resembles the "Fl" facies type in Miall´s (1978) facies classification. This facies represents overbank or waning floodplain or deltaic distal bar deposits, which were depoisted in an oxidizing environment (Plates 4.1, 4.2 & 4.3).

### 4.2.8 Massive to Desiccated Mudstone

This facies is only present in cores from Bentiu and Aradeiba Formations. It reaches a total thickness of 2.1 m and 0.5 m respectively (Table 4.1; Figs. 4.2 & 4.5). The colour of this facies varies from purple to grey, purple to red and from red to brown. The most common sedimentary structures of this facies in the Bentiu Formation are desiccation cracks. In the Aradeiba Formation, most of this lithofacies is massive. This facies is classified as "Fm" according to Miall (1978). It can be interpreted as overbank deposits (Plates 4.1 & 4.2).

### 4.2.9 Fine Laminated to Massive Mudstone

The thickness of this facies is about 5.1 m in the Bentiu, 3.0 m in the Aradeiba and 6.0 m in the Zarga Formations (Tables 4.1; Figs. 4.4, 4.6 & 4.7). It is grey in colour and rich in kaolinite. This facies resembles the "Fcf" facies in Miall´s (1978) classification. It is interpreted as prodelta or backswamp pond deposits deposited in a reducing environment (Plates 4.1, 4.2 & 4.3).

Lithology

| | Claystone |
| | Silty claystone |
| | Siltstone |
| | Sandy siltstone |
| | Sandstone |

Lithologic Accessories

| o o<br>o o | Pepples/ granules |
| Δ Δ | Mud clasts |
| c c | Carbonate |
| ☐ | Photograph location |
| ○ | Petrographic sample position |

Sedimentary Structures

| | Trough cross stratification |
| | Planar cross- bedded |
| | Low angle cross bedded |
| | Ripple marks |
| | Plane parallel beds |
| | Horizontal to wavy beds |
| | Plane parallel lamination |
| | Plane parallel to low angle laminae |
| | Desiccation cracks |
| | Plant roots |
| | Plant peats/ Fresh water molluscs |

**Figure 4.1: Legend of the symbols used int he description of the cores and throughout this study.**

**Well name: Unity -9**
**Formation: Bentiu**  Core No 14  Interval : 8891 - 8861 ft.

| Lithology | Samples | Photos | Depth (ft.) | Comments | Interpretation |
|---|---|---|---|---|---|
| | | □ | 8877 | Grey coarse pebbly sandstone, well rounded, well sorted, kaolinitic, trough cross-bedded. | Channel/ bar deposits |
| | | | 8879 | Sandstone, grey, fine grained, well sorted, low angle cross-bedded to plane parallel stratification. | |
| | | | 8881 | Sandstone, white, medium grained, subrounded to well rounded, well to moderately sorted, kaolinitic, horizontal to wavy bedded. | |
| | | | | Sandstone, white, v. fine grained, well rounded, well sorted, kaolinitic, mud clasts are present, low angle cross stratification. | |
| | | | 8883 | Sandstone, white, fine grained with mud clasts, horizontal to wavy bedded. | |
| | | | 8885 | Sandstone, grey, medium grained, rounded, well sorted, few mud clasts, trough cross-bedded. | |
| | | | | Sandstone, grey, fine grained, moderately sorted, ripple marks with some lamination. | |
| | O | | 8887 | | |
| | O | | 8889 | Sandstone, white with red stains, medium grained, well sorted, kaolinitic, few mud clasts, traces of carbonates, trough cross-bedded. | |
| | | | 8891 | | |

| Lithology | Samples | Photos | Depth (ft.) | Comments | Interpretation |
|---|---|---|---|---|---|
| | | | 8861 | | Overbank deposits |
| | | | 8863 | Mudstone, reddish to brown, has desiccation cracks. | |
| | | | 8865 | | |
| | | | 8867 | Sandstone, white, v. fine , moderately sorted, has mud clasts, ripple marks, with some lamination. | |
| | | | | Mudstone, grey, minor swelling clay laminae, desiccated, burrows and plant roots. | |
| | | | 8869 | Sandstone, dark grey, gradual fining upwards, subrounded, moderately sorted, massive. | Channel/ bar deposits |
| | | | 8871 | Sandstone, white, medium grained rounded, well sorted, kaolinitic, with few mud clasts, traces of carbonates, presence of silt filled burrows, trough cross-bedded. | |
| | O | □ | 8873 | | |

**Figure 4.2: Description and interpretation of core no. 14 from the Bentiu Formation in well Unity-9.**

**Well name: Toma -1**
**Formation: Bentiu**  Core No 2  Interval : 5338 - 5310 ft.

| Lithology | Samples | Photos | Depth (ft.) | Comments | Interpretation |
|---|---|---|---|---|---|
| | | | 5324 | Black shale. | Channel/ bar deposits |
| | | | | Grey medium grained sandstone, well rounded, well sorted, trough cross-bedded, oil shows. | |
| | | | 5326 | | |
| | | | 5328 | Fine grey sandstone, subrounded, moderately sorted, ripple marks with some lamination. | |
| | | | 5330 | Sandstone, grey, medium grained, mud clasts, kaolinitic, subrounded moderately sorted, trough cross-bedded, oil shows. | |
| | | | 5332 | | |
| | | | 5334 | Sandstone, grey, medium grained, well sorted, plane parallel and planar tabular cross beds. | |
| | | | | Siltstone, grey, horizontally laminated. | |
| | | | 5336 | Sandstone, grey in colour, medium grained, well sorted, planar tabular cross-bedded. | Overbank deposits |
| | | | 5338 | sandstone, grey, subrounded, fine grained, moderately sorted, kaolinitic, mud clasts, low angle to parallel laminae. | |

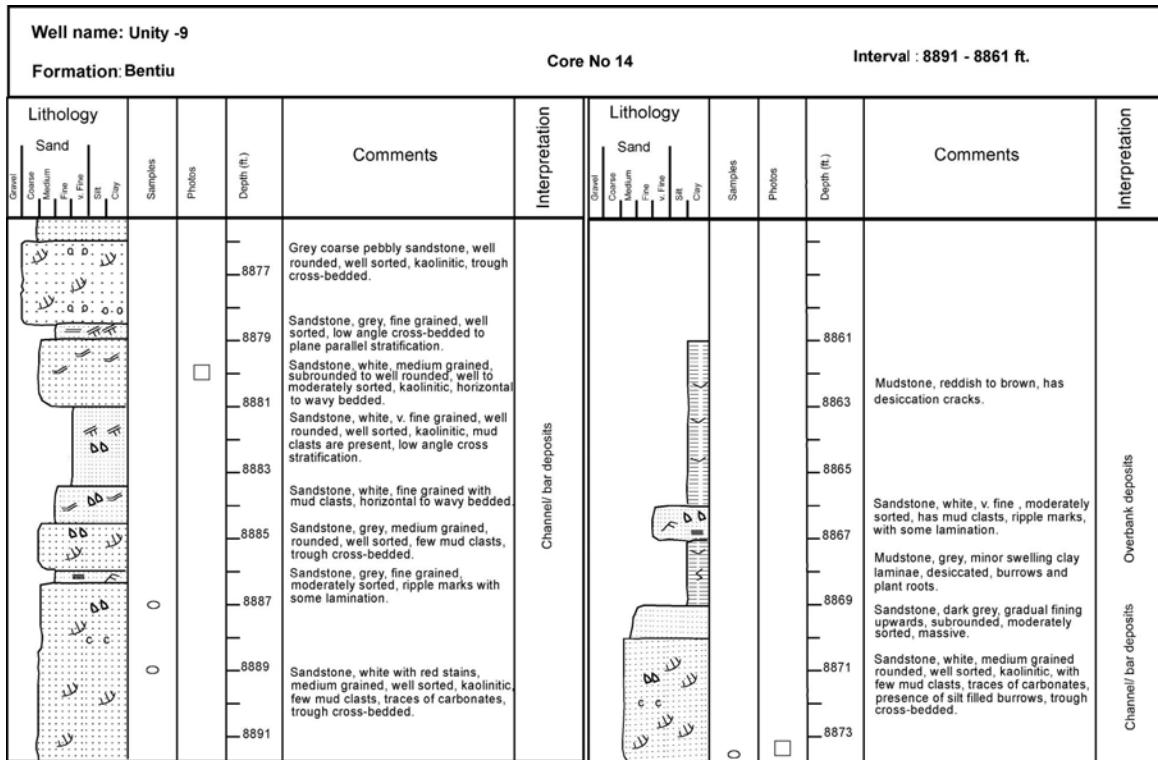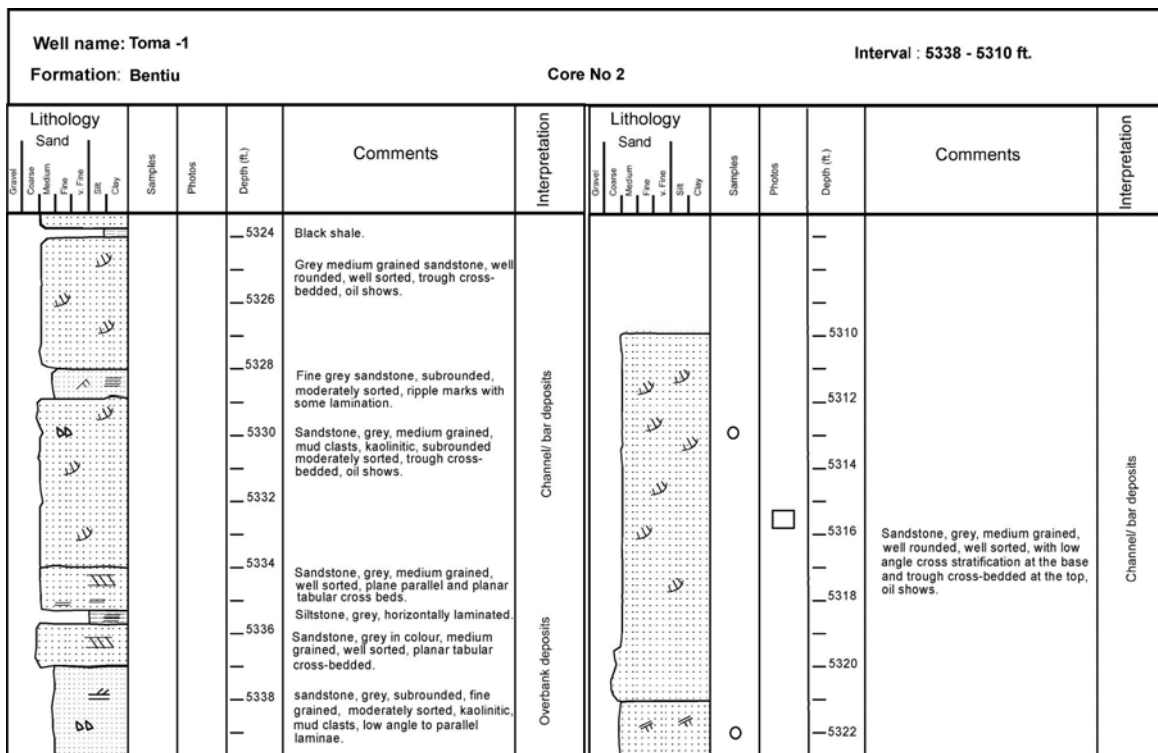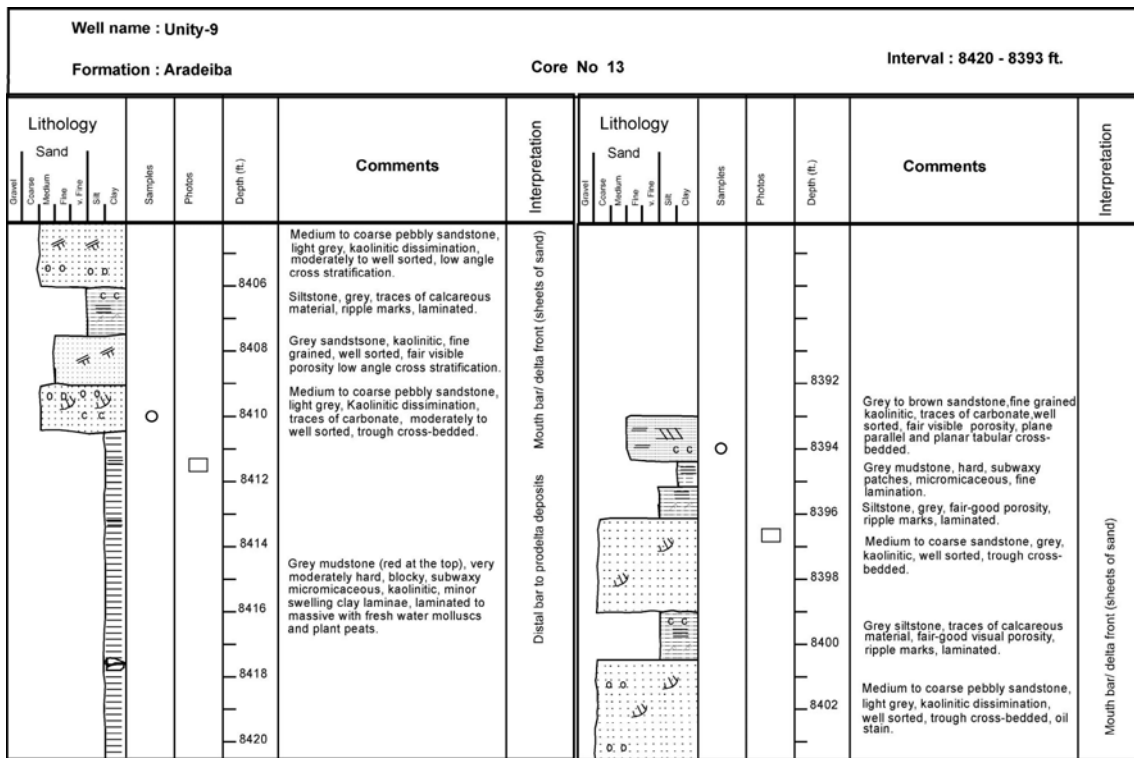| Lithology | Samples | Photos | Depth (ft.) | Comments | Interpretation |
|---|---|---|---|---|---|
| | | | | | Channel/ bar deposits |
| | | | 5310 | | |
| | O | | 5312 | | |
| | | □ | 5314 | | |
| | | | 5316 | Sandstone, grey, medium grained, well rounded, well sorted, with low angle cross stratification at the base and trough cross-bedded at the top, oil shows. | |
| | | | 5318 | | |
| | | | 5320 | | |
| | O | | 5322 | | |

**Figure 4.3: Description and interpretation of core no. 2 from the Bentiu Formation in well Toma-1.**

**Figure 4.4: Description and interpretation of core no. 13 from the Aradeiba Formation in well Unity-9.**
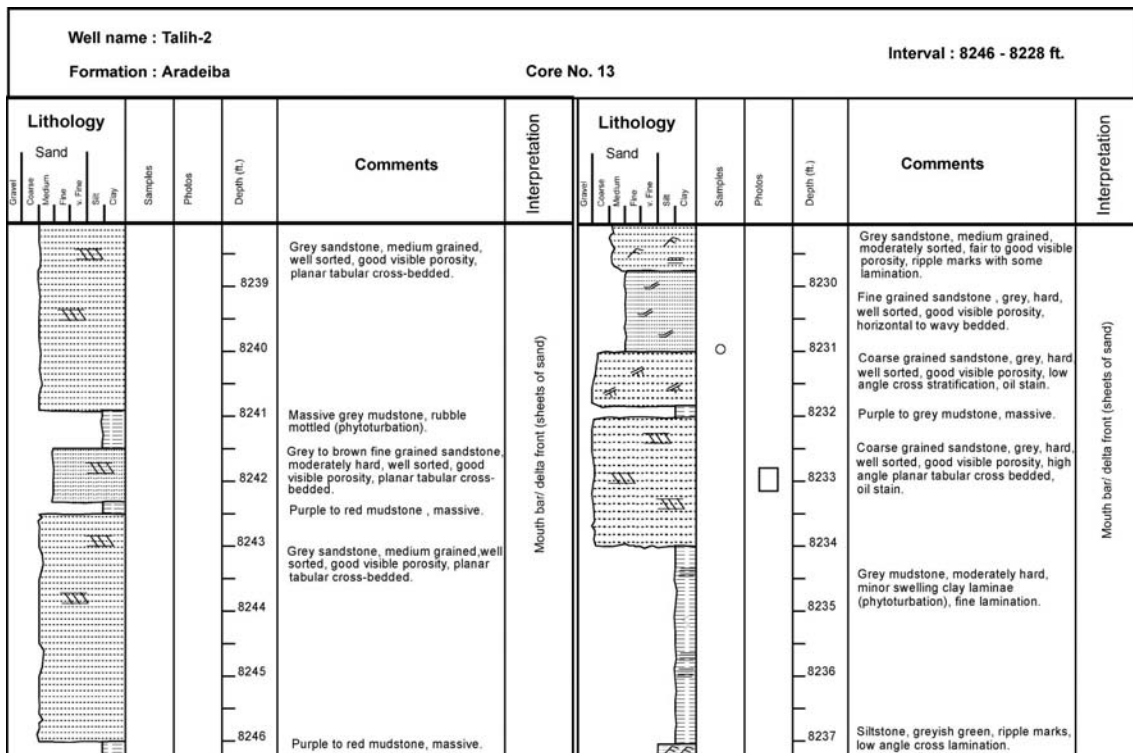
Well name : Unity-9
Formation : Aradeiba — Core No 13 — Interval : 8420 - 8393 ft.

Left panel — Lithology / Samples / Photos / Depth (ft.) / Comments / Interpretation:

- 8406 — Medium to coarse pebbly sandstone, light grey, kaolinitic dissimination, moderately to well sorted, low angle cross stratification.
- Siltstone, grey, traces of calcareous material, ripple marks, laminated.
- 8408 — Grey sandstsone, kaolinitic, fine grained, well sorted, fair visible porosity low angle cross stratification.
- 8410 — Medium to coarse pebbly sandstone, light grey, Kaolinitic dissimination, traces of carbonate, moderately to well sorted, trough cross-bedded.
- 8412
- 8414 — Grey mudstone (red at the top), very moderately hard, blocky, subwaxy micromicaceous, kaolinitic, minor swelling clay laminae, laminated to massive with fresh water molluscs and plant peats.
- 8416
- 8418
- 8420

Interpretation: Mouth bar/ delta front (sheets of sand); Distal bar to prodelta deposits

Right panel — Lithology / Samples / Photos / Depth (ft.) / Comments / Interpretation:

- 8392
- 8394 — Grey to brown sandstone, fine grained kaolinitic, traces of carbonate, well sorted, fair visible porosity, plane parallel and planar tabular cross-bedded.
- Grey mudstone, hard, subwaxy patches, micromicaceous, fine lamination.
- 8396 — Siltstone, grey, fair-good porosity, ripple marks, laminated.
- Medium to coarse sandstone, grey, kaolinitic, well sorted, trough cross-bedded.
- 8398
- 8400 — Grey siltstone, traces of calcareous material, fair-good visual porosity, ripple marks, laminated.
- 8402 — Medium to coarse pebbly sandstone, light grey, kaolinitic dissimination, well sorted, trough cross-bedded, oil stain.

Interpretation: Mouth bar/ delta front (sheets of sand)

**Figure 4.5: Description and interpretation of core no. 13 from the Aradeiba Formation in well Talih-2.**

Well name : Talih-2
Formation : Aradeiba — Core No. 13 — Interval : 8246 - 8228 ft.

Left panel — Lithology / Samples / Photos / Depth (ft.) / Comments / Interpretation:

- 8239 — Grey sandstone, medium grained, well sorted, good visible porosity, planar tabular cross-bedded.
- 8240
- 8241 — Massive grey mudstone, rubble mottled (phytoturbation).
- Grey to brown fine grained sandstone, moderately hard, well sorted, good visible porosity, planar tabular cross-bedded.
- 8242 — Purple to red mudstone, massive.
- 8243 — Grey sandstone, medium grained, well sorted, good visible porosity, planar tabular cross-bedded.
- 8244
- 8245
- 8246 — Purple to red mudstone, massive.

Interpretation: Mouth bar/ delta front (sheets of sand)

Right panel — Lithology / Samples / Photos / Depth (ft.) / Comments / Interpretation:

- 8230 — Grey sandstone, medium grained, moderately sorted, fair to good porosity, ripple marks with some lamination.
- Fine grained sandstone, grey, hard, well sorted, good visible porosity, horizontal to wavy bedded.
- 8231 — Coarse grained sandstone, grey, hard, well sorted, good visible porosity, low angle cross stratification, oil stain.
- 8232 — Purple to grey mudstone, massive.
- Coarse grained sandstone, grey, hard, well sorted, good visible porosity, high angle planar tabular cross bedded, oil stain.
- 8233
- 8234 — Grey mudstone, moderately hard, minor swelling clay laminae (phytoturbation), fine lamination.
- 8235
- 8236
- 8237 — Siltstone, greyish green, ripple marks, low angle cross lamination.

Interpretation: Mouth bar/ delta front (sheets of sand)

**Well name: Heglig -2**

**Formation: Bentiu / Aradeiba**  Core No 4  Interval: 5557 - 5497 ft.

| Lithology Sand | Samples | Photos | Depth (ft.) | Comments | Interpretation |
|---|---|---|---|---|---|
| | | | 5525 | Sandstone, white, coarse grained, rounded, well sorted, kaolinitic, few mud clasts, trough cross-bedded. | Channel/ bar deposits |
| | | | 5529 | | |
| | | | 5533 | | |
| | | | 5537 | | |
| | | | 5541 | Mudstone, grey, kaolinitic, laminated to massive. | Backswamp pond deposits |
| | | □ | 5545 | | |
| | | | 5549 | | |
| | | | 5553 | Sandstone, white, medium to fine, gradual fining upwards, moderately sorted, kaolinitic, massive with some mud clasts. | Overbank deposits |
| | | | 5557 | Sandstone, grey, coarse grained, well rounded, well sorted, kaolinitic, traces of carbonates, trough cross-bedded, has oil shows. | |

| Lithology Sand | Samples | Photos | Depth (ft.) | Comments | Interpretation |
|---|---|---|---|---|---|
| | | | 5495 | Grey sandstone, coarse, subrounded tol rounded, well sorted, kaolinitic, trough cross-bedded. | Floodplain deposits |
| | | | 5499 | | |
| | | | 5503 | Mudstone, red, fine laminated with some plant roots. | |
| | | | 5507 | Sandstone, grey, v. fine grained, subagular to subrounded, moderately sorted, mud clasts, plane parallel laminae. | Overbank deposits |
| | O | | 5511 | Grey v. fine sandstone, subrounded grains, moderately sorted, massive. Sandstone, grey, medium grained, rounded grains, well sorted, kaolinitic, low angle trough cross-bedded. | |
| | | □ | 5515 | Sandstone, white, fine grained, rounded grains, moderately sorted, traces of carbonates, ripple marks, kaolinitic, low angle trough cross-bedded. | Channel/ bar deposits |
| | O | | 5519 | Grey sandstone, coarse, rounded grains, well sorted, kaolinitic, trough cross-bedded. | |
| | | | 5523 | Gery fine sandstone, rounded grains, well sorted, low angle cross-bedded with ripple marks. | |

**Figure 4.6: Description and interpretation of core no. 4 from the boundary between the Bentiu and Aradeiba Formations in well Heglig-2.**

**Well name: Talih-2**

**Formation: Zarga**  Core No.10  Interval : 7740 -7699 ft.

| Lithology Sand | Samples | Photos | Depth (ft.) | Comments | Interpretation |
|---|---|---|---|---|---|
| | O | | 7714 | Sandy siltstone, grey, traces of carbonates, ripples marks, laminated. Coarse sandstone,white, kaolinitic granules, siliceous cement material moderately to well sorted, trough cross-bedded. | Overbank deposits |
| | O | □ | 7720 | Grey silty sandstone, traces of carbonates, ripple marks. Fine sandstone, light grey,moderately to well sorted, low angle cross stratification. | |
| | | | 7726 | | Backswamp pond deposits |
| | | | 7732 | Light grey mudstone, kaolinitic, laminated to massive. | |
| | | | 7738 | | |
| | | | 7744 | | |

| Lithology Sand | Samples | Photos | Depth (ft.) | Comments | Interpretation |
|---|---|---|---|---|---|
| | | | 7693 | | |
| | | | 7699 | Grey mudstone, kaolinitic, fine laminated. | Overbank deposits |
| | | | 7705 | Grey to greenish siltstone, kaolinite granules, horizontally laminated with ripple marks. | |
| | | | 7711 | Very fine sanstone, grey to white, moderately sorted, planar tabular cross bedded at the base, horizontal to wavy bedded with streaks of mud at the top. | |

**Figure 4.7: Description and interpretation of core no. 10 from the Zarga Formation in well Talih-2.**

Well name : Unity-9

Formation : Zarga

Core No 9

Interval : 7473 - 7457

**Left panel**

Lithology — Sand (Gravel, Coarse, Medium, Fine, v. Fine, Silt, Clay) | Samples | Photos | Depth (ft.) | Comments | Interpretation

| Depth (ft.) | Comments |
|---|---|
| 7466 | Light grey to white v. fine sandstone, kaolinitic, well sorted, low angle cross-bedded at the base with ripple marks at the top. |
| 7467 | |
| 7468 | Dark grey mudstone, fine laminated with some plant peats and fresh water molluscs. |
| 7469 | |
| 7470 | Light grey, v. fine sandstone, Kaolinitic, well sorted, traces of carbonates, low angle cross-bedded. |
| 7471 | |
| 7472 | Red to brown mudstone, fine laminated with some plant peats and fresh water molluscs, oil stain. |
| 7473 | |

Interpretation: Distal bar to prodelta deposits

**Right panel**

Lithology — Sand (Gravel, Coarse, Medium, Fine, v. Fine, Silt, Clay) | Samples | Photos | Depth (ft.) | Comments | Interpretation

| Depth (ft.) | Comments |
|---|---|
| 7457 | Grey mudstone, minor swelling clay laminae, fine lamination, some plant roots. |
| 7458 | |
| 7459 | Fine sandstone, white in colour with kaolinite granules, well sorted, low angle cross-bedded. |
| 7460 | |
| 7461 | Sandy siltstone , grey in colour, plane parallel to low angle laminae. |
| 7462 | |
| 7463 | V. fine sandstone, white to grey, well sorted, traces of carbonates, low angle trough cross-bedded. |
| 7464 | Siltstone, light grey, hard blocky, laminated with ripple marks. |

Interpretation: Distal bar/ delta front deposits

**Figure 4.8: Description and interpretation of core no. 9 from the Zarga Formation in well Unity-9.**

**Table 4.1: Summary of facies description and interpretation from the conventional cores (facies codes are taken from Miall, 1978).**

| Facies code | Lithofacies | Sedimentary structures | Total thickness in Formation (m) | | Interpretation |
|---|---|---|---|---|---|
| St | Sand, medium to coarse | Trough cross-bedded | Bentiu Aradeiba Zarga | 16.4 3.0 0.9 | Dunes (fluvial channel or delta distributary channel). |
| Sp | Sand, fine to coarse | Planar cross-bedded | Bentiu Aradeiba Zarga | 0.8 3.3 1.0 | Linguoids, transverse bars, sand waves (fluvial channel or delta mouth bar). |
| Sl | Sand, very fine to coarse | Low angle cross-bedded | Bentiu Aradeiba Zarga | 1.8 3.6 1.5 | Scour fills, washout dune, antidunes (fluvial channel or delta distributary channel). |
| Sr | Sand, very fine to medium | Ripples marks of all types | Bentiu Aradeiba Zarga | 0.8 1.8 1.5 | Ripples (top fluvial bar or delta mouth bar or floodplain or levee). |
| Sm | Sand, very fine to medium | Massive | Bentiu Aradeiba Zarga | 0.6 0.3 - | Rapid sedimentation (high-discharge event). |
| Sh | Sand, very fine to medium | Horizontal lamination & parting | Bentiu Aradeiba Zarga | 0.9 0.5 0.6 | Planar bed flow (fluvial channel bar deposits or delta mouth bar deposits). |
| Fl | Sandy siltstone, siltstone and mudstone | Fine lamination, very small ripples | Bentiu Aradeiba Zarga | 0.2 4.8 7.8 | Overbank or waning flood deposits or delta distal bar deposits. |
| Fm | Mudstone | Massive, desiccation cracks | Bentiu Aradeiba Zarga | 2.1 0.5 - | Overbank deposits |
| Fcf | Mudstone | Laminated to massive | Bentiu Aradeiba Zarga | 5.1 3.0 6.0 | Backswamp pond deposits or prodelta deposits. |

## 4.3 Subsurface Facies Analysis from Wire line Logs and Cutting Samples

Well logs are extensively used in petroleum exploration for evaluation of fluid type and content in rocks. In most subsurface studies, geophysical logs are the fundamental source of

data because well logging is a very valuable method of analyzing downhole formations (Cant 1984; Miall 1984; Allen and Allen 1990). In the present study, wire line logs besides the investigations of cutting samples were used to investigate the uncored facies successions, to detect changes in grain size distribution, lithology and sedimentary facies and hence to interpret depositional environment. Confirmation of the log behaviour using the cores and the cutting samples was undertaken. Furthermore, core to gamma-ray and spontaneous potential log correlations were set up (Figs. 4.9 – 4.15).

The gamma-ray and the spontaneous potential log response throughout Bentiu, Aradeiba and Zarga Formations in the six studied wells exhibits a serrated cyclic log shape. This corresponds to the changes of the sedimentary facies as a result of changes in the both autocyclic and allocyclic controls. Four basic types could be noticed in these logs patterns: a bell shape with a abrupt base (a fining upward pattern), a cylinderical shape (no trend), an irregular shape (an irregular mixture of sand and mud) and a funnel shape with abrupt top (coarsening upward pattern) (Figs. 4.9. – 4.15). The dominant pattern types in the Bentiu Formation are the bell shape with a long abrupt base and the cylindrical shape (Figs. 4.9, 4.10 & 4.13). The wire line logs patterns in the Aradeiba Formation are more or less similar to that of the Bentiu Formation. However, the bell shape patterns show a shorter abrupt base and a longer top in comparison to that of the Bentiu Formation. Moreover, there are multiple fining up-ward patterns (bell shape patterns) stacked on each others in the Aradeiba Formation. In addition to that in the strata near the upper part of the Aradeiba Formation, the funnel shape of long base patterns are dominant (Figs. 4.11, 4.12 & 4.13). On the other hand, the gamma-ray and the spontaneous potential logs of the Zarga Formation generally show relatively low API readings with dominant irregular shape patterns (Figs. 4.14 & 4.15).

The results obtained from the lithofacies analysis of the wire line logs, the conventional cores and the cutting samples were tabulated and the sand/mud ratios were calculated separately for each formation in Unity and Heglig Fields (Tables 4.2 & 4.3). On the basis of lithofacies analysis of the wire line logs, the conventional cores and the cutting samples, the vertical profiles of the studied intervals in the six wells under investigation have been plotted separately in each field in order to reveal the vertical and the lateral correlations in the two fields (Figs. 4.16 & 4.17).

The average sand/mud ratios of the Bentiu, Aradeiba and Zarga Formations in the studied wells of Unity Fields are 6.6, 1.17 and 0.62 respectively. The average sand/mud ratios

of the Bentiu, Aradeiba and Zarga Formations in the studied wells of Heglig Field are 3.5, 0.95 and 0.57 respectively, which are lesser in comparison with the average sand/mud ratios of these formations in the studied wells of the Unity Field. Generally, this trend is also indicated by the relatively low and stable gamma-ray readings as well as by the relatively low and more stable millivolts readings of the studied intervals in the Unity Field in comparison to the studied intervals in the Heglig Field (Figs. 4.9 – 4.15). Moreover, the travel time readings of the sonic wire line logs as well as the density values of the density and neutron wire line logs are high in the Unity Field in comparison to the Heglig Field. This indicates, that the sandstone beds are thicker in the Unity Field than in the studied intervals of the Heglig Field (Tables 4.2 & 4.3; Figs. 4.16 & 4.17).
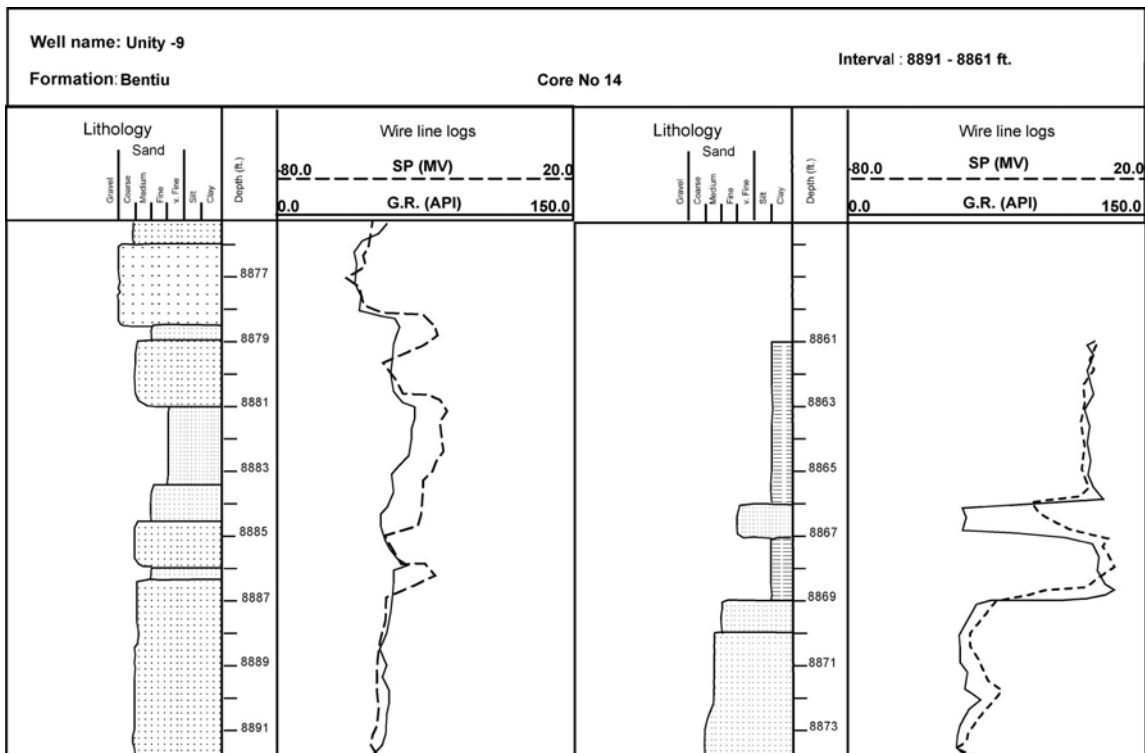
**Figure 4.9: Correlation of gamma-ray and spontaneous potential logs of core no. 14 in the Bentiu Formation, well Unity-9.**
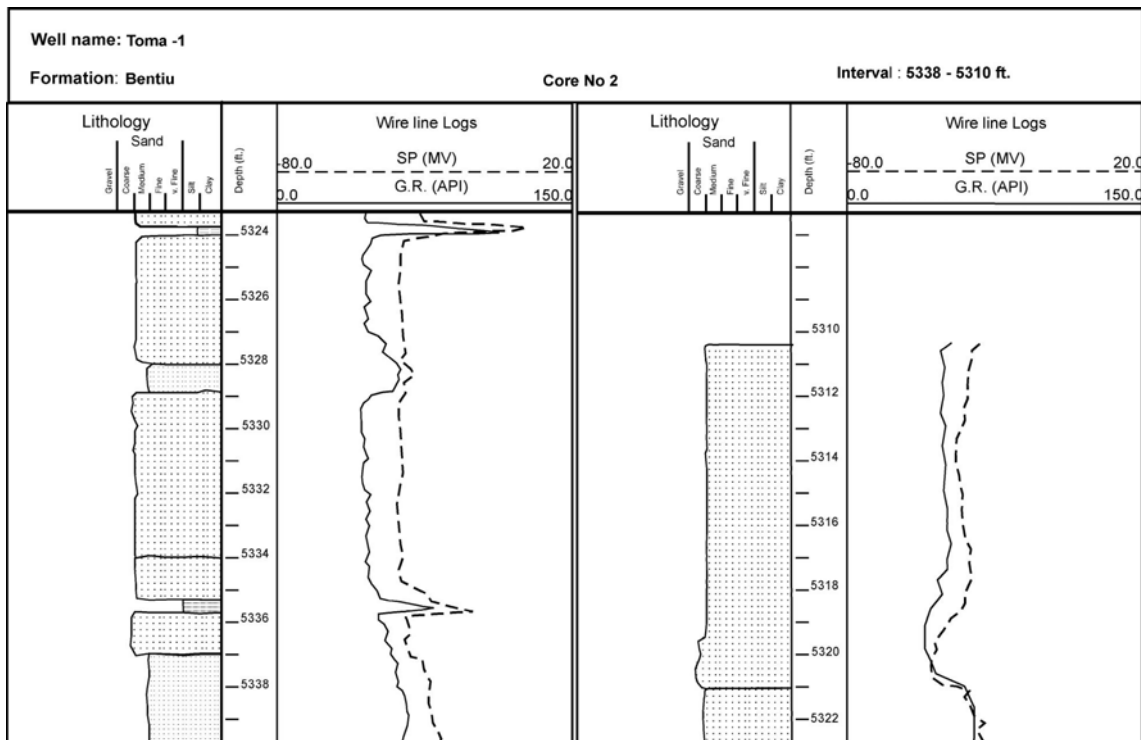


**Figure 4.10: Correlation of gamma-ray and spontaneous potential logs of core no. 2 in the Bentiu Formation, well Toma-1.**
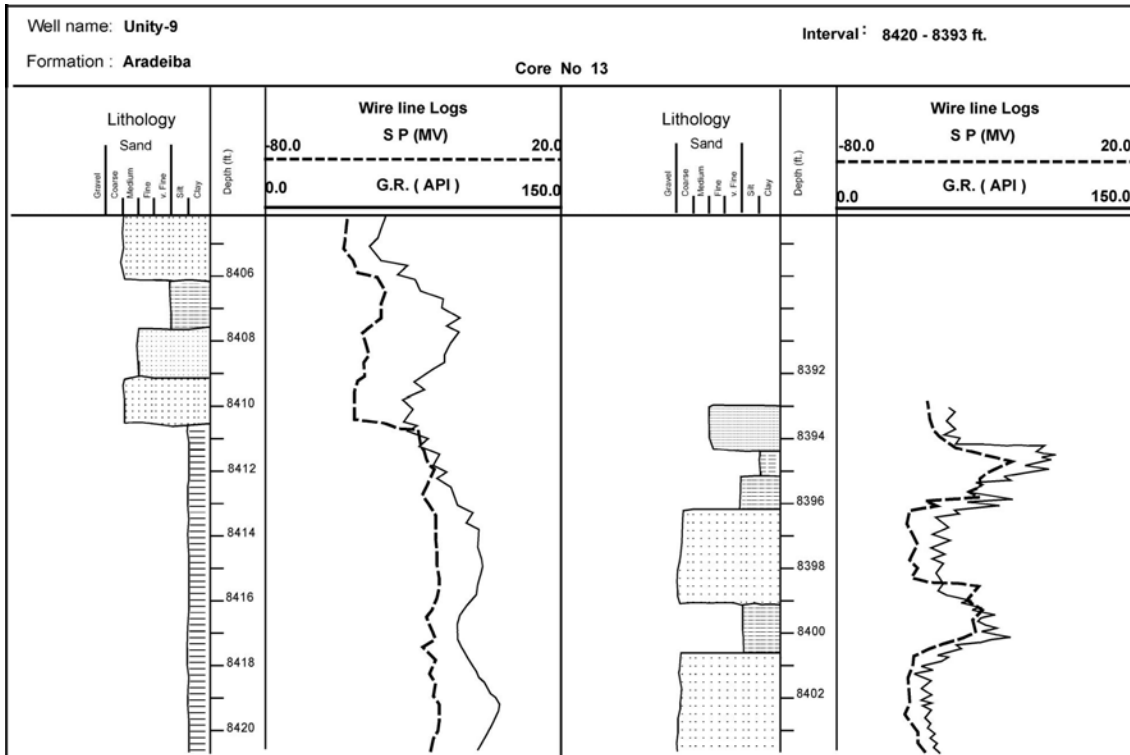
**Figure 4.11: Correlation of gamma-ray and spontaneous potential logs of core no. 13 in the Aradeiba Formation, well Unity-9.**
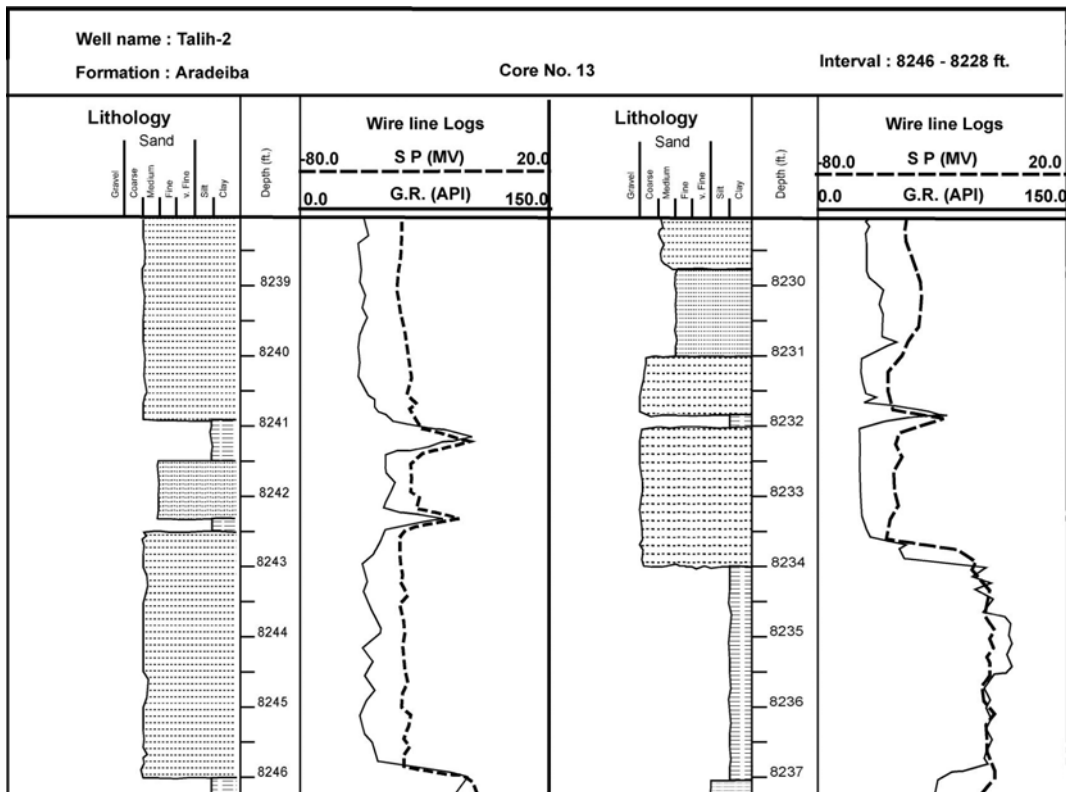


**Figure 4.12: Correlation of gamma-ray and spontaneous potential logs of core no. 13 in the Aradeiba Formation, well Talih-2.**
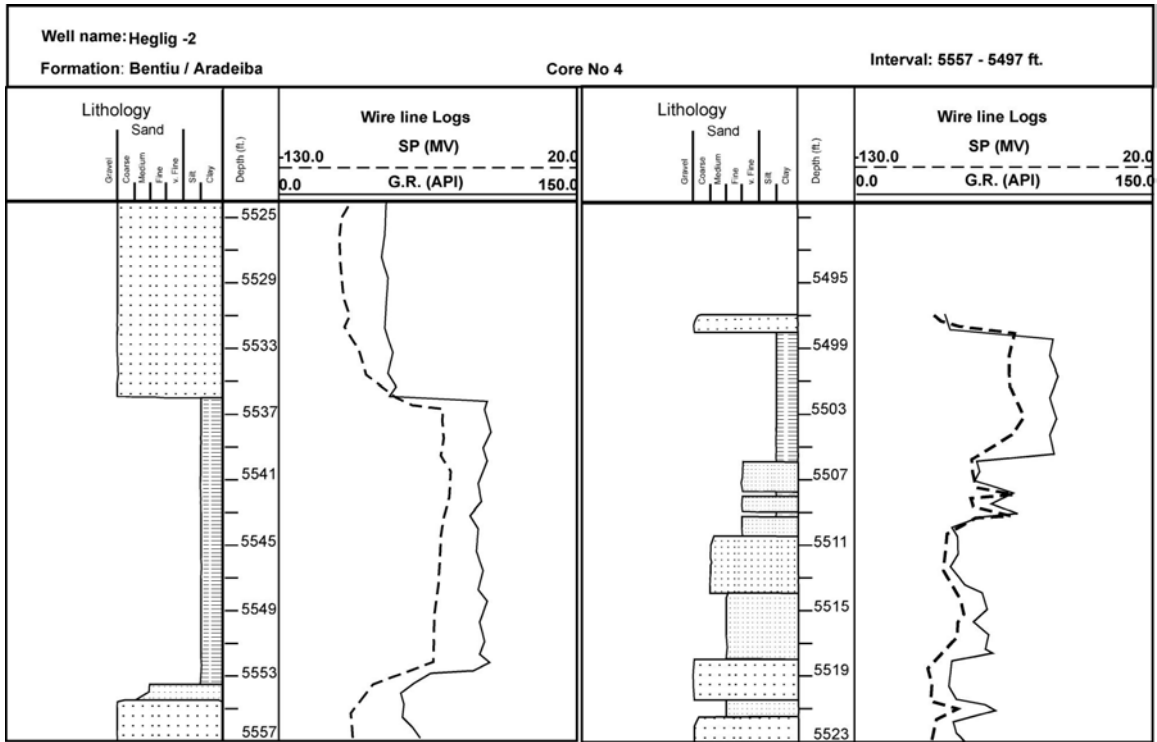
**Figure 4.13: Correlation of gamma-ray and spontaneous potential logs of core no. 4 in the Bentiu / Aradeiba Formations, well Heglig-2.**
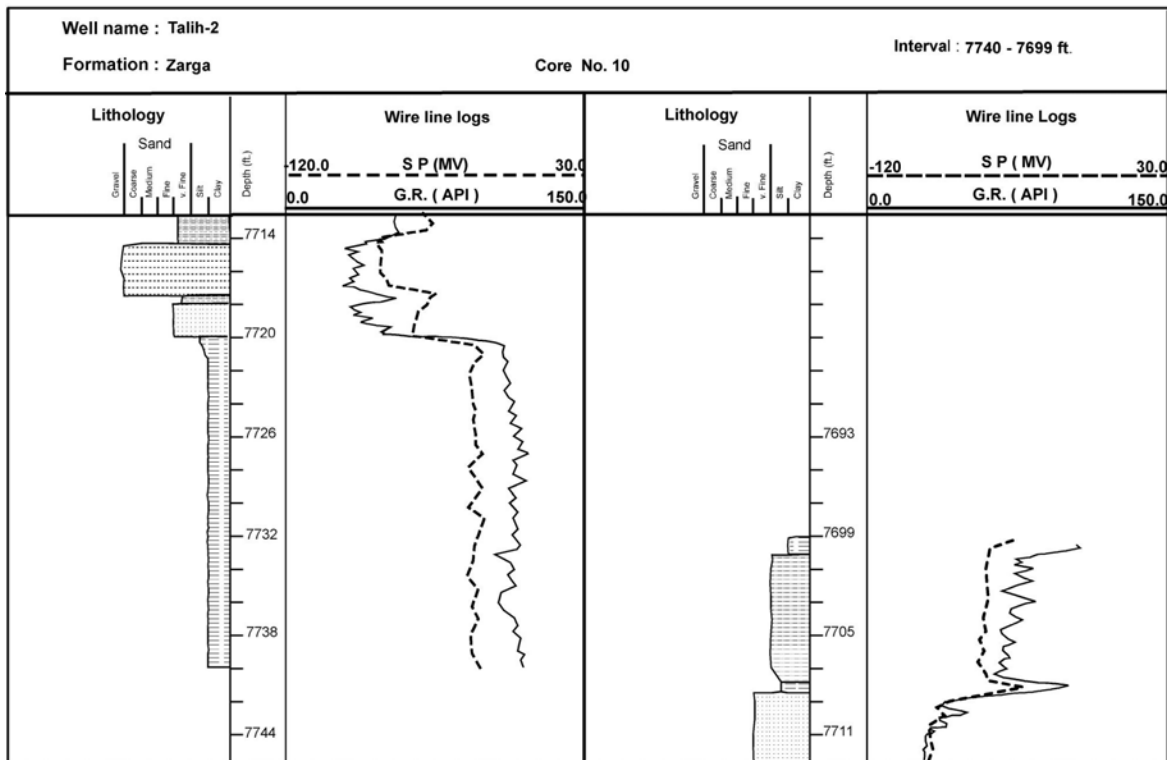


**Figure 4.14: Correlation of gamma-ray and spontaneous potential logs of core no. 10 in the Zarga Formation, well Talih-2.**
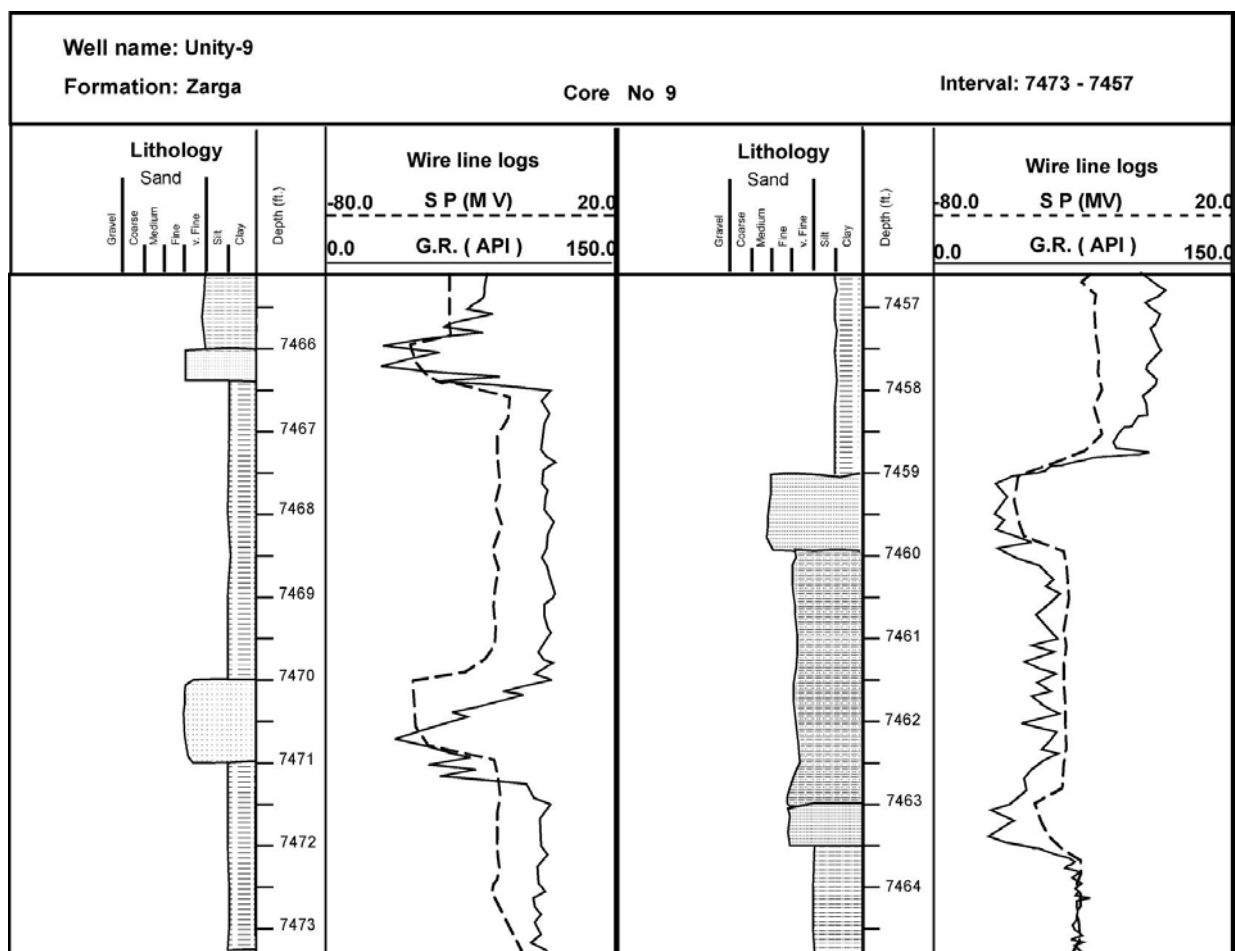
**Figure 4.15: Correlation of gamma-ray and spontaneous potential logs of core no. 9 in the Zarga Formation, well Unity-9.**

**Table 4.2: Sedimentological characteristics of Bentiu, Aradeiba and Zarga Formations in the studied wells of the Unity Field based on cutting samples and wire line logs.**

| Characteristics | | | Bentiu Fm. | Aradeiba Fm. | Zarga Fm. |
|---|---|---|---|---|---|
| Lithology | Maximum facies thickness (m) | Coarse sandstone | 103 | 10 | 6 |
| | | Medium sandstone | 127 | 42 | - |
| | | Fine sandstone | 163 | 33 | 30 |
| | | Silty sandstone | - | 18 | 6 |
| | | Siltstone | - | 45 | 30 |
| | | Mudstone | 18 | 60 | 90 |
| Sequences thickness ranges (m) | Fluvial | | 18-169 | 12-81 | 18-84 |
| | Lacustrine | | - | 24-60 | 30-90 |
| | Deltaic | | - | 21-67 | 18-30 |
| Sand/mud ratios | | | 6.60 | 1.17 | 0.62 |

68

**Table 4.3: Sedimentological characteristics of Bentiu, Aradeiba and Zarga Formations in the studied wells of the Heglig Field based on cutting samples and wire line logs.**

| Characteristics | | | Bentiu Fm. | Aradeiba Fm. | Zarga Fm. |
|---|---|---|---|---|---|
| Lithology | Maximum facies thickness (m) | Coarse sandstone | 133 | 30 | - |
| | | Medium sandstone | 90 | 18 | 12 |
| | | Fine sandstone | 72 | 67 | 9 |
| | | Silty sandstone | 12 | 54 | 6 |
| | | Siltstone | 18 | 21 | 109 |
| | | Silty mudstone | - | 3 | - |
| | | Mudstone | 60 | 145 | 79 |
| Sequences thickness ranges (m) | Fluvial | | 30-169 | 18-64 | 15-70 |
| | Lacustrine | | - | 12-133 | 18-121 |
| | Deltaic | | - | 24-72 | 12-61 |
| Sand/mud ratios | | | 3.50 | 0.95 | 0.57 |

## 4.4 Discussion and Interpretation

### 4.4.1 Vertical and Lateral Facies Distribution of the Middle – Upper Cretaceous Strata

The depositional framework of the Middle – Upper Cretaceous Strata was lakes influenced by contributions from surrounding fluvial systems as well as by tectonism. The lacustrine and the fluvial deposits are characterized by a striking asymmetric facies distribution and by a hierarchical sequential arrangement. The hierarchical arrangement of the basin fill resulted from the evolution of the lacustrine-fluvial system. The fluctuating water level of the lake and of the lake areal extent of this lacustrine-fluvial system have defined and controlled three major sediment cycles, which had been also controlled by tectonism. The lithofacies analysis of the Bentiu Formation, which belongs to the first sediment cycle and of the Aradeiba and Zarga Formations, which belong to the second sediment cycle, allows the subdivision of these sediments into three units of first-order sequences that represent a fluvial-dominated sequence unit, a lacustrine-dominated sequence unit and a deltaic-dominated sequence unit.

### 4.4.2 Fluvial-dominated Unit

Both braided and meandering fluvial sedimentary sequences occur in the studied intervals. The braided sequences are characterized by lower amounts of fine grained floodplain sediments and by more irregular in grain-size trends within the sequences (Maill 1978;

Ethridge et al., 1981; Abdullatif 1989; Godin 1991). The bar sediments are represented by sandstone beds, which have complex structures, mainly trough and planar cross-bedding, whereas the overbank and the floodplain sediments are siltstone and mudstone beds. The siltstone beds are ripple-laminated, whereas the mudstone beds, which cap the fluvial sequences, are horizontally laminated with some root casts (Figs 4.2, 4.3, 4.6 & 4.7). This fluvial-dominated sequence unit characterizes the whole of the Bentiu Formation as well as the lowermost part of the Aradeiba Formation in all of the studied wells of Unity Field, the middle part of the Aradeiba Formation in Unity-9 well and the upper part of Aradeiba Formation as well as the middle part of Zarga Formation in all of the studied wells of the Unity Field (Fig 4.17). Moreover, this fluvial sequence unit is found throughout the Bentiu Formation in the studied wells of Heglig Field, in the lower and middle parts of Aradeiba Formation in Heglig-2 as well as in the lower and the middle parts of Zarga Formation in Toma-1 and Nabag-1 wells (Fig 4.16). The thickness of the fluvial sequences in the Bentiu, Aradeiba and Zarga Formations in the Unity Field ranges between $18 - 169$ m, $12 - 81$ m and $18 - 84$ m respectively, whereas that of the same formations in the Heglig Field ranges between $30 - 169$ m, $18 - 64$ m and $15 - 70$ m respectively (Tables 4.2 & 4.3). The fluvial sequences of the Bentiu Formation are braided river deposits, whereas the fluvial sequences of the Aradeiba Formation are both braided and meandering river sediments. The fluvial sequences of the Zarga Formation consist mainly of meandering river deposits. The floodplain sediments act as a permeability barrier and thus separate the potential reservoir sand bar bodies in the study area.

### 4.4.3  Lacustrine-dominated Sequences Unit

The lacustrine-dominated sequence unit occurs in the lower and upper part of the Aradeiba Formation in Unity-9 well, in the lower part of the Aradeiba Formation in Talih-2 and Barki-1 wells as well as in the lower and upper part of the Zarga Formation in Unity-9 and Talih-2 wells (Fig. 4.17). This sequence unit also characterizes the lower part of the Aradeiba Formation in Toma-1 and Nabag-1 wells. Some lacustrine sequences occur in the strata near the middle part of the Aradeiba Formation in Heglig-2 well. Furthermore, the lacustrine sequence unit characterizes the middle part of the Zarga Formation in Heglig-2 and Nabag-1 wells as well as the upper part of the Zarga Formation in Toma-1 well (Fig. 4.16). The thickness of the lacustrine sequences in the Aradeiba and Zarga Formations in the studied wells of the Unity Field are $24 - 60$ m and $30 - 90$ m respectively (Tables 4.2). On the other

hand, the thickness of this sequence in the Aradeiba and Zarga Formations in the studied wells of the Heglig Field are 12 – 133 m and 18 – 121 m respectively (Table 4.3). The deposits of this lacustrine sequence unit resulted from sediment-laden rivers, which deposited fine laminated sediments (rhythmites) in the centres of the lakes by dilute density currents and by settling out of clays from suspension. Moreover, during the flood seasons these distributary channels aggraded or meandered resulting in a deposition of thin sheets of sand bodies within the lakes (Sturm, 1979). The rhythmites represent the source rock in the study area.

### 4.4.4  Deltaic-dominated Sequences Unit

One long and one short type of coarsening-upward deltaic sequence are found in the studied intervals. These sequences occur near the middle and near the upper part of the Aradeiba Formation in Unity-9 well, in the middle part and near the upper part of the Aradeiba Formation in Talih-2 well, in the lower part of the Zarga Formation in Unity-9 well as well as in the lower and middle part of the Zarga Formation in Talih-2 well (Fig. 4.17). Moreover, this sequence unit characterizes the middle part and the strata near the upper horizons of the Aradeiba Formation in Toma-1 well, the top of the Aradeiba Formation in Heglig-2 well and the top horizons of the Zarga Formation in Heglig-2 and Nabag-1 wells (Fig 4.16). The deltaic sequence thickness ranges between 21 – 67 m in the Aradeiba Formation and between 18 – 30 m in the Zarga Formation in the studied wells of the Unity Field (Table 4.2). However, the thickness of the deltaic sequences in the Aradeiba and Zarga Formations in Heglig Field ranges between 24 – 72 m and 12 – 61 m respectively (Table 4.3). The thick deltaic sequences of the study area were formed due to the direct drain of rivers into the lakes, whereas the thin deltaic sequences were formed due to the break of the fluvial channels to their banks by crevassing (Coleman and Prior 1982; Gawthorpe and Colella 1990), thus small coarsening-upward sequences of clay and silt grading into sand formed in the area (Figs 4.4, 4.5 and 4.8). The delta fronts were areas of progradation. Deposition on the mouth and distal bars resulted in lakeward building of these delta fronts so that coarser sediments of the mouth bar came to overlie finer sediments of the distal bar and prodelta. The delta mouth bar sandstones provide some important oil reservoirs in the study area.
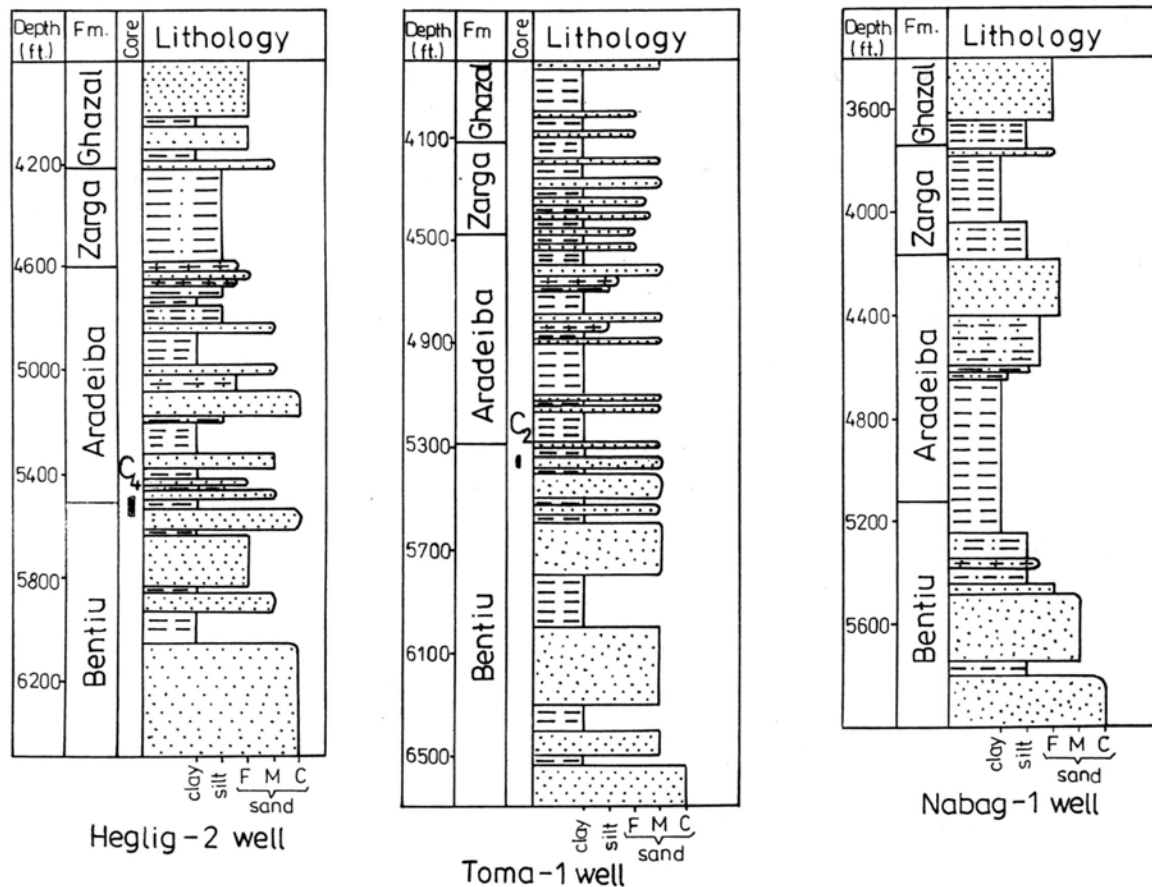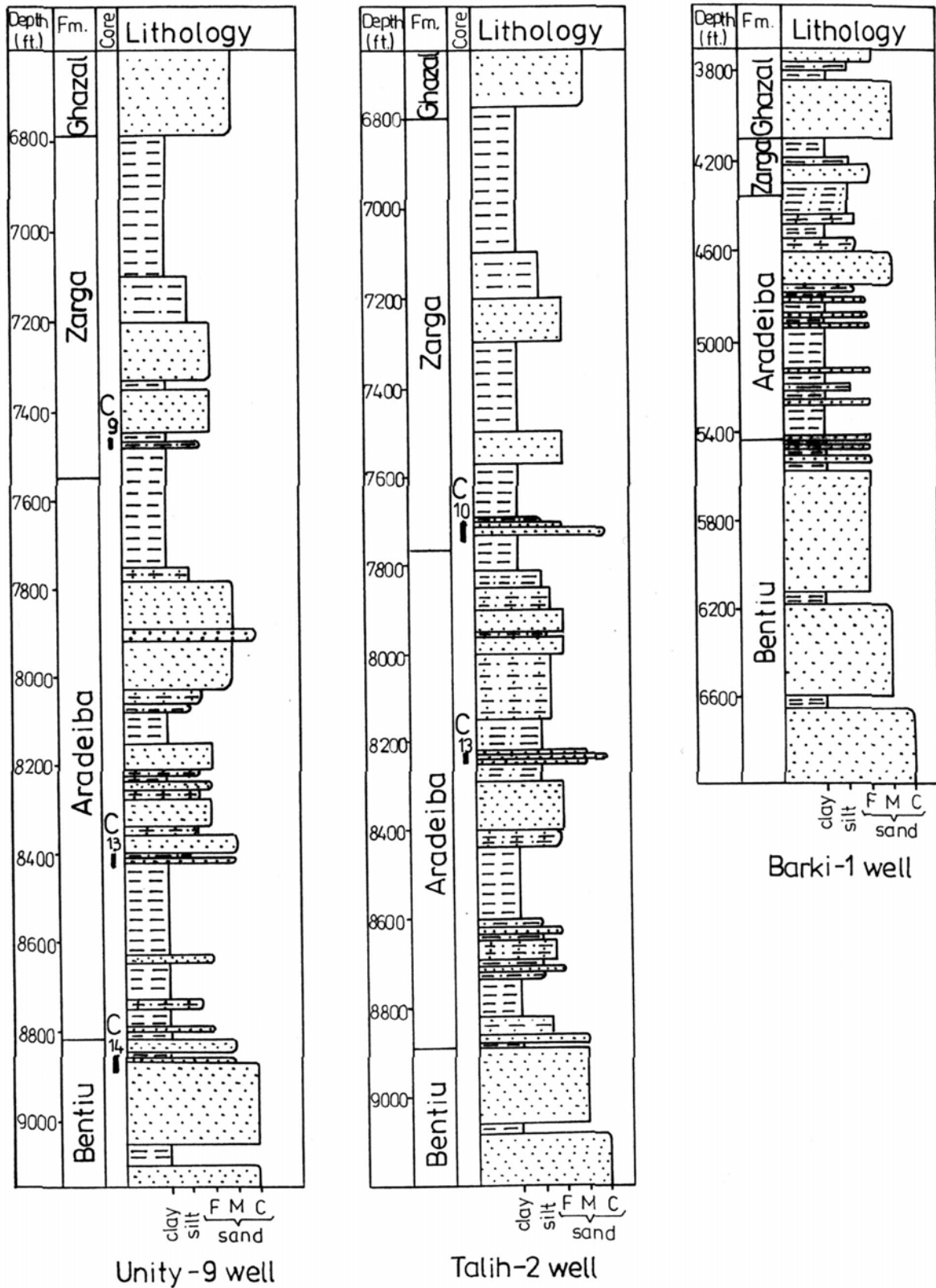
**Figure 4.16: Lateral correlation of Bentiu, Aradeiba and Zarga Formations in wells Heglig-2, Toma-1 and Nabag-1 in the Heglig Field, SE Muglad Basin (based on wire line logs, cores and cutting samples).**

## 4.5 Seismic Analysis and Interpretation

The seismic data gn 98-010, sd 81-013 and sd 82-202 (Figs. 4.18, 4.20 & 4.22) were used in this study in stratigraphic applications to give some lateral extended facies interpretation of the study area. Moreover, these seismically defined units contain some essential depositional and structural information.

Furthermore, this analysis revealed that the maximum thickness of the sediment in the southern part of the Heglig Field and in the Unity Field is about 2550 m and 3190 m respectively, whereas the sediment thickness in the NE part of the Heglig Field reaches about 2500 m (Figs 4.19, 4.21 & 4.23). Generally, the thickness of sediments in the study area increases in the western flank towards the Kaikang Trough (Fig. 1.2), which represents the deepest sub-basin of the Muglad Rift Basin. Therefore, the maximum thickness of the burial sediment in the NW part of the Heglig Field reaches about 6000 m (Fig. 4.23). The first sediment cycle started during the first rifting phase (Early Cretaceous) by the deposition of the Sharaf and Abu Gabra Formations, which consist mainly of lacustrine mudstones. The first sediment cycle ended with the deposition of the Late Albian to Cenomanian Bentiu

Formation. This cycle is bounded at the top by an erosional unconformity. However, the lower strata of this cycle, which are Sharaf and Abu Gabra Formations, do neither exist in the southern part of the Heglig Field nor in the Unity Field (Figs. 4. 18 – 4.23). On the other hand, the second sediment cycle formed during the Turonian – Late Senonian second rifting phase by the deposition of the Darfur Group. Aradeiba and Zarga Formations represent the basalstrata of the Darfur Group, whereas Ghazal and Baraka Formations represent the upper strata of the group. This second sediment cycle ended by the deposition of the Amal Formation. However, the members of this cycle are only differentiated in the Unity Field and in the central and southern areas of the Heglig Field (Figs. 4.18, 4.19, 4.20 & 4.21). Moreover, the Kordofan Group, which forms the third sediment cycle, was deposited unconformably on the top of the Amal Formation during and after the Late Eocene – Oligocene third rifting phase and consists of Nayil, Tendi, Adok and Zeraf Formations (Figs. 4.18 – 4.23).

**Figure 4.17: Lateral correlation of Bentiu, Aradeiba and Zarga Formations in wells Unity-9, Talih-2 and Barki-1 in the Unity Field, SE Muglad Basin (based on wire line logs, cores and cutting samples).**

The main styles of seismic facies reflection patterns that could be recognized within the three seismically defined units are: parallel and subparallel reflection patterns, divergent reflection patterns and hummocky clinoform patterns (Miall 1984; Emery and Myers 1996). The parallel and subparallel reflections patterns, which indicate uniform rates of deposition could be clearly noted in the Amal, Nayil, Tendi and Adok Formations in the Unity Field, as well as in the Amal and Nayil Formations in the Heglig Field (Figs. 4.18 & 4.20). The divergent reflection pattern, which resulted from the differential subsidence rates in the half-graben SE Muglad Basin could be noted generally in the stratigraphic unit of the seismic line gn 98-010, which extends from the NE of the study area and runs across the Heglig Field to Kaikang Trough in the West of the study area (Fig. 4.22). The hummocky clinoform pattern, which is a pattern of prograding reflection, indicates small clinoform lobes of a delta, that had undergone distributary switching. This type of reflection pattern can be noted in the Aradeiba, Zarga, Ghazal and Baraka Formations in the Unity Field (Fig. 4.18). Moreover, this reflection pattern of progradational delta was confirmed by the dominant coarsing upward funnel shape pattern behaviour of the gamma-ray and the spontaneous potential wire line logs of the above mentioned strata in unity-9 well (Figs. 4.11, 4.15 & 4. 17).

The interpreted seismic sections of lines sd 81-013 and gn 98-010, which trend NE-SW across the study area indicate several structural oil traps related to faults (Figs. 4.21 and 4.23). The interpreted seismic line sd 82-202, which trends NW-SE and runs parallel to the major fault planes shows very few structural oil traps (Fig. 4.19).

## 4.6 Facies Controls

The studied fluvial, deltaic and lacustrine facies were controlled by autocyclic and allocyclic processes. Autocyclic mechanisms are those which result in the natural redistribution of energy within a depositional system, whereas allocyclic mechanisms are those, in which the change in a sedimentary system is generated by some external cause (Miall 1984; Reading and Levell 1996). Changes in base level, subsidence rate and sediment supply are claimed as the main factors that influence the evolution of any basin (Anadon et al., 1991). Climate provides another fundamental control (Frostick and Reid, 1989). Anadon et al. (1991) attributed changes in lake levels to:

(a) Changes in basin geometry caused by variations in the relative subsidence and sedimentation rates. The resulting variations in the basin volume would change the water and sediment capacities.

(a) Variations in water balance caused by climatic change (i.e evaporation/precipitation balance) and/or by watershed modification (i.e by river diversion owing to the evolution of the surrounding drainage network through blockage, avulsion or stream capture).

## 4.7 Allocyclic Controls

### 4.7.1 Tectonic Influences

The lacustrine system of the Muglad Basin evolved in response to active rift tectonics that had occurred during Late Jurassic to Early Cretaceous time. The early lacustrine and fluvial deposits in the SE Muglad Basin record the onset of differential tectonic subsidence along the basin-bounding faults. As a result of varation in tectonic and subsidence intensity of the different sub-basinal areas, the lacustrine and the fluvial facies vary across the Muglad Basin. The occurrence of a thick lacustrine section in the Kaikang sub-basin is due to the greater subsidence (Figs. 1.2 & 4.23). Tectonics appear to have played also an important role on facies type, distribution and architectural styles of the fluvial system. This because the structural developments caused rifting and controlled the topography on the flanks and the adjacent land masses. Consequently, this affected the river drainage pattern, channel sinuosity, lateral migration, avulsion and facies distribution (Maill 1988; Frostick and Reid 1989). Moreover, a more extensive development of a lacustrine facies could be related to lakes with higher gradient (bench-type) margins as shown in figure 4.23. In contrast, lakes with low gradient (ramp-type) margins as in the NW Muglad Basin are commonly dominated by marginal lake facies (Mohammed, 1997). The rate of subsidence and the lake morphology appear to represent controls on hydrocarbon source rocks potential. The areal extent of the anoxic lacustrine zones were controlled by the relationship between oxic oscillations and the gradient of the lake bottom. This suggests that deep and anoxic lacustrine condition have prevailed generally in the SE Muglad Basin. Within the framework of the Muglad Basin Complex, the subsidence rate is relatively slow in the Unity Field and in the southern part of the Heglig field compared to the subsidence rate in the Kaikang and NW Muglad sub-basinal areas (Mohamed et al., 2002). The slow rate of subsidence in the Unity Field and in the

southern part of the Heglig Field resulted in the deposition of a well differentiated Darfur Group (Figs 4.18 – 4.21) in contrast to a poorly differentiated Darfur Group in the northern part of the Heglig Field (Figs. 4.22 & 4.23), Kaikang Trough and NW Muglad Basin. As a result of the syntectonic sedimentation adjustment, a nearly continuous deposition of anoxic and oxic lacustrine sediments linked to a permanent existing deep lacustrine depositional setting took place in the SE Muglad Basin, where rather narrow and high gradient marginal zones developed (Fig. 4.23). In contrast, oxic facies occurred in the NW Muglad Basin, which is characterized by a terrigenous-dominated lacustrine facies (Abdullatif 1992; Bakr, 1995).

## 4.7.2  Palaeoclimatic Factor

Apart from the above mentioned major deepening trend of the lake system, which is mainly controlled by tectonism, small-scale fluctuations of the lake level also exerted a strong influence on the basin fill development. These palaeoclimate oscillations resulted in small-scale cyclical transgressive-regressive sequences. However, it is not possible to neglect the control of tectonic subsidence and sedimentation rates on the previous mentioned units. Moreover, the palaeoclimatic setting and the sedimentological features of the three different sequences units suggest the possible influence of water balance changes on the basin fill evolution.

A warm, subtropical to tropical climatic regime was well established in the Central and Southern Sudan rift basins by Early Cretaceous to Early Tertiary (Abdullatif 1992; Ahmed 1996). The palynological and macrophyte fossil remains recorded in these basins agree with this fact (Omer 1983; Kaska 1989; Awad and Schrank 1990). Such a climate would have favoured thermal stratification of the water column in the lake. Lithofacies association within the fluvial, the lacustrine and the deltaic units indicate periods of low discharge and/or low water stages of fluctuations influences on the system and the base level in lakes. This probably testifies to seasonal dry and wet climatic conditions. In addition, the palaeoclimatic changes (i.e. from rainy to dry conditions) caused changes in four principal factors: lake level, the chemistry of lake water, position of the shoreline as well as the amount and quality of sediment supplied.

The presence of fresh water flora and fauna (Kaska, 1989) and the lack of a significant amount of evaporite sediments suggest that the Muglad Basin was an open lake with an outlet and so characterized by relatively stable shoreline and limited residence time for solutes.

However, in the Blue Nile and the White Nile Rift Basins loss by evaporation and infiltration exceeded the inflow plus the precipitation, which allowed high ionic concentrations to develop with consequent chemical evaporites (Abdullatif 1992; Awad 1994; Bakr 1995). Therefore, palaeoclimatic and tectonic factors must have favoured the development of a closed lake system in the Blue and the White Nile Rift Basins. Good source rock accumulation in the Muglad Basin seems to have been associated with deep anoxic fresh to mildly brackish lake water that was permanently stratified under a relative humid warm climate with minimal seasonal contrasts. Moreover, the dense vegetation must have been reduced the clastic sediment supply but enhanced the accumulation of organic matter relative to the clastic content of the lake sediments. Furthermore, the intense chemical weathering during the warm humid climate produced a large supply of dissolved nutrients, which promoted high rate of primary productivity (Talbot, 1988) within the sub-basinal lakes of the Muglad Basin.

## 4.8 Autocyclic Controls

The autocyclic controls, that affected the sedimentary facies of the Muglad Basin in general were of various kinds: fluvial effects (discharge and channel processes), sediment supply and lake currents. In the near shore zone, currents were strong and were directed parallel to the shoreline, whereas in the deep lacustrine zone currents tend to be weaker and lacking a preferred direction. As a result the coarse-grained sediments were generally concentrated at the margins of the lakes, meanwhile the fine-grained sediments were concentrated in the centres of the lakes.

**Figure 4.18: Interpreted seismic section of line sd 82-202 (see Figure 4.2 for location).**
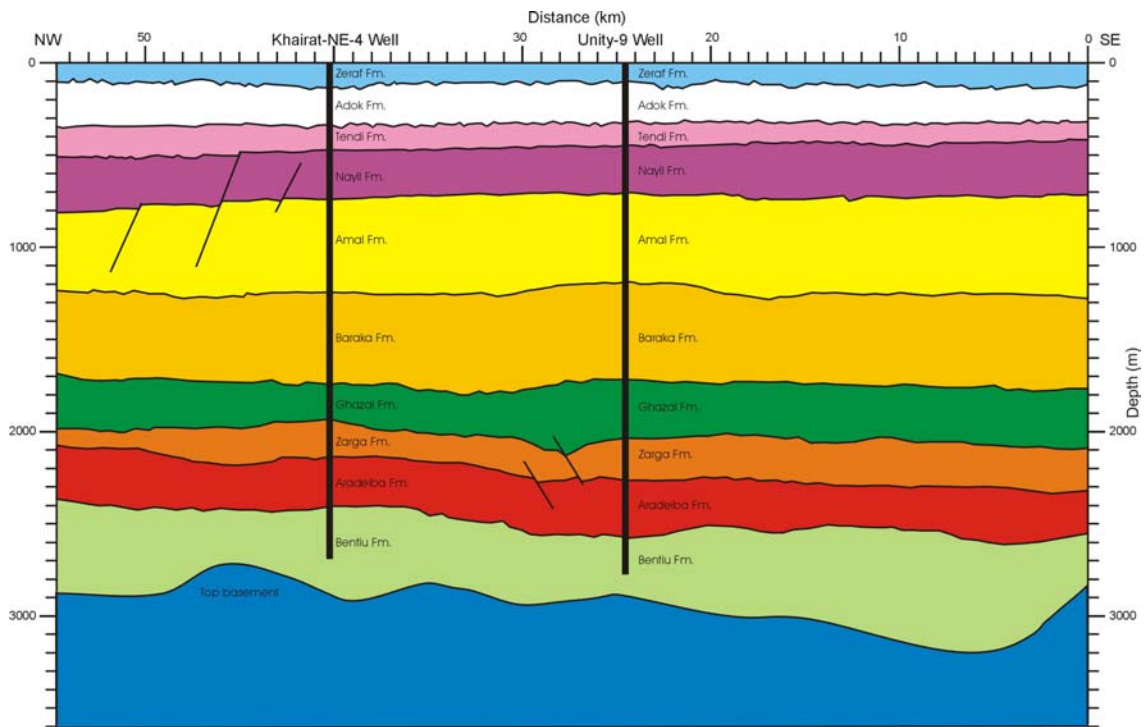


**Figure 4.19: Cross section constructed from the interpretation of seismic line sd 82-202 (Fig. 4.18).**

Un.=unconformity.
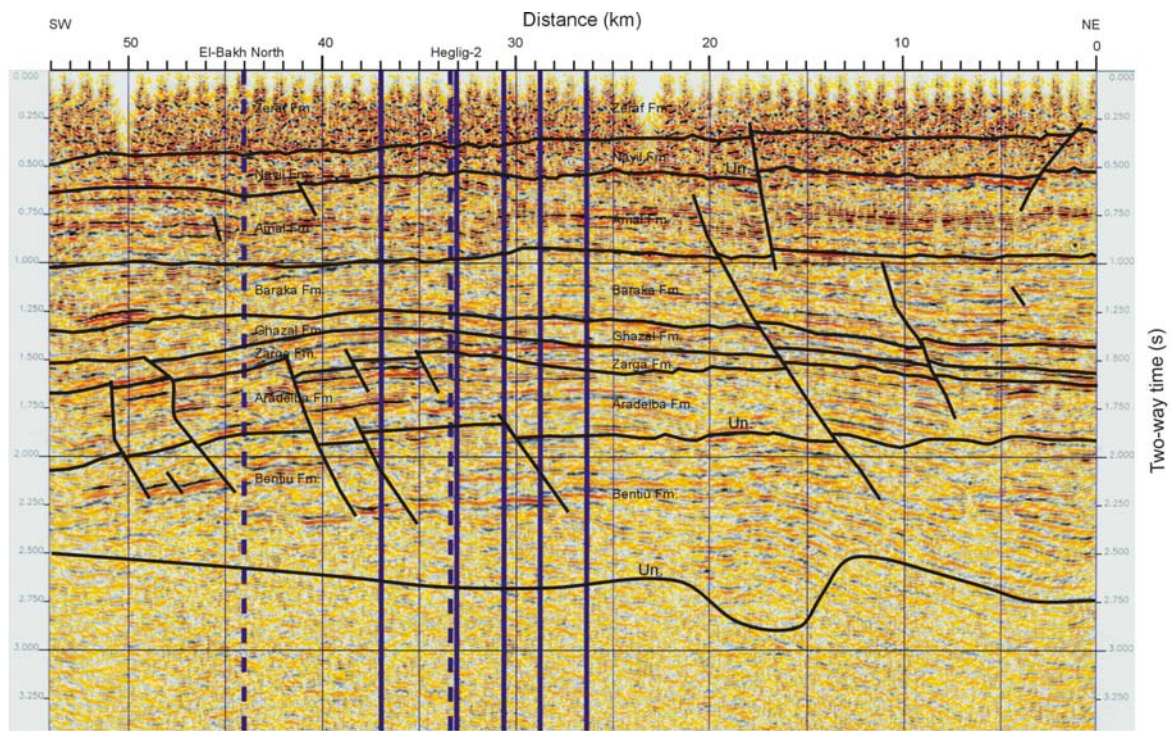
**Figure 4.20: Interpreted seismic section of line sd 81-013 (see Fig. 1.2 for location).**
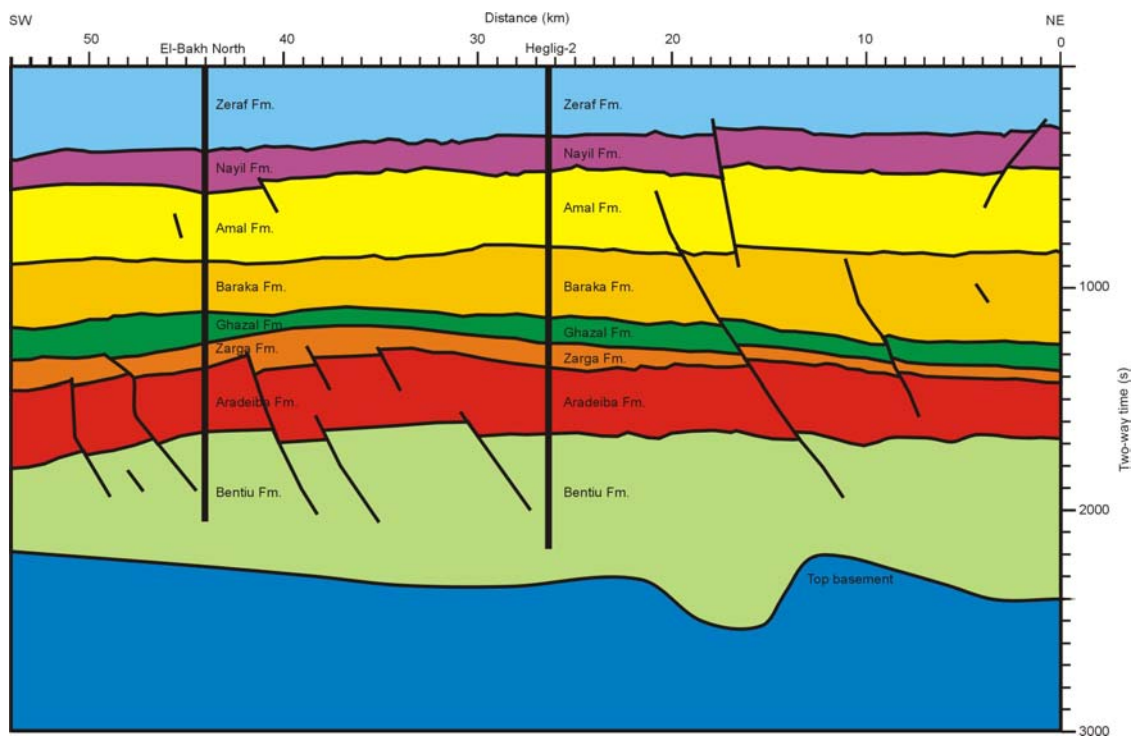


**Figure 4.21: Cross section constructed from the interpretation of seismic line sd 81-013 (Fig. 4.20).**
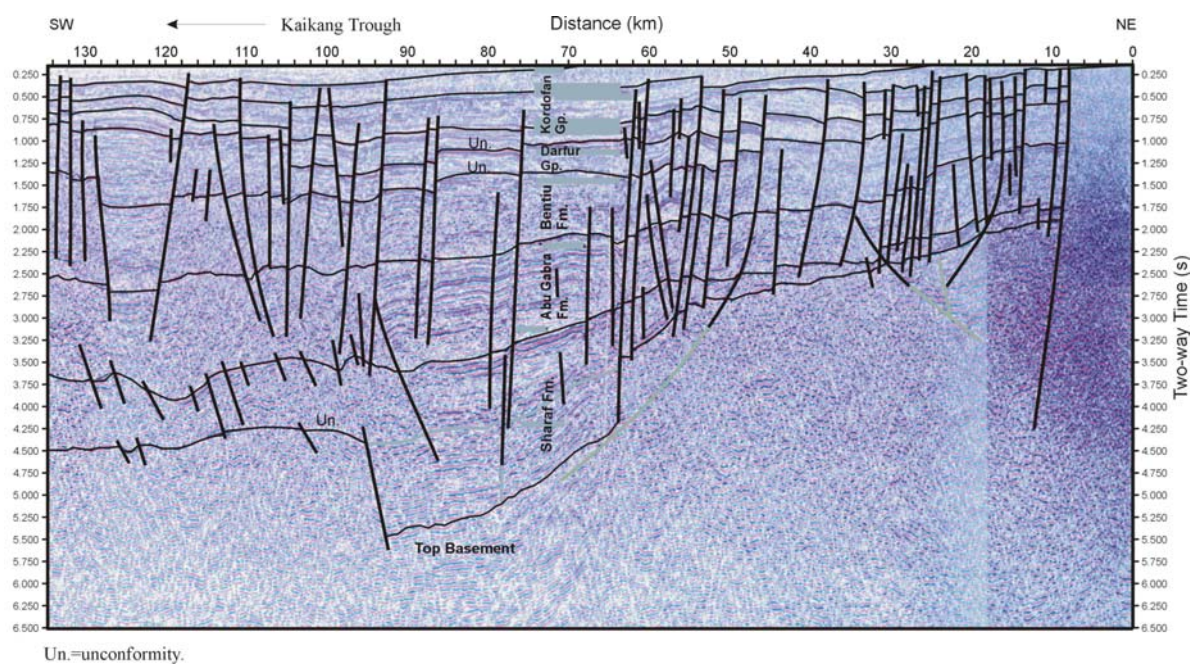
**Figure 4.22: Interpreted seismic section of line gn 98-010 (see Fig. 1.2 for location).**
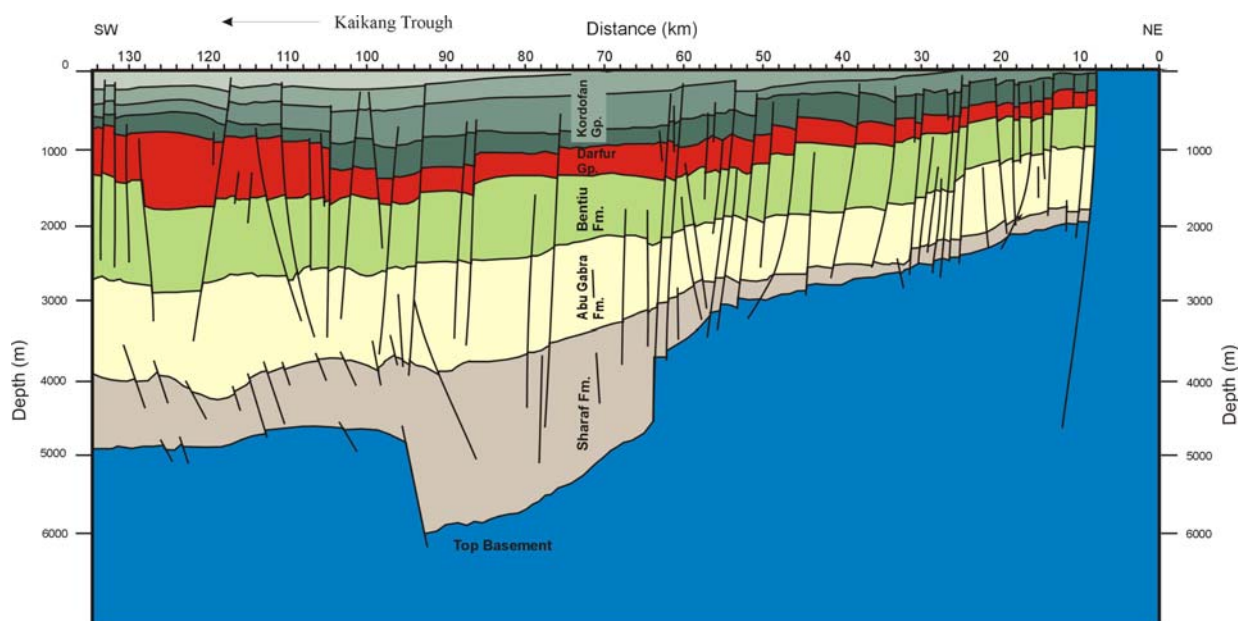


**Figure 4.23: Cross section constructed from interpretation of seismic line gn 98-010 (Fig. 4.22).**

# Plate 4.1 (for cores from the Bentiu Formation)



Photo. (a) Shows part of the Core 14 from Bentiu Formation, Unity-9 Well in the Unity Field.
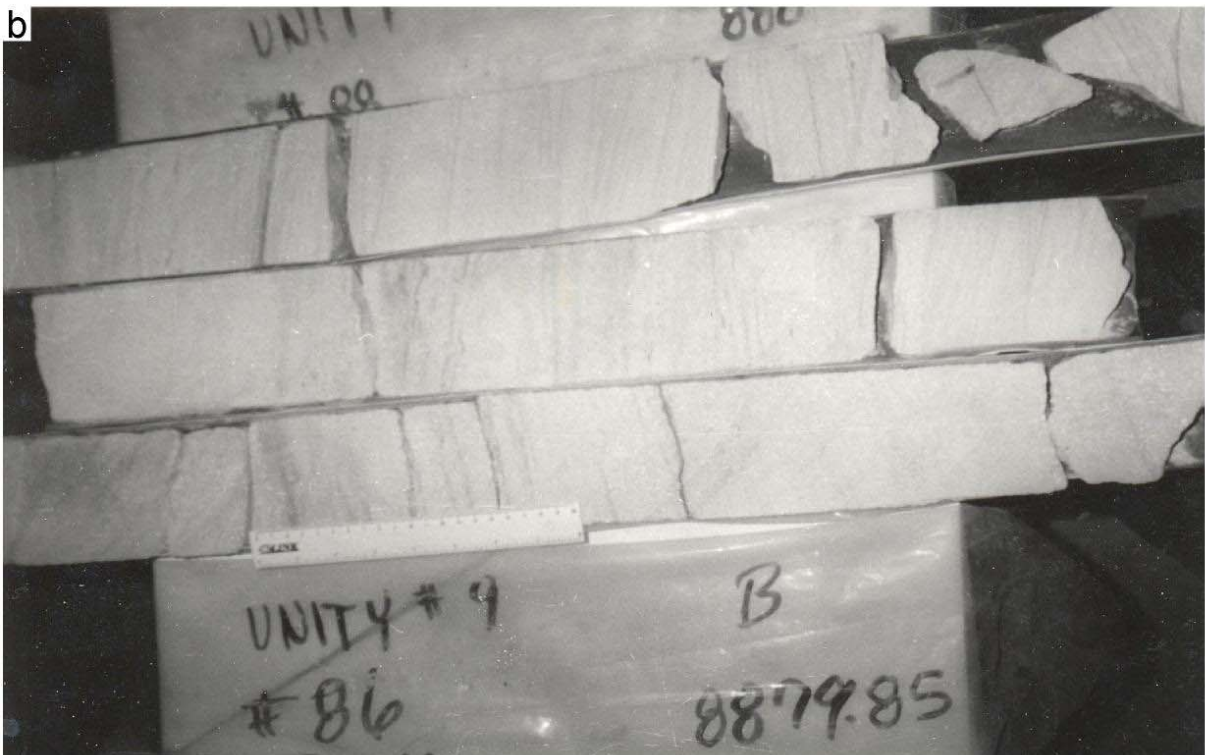


Photo. (b) Shows part of the Core 14 from Bentiu Formation, Unity-9 well in the Unity Field.

# Plate 4.1 cont.
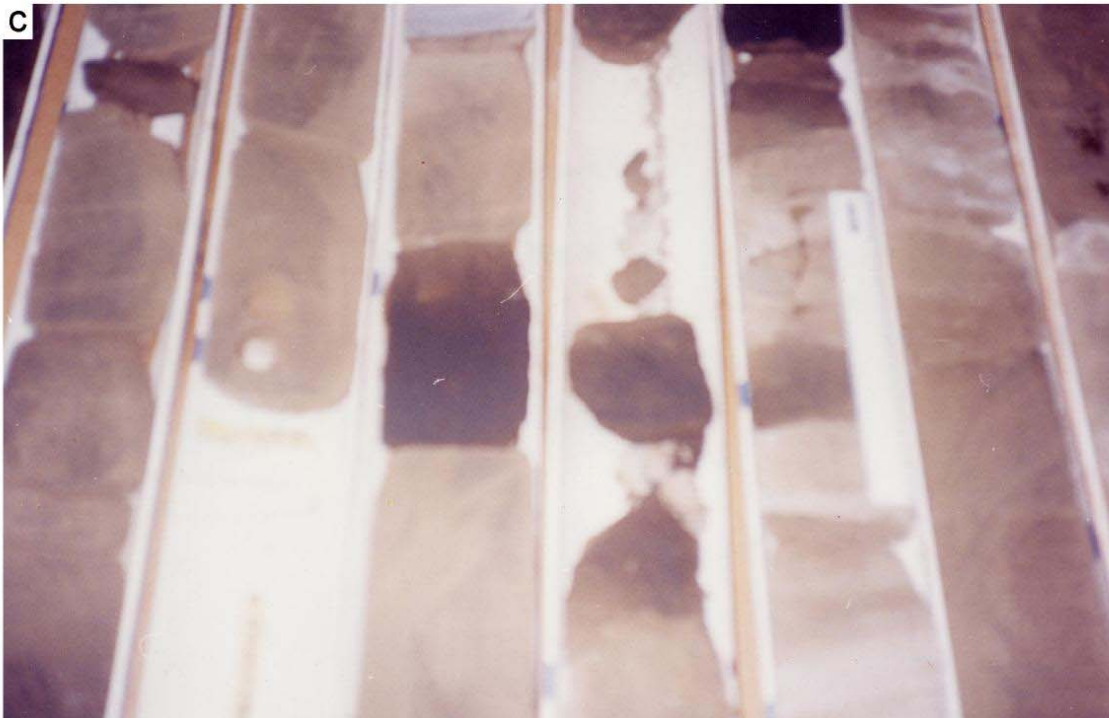


Photo. (c) Shows part of the Core 2 from Bentiu Formation, Toma.1 well in the Heglig Field.



Photo. (d) Shows part of the Core 4 from Bentiu Formation, Heglig-2 well in the Heglig Field.

# Plate 4.2 (for cores from the Aradeiba Formation)
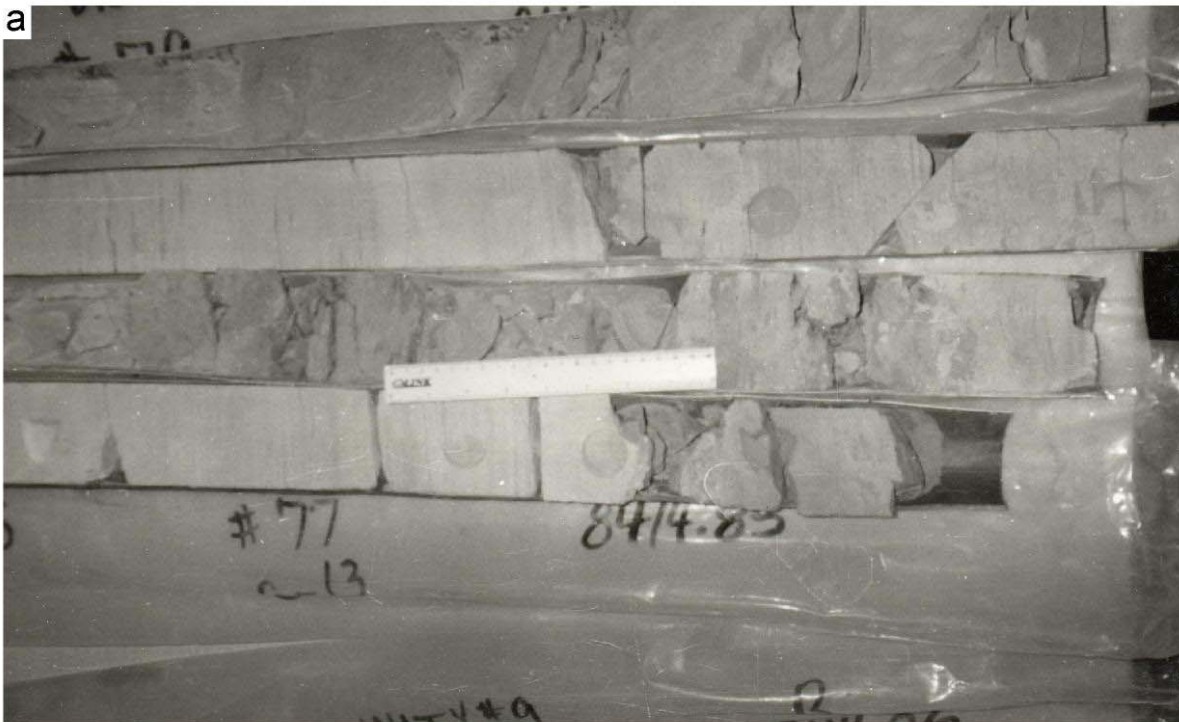


Photo. (a) Shows part of Core 13 from the Aradeiba Formation, Unity-9 well in Unity Field.
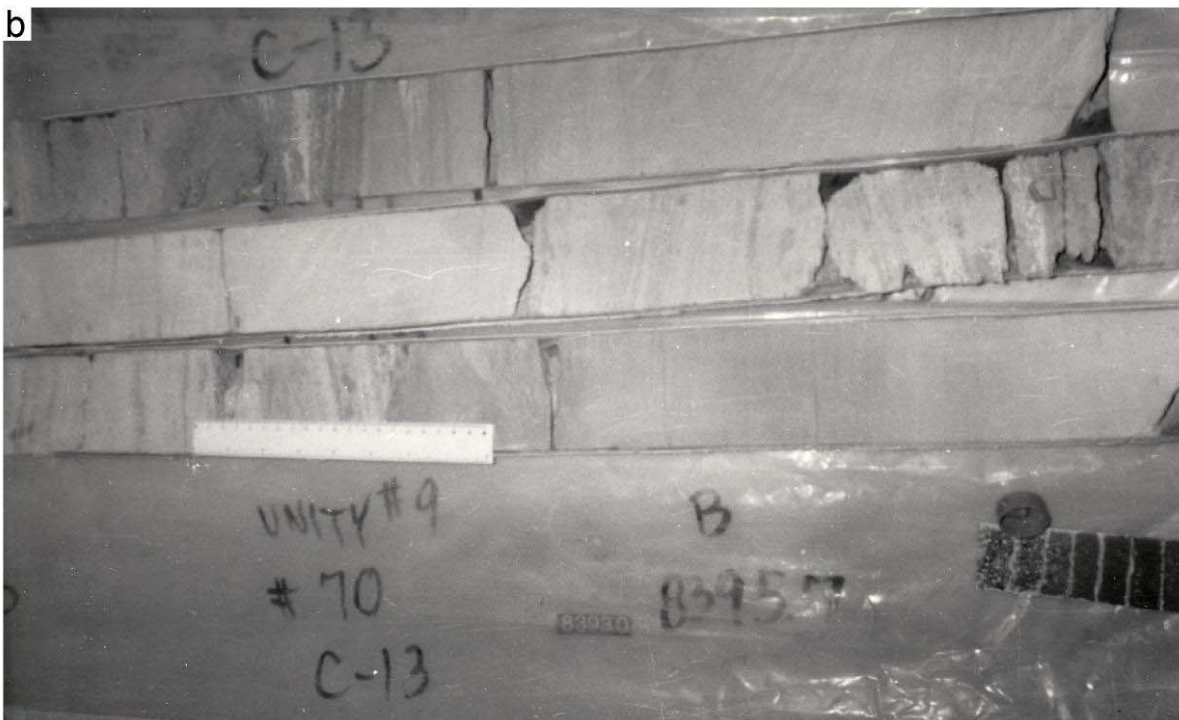


Photo. (b) Shows part of Core 13 from the Aradeiba Formation, Unity-9 well in Unity Field.

# Plate 4.2 cont.



Photo. (c) Shows part of Core 13 from the Aradeiba Formation, Talih-2 well in Unity Field.



Photo. (d) Shows part of Core 4 from the Aradeiba Formation, Heglig-2 well in Heglig Field.

# Plate 4.3 (for cores from the Zarqa Formation)



Photo. (a) Shows part of Core 9 from the Zarga Formation, Unity-9 well in Unity Field.



Photo. (b) Shows part of Core 10 from the Zarga Formation, Talih-2 well in Unity Field.



Photo. (c) Shows part of Core 10 from the Zarga Formation, Talih-2 well in Unity Field.

# 5 Sandstone Petrography

## 5.1 Introduction

Sandstone types and compositions are useful indicators for the source rock origin, depositional environments, diagenesis and tectonic setting. This part of the study deals with the petrography of the sandstones of Bentiu, Arabdeiba and Zarga Formations. It´s main objective is to determine the mineralogical composition and to classify the sandstone types to get information about their source areas, depositional environments, palaeoclimate, diagenetic processes and to infer the tectonic history of the study area by relate the detrital composition of the studied sandstones to the tectonic setting of it´s provenance region. Detritus from different tectonic provenances generally has a particular composition and the debris is deposited in associated sedimentary basins which occur in a limited number of plate-tectonic settings (Dickinson, 1985).

Twenty-one sandstone samples were selected from the previous seven mentioned conventional cores from Unity-9 and Talih-2 wells at Unity Field as well as from Heglig-2 and Toma-1 wells at Heglig Field. The samples were selected during the core description and lithofacies analysis for the preparation of thin sections as well as for the scanning electron microscopy (SEM) analysis.

The thin sections were studied using a polarizing microscope with different magnifications. The identification of minerals was based on their optical properties such as colour, form, relief, extinction angle, pleocroism, twining and bifringence. Ribbon traverses were drawn on the slides to facilitate the counting of the minerals for quantitative estimation of the minerals percentages in each slide.

## 5.2 Mineralogical Description

The composition of the sandstone depends mainly on the nature of the source rocks and on the weathering processes. The minerals and components which were recognized in the thin sections include: quartz, feldspar, micas (mainly biotite and muscovite), carbonates, iron oxides, and rock fragments.

### 5.2.1 Quartz

The most common mineral in the studied sandstones is quartz. It appears in thin sections as relatively clear colourless grains having a weak bifringence and a low refractive index that is only slightly higher than that of the mounting medium (Kerr, 1977; Adams et al., 1995). Both polycrystalline quartz (Qp) and monocrystalline quartz (Qm) are present. Some of the polycrystalline and monocrystalline quartz crystals exhibit undulose extinction. Moreover, some of the composite quartz grains (polycrystalline quartz grains) are elongated and within some of them, the crystals boundaries are sutured. Many of the quartz grains incorporate mineral inclusions such as rutile, zircon, iron oxides and tourmaline. Fractured quartz grains are also common (Plates 5.1, 5.2 & 5.3). The studied sandstones have high percentages of quartz ranging between 50 – 60% (Tables 5.1, 5.2 and 5.3).

In all of the examined samples, polycrystalline quartz, occurs in higher percentages than monocrystalline quartz (Tables 5.1, 5.2 & 5.3 and Plates; 5.1, 5.2 & 5.3). These high rations of polycrystalline to monocrystalline quartz suggest a metamorphic source region (Basu et al., 1975). However, the studied sandstones of Unity Field in Unity-9 and Talih-2 wells (Tables 5.1, 5.2 and 5.3), have lower percentages of polycrystalline quartz than the examined samples of the Heglig Field in Heglig-2 and Toma-1 wells (Tables 5.1 and 5.2). The monocrystalline quartz grains in the sandstones of Heglig Field are subangular to subrounded and are poorly to moderately sorted whereas, in the sandstones of Unity Field, the monocrystalline quartz grains are subrounded to rounded and are moderately to well sorted (Plates 5.1, 5.2 & 5.3). This could be attributed to longer distance of transport and to a relative prolonged abrasion of the Unity Field sediments.

### 5.2.2 Feldspar

Like quartz, feldspars in thin sections are typically clear, colourless and show low bifringence, but they can be distinguished from quartz by their cleavage, twining and refractive indices. Nevertheless, distinguishing between untwinned orthoclase and quartz can be difficult. However, feldspar grains may sometimes be partly decomposed, and then they appear cloudy or turbid in contrast to quartz grains, which are invariable unaltered and relatively clear (Adams et al., 1995).

Of the different types of feldspar, the potash feldspar (Fk), orthoclase (Or), and microcline (Mi) (Plates 5.1, 5.2 & 5.3) are much more common in the studied sandstones of

the two fields than the plagioclases (Pl) (Tables 5.1, 5.2 & 5.3). There are two reasons for this: K-feldspar has a greater chemical stability than plagioclase (Tucker, 1991), and so the latter is altered preferentially in the source area. In addition, K-feldspar is much more common in continental basement rocks (acid gneisses) (Tucker, 1991), which are probably the provenance of many sandstones in the study area. However, the percentages of the sodic plagioclase (e.g. albite) are increased in the deeper horizons of the Bentiu Formation and in the lower strata of Aradeiba Formation (Tables 5.1 & 5.2 and Plates 5.1 & 5.2). This increase of plagioclase in the deeper horizons could be due to albitization of the detrital plagioclases and K-feldspars. Moreover, the amount of the potasic and sodic feldspars is greater in the studied sandstones of Heglig Field wells (Heglig-2 and Toma-1), than in the studied sandstones of Unity Field wells, (Unity-9 and Talih-2) (Tables 5.1, 5.2 & 5.3). This could be attributed to the relatively shorter distance of transportation of the Heglig Field sediments.

### 5.2.3  Micas

Biotite (Bi) and muscovite (Mu) were identified by their platey shape and parallel extinction. Biotite has a brown – green pleochroism, which masks the interference colours whereas, muscovite is colourless in the plane-polarized light, but has bright second-order colours under crossed polars (Kerr, 1977). They were observed with rather low concentrations in most of the investigated samples. The highest percentage of biotite (4%) was recorded at Aradeiba Formation in Talih-2 well, whereas that of muscovite (3%) was recorded at Aradeiba Formation in Unity-9 well (Table 5.2 & Plate 5.2 ). Biotite occurs as large detrital flakes (Plate 5.2 e,f), which are concentrated along partings, laminae and bedding planes. This distribution is primarily a function of sorting and is determined largely by the hydraulic behavior of the mica flakes (Tucker, 1991).

### 5.2.4  Rock Fragments

Only minor amounts of rock fragments were observed in the studied samples (Tables 5.1, 5.2 & 5.3). These rock fragments include shale, mudstone and siltstone.

### 5.2.5  Carbonates

Siderite and calcite (Ca) were observed as patchy cements in most of the examined samples of the two fields (Plates 5.1, 5.2 and 5.3), with a concentration ranging between 1 – 13 % (Tables 5.1, 5.2 and 5.3). Both siderite and calcite can be identified by their perfect

rhombohedral cleavage and a pearl grey or white interference colour of higher order. Calcite is colourless, but it is often cloudy, usually anhedral, whereas siderite resembles calcite, but may often be distinguished by the brown stain around the borders of the grains and along cleavage cracks (Plate 5.3) (Kerr, 1977). The highest amount of carbonates (8 %) was observed at Zarga Formation in Unity-9 and Talih-2 wells (Table 5.3 & Plate 5.3).

### 5.2.6 Iron Oxides

Iron oxides are not wide spread in the examined samples, but they were recorded as a minor cementing material. Their percentages do not exceed 3.8 %. The maximum amount was found in the Aradeiba Formation in Unity-9 well (Table 5.2 & Plate 5.2 g,h).

### 5.2.7 Porosity

Porosity is a characteristic feature of sedimentary rocks, and is a measure of pore space percentage (Tucker, 1991). The two fundamental types of porosity were observed in the investigated samples. The primary porosity developed as the sediment was deposited and includes interparticle and intraparticle porosities; it constitutes the dominant type. It occurs in all of the investigated samples (Plates 5.1, 5.2 and 5.3). The secondary porosity, which was developed by diagenetic dissolution processes and during the tectonic movements that produced fractures in the rocks, represents the lesser type. The secondary porosity, which is related to the dissolution of carbonates, occurs mainly in the Bentiu and Zarga Formations (Plates 5.1 l and 5.3 d,g arrows 1), whereas that one which is due to the dissolution of the feldspars occurrs throughout the whole three formation with a minor amount (Plates 5.1 g,i,l, 5.2 b,d,f,h,j and 5.3 b,e arrow 2). In the examined samples, both of the two pore types have been stained with brown coloured Canada Balsam, and have been counted. The calculated porosity is found to range between 16.3 – 30 % (Tables 5.1, 5.2 and 5.3). The primary porosity in sandstones is principally interparticle porosity, dependent on the textural maturity of the sediment, controlled largely by depositional processes and environments, and to a lesser extent by compositional maturity. Permeability, which is the ability of a sediment to transmit fluids, depends on the effective porosity, the shape and size of the pores and pore interconnections (throats) and on the properties of the fluid itself (Tucker, 1991).Table (5.3): The petrographic point counting results of samples from the Zarga Formation in Unity-9 and Talih-2 wells.

**Table 5.1: The petrographic point counting results of samples from the Bentiu Formation in Heglig-2, unity-9 and Toma-1 wells.**

| Well Name | Core No. | Sample Depth (ft.) | Quartz | | Feldspars | | | Micas | | Cements | | Other Components | | Matrix % | Porosity % |
| --- | --- | --- | --- | --- | --- | --- | --- | --- | --- | --- | --- | --- | --- | --- | --- |
| | | | Monocrystalline % | Polycrystalline % | Orthoklase % | Plagioklase % | Microcline % | Muscovite % | Biotite % | Carbonates % | Iron Oxides % | Amphiboles % | Zircon / Rutile % | | |
| Toma-1 | 2 | 5313.0 | 24.2 | 31.0 | 6.0 | 3.5 | 4.5 | 1.6 | * | 2.7 | 1.3 | * | * | 2.0 | 23.2 |
| | 2 | 5322.0 | 28.0 | 30.7 | 6.0 | 3.8 | 4.3 | 0.2 | * | 2.9 | 2.0 | 0.4 | * | 5.0 | 16.7 |
| Unity-9 | 14 | 8874.0 | 25.3 | 28.1 | 4.5 | 2.6 | 3.5 | * | * | 3.5 | 1.3 | * | 0.2 | 1.0 | 30.0 |
| | 14 | 8887.0 | 26.9 | 28.3 | 4.0 | 2.8 | 3.5 | 2.0 | * | 3.0 | 2.0 | 0.3 | * | 5.0 | 22.2 |
| | 14 | 8889.0 | 27.6 | 28.2 | 3.8 | 2.8 | 3.2 | 1.0 | * | 6.0 | 1.3 | * | * | 6.0 | 20..1 |
| Heglig-2 | 5 | 5561.8 | 27.0 | 27.0 | 6.5 | 3.0 | 4.0 | 0.5 | * | 1.2 | 1.4 | * | * | 2.0 | 22.7 |
| | 5 | 5576.0 | 19.2 | 19.2 | 6.3 | 3.0 | 4.2 | 1.4 | * | 4.8 | 2.0 | * | 0.1 | 5.0 | 20.7 |
| | 6 | 5723.0 | 19.0 | 31.4 | 6.0 | 3.5 | 4.0 | 0.3 | * | 2.0 | 1.7 | 0.7 | * | 6.0 | 25.4 |

Note :*=traces

**Table 5.2: The petrographic point counting results of samples from the Aradeiba Formation in Heglig-2, unity-9 and Toma-1 wells.**

| Well Name | Core No. | Sample Depth (ft.) | Quartz | | Feldspars | | | Micas | | Cements | | Other Components | | Matrix % | Porosity % |
| --- | --- | --- | --- | --- | --- | --- | --- | --- | --- | --- | --- | --- | --- | --- | --- |
| | | | Monocrystalline % | Polycrystalline % | Orthoklase % | Plagioklase % | Microcline % | Muscovite % | Biotite % | Carbonates % | Iron Oxides % | Amphiboles % | Zircon / Rutile % | | |
| Heglig-2 | 4 | 5512.0 | 22.4 | 32.5 | 8.0 | 2.9 | 4.9 | 1.1 | * | 1.0 | 1.0 | 0.1 | * | 5.0 | 21.1 |
| | 4 | 5520.8 | 25.0 | 30.5 | 7.8 | 2.9 | 4.7 | 0.2 | 2.0 | 2.0 | 0.5 | 0.3 | * | 5.0 | 19.4 |
| Unity-9 | 10 | 7904.6 | 22.0 | 30.0 | 5.6 | 1.6 | 3.7 | 2.0 | * | 0.0 | 3.8 | 0.1 | * | 6.0 | 25.2 |
| | 10 | 8015.0 | 25.0 | 30.0 | 5.6 | 1.8 | 3.6 | * | 1.0 | 1.0 | 2.0 | * | 0.2 | 5.0 | 24.8 |
| | 13 | 8394.0 | 27.0 | 29.0 | 5.4 | 2.0 | 2.6 | 1.0 | * | 3.0 | 0.5 | * | 0.1 | 6.0 | 23.4 |
| | 13 | 8410.1 | 28.0 | 31.0 | 5.2 | 2.0 | 2.2 | 3.0 | * | 3.0 | 1.0 | * | * | 6.0 | 18.6 |
| Talih-2 | 13 | 8231.0 | 25.0 | 27.0 | 5.7 | 2.1 | 3.9 | 1.0 | 4.0 | 0.0 | 0.8 | 0.2 | * | 5.0 | 25.3 |
| | 14 | 8634.0 | 24.0 | 28.0 | 5.5 | 2.4 | 3.8 | 2.0 | * | 2.0 | 1.0 | * | * | 6.0 | 25.3 |

Note :*=traces

**Table 5.3: The petrographic point counting results of samples from the Zarga Formation in Unity-9 and Talih-2 wells.**

| Well Name | Core No. | Sample Depth (ft.) | Quartz | | Feldspar | | | Micas | | Cements | | Other Components | | Matrix % | Porosity % |
|---|---|---|---|---|---|---|---|---|---|---|---|---|---|---|---|
| | | | Monocrystalline % | Polycrystalline % | Orthoclase % | Plagioclase % | Microcline % | Muscovite % | Biotite % | Carbonates % | Iron Oxides % | Amphiboles % | Zircon/Rutile % | | |
| Unity-9 | 8 | 7241.0 | 25.0 | 27.7 | 5.7 | 1.4 | 3.6 | 2.0 | 0.4 | 4.0 | 0.3 | * | 0.2 | 6.0 | 23.7 |
| | 9 | 7463.0 | 22.0 | 28.0 | 5.4 | 1.5 | 3.5 | * | * | 8.0 | 0.5 | * | 0.2 | 13.0 | 18.9 |
| | 9 | 7470.0 | 23.0 | 27.0 | 5.7 | 1.5 | 3.2 | * | * | 8.0 | 0.3 | * | * | 15.0 | 16.3 |
| Talih-2 | 10 | 7713.5 | 21.0 | 29.0 | 5.9 | 1.6 | 3.9 | 1.0 | * | 8.0 | * | * | * | 13.0 | 16.6 |
| | 10 | 7718.0 | 21.0 | 28.0 | 5.9 | 1.8 | 3.8 | * | * | 7.0 | * | * | * | 13.0 | 17.5 |

Note: * = traces

## 5.3  Sandstone Classifications

The scheme of Folk (1974) and Pettijohn et al. (1987) was used to classify the sandstones of this study. The triangular diagram shown in Fig. 5.1, is based on plotting the percentages of quartz, feldspar and rock fragments, which were counted under the polarized microscope (Table 5.4). All of the studied samples can be classified as subarkoses.

Sandstones are generally accepted as arkoses when they contain more than 25 % feldspar, not more than 75 % quartz and less than 50 % lithic fragments (Folk, 1974). In the studied samples, the feldspar percent is between 13.5 – 22 %. Whereas, that of the quartz and the lithic fragments are ranging between 75.7 – 85.2 % and 0.0 – 7.3 % respectively (Table 5.4). Consequently the sandstones are classified as subarkose (Folk, 1974). Besides quartz and feldspar, detrital micas are present. The feldspars are usually altered.

**Table 5.4: The percentages of quartz, feldspar and all other rock fragments which were used in the sandstones classification.**

| Well Name | Formation | Sample Depth (ft) | Total Quartz (Qt %) | Monocrystalline Quartz (Qm %) | Polycrystalline Quartz (Qp %) | Feldspar (%) | All other rock frag– ments (%) |
|---|---|---|---|---|---|---|---|
| Unity-9 | Zarga | 7241.0 | 80.80 | 37.99 | 42.09 | 16.26 | 3.64 |
| | | 7463.0 | 85.16 | 41.00 | 44.16 | 14.82 | 0.00 |
| | | 7470.0 | 81.96 | 37.70 | 44.26 | 18.03 | 0.00 |
| | Aradeiba | 7904.6 | 79.48 | 34.97 | 44.51 | 17.32 | 3.17 |
| | | 8015.0 | 81.80 | 37.87 | 43.93 | 16.66 | 1.51 |
| | | 8394.0 | 83.07 | 40.00 | 43.07 | 15.38 | 1.53 |
| | | 8410.0 | 82.12 | 40.34 | 41.78 | 13.54 | 4.32 |
| | Bentiu | 8874.0 | 83.43 | 39.53 | 43.90 | 16.56 | 0.00 |
| | | 8887.0 | 81.77 | 39.85 | 41.92 | 15.25 | 2.96 |
| | | 8889.0 | 83.78 | 41.44 | 42.34 | 14.71 | 1.50 |
| Talih-2 | Zarga | 7713.5 | 80.74 | 35.71 | 45.03 | 17.70 | 1.55 |
| | | 7718.0 | 81.60 | 35.20 | 46.40 | 18.40 | 0.00 |
| | Aradeiba | 8231.0 | 75.69 | 36.39 | 39.30 | 17.03 | 7.27 |
| | | 8634.0 | 79.13 | 36.52 | 42.61 | 17.80 | 3.04 |
| Heglig-2 | Aradeiba | 5512.0 | 76.45 | 31.19 | 45.26 | 22.00 | 1.53 |
| | | 5520.8 | 75.82 | 34.34 | 41.48 | 21.15 | 3.02 |
| | Bentiu | 5561.8 | 80.73 | 37.13 | 43.60 | 18.56 | 0.68 |
| | | 5576.0 | 77.88 | 28.48 | 49.40 | 20.02 | 2.07 |
| | | 5723.0 | 78.49 | 29.90 | 48.59 | 21.02 | 0.46 |
| Toma-1 | Bentiu | 5313.0 | 77.96 | 34.18 | 43.78 | 19.77 | 2.25 |
| | | 5322.0 | 80.40 | 38.35 | 42.05 | 19.81 | 0.27 |

## 5.4 Interpretation and Discussion

### 5.4.1 Tectonic Setting

Based on the modal analysis of the sandstones, the percentages of the different grains were plotted on a triangular diagram, which was used to interpret their provenance. A triangular plot of QmFLt takes into account the monocrystalline quartz grains, the feldspars and the lithic fragments was drawn. This diagram, which was drawn after Dickinson et al. (1985) and Tucker (1991) is very useful in discriminating sandstones from major tectonic settings. However, the results are affected by those amounts of the feldspar and of the lithic fragments, which had been reduced by diagenetic processes.

The plots of Fig. 5.2 revealed, that these sandstones were derived mainly from a transitional provenance in the continental block, between the stable interior of the craton and the basement uplift provenance, which is an area of relatively high relief basement along rifts. This enables the detrital constituents to be recycled and transported for a relatively long distance and to be deposited in a rift or a pull-apart basin.
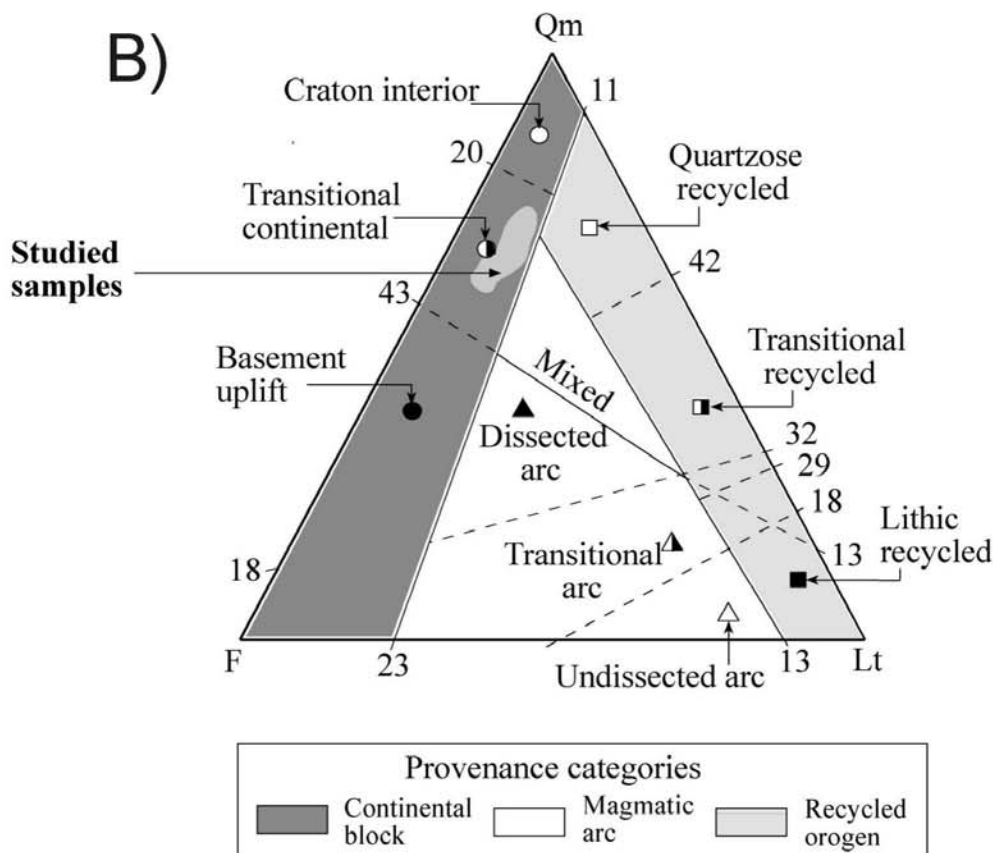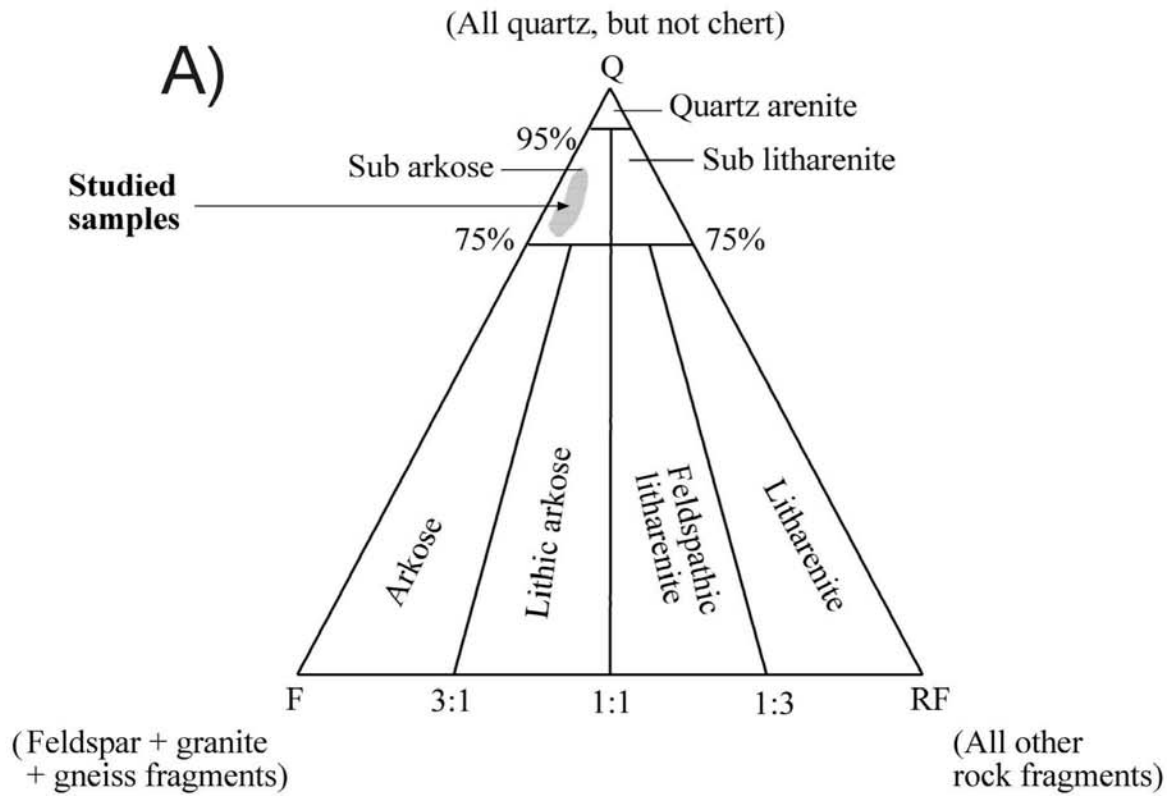
Figure 5.1: A) Classification of sandstones in the study area (after Folk, 1974; Pettijohn et al., 1987). B)The tectonic setting of the studied sandstones (after Dickinson, 1985; Tucker, 1991).

## 5.4.2 Diagenesis

The key points that should be considered in analysing diagenetic changes in sandstones are depositional environment, temperature gradient (burial depth), composition of the sandstone source rock, composition of the original interstitial fluid, and time (Blatt et al., 1980; Tang et al., 1997).

The increase in the temperature that accompanies the burial of sediments affects not only the organic constituents, but also the inorganic ones. The maximum recorded temperature in Unity-9 well was 219° F/103° C at 9095 ft/2772 m depth with a temperature gradient of 1.49° F/100 ft or 27.1° C/1000 m. The maximum recorded temperature in Talih-2 well was 204° F/96° C at 9251 ft/2820 m depth with a temperature gradient of 1.47° F/100 ft or 26.9° C/1000 m. Moreover, the maximum recorded temperature in Heglig-2 well was 190° F/88° C at 7084 ft/2159 m depth with a temperature gradient of 1.48° F/100 ft or 27° C/1000 m. The maximum recorded temperature in Toma-1 well was 192° F/89° C at 8824 ft/2689 m depth with a temperature gradient of 1.35° F/100 ft or 24.9° C/ 1000 m. The fundamental effect of increased temperature is the change in the solubility of the substances as temperature and pore fluid-pH change (Tucker, 1991). In the study area, carbonate precipitation has been brought about by an increase in the pH and/or temperature. Probably the decomposition of the plagioclase supplied the pore water with $Ca^{2+}$ ions. Whereas, the organic-matter degradation increased the $HCO_3^-$ ion concentration in the pore water. The carbonate mineral content reaches 8 % in Zarga Formation at Unity-9 and Talih-2 wells (Table 5.3). The relative low porosity of Bentiu and Aradeiba Formations in Unity-9 well at depths of 8889 ft and 8410 ft respectively and also of Zarga Formation in Unity-9 well at a depth of 7470 ft as well as in Talih-2 well at depths of 7713 ft and 7718 ft could be due to the carbonate precipitation (Tables 5.1, 5.2 & 5.3 and Plates 5.1 l, 5.2 j & 5.3 b,d,h).

Ahmed (1983) and Ahmed (1993) noted that carbonate cementation had reduced the porosity up to 10 % in the Abu Gabra Formation in NW Muglad Basin.

Quartz overgrowth, which is one of the most common types of silica cement, is not widely spread in the examined samples. However, it was noted during the examination with the polarized microscope as well as during the examination with the scanning electron microscope at Bentiu and Aradeiba Formations in Heglig-2 well at depths of 5562 ft. and 5512 ft respectively as well as at Bentiu Formation in Toma-1 well at depths of 5322 ft. and 5313 ft . Silica cement was partially precipitated around the detrital quartz grains and in

optical continuity, so that the grain and cement extinguish together under crossed polarizers. In a few cases, the shape of the grains are delineated by a thin iron oxide – clay coating between the overgrowth and the grain (a "dust-line") (Plates 5.1 d,f,j; 5.2 d and 5.3 f, arrow 3) but in many cases the boundary between the grain and the overgrowth can not be discriminated with the plane polarized light microscope. The scanning electron microscope investigation also reveals detrital quartz grains partially rimmed with authigenic quartz overgrowths. The authigenic quartz forms discontinous rims of small rhombic quartz crystals or druses around the detrital quartz grains (Plate 5.4 a, arrow 3). This growth of the druses was eventually inhibited by the formation of clay mats which covered many of the quartz nucleation sites reducing quartz development. However, at gaps in the clay coatings, some quartz continued to develop, forming large euhedral overgrowths (Plate 5.4 a, arrow 4). The origin of the silica cementation could be attributed to pressure dissolution. Dissolution of silica dust and feldspars would provide silica, as would the transformation of montmorillonite to illite (Tucker, 1991). Silicification was already reported during the description of the conventional cores. One important positive feature, that arises from the quartz cementation of sandstones, is that they are then able to withstand better the effects of compaction and pressure dissolution during later burial (Tucker, 1991).

In many of the studied samples, some of the feldspars have altered to clay minerals (Plate 7.1 f), whereas in other samples, e.g. in the Zarga Formation in Unity-9 well, they have been replaced by carbonate (Plate 5.3 f, arrow 5). In the deeper strata as in the Bentiu Formation and in the lower part of Aradeiba Formation, authigenic albite overgrowths do grow on detrital K-feldspars and plagioclase grains (Plate 5.4 b,c,d arrows 6). For authigenic albitization of detrital K-feldspars and plagioclase, alkaline pore waters rich in $Na^+$, $Al^{3+}$ and $Si^{4+}$ are necessary. The required ions probably come from the breakdown of smectite to illite (Boles, 1982; Saigal et al., 1988; Milliken, 1989).

The precipitation of clay minerals in a sandstone is very significant since it can have a great effect on its permeability and porosity, and this may seriously reduce its reservoir potential (Wilson & Pittman, 1977). Clay may also filter into a sandstone, carried down by pore waters from muddy interbeds. Extensive infiltration drastically alters the texture of the sediment and decreases the original texture and compositional maturity (Walker et al., 1978). The SEM analysis reveals, that an authigenic precipitation of clay minerals has occurred within the studied samples. Kaolinite is the most common authigenic clay in the sandstones of

Aradeiba and Zarga Formations, whereas illite and mixed-layer illite/montmorillonite are the most dominant authigenic clays in the sandstones of Bentiu Formation (Plates 5.4 e, 7.1 c,d and 7.2 c,d) The authigenic clay minerals occur as pore-filling cements and as clay rims around the grains (Plates 5.4 e, 7.1 d, 7.2 c,d, 7.3 c,d). The attenuation and absence of rims near and at grain contacts demonstrates their diagenetic origin as seen under the plane polarized microscope (Plates 5.1, 5.2, 5.3).

As mentioned before, secondary porosity is intensively developed in the Zarga Formation at Unity-9 and Talih-2 wells as well as in the Bentiu Formation at Unity-9 well. This secondary porosity was developed as a result of dissolution of carbonate or calcite. The dissolution of feldspars and other unstable grains may lead also to secondary porosity, but is not as significant as that caused by calcite dissolution. Moreover, the late dissolution of the carbonate and of the labile detrital grains may also be related to the release of fluids from the oil shale interbeds when thermal maturity was reached (Surdam et al., 1985). However, the dissolution and the authigenic precipitation processes, which affect the secondary porosity are intermittent processes alternating each other and depend mainly on the pore water chemistry and/or temperature (Tucker, 1991).

### 5.4.3  Reservoir Quality

Data concerning the distribution of porosity in the wells generally shows a predictable continuous decrease with depth but actually this gradual decrease changes in some of the deeper horizons and is locally reversed. This progressive reduction is due to the diagenetic processes, which include: mechanical compaction factors (grain slippage and crushing of the ductile grains), quartz overgrowths, precipitation of cements (siderite, calcite and iron oxides), precipitation of intergranular clays (mainly illite and kaolinite) and feldspar overgrowths. In general, Bentiu and Aradeiba Formations have higher porosity than Zarga Formation. The porosity of the Bentiu and Aradeiba Formations ranges between 16.7 – 30 % and 18.6 – 25.3 % respectively, whereas the porosity of the Zarga Formation ranges between 16.3 – 23.7 % . The sandstones of the Bentiu and Aradeiba Formations are mainly cemented with quartz, thus the two formations had suffered less from compaction. However, Zarga Formation sandstones contain a higher amount of phyllosilicate grains and carbonate cement, hence the formation had lost part of its porosity through the compactive deformation of the ductile grains, which was followed by the authigenic precipitation of clays within the pore spaces, which in turn reduced the porosity of this formation. On the other hand and as

mentioned before, the dissolution of the carbonates in the sandstones of the Zarga and Bentiu Formations gave rise to the development of secondary porosity (Plates 5.1 l and 5.3 d,g arrow 1). In contrast, the transformation of smectite to illite and to illite/smectite mixed-layers in the deeper horizons (Bentiu Formation and lower part of Aradeiba Formation), besides the clay infiltration and the formation of authigenic kaolinite, smectite and illite within the sandstones of the three formations, resulted in the reduction of the porosity (Plates 7.1 – 7.4).

Lastly, the reservoir quality of the study intervals was affected not only by the above mentioned diagenetic processes but also in a large-scale by the depositional evironments, which had controlled the distribution of the facies and sediment thickness within the basin as well as by the subsidence of the basin besides the structural relief variations that had happened during the initiation of the second rifting phase, which gave rise to the quick transportation and the rapid burial of the sediments. Moreover, the reservoir quality was influenced by the sandstone composition, by sedimentary textures and by grain size, as well as by clay infiltration.

For Muglad Rift Basin, Schull (1988) reported that the reservoir quality in the basin decreases with depth. He attributed this to diagenetic processes which include: compaction, quartz overgrowths as well as feldspar and clay mineral authigenesis. He noted, that the reservoir quality decreases with decreasing grain size and with increasing of feldspars amounts and lithic fragments. El Amin (1993) found that porosity decreases with depth, but with a gradient, which changes in some of the deeper strata and is locally reversed. He attributed this progressive reduction to several processes which include: mechanical factors such as grain slippage and crushing, and to diagenetic processes such as quartz overgrowth and precipitation of intergranular clay minerals such as illite and kaolinite. Hussein (1997) noted the control of the facies on the porosity and the permeability of the Bentiu Formation. Idriss (2001) found that the sandstones of the Bentiu Formation at Heglig and Unity Fields are subarkoses with some minor quartz arenites. The sandstones are very fine- to very coarse-grained with angular to well rounded and moderately to well sorted grains. These sandstones consist of polycrystalline and monocrystalline quartz, feldspar, calcite, mica, iron oxides and clay minerals. The mean porosity is 27 %. The diagenetic features which affect the sandstones, are: quartz overgrowths, clay infiltration and authigenesis, feldspar alteration and calcite cementation and dissolution. The later was thought to have had the greatest influence on the formation of secondary porosity.

# Plate 5.1 (for samples from the Bentiu Formation)
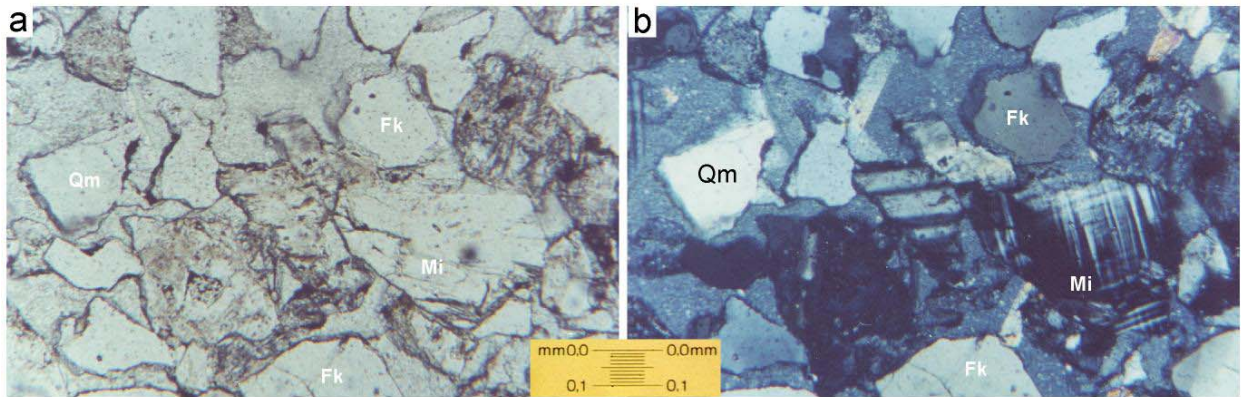


Photos. a (PPL.) and b (XNL.) Show subarkose sandstone from Core 14 in Bentiu Formation, Unity-9 well, Unity Field.
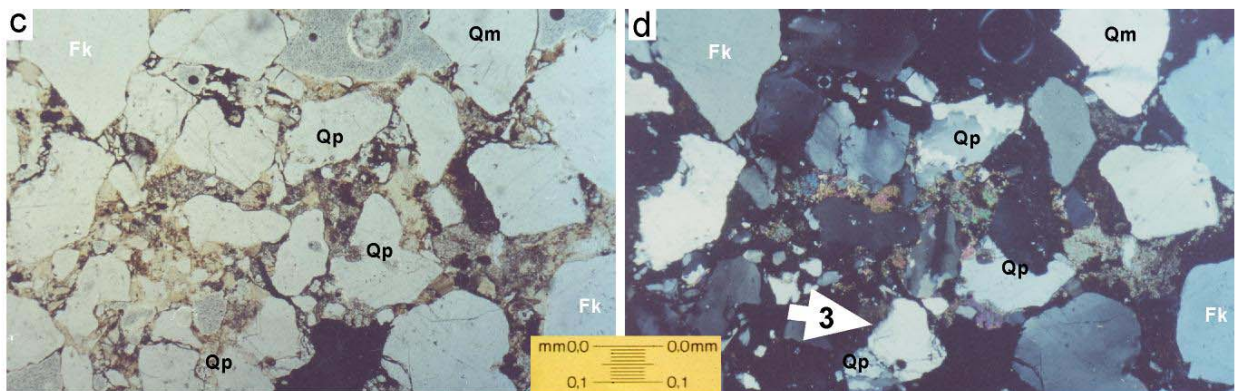


Photos. c (PPL.) and d (XNL.) Show subarkose sandstone from Core 2 in Bentiu Formation, Toma-1 well, Heglig Field.
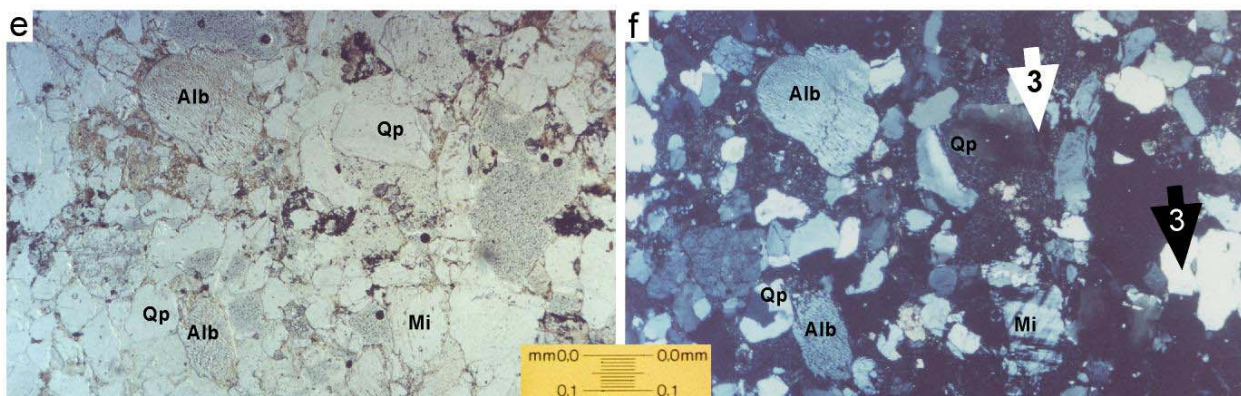


Photos. e (PPL.) and f (XNL.) Show subarkose sandstone from Core 5 in Bentiu Formation, Heglig-2 well, Heglig Field.
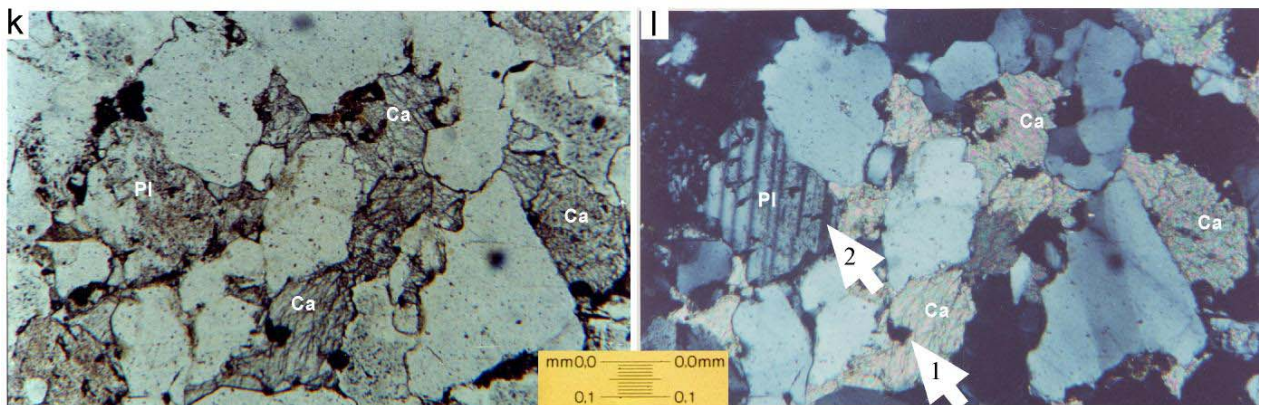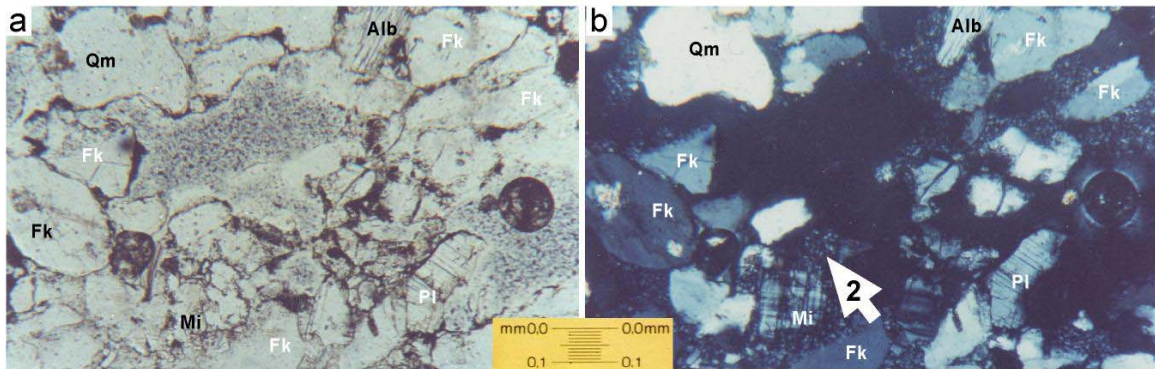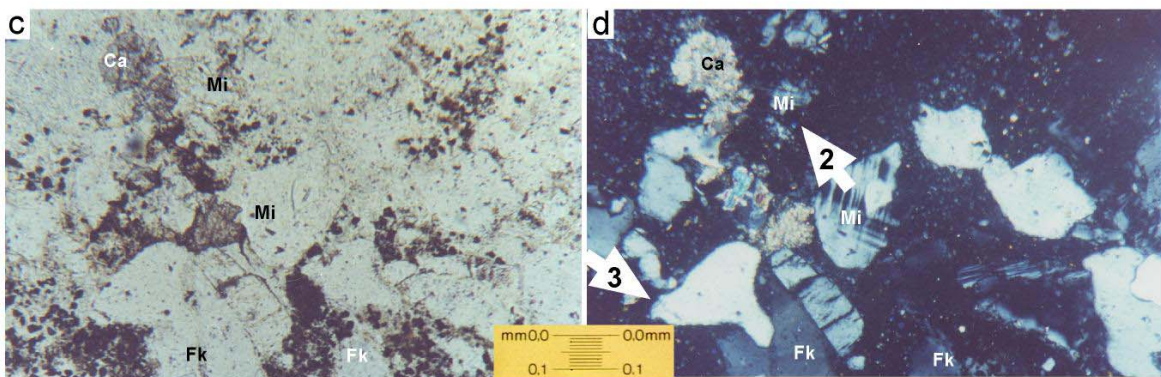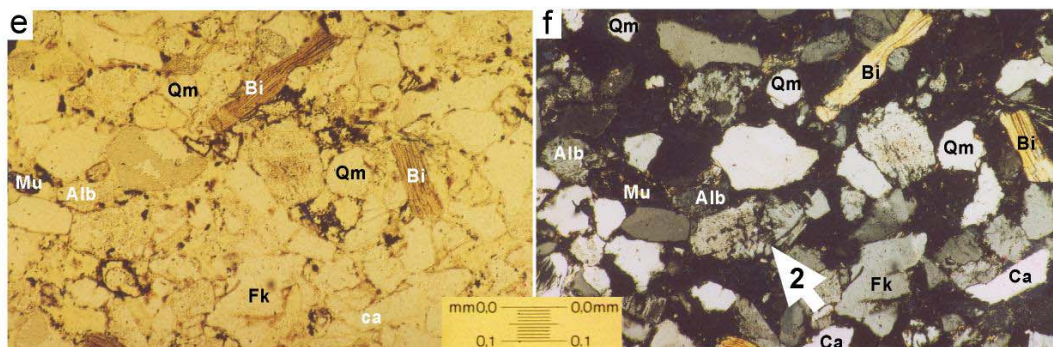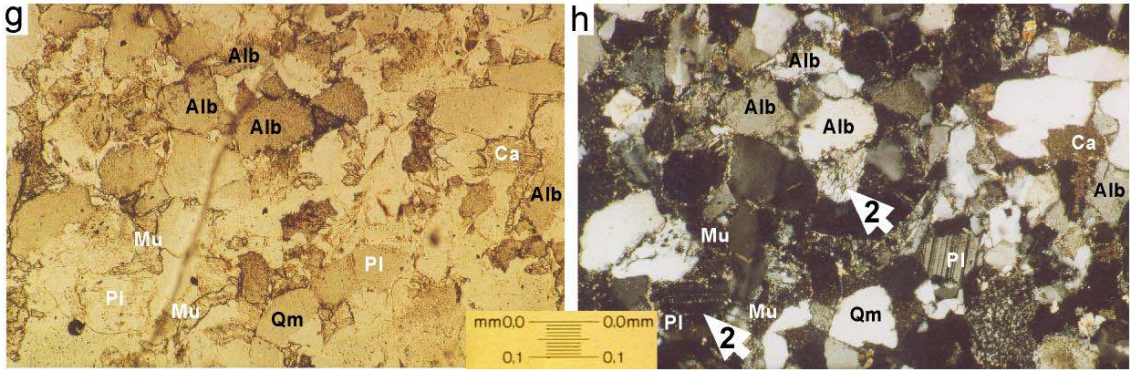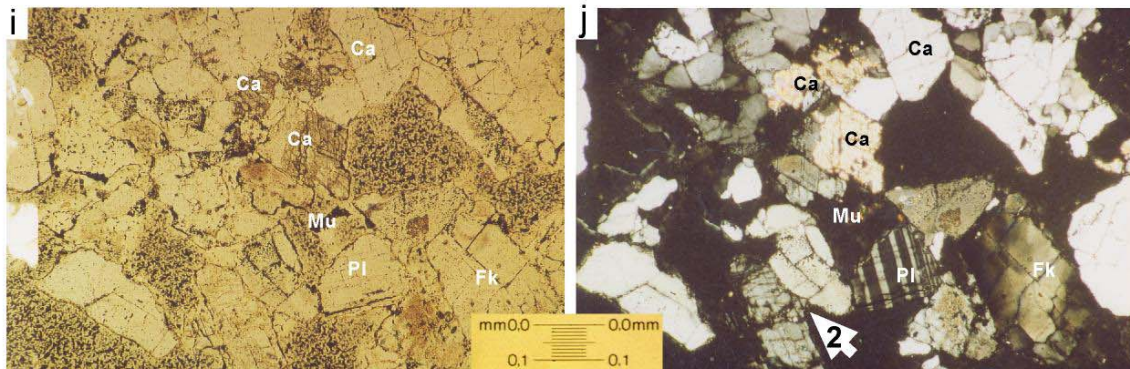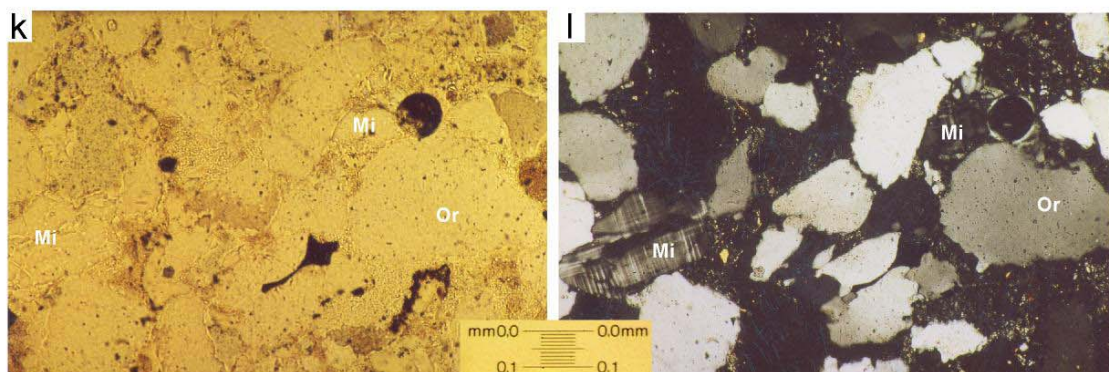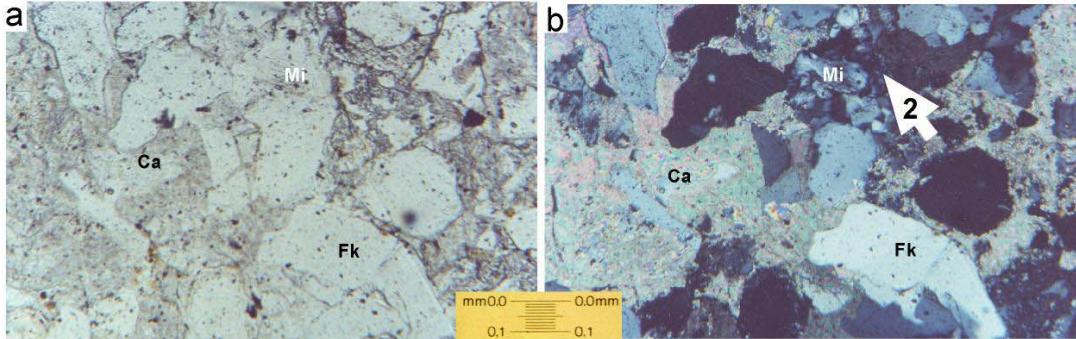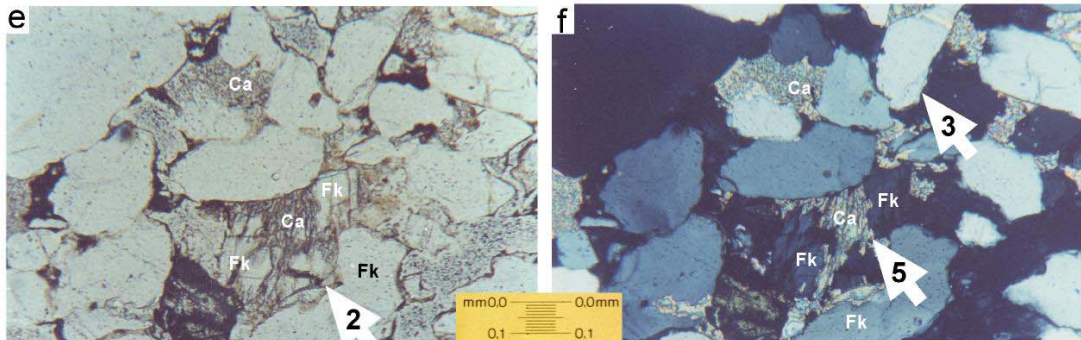
# Plate 5.1 cont.
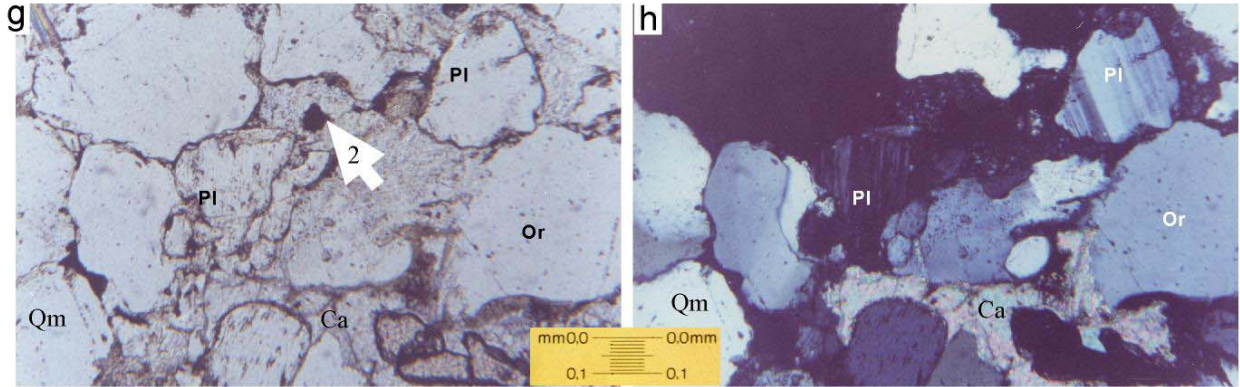
Photos. g (PPL.) and h (XNL.) Show subarkose sandstone from Core 14 in Bentiu Formation, Unity-9 well, Unity Field.
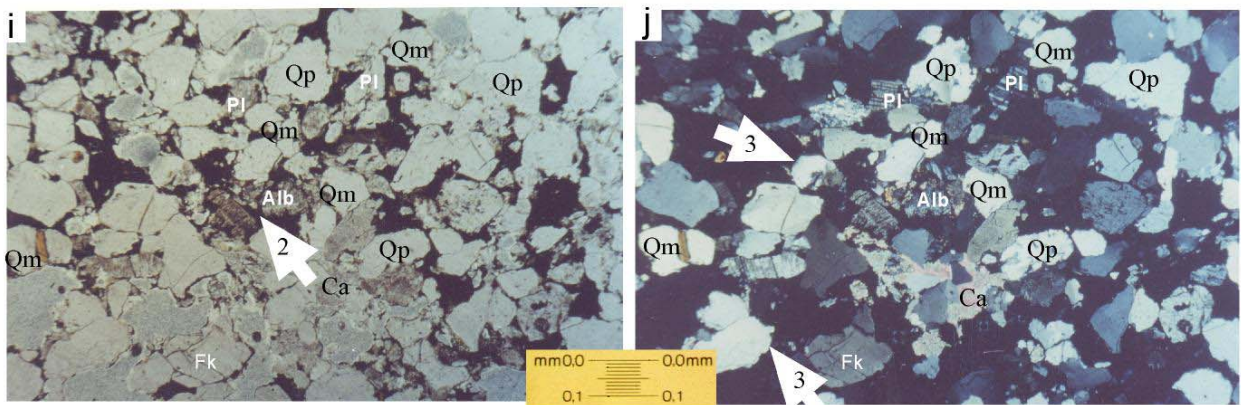


Photos. i (PPL.) and j (XNL.) Show subarkose sandstone from Core 14 in Bentiu Formation, Unity-9 well, Unity Field.



Photos. k (PPL.) and l (XNL.) Show subarkose sandstone from Core 14 in Bentiu Formation, Unity-9 well, Unity Field.

# Plate 5.2 (for samples from the Aradeiba Formation)



Photos. a (PPL.) and b (XNL.) Show subarkose sandstone from Core 4 in the Aradeiba Formation, Heglig-2 well in the Heglig Field.



Photos. c (PPL.) and d (XNL.) Show subarkose sandstone from Core 4 in the Aradeiba Formation, Heglig-2 well in the Heglig Field.



Photos. e (PPL.) and f (XNL.) Show subarkose sandstone from Core 13 in the Aradeiba Formation, Talih-2 well in the Unity Field.

# Plate 5.2 cont.



Photos. g (PPL.) and h (XNL.) Show subarkose sandstone from Core 13 in the Aradeiba Formation, Unity-9 well in the Unity Field.



Photos. i (PPL.) and j (XNL.) Show subarkose sandstone from Core 14 in the Aradeiba Formation, Talih-2 well in the Unity Field.



Photos. k (PPL.) and l (XNL.) Show subarkose sandstone from Core 13 in the Aradeiba Formation, Talih-2 well in the Unity Field.

# Plate 5.3 (for samples from the Zarga Formation)



Photos. a (PPL.) and b (XNL.) Show subarkose sandstone from Core 10 in the Zarga Formation, Talih-2 well in the Unity Field.
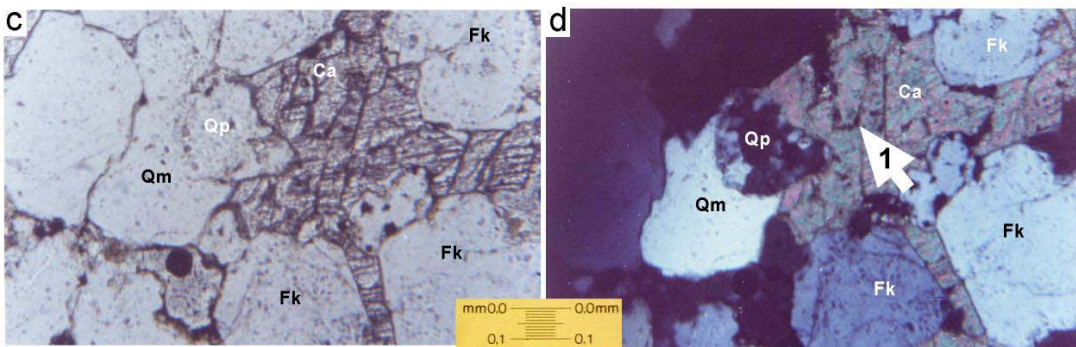


Photos. c (PPL.) and d (XNL.) Show subarkose sandstone from Core 10 in the Zarga Formation, Talih-2 well in the Unity Field.



Photos. e (PPL.) and f (XNL.) Show subarkose sandstone from Core 8 in the Zarga Formation, Unity-9 well in the Unity Field.
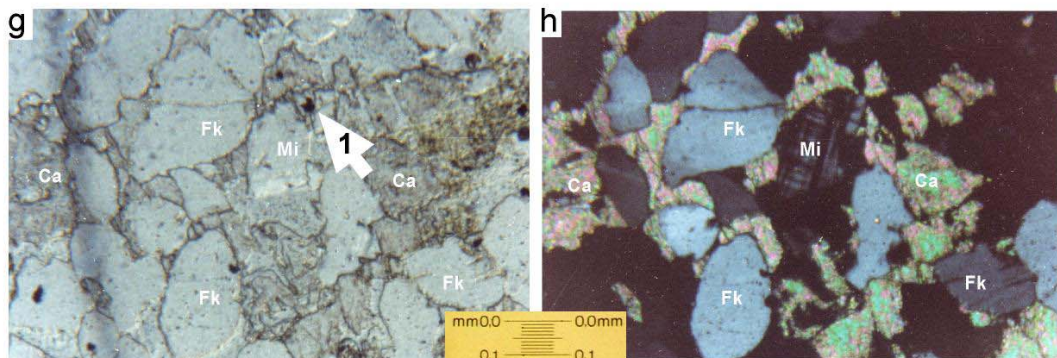


Photos. g (PPL.) and h (XNL.) Show subarkose sandstone from Core 9 in the Zarga Formation, Unity-9 well in the Unity Field.

# Plate 5.4
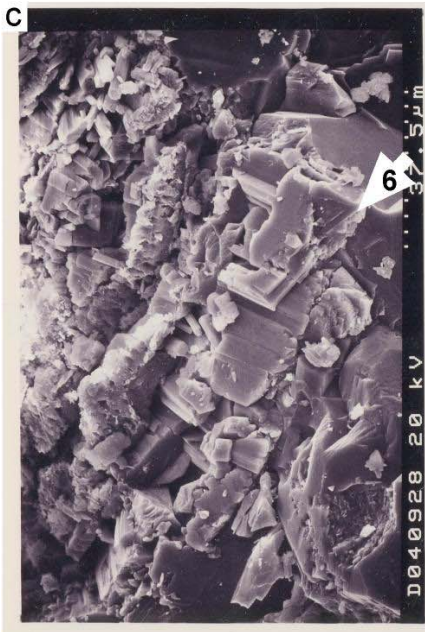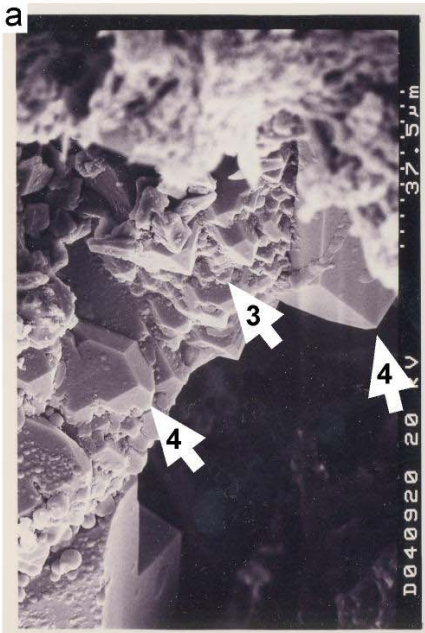
# 6 Heavy Mineral Analysis

By microscopic investigation of eighty samples from Aradeiba, the upper part of Bentiu and the lower part of Zarga Formations in the six previous mentioned wells, ten major heavy minerals (zircon, tourmaline, rutile, kyanite, staurolite, andalusite, sillimanite, epidote, garnet and hornblende) were identified and counted separately. Some heavy minerals such as glaucophane – riebeckite were also recorded, but in lesser amounts. In general the metastable heavy minerals kyanite and garnet supersede the ultrastable heavy minerals zircon, tourmaline and rutile.

## 6.1 Zircon

The ultrastable heavy mineral zircon was recorded in almost all of the examined samples. Several varieties of zircon with different forms, sizes and inclusions were noticed. Zircon is commonly colourless with a light core and a darker rim. It is distinguished from apatite by its higher relief, form and stronger bifringence (Kerr, 1977). Inclusions which were observed within the zircon grains are minute grains of tourmaline and opaque minerals, possibly graphite (Plate 6.1 a – e). The concentration of zircon ranges between 3.4 – 25 % (Appendices 1A & 1B). Zircon is dominantly subrounded to subangular, indicating a relatively far distance of transportation from the source area, as well as relatively strong reworking effects. Furthermore, the subrounded to rounded zircon grains were recorded in almost all of the analysed samples from the Unity Field (Plate 6.1 a,b,c). However, there is a small amount of similar subrounded zircon grains observed in the samples from Heglig Field, hence the dominant subangular zircon grains in the samples from the three wells of Heglig Field indicate relatively short distances of transportation and the relatively lesser recycling of the Heglig Field sediments (Plate 6.1 d,e). The highest precentage of zircon (25 %) was observed in the samples from Aradeiba Formation in Unity-9 well in the Unity Field (Fig. 6.1 & Appendix 1A). This exceptional increase in the amount of zircon could be attributed to the prolonged abrasion and/or diagenesis, which reduced the amount of the metastable and the unstable heavy mineral grains. Idiomorphic zircon grains of igneous origin were not observed in the analysed samples. Some grains of zircon from the analysed samples of the two fields show coloured concentric rings and an odd strong birefringence. These grains are most probably derived from a metamorphic source. It is therefore possible to conclude, that zircon

from the sediments of Aradeiba, the upper part of Bentiu and the lower part of Zarga Formations in the two fields is likely to have been derived from a predominantly metamorphic source.

## 6.2 Tourmaline

The ultrastable heavy mineral tourmaline is diagnosed by it´s high relief, highly variable morphology and colours (brown, green, blue and sometimes pink) as well as marked pleochroism, negative elongation, lack of cleavage, parallel extinction, interference colours of second order and moderate bifringence (Kerr, 1977). It was observed in low concentrations in the majority of the examined samples. In terms of colours, three varieties of tourmaline were observed. These are brown-reddish brown, green-yellowish green and blue-light blue varieties (Plate 6.1 f – j). Some varieties particularly in the lower strata of Aradeiba and in the upper horizons of Bentiu Formations exhibit pale grey colours; sometimes they are colourless. This phenomenon could be attributed to the decolouration of the brown-reddish brown and the green-yellowish green varieties caused by burial diagenesis. Some tourmaline varieties are tabular and other are columnar to acicular in form with regular to irregular edges. Inclusions are mainly minute grains of zircon, tourmaline and opaque minerals. The concentration of the tourmaline ranges between 0.0 – 4.2 % (Appendices 1A & 1B).

The green-yellowish green species (Plate 6.1 f,h) is recorded in samples from the lower horizon of Aradeiba Formation in Heglig-2 well and in samples from the lower strata of Zarga Formation in Barki-1 well. On the other hand, the brown-reddish brown variety (Plate 6.1 g,i) which is less abundant, seems to have a stratigraphic and/or diagenetic control. Its occurrence is restricted to the upper part of Bentiu Formation. Furthermore, the blue tourmaline grains (Plate 6.1 j) were scarce and only seen in some few samples from the Aradeiba Formation in Heglig-2 and Nabag-1 wells. Such blue variety was documented by Mansour (1990) in higher percentage in the Gilf Kebir Formation (Lower Cretaceous) in southern Egypt, and in the Selima Formation in northern Sudan. It is possible to assign gneisses and schists as source rocks to the brown and the green tourmaline varieties, which would be formed by metasomatism, and pegmatite veins for the blue one (Mange and Maurer, 1992).

## 6.3 Rutile

Rutile is the third ultrastable heavy mineral recorded in the investigated samples. According to Mange and Maurer (1992), rutile may be confused with cassiterite. The dark colours (red and yellowish brown), the very high relief, the prismatic form, the extreme bifringence, the parallel extinction and the positive elongation are characteristic features for all rutile grains identified in the examined samples. Rutile is recorded as subangular and subrounded grains in most of the investigated samples. Similar to zircon, the subangular grains were dominantly observed in the samples from the studied intervals of the Heglig Field. The subrounded grains were dominantly observed in the samples from the studied intervals of the Unity Field. The rutile grains are sometimes partially or completely covered by iron oxides (Plate 6.1 k – o). Its concentration in the studied strata ranges between 7.3 – 19 % (Figs. 6.1, 6.2, 6.3, 6.4, 6.5 and 6.6 & Appendices 1A & 1B). The highest percentage of rutile (18 – 19 %) was noted in the lower horizon of Zarga Formation in Talih-2 well and in the upper strata of Bentiu Formation in the same well (Fig. 6.2 & Appendix 1A) as well as in the upper strata of the Bentiu Formation in Barki-1 well (Fig. 6.3 & Appendix 1A).

Generally, rutile is a rather widespread heavy mineral in various metamorphic rocks, sometimes it is found in igneous rocks (Kerr, 1977). The Basement complex north-east of the Muglad Basin is most probably the source area.

## 6.4 Kyanite

Kyanite is a metastable heavy mineral. It is observed in all of the analysed samples. It is commonly colourless, sometimes with very faint shadows of bluish colour. The combination of perfect cleavage and parting, together with a large extinction angle and the good interference figure allows an easy diagnosis (Mange and Maurer, 1992). It occurs as elongated tabular grains with strongly corroded edges (Plate 6.1 p – r).

Kyanite is recorded in all strata studied with a concentration ranging between 17 – 42 % (Figs. 6.1, 6.2, 6.3, 6.4, 6.5, and 6.6 & Appendices 1A and 1B). Generally the amount of kyanite in the wells of the two fields exceeds the amount of any other heavy mineral present except of garnet. This reflects a metamorphic source origin for these sediments. The highest occurrences of the heavy mineral kyanite (37 – 42 %) were notably observed in the examined samples from Heglig Field, as in the upper horizons of the Aradeiba Formation as well as in

the lower strata of the Zarga Formation at Nabag-1, Heglig-2 and Toma-1 wells (Figs. 6.4, 6.5 and 6.6 & Appendix 1B). There are several reasons that can account for these higher occurrences of kyanite and for the preservation of the unstable heavy minerals in general at the studied intervals:

(1)     The structural relief during the initiation of the second rifting phase has led to an increase in the detrital input, quick transportation and rapid burial, which favoured the preservation of the unstable heavy minerals.

(2)     The prevalence of a shallow lacustrine environment has led to the deposition of vertically stacked, thinly bedding sequences of shale and argillaceous sandstone. As a result of this depositional regime, both the horizontal and the vertical permeabilities were substantially decreased. This will allow only very limited circulation and percolation of pore water which reduces the intensity of intrastratal dissolution.

(3)     The early cementation by calcrete may have led to the preservation of kyanite and also of other rather unstable heavy minerals such as staurolite, andalusite, sillimanite, garnet, epidote and hornblende. Fragments of calcretes were observed not only in the cutting samples but also in the thin sections of the core samples from the upper strata of Bentiu Formation in Heglig-2 and Toma-1 wells and from the lower strata of Aradieba and Zarga Formations at Unity-9 and Talih-2 wells (Plates 5.1, 5.2 & 5.3), as well as in the drill cutting samples from the boundary between Bentiu and Aradeiba Formations at Barki-1 well. This cementation might have contributed to the preservation of the unstable heavy minerals in the above mentioned horizons (Figs. 6.1, 6.2, 6.3, 6.4 and 6.5).

(4)     The presence of residual oil due to the early migration of oil into the Cretaceous reservoir horizons may have inhibited further dissolution of kyanite and the other unstable heavy minerals grains by intrastratal solutions. Morton (1979) observed relatively higher concentrations of kyanite and staurolite in the Palaeocene oil bearing sands of the North Sea.

(5)     The short distance of transportation for Heglig Field sediments in comparison with the relatively longer distances of transportation that the

sediments of Unity Field have been subjected to. This is indicated by the textural characteristics together with the increased amounts of sillimanite and hornblende in the studied horizons of Heglig Field.

## 6.5 Staurolite

Staurolite is a metamorphoc metastable heavy mineral. It is the product of medium- grade regional metamorphism (Mange and Maurer, 1992). It is observed in almost all of the examined samples, but with very low concentrations compared to kyanite. All staurolite grains were identified by their goldish and yellowish-orange colours and weak pleochroism. The presence of liquid inclusions is also distinctive (Kerr, 1977). Generally, staurolite occurs as large angular to subangular grains with corroded edges, that sometimes contain wavy quartz inclusions (Plate 6.2 a – e). Staurolite occurs only in small quantities in most of the studied intervals, with a concentration of 0.0 – 5.2 % (Apendices 1A & 1B). The dissolution of this heavy mineral by pre- and post-depositional processes could not account for this, since the other low stable heavy minerals such as kyanite, sillimanite, andulasite and epidote were recorded in the same intervals. Hence, the source area is more likely to be the main reason.

According to Mange and Maurer (1992), staurolite is commonly derived from schists and less frequently from gneisses. Therefore, the source rocks for this staurolite may be the schists or the gneisses at the north-eastern border of the Muglad Basin.

## 6.6 Andalusite

Andalusite is an unstable heavy mineral. It is observed as subrounded to rounded grains and occasionally in a prismatic form in most of the examined samples. It is commonly colourless covered with iron oxides and sometimes light green in colour (Plate 6.2 f,g,h). Some andalusites are non-pleochroic, others display a distinctive pleochroism (pleochroic in shades of light green and yellowish green). It is also characterized by weak bifringence, parallel extinction and negative elongation (Mange and Maurer, 1992).

The amounts of andalusite in the studied intervals at Heglig Field are greater than the amounts of the minerals in the studied intervals of the Unity Field. Moreover, the highest occurrence of andalusite in the studied intervals of Heglig Field reaches 12 % as noted in the Aradeiba Formation in Toma-1 Well and in the Zarga Formation in Heglig-2 Well (Figs. 6.4

and 6.5 & Apendix 1B). In the studied intervals of the Unity Field andalusite reaches 10 % as seen in the Zarga Formation in Talih-2 Well and also in the Aradeiba Formation in Barki-1 Well (Figs. 6.2 and 6.3 & Apendix 1A). As mentioned earlier in the clarification of the reasons for the higher kyanite contents in Heglig Field, this might also be explained by a short distance of transport of Heglig Field sediments in comparsion with the relatively longer distance of transport that the sediments of Unity Field were subjected to. Generally, in both of the two oil fields, the amount of andalusite decreases down along the studied intervals. This could be explained by increasing weathering, transportation and dissolution effects rather than differences in the source rocks. Andalusite is a typical metamorphic mineral and appears most commonly in argillaceous rocks derived from gneisses and/or schists (Mange and Maurer, 1992).

## 6.7 Sillimanite

Sillimanite is an unstable heavy mineral. It is recorded in the studied samples in lower concentrations compared to andalusite. It usually occurs in small, slender prismatic grains and in a felted mass of fibers (Plate 6.2 i – l). It is commonly colourless. It is also characterized by perfect parallel cleavage, high relief, moderate bifringence, parallel extinction and positive elongation. Moreover, the prismatic habit and the brilliant interference colours provide an easy diagnosis (Mange and Maurer, 1992).

Similar to kyanite and andalusite, the sillimanite contents in the studied intervals at Heglig Field are greater than those in the studied intervals of Unity Field. The highest amounts of sillimanite in the studied intervals of Heglig Field reaches 6 – 7 % as noted at the upper strata of Aradeiba Formation in Toma-1 well and at the lower horizon of Zarga Formation in Nabag-1 well (Figs. 6.5 and 6.6 & Appendix 1B). However, the highest amount of sillimanite in the studied intervals of Unity Field reaches 3.6 % as seen in the lower strata of Zarga Formation at Bark-1 well (Fig. 6.3 & Appendix 1B). As mentioned earlier, this could be attributed to the short distance of transport of Heglig Field sediments in comparsion with the relatively longer distance of transport for the Unity Field sediments. On the other hand, the amount of the heavy mineral sillimanite is not graded regulary down along the studied intervals in both of the two fields. This might reflect changes in weathering, transport distance and diagenesis rather than changes in the source rocks. Detrital sillimanite is derived from

metamorphic rocks which were formed in high-temperature conditions such as sillimanite – cordierite gneisses and biotite – sillimanite hornfelses (Mange and Maurer, 1992).

## 6.8 Garnet

Detrital garnets were observed in the studied intervals as subhedral grains, sharp irregular fragments (studied intervals of Heglig Field), and subrounded to rounded grains (studied intervals of Unity Field). Garnets generally show high relief and can easily be distinguished by their isotropic character under crossed nicols (Mange and Maurer, 1992). Their colour ranges from light green to yellowish green and sometimes to reddish brown (Plate 6.2 m – q). This variation in colour was even noted within the same sample.

Generally the amount of garnet in the studied intervals of the two fields is high. However, its amount in the studied sediments of Unity Field is a bit higher than that in the studied sediments of Heglig Field. The greatest amounts of garnet (46 – 53 %) were recorded in the upper strata of Bentiu Formation and in the lower strata of Aradeiba Formation at Unity-9 and Talih-2 wells (Figs. 6.1 and 6.2 & Appendix 1A), in Unity Field. In the same stratigraphic horizons in Barki-1 well in Unity Field the garnet contents are also high (42 %) (Fig. 6.3 & Appendix 1A). The maximum recorded amount of garnet in Heglig Field 39 – 40 % was recorded in the upper strata of Bentiu Formation and in the lower strata of Aradeiba Formation at Heglig-2 well as well as in the upper strata of Bentiu Formation at Toma-1 well (Figs. 6.4 and 6.5 & Appendix 1B). The higher amount of garnet in the Unity Field sediments compared to that of the Heglig Field sediments may be attributed to differences in metamorphic source rock origin.

Garnet is normally derived from metamorphic rocks, and very rarely associated with ultrabasic igneous rocks such as peridotite (Kerr, 1977).

## 6.9 Epidote

Epidote is identified by its yellowish green colour, high relief, prismatic habit, very weak pleochroism, moderate birefringence, contrasting anomalous interference colours and parallel extinction (Mange and Maurer, 1992). Its colour is ranging from yellowish green to brownish green (Plate 6.3 a – c).

In the study intervals in Unity and Heglig Fields wells, two or three small positive anomalies of epidote were noted. The first anomaly is found within the upper strata of Bentiu Formation (Middle Cretaceous). The second one is restricted to the lower strata of Aradeiba Formations, whereas the third anomaly is extended from the uppermost of Aradeiba up to the lower strata of Zarga Formations (Figs. 6.1, 6.2, 6.3, 6.4, 6.5 and 6.6 & Appendices 1A and 1B). In the middle part of the Aradeiba Formation between the anomalies of the epidote, epidote completely disappears with exception of few sporadic occurrences in Nabag-1 and Heglig-2 wells. Some angular zircon grains were noted in association with the above mentioned positive anomalies, which indicate partial reworking effects acted on these sediments. Therefore, this restricted occurrence of epidote is an evidence for tectonism that had occurred in the area. As mentioned earlier, the subsidence of the basin besides the structural relief variations that acting in the area during the initiation of the second rifting phase have given rise to an increase in the detrital directly derived from parent rocks of the Basement Complex. Quick transportation and rapid burial favour the preservation of unstable heavy minerals. However, the role of the other previous mentioned preserving factors can not be excluded.

According to Kerr (1977), epidote might stem from different source rocks. It is equally common in igneous and metamorphic rocks. However, the source rock of the heavy mineral epidote in the studied intervals at Heglig and Unity Fields is most probably a metamorphic one.

## 6.10 Hornblende

Hornblende, which belongs to the unstable heavy minerals, was observed in low contents in some of the investigated samples from the study wells. It occurs as prismatic, rounded and angular grains. Its colour is light green, yellowish green or sometimes brown (Plate 6.3 d,e,f). Decoloration of hornblende was also noted.

Due to its low chemical stability (Mange and Maurer, 1992), it usually shows a discontinuous occurrence through the sedimentary succession with a concentration between 0 – 5 % (Appendices 1A and 1B). The occurrence of hornblende is more sporadic in the study intervals of Unity Field than in the study intervals of Heglig Field (Figs. 6.1, 6.2, 6.3, 6.4, 6.5 and 6.6). Furthermore, the amounts of the hornblende in the study intervals of Heglig Field are higher than in the study intervals of Unity Field. The higher percentage of hornblende in

the sediments of Heglig Field compared to it´s percentage in the Unity Field sediments is possibly due to the short distance of transportation and to a less intensive weathering, besides the rapid burial of these sediments during the initial of the rifting phase. Generally the sporadic occurrence reflects periods of only partial reworking followed by periods of intensive reworking. In part, hornblende is preserved due to an early cementation of calcite, e.g. in the upper strata of Bentiu Formation in Heglig-2 and Toma-1 wells (Figs. 6.4 and 6.5). The same can be noted in the lower strata of Aradeiba Formation at Unity-9 and Talih-2 wells and at the boundary between Bentiu and Aradeiba Formations in Barki-1 well (Figs. 6.1, 6.2 and 6.3). Furthermore, the cementation by calcite plays an important role in preserving the unstable heavy minerals in general, e.g. in Zarga Formation at Unity-9 and Talih-2 wells. This calcite cementation is clearly observed in thin sections of the core samples from the above mentioned horizons (Plates 5.1, 5.2 and 5.3). However, the role of the other previous mentioned preserving factors can not be excluded.

In fact, hornblende is widely present in different varieties of igneous rocks. However, it could also be derived from metamorphic rocks such as amphibolites and gneisses (Kerr, 1977).

## 6.11 Glaucophane – riebeckite

Glaucophane – riebeckite is only identified in a few samples from the lower horizons of Zarga Formation at Nabag-1 well, reaching a amount of 2 % (Appendix 1B & Fig. 6.6). It is found as blue coloured subrounded to rounded grains and/or as fibrous asbestiform aggregates (Plate 6.3 g,h). The blue colour, the characteristic pleochroism (bright blue to greenish blue), the fibrous morphology and the amphibole cleavages ensure an easy diagnosis of this heavy mineral (Mange and Maurer, 1992).

Glaucophane and crossite are characteristic minerals of the glaucophane schist and glaucophanitic green-schist facies (Mange and Maurer, 1992), hence it is possible to assign glaucophane – riebeckite-rich schists as source rocks for this heavy mineral.

## 6.12 Presentation of the Results

The results of the heavy minerals investigation are stratigraphically tabulated in Appendices 1A and 1B. The individual heavy minerals are expressed in percentages. This gave the first

insight into the heavy mineral spectrum and provides the basis for further data treatment. The vertical distribution of the heavy minerals percentages for each of the studied intervals at the six studied wells and their possibly interpreted mineralogical assemblage zones (A.Z.) are reflected by figures 6.1, 6.2, 6.3, 6.4, 6.5 and 6.6. Zircon – tourmaline – rutile indices (ZTR %), besides the total percentages of the rather unstable heavy minerals sillimanite, epidote and hornblende (SEH %) were used as mineralogical maturity indicators combined with the textural maturity observations, and were vertically plotted versus depth for each of the studied intervals at the study wells (Figs. 6.7 and 6.8).
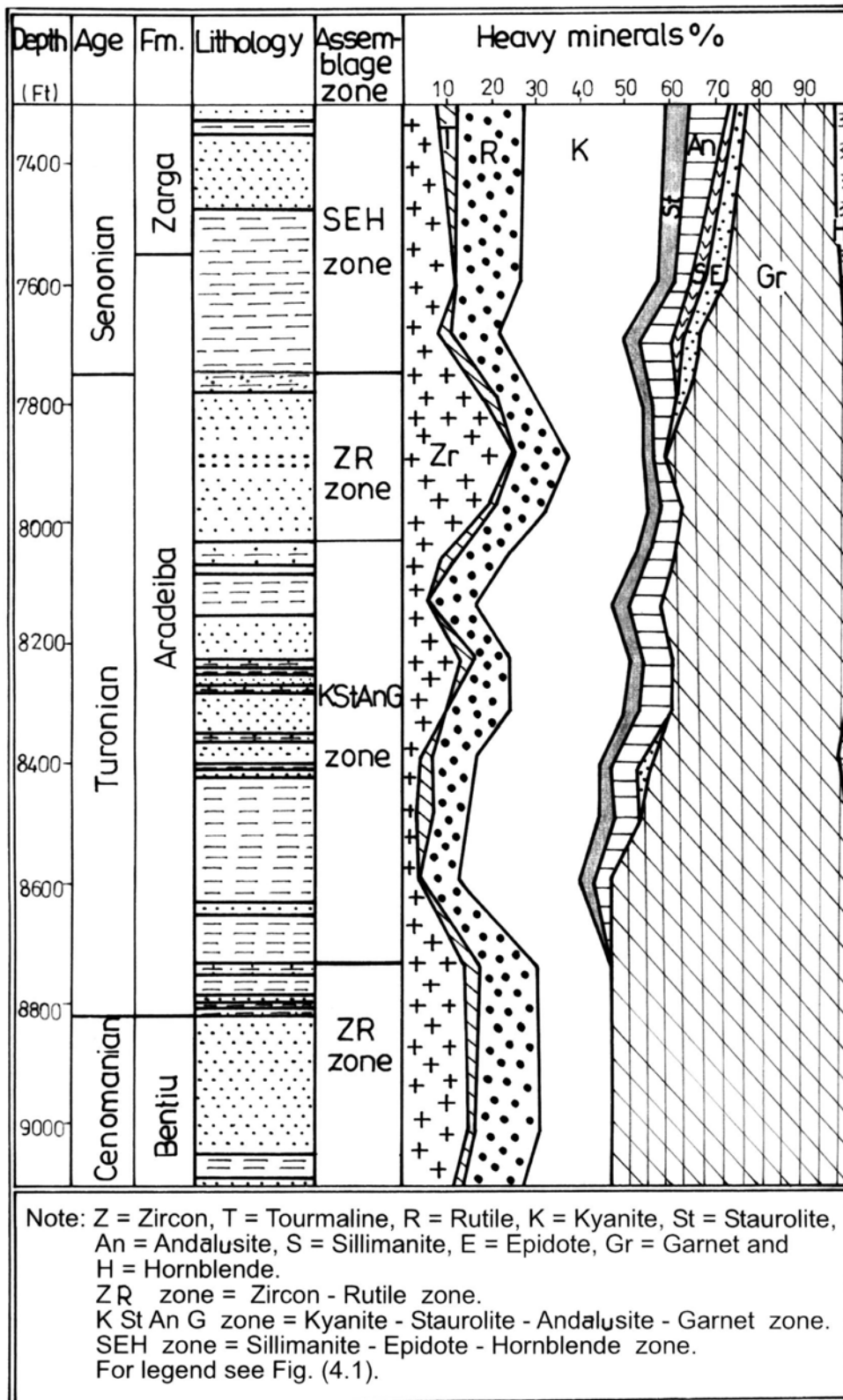
**Figure 6.1: Vertical distribution of heavy minerals and their relevant assemblage zones in the upper Bentiu, Aradeiba and lower Zarga Formations, (well Unity-9), SE Muglad Basin.**
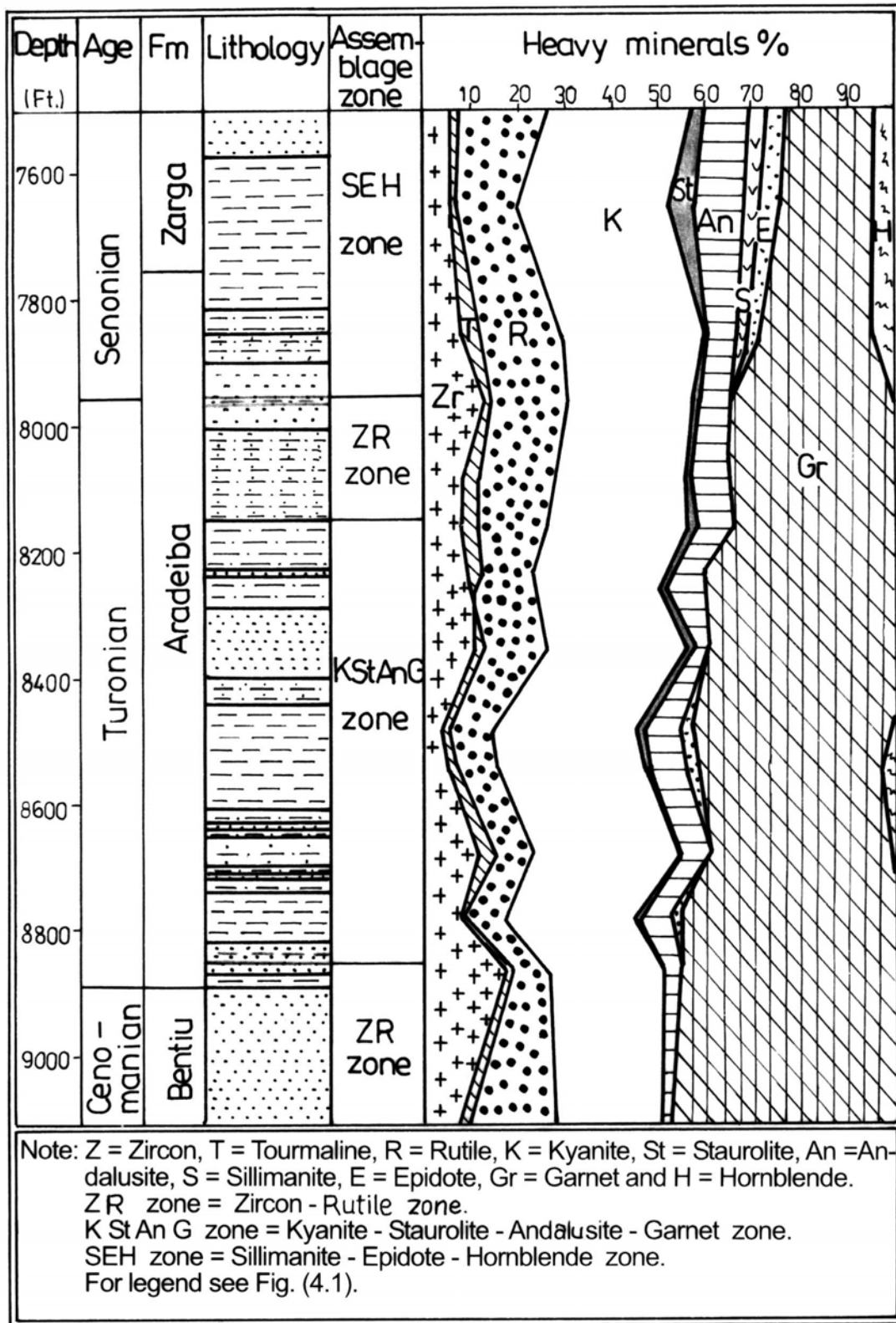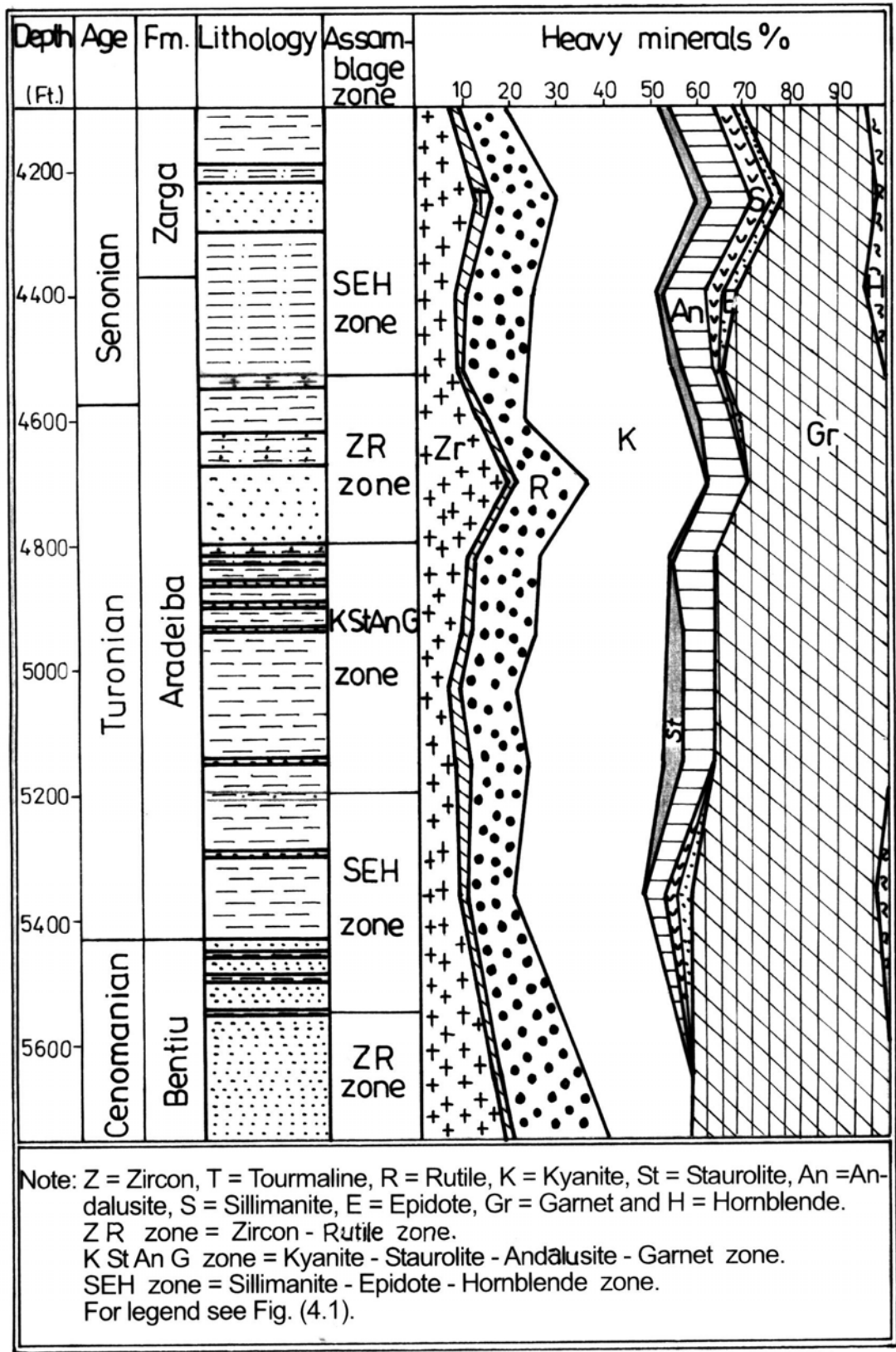
| Depth (Ft.) | Age | Fm | Lithology | Assemblage zone | Heavy minerals % |
|---|---|---|---|---|---|

Figure 6.2: Vertical distribution of heavy minerals and their relevant assemblage zones in the upper Bentiu, Aradeiba and lower Zarga Formations, well Talih-2, SE Muglad Basin.

116

**Figure 6.3: Vertical distribution of heavy minerals and their relevant assemblage zones inthe upper Bentiu, Aradeiba and lower Zarga Formations, well Barki-1, SE Muglad Basin.**
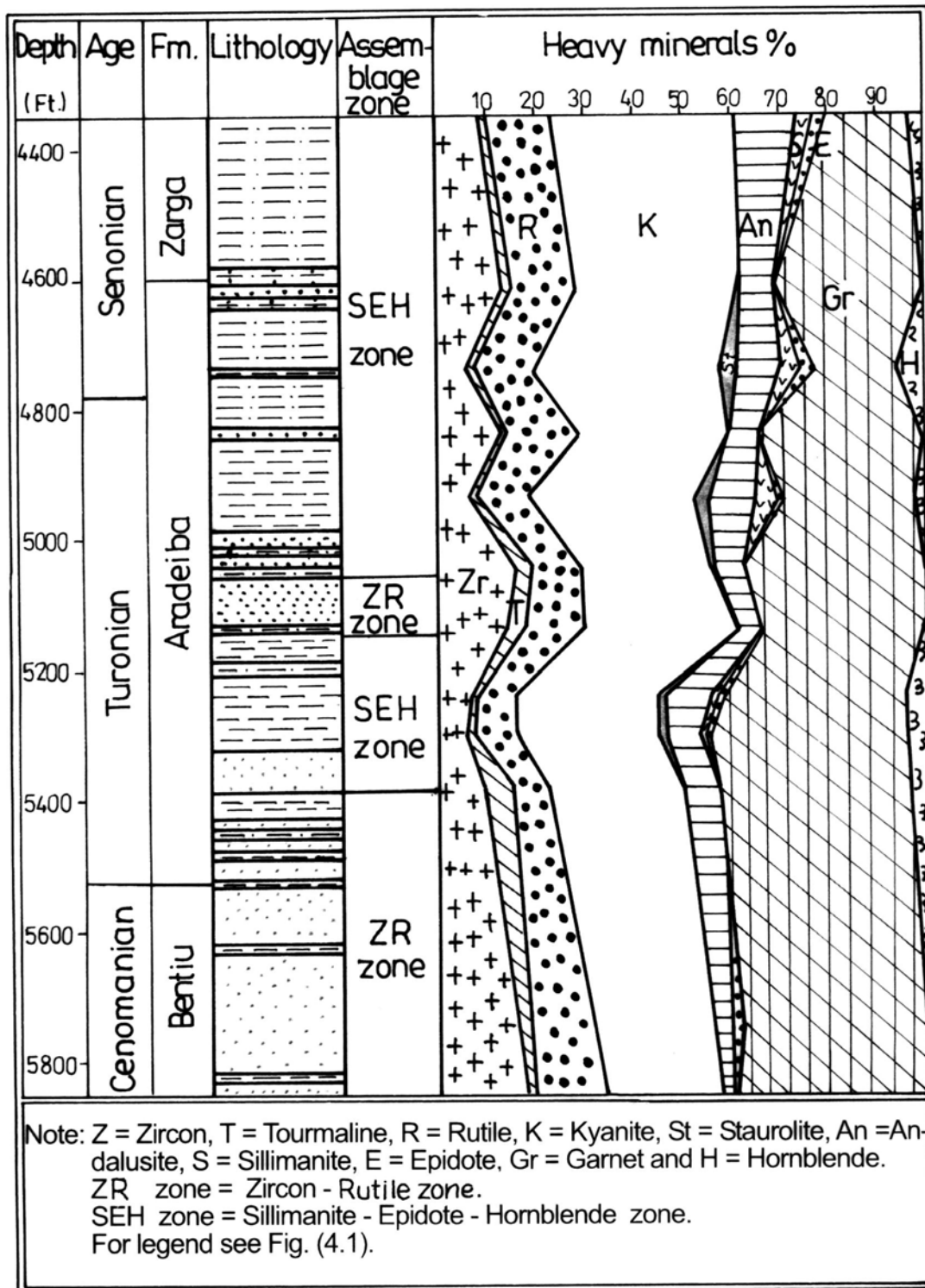
**Figure 6.4: Vertical distribution of heavy minerals in the upper Bentiu, Aradeiba and lower Zarga Formations, well Heglig-2, SE Muglad Basin.**
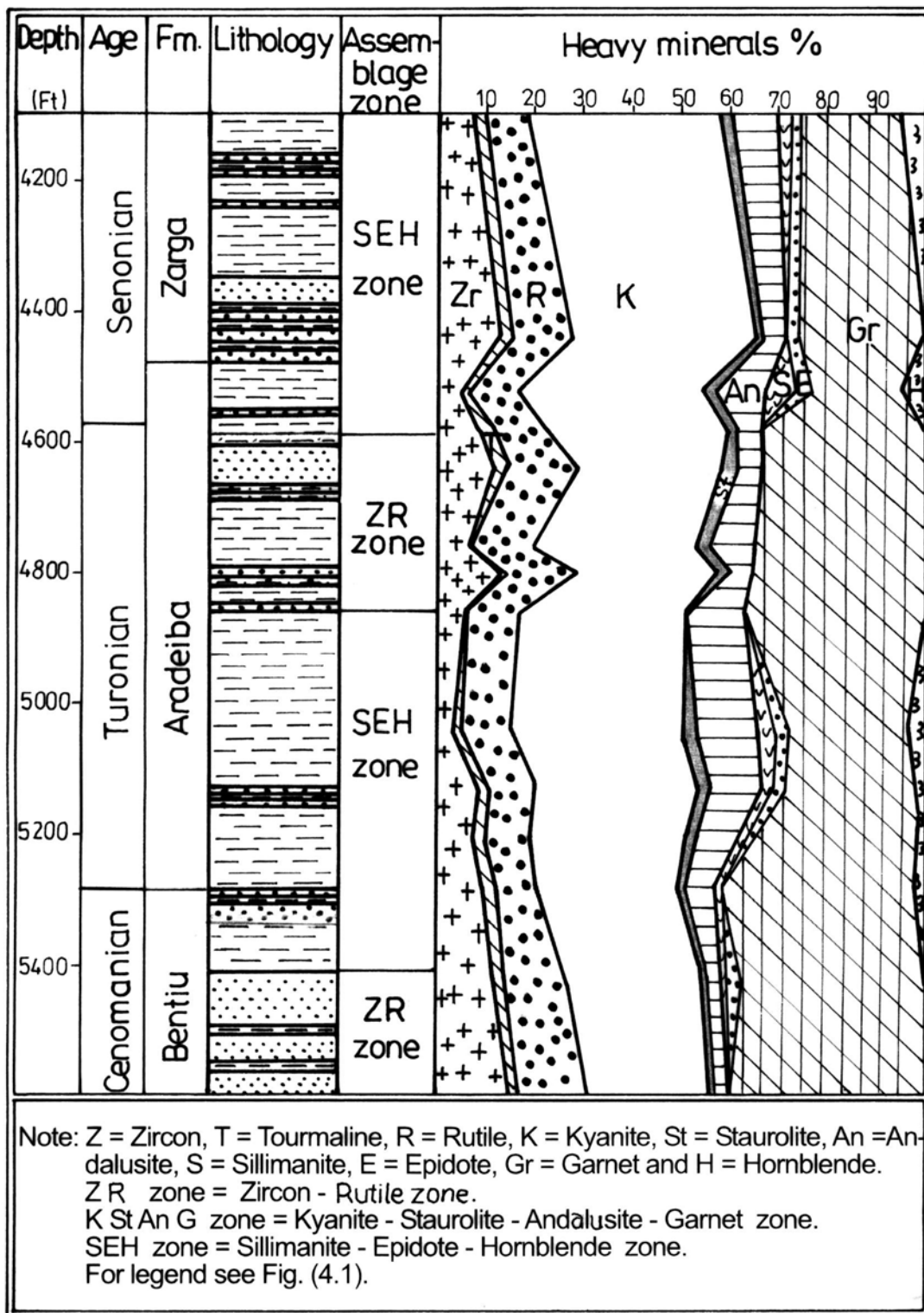
118

**Figure 6.5: Vertical distribution of heavy inerals and their relevant assemblage zones in the upp erBentiu, Aradeiba and lower Zarga Formations, well Toma-1, SE Muglad Basin.**
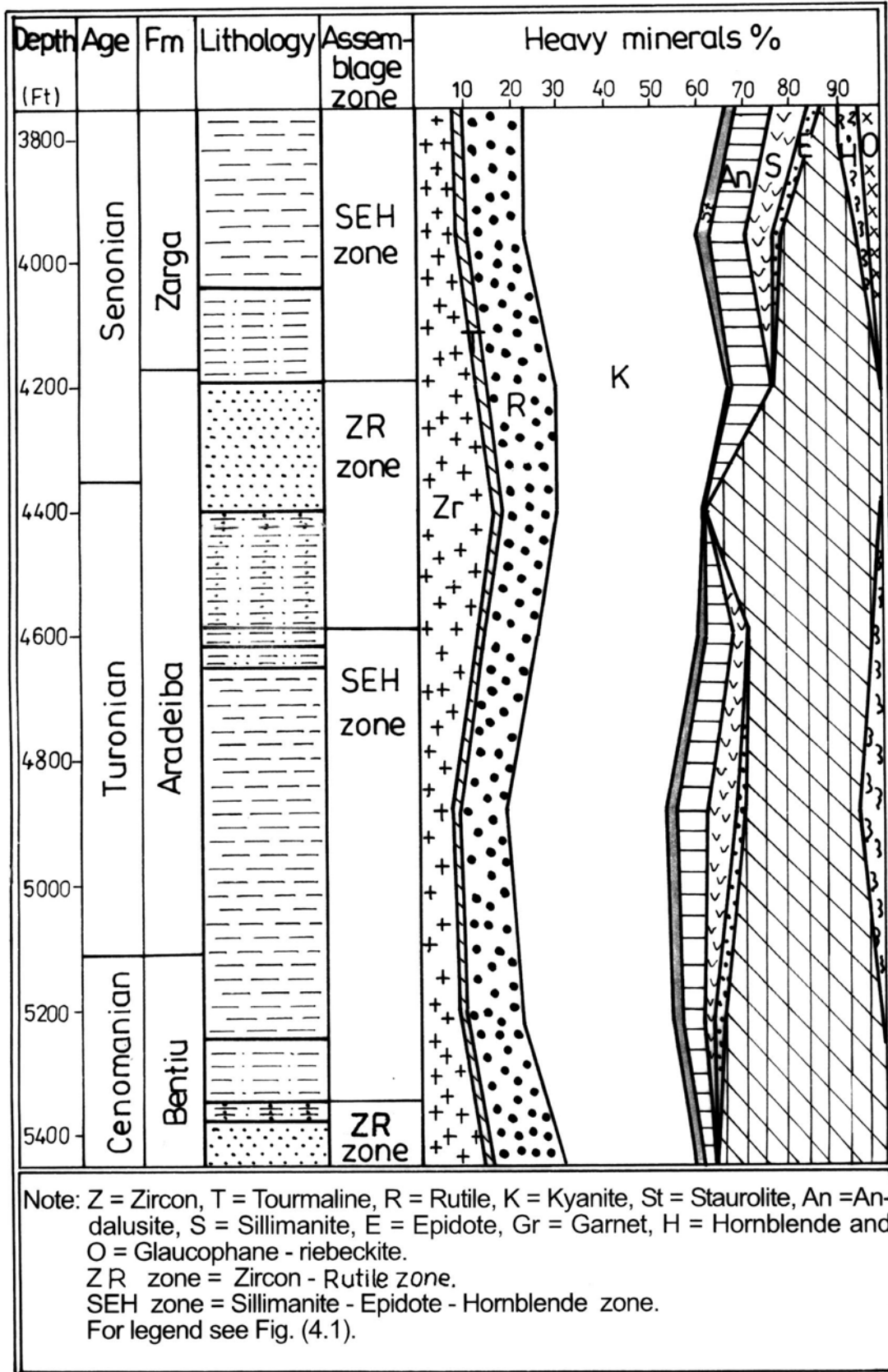
**Figure 6.6: Vertical distribution of heavy minerals and their relevant assemblage zones in the upper Bentiu, Aradeiba and lower Zarga Formations, well Nabag-1, SE Muglad Basin.**

## 6.13 Discussion of the Results

Determination of the source rocks, the palaeogeographic situation and the provenance of the sedimentary rocks are the objectives of most petrographic studies of heavy minerals. Moreover, heavy minerals provide information about weathering, transportation and diagenetic processes. Although some of the heavy mineral species, such as olivenes, pyroxenes and the other low stable minerals may selectively be destroyed by pre- and post-depositional processes, the remaining heavy minerals are sometimes the best guides for the provenance of sandstones (Carver, 1971).

Before reaching any satisfactory conclusions regarding the provenance of the Upper Cretaceous sedimentary rocks in Unity and Heglig Fields, many parameters have to be evaluated first. It is essential to determine how close the present mineralogical composition of the sedimentary rocks resembles the petrological character of the source area. The parameters include the weathering conditions in the source area, distance of transport, reworking and recycling effects, variations of the palaeorelief, climatic conditions, tectonic activities and post-depositional diagenetic changes. All these variables and attributes could be reflected as mineralogical and/or textural changes.

## 6.14 Zircon – Tourmaline – Rutile Index (ZTR)

The ZTR index (Hubert, 1962) is the total percentage of the three ultrastable heavy minerals zircon, tourmaline and rutile. This index is used as a indicator for the degree of textural maturity or modification of the entire heavy mineral assemblage of a sandstone. Furthermore, any increase in the ZTR index is the result of the progressive dissolution of the unstable minerals. A new and far better classification for the sedimentary rocks in the studied intervals is approached. Some terms such as immature, moderately mature, mature and overmature are used in this study to describe very low, low, average and above average ZTR percentages respectively. Also terms such as slightly reworked, moderately reworked, reworked and extensively reworked are used in this study to denote textural observations of zircon grains like angular, subangular, subrounded and rounded respectively. These terms are however not absolute. They indicate relative mineralogical and textural trends. Generally, the ZTR indices show parallel trends with the textural maturity of the examined sedimentary rocks as visually inferred from the angularity and the roundness of the zircon grains.

# 6.15 Sillimanite – Epidote – Hornblende Indicator (SEH)

Sillimanite, epidote and hornblende are mechanically and chemically rather unstable heavy minerals. The total sum percentages of these three minerals can be used in conjunction with the ZTR indices as a measure for the degree of textural maturity of the studied sediments. The amount of these three rather unstable heavy minerals varies between 0 – 15 % in the investigated samples. If we assume that the actual percentage of these three heavy minerals in the source area, is reflected by the maximum amount of 15 %, then many processes must have been active to bring that level to zero in some stratigraphic horizons. These processes were mainly weathering, transportation and diagenesis.

In fact, four major textural maturation levels were established on the basis of the above criteria (Figs. 6.7 and 6.8). The more defining parameters for the maturation level is however the absolute percentage of the three ultrastable heavy minerals zircon, tourmaline and rutile, besides the total sum percentages of the three rather unstable heavy minerals sillimanite, epidote and hornblende as well as the similarity in the textural characteristics of the zircon grains. The four textural maturation levels are:

## 6.15.1 Immature Level

This level of maturation is widely spread in the study area. It includes about 42 – 60 % of the studied intervals in the Heglig Field (Fig. 6.7) and it covers about 45 – 56 % of the studied intervals in the Unity Field (Fig. 6.8). This level of maturation is generally characterized by low ZTR indices (< 25 %) and by relatively high SEH indices (8 – 15 %). The sedimentary rocks, which represent this level, are characterized by ubiquitous occurrences of the heavy minerals kyanite, garnet, andalusite and staurolite. The total percentage of these minerals ranges between 60 – 82 %. Moreover, the shape of the zircon grains in the sediments of this level is commonly angular (Plate 6.1 d). Sedimentary rocks of such characteristics are possibly derived from an elevated source area by low intense weathering processes, transported for a short distance, deposited in a rapidly subsiding basin and suffered only from insignificant losses of the low stable heavy minerals by dissolution.

## 6.15.2 Moderately Mature Level

The sediments of this level of maturation show mostly moderate maturity and reworking. This level forms 25 – 42 % of the sediments from Heglig Field and also forms 19 – 23 % of the

sediments from Unity Field. The ZTR indices are generally between 25 – 30 %, whereas that of the SEH are between 4 – 7 % (Figs. 6.7 and 6.8). Most of the zircon grains are subangular, sometimes they are subrounded and very rarely angular. Moreover, the average amount of kyanite, garnet, andalusite and staurolite in this level is ranging between 63 – 71 %. Sedimentary rocks of such character resemble the previous one, but have undergone partial losses of the unstable heavy minerals by intrastratal solution and/or short term abrasion.

### 6.15.3 Mature Level

This level of maturation contains mature and highly reworked sedimentary rocks. It covers about 13 – 16 % of the studied intervals in the Heglig Field and also about 16 – 23 % of the studied intervals in the Unity Field (Figs. 6.7 and 6.8). This level of maturation is generally characterized by high ZTR indices (30 – 35 %), low SEH indices (< 4 %), predominance of subrounded zircon grains and low occurrences of the metastable heavy minerals kyanite and staurolite as well as by a small amount of the unstable mineral andalusite. The presence of the subrounded zircon grains together with the small amounts of unstable minerals indicates relatively strong reworking effects. Sedimentary rocks of such a character must have been derived from low relief areas by relatively intense weathering processes and must have underwent significant losses of the low stable heavy minerals such as hornblende, sillimanite, epidote, andulasite, kyanite and staurolite by either prolonged abrasion and/or strong intrastratal solution attack.

### 6.15.4 Overmature Level

This level of maturation includes extensively reworked and overmature sedimentary rocks. It is characterized by high ZTR indices (> 35 %), subrounded to well rounded heavy mineral grains, and the absence of even traces of the rather unstable heavy minerals sillimanite, epidote and hornblende. It is only present in Bentiu and Aradeiba Formations in Barki-1 well and in the Aradeiba Formation in Unity-9 well. It covers about 7.6 % and 4.6 % of the study intervals in the two wells, respectively (Fig. 6.8). This level was achieved by highly extensive weathering of the source areas, long distances of transport, extensive recycling of the pre-existing sediments and/or severe intrastratal dissolution.
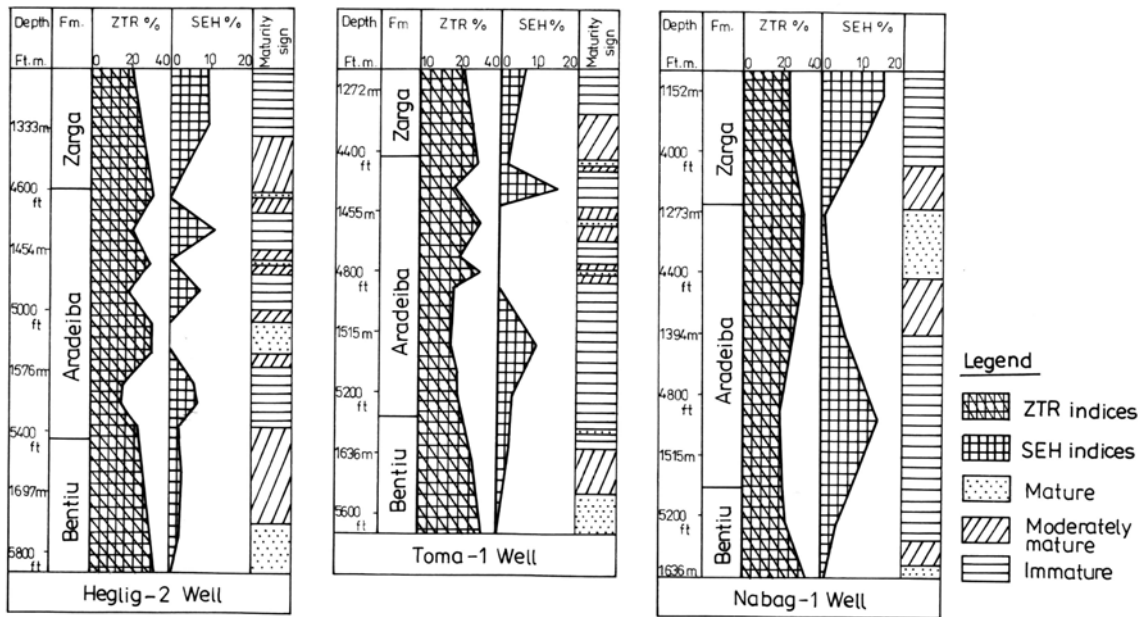
**Figure 6.7: Diagrams of Zircon–Tourmaline–Rutile (ZTR) and Sillimanite–Epidote–Hornblende (SEH) indices with sediment maturity indications at the studied intervals in the three wells of the Heglig Field.**
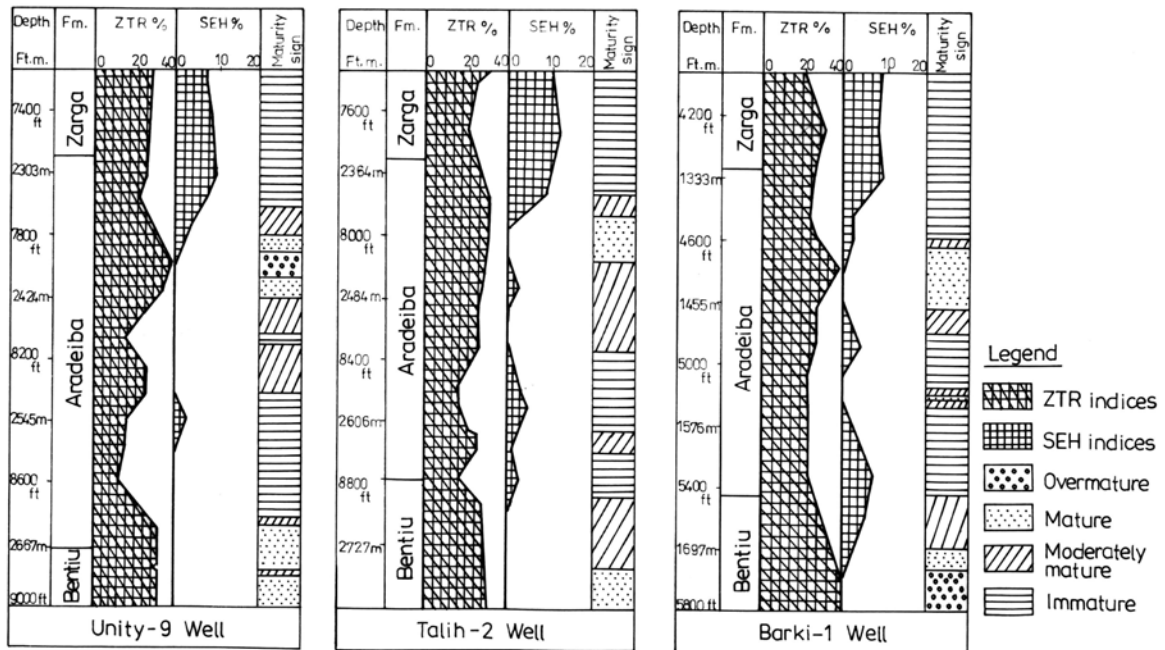


**Figure 6.8: Diagrams of Zircon–Tourmaline–Rutile (ZTR) and Sillimanite–Epidote–Hornblende (SEH) indices with sediment maturity indications at the studied intervals in the three wells of the Unity Field.**

## 6.16 Zonation and Stratigraphic Significance

The study of the heavy minerals associations of the subsurface Middle – Upper Cretaceous strata in the SE Muglad Basin has made it possible to establish three assemblage zones with

obvious lateral and vertical continuity. The boundaries of these assemblage zones broadly coincide with the boundaries already established by the lithofacies criteria. The defining criteria for a heavy mineral assemblage zone is however, the amount of the ultrastable, metastable or the unstable heavy minerals mentioned earlier. Moreover, the more abundant and ubiquitous minerals such as kyanite and garnet are not as useful as those minerals whose presence is discontinuous (e.g. sillimanite, epidote and hornblende). For the purpose of zonation and vertical continuity, the ubiquitous heavy minerals of zircon, rutile, tourmaline, kyanite, staurolite, andalusite and garnet as well as those which occur only sporadically such as sillimanite, epidote and hornblende are considered.

### 6.16.1 Zircon – Rutile Zone (ZR)

This zone generally defines the upper parts of Bentiu and Aradeiba Formations in most of the study intervals except at Heglig-2 well; it covers the upper part of the Bentiu Formation besides the lowermost part and the middle part of Aradeiba Formation (Figs. 6.1, 6.2, 6.3, 6.4, 6.5 and 6.6). It is characterized by a ZR index of 20 – 38 %. Associated with these heavy minerals are tourmaline, kyanite, staurolite, garnet and andalusite with some traces of sillimanite, epidote and hornblende. The confined occurrence of the ZR zone at the upper strata of Bentiu and Aradeiba Formations suggest a subdivision of the study intervals into two subdivisions. The first subdivision, which is relatively sand-rich, includes the upper parts of Bentiu and Aradeiba Formations, whereas the second one, which is relatively argillaceous, includes the lower parts of Aradeiba and Zarga Formations.

Reduction of the unstable heavy minerals in the former subdivision could be interpreted as due to the effects of intrastratal solution, which are specially strong in porous and permeable sandy horizons.

### 6.16.2 Sillimanite - Epidote - Hornblende Zone (SEH)

The SEH zone covers the uppermost horizons of Bentiu, the lower as well as the uppermost parts of Aradeiba and the lower part of Zarga Formations in Barki-1, Toma-1 and Nabag-1 wells (Figs. 6.3, 6.5 and 6.6). Moreover, it covers the lower part of Aradeiba Formation in Heglig-2 well (Fig. 6.4). In addition to that, the SEH zone covers the uppermost part of Aradeiba as well as the lower part of Zarga Formations in Unity-9 and Talih-2 wells (Figs. 6.1 & 6.2). This SEH zone which often overlies the ZR zone, is characterized by a SEH index of 2 – 15 %, low ZR indices and by presence of kyanite, staurolite, andalusite and garnet. All of

the sillimanite, epidote and hornblende vanish at the base of this zone and in the subsequent underlying ZR zone.

The presence of unstable heavy minerals in higher quantities as normal suggests a low intensity of weathering and a short distance of transport, particulary indicated by the presence of hornblende. Moreover, the SEH zone is expected to have formed as a result of less intensive chemical weathering in the source area during relief rejuvenation parallel with the onset of the second rifting phase during Cretaceous time.

### 6.16.3 Kyanite - Staurolite - Andalusite - Garnet Zone (KStAnG)

This KStAnG zone encompasses the lower and the middle parts of Aradeiba Formation in all of the Unity Field except at Barki-1 well, where it is found in the middle part of Aradeiba Formation (Figs. 6.1, 6.2 and 6.3). In the Heglig Field, the zone does not clearly prominent due to the continuous occurrences of the defining heavy minerals group of this zone (Figs. 6.4, 6.5 and 6.6). This zone overlies the lower ZR zone and underlies the upper ZR zone in Unity-9 and Talih-2 wells but in Barki-1 well, it overlies the SEH zone and underlies the upper ZR zone. This zone is characterized by range of 70 – 88 % KstAnG indices, low ZR indices and presence of sillimanite, epidote and hornblende.

The sediments of the lower strata in this zone are poorly reworked, but that of the upper horizons are moderately reworked, in which the amount of the heavy minerals zircon and rutile is increased.

## 6.17 Integration

Heavy mineral analysis is one of the most sensitive and widely used technique in the determination of sandstone provenance (Morton and Hallsworth, 1994). Metamorphic source rocks rich in kyanite, garnet, andalusite, staurolite, sillimanite and hornblende are found in the Nuba Mountains (Vail, 1978), consequently these might have been the source rocks for the studied sediments. However, the variations of the heavy minerals proportions within the studied intervals were caused by one or several of the following influences: The subsidence of the basin, which was accompanied by structural relief variation, which enhanced transport and rapid burial of the detrital components. The quick transportation and rapid burial led to the preservation of the unstable heavy mineals as noted in the upper strata of Bentiu Formation, in

the lower and uppermost strata of Aradeiba Formation as well as in the lower strata of Zarga Formation.

Moreover, the prevalence of the shallow lacustrine environment led to the deposition of thin interbeds of shale and argillaceous sandstone which in turn decreased the vertical and lateral permeabilities and allowed only very limited percolation of fresh water and hence, reduced the effect of the intrastratal dissolution. On the other hand, the effect of the fluvial and deltaic reworking in the upper part of the Bentiu Formation (in all of the studied wells), in the middle and upper parts of the Aradeiba Formation (in Unity-9 and Talih-2 wells), in the middle part of the Aradeiba Formation (in Heglig-2 well), in the upper part of the Aradeiba Formation (in Barki-1, Toma-1 and Nabag-1 wells) and in the lower strata of the Zarga Formation (in Unity-9, Talih-2, Barki-1, Heglig-2 and Toma-1 wells) severely reduced the amount of the unstable and metastable heavy minerals in the above horizons. The relatively long distances of transportation, that the Unity Field sediments had been subjected to, also reduced the amount of the unstable heavy minerals in the Unity Field sediments.

However, carbonate cement in the upper strata of the Bentiu Formation as well as in the lower strata of the Aradeiba and Zarga Formations had isolated some rocks from circulating pore fluids and hence, inhibited the dissolution of the unstable heavy minerals in these horizons. Similarly, the presence of residual oil due to the early migration of oil into the reservoir horizons also inhibited the dissolution of the unstable heavy minerals.

Regarding the previous heavy minerals studies of the subsurface facies in the Central Sudan rift basins: Bakr (1995) studied the Mesozoic and Cenozoic subsurface sediments of Muglad, Melut and Blue Nile Rift Basins. He found that three sedimentary provinces could be interpreted from the heavy minerals associations. The sediments of these provinces have been predominantly derived from low to high grade metamorphic terrains of originally granitic and granodioritic composition. Mohammed (1997) characterized the Lower Cretaceous strata of the NW Muglad Basin by the following zones: the Sharaf Formation was characterized by the heavy mineral zones garnet – staurolite – hornblende and kyanite – garnet, whereas the Abu Gabra Formation was characterized by zircon – tourmaline – rutile and garnet – staurolite – hornblende. He concluded, that the source rocks of these Lower Cretaceous strata are mainly metamorphic rocks of granitic and granodioritic origin. Maarouf (1998) showed, that the heavy minerals associations of the Darfur Group and Amal Formation in NW Muglad Basin comprise three heavy mineral zones: The ultrastable heavy minerals zircon, tourmaline and

rutile characterize the first zone. The second zone is characterized by the presence of the rather unstable heavy minerals sillimanite, epidote and hornblende, and she related this zone to the second rifting phase. The third zone is characterized by the metastable heavy minerals kyanite and garnet. She concluded that the source rocks are mainly metamorphic rocks. A'amir (2000), in his study of the Cretaceous sandstones outcropping at the NE margin of the Muglad Rift Basin, found that the sediments are characterized by relatively high ZTR index and attributed this to a prolonged abrasion and/or diagenesis which reduced the amount of the unstable and the metastable heavy minerals grains and hence, increased the ratios of the ultrastable heavy minerals in the sediments. Furthermore, he suggested that the source rocks of these sediments must have been mainly metamorphic rocks of acidic nature, which were subjected to intensive chemical weathering and physical reworking processes.

In the sediments of the present study, the ZTR index is generally low. Kyanite and garnet form the dominant heavy minerals. This indicates mainly metamorphic source rocks of acidic nature for the sediments of the study intervals. However, the difference between the heavy minerals zones of this study and the studies carried out by Bakr (1995), Mohammed (1997), Maarouf (1998) and A'amir (2000) could be due to differences in the studied subbasins, which were subjected to different weathering, transportation and diagenetic conditions.

# Plate 6.1

a, b and c      X100, X100 and X50 subrounded to rounded zircon grains with light core and small inclusions from the studied strata in Unity-9 and Talib-2 wells at Unity Field indicating a relatively long distance of transport as well as relatively strong reworking effects.

d and e      X50 subangular to angular zircon grains with sharp edges from the studied intervals in Heglig-2 and Toma-1 wells at the Heglig Field suggesting a relatively short distance of transport and/or moderately reworking effects

f and h      X100 acicular to columnar green-yellowish green tourmaline grains with irregular edges from the lower horizon of Aradeiba Formation in the Heglig-2 well and also from the lower strata of Zarga Formation in Barki-1 (Heglig Field) suggesting moderately reworked sediments, which most probably had come from gneisses and schists source rocks.

g      X50 rounded brown-reddish brown tourmaline from the Bentiu Formation in the Unity Field studied wells showing dissolved edges due to the relatively long distance of transport and/or intrastratal solution effects.

i      X50 subrounded brown-reddish brown tourmaline from the upper part of Bentiu Formation in Heglig Field studied wells indicating most probably gneisses and schists source rocks.

j      X100 tabular light blue tourmaline grain seen only in some samples from the Aradeiba Formation in Nabaq-1 and Heglig-2 wells indicating most probably some pegmatite veins occurred within the source rocks.

k, l, m and o      X100, X100, X50 and X100 subrounded to rounded red to reddish brown rutile grains from the studied strata in the Unity Field indicating reworked sediments most probably had come from metamorphic source rocks.

n      X100 prismatic yellowish brown rutile from the studied strata in the Heglig Field suggesting moderately reworked sediments most probably had come from metamorphic source rocks.

p, q and r      X100, X100 and X50 etched kyanite grains from the studied intervals in Heglig and Unity Fields showing alteration along the edges and cleavages, which was due to the action of intrastratal dissolution.
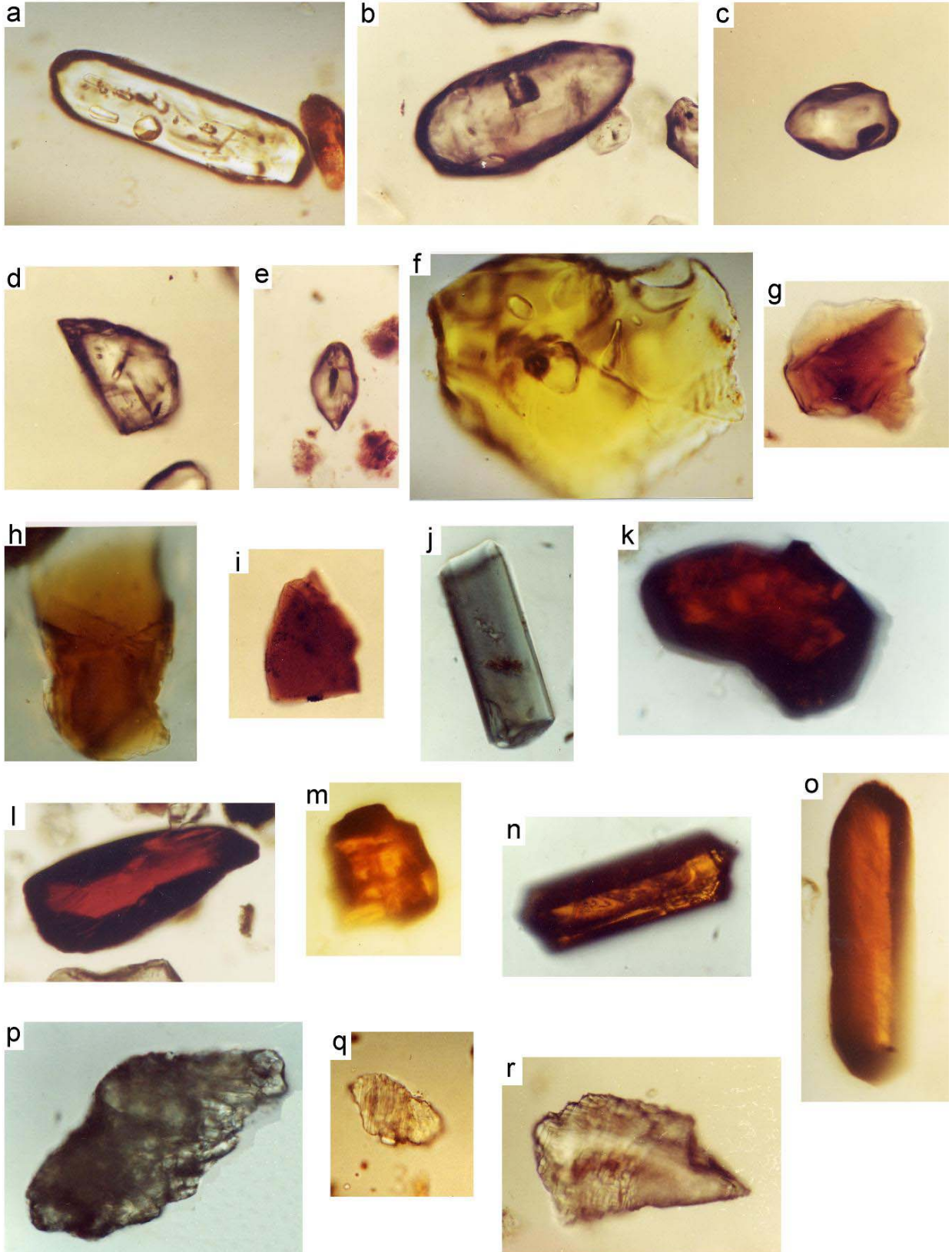
# Plate 6.1

# Plate 6.2

a – e  X100, X100, X50, X100 and X50 subangular to angular staurolite grains from the studied sediments of the two fields indicating most probably schists and/or gneissic source rocks.

f  X100 subrounded to rounded analusite grain covered partially by iron oxides from the Aradeiba Formation in the Talih-2 well at Unity Field suggesting most probably gneisses and/or schists as source rocks.

g  X50 subrounded andalusite grain from the Bentiu Formation in Toma-1 well at Heglig Field suggesting most probably gneisses and/or schists as source rocks.

h  X50 subrounded to rounded andalusite grains covered by iron oxides from the Zarga Formation in Unity-9 well at Unity Field suggesting most probably gneisses and/or schists as source rocks.

i, j and k  X100, X50 and X100 prismatic and felted mass fibrous grains of sillimanite from the studied strata in the Heglig Field indicating metamorphic source rocks.

l  X100 prismatic sillimanite dissolved grain from the Aradeiba Formation in Unity-9 well indicating the effect of intrastratal dissolution.

m and q  X100 and X50 subangular reddish brown garnet grains from the Bentiu Formation in Heglig-2 well and from the Aradeiba Formation in Toma-1 well (Heglig Field) indicating moderately reworked sediments, which most probably had come from metamorphic source rocks.

n  X100 angular light green garnet grain from the Zarga Formation in Nabag-1 well in Heglig Field suggesting moderately reworked sediments, which most probably had come from metamorphic source rocks.

o and p  X50 and X100 subrounded to rounded green to yellowish green garnet grains from the Aradeiba Formation in Unity-9 well at Unity Field indicating a relatively long distance of transport.
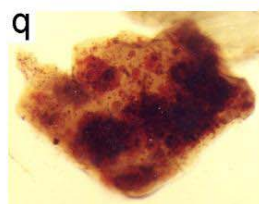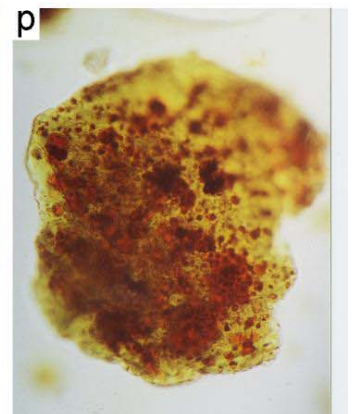
# Plate 6.2
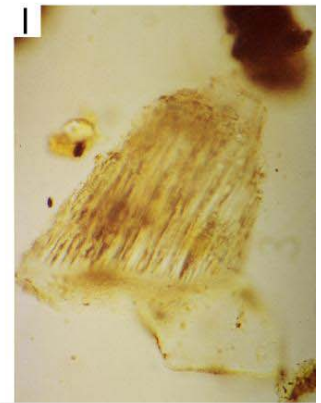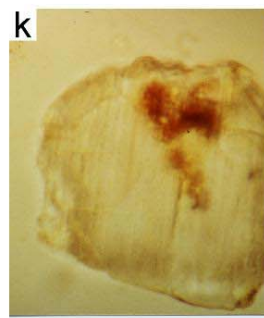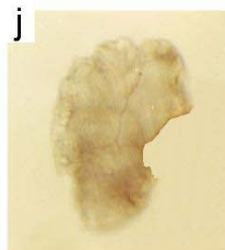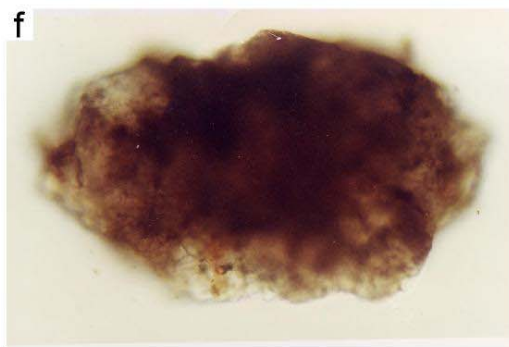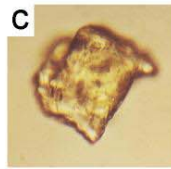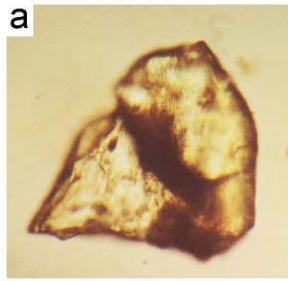
# Plate 6.3

a, b and c      X50, X100 and X100 yellowish green to brownish green epidote grains from the upper strata of Bentiu Formation in Heglig-2 well and from the Aradeiba Formation in Unity-9 well as well as from the Zarga Formation in Nabag-1 well suggesting most probably metamorphic source rocks.

d, e and f      X100, X100 and X100 long prismatic green, brown and yellowish green hornblende grains from the Zarga Formation in Talih-2 well, from the Aradeiba Formation in Unity-9 well and from the Bentiu Formation in Heglig-2 well suggesting most probably metamorphic source rocks.

g and h      X50 and X50 subrounded to rounded blue to greenish blue glaucophane-riebeckite grains from the lower strata of Zarga Formation at Nabag-1 well indicating most probably glaucophane-riebeckite schists as source rocks.

# Plate 6.3
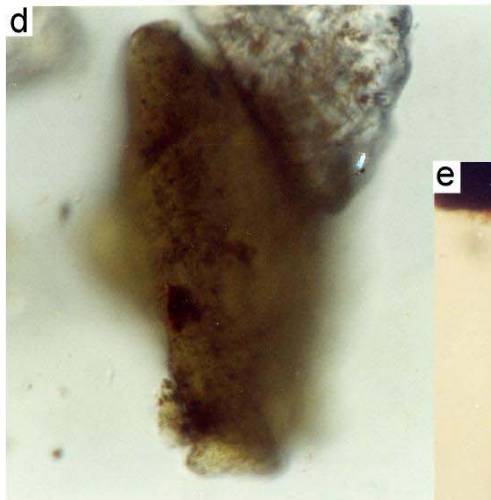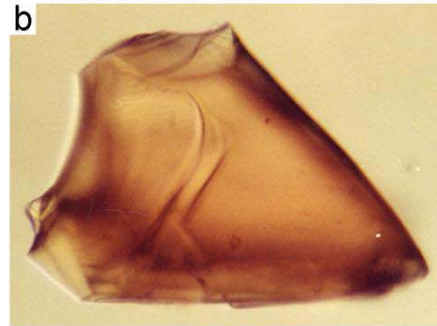
# 7 Clay Minerals and Geochemical Analyses

## 7.1 Clay Mineral Analysis

### 7.1.1 Introduction

The study of the clay minerals has involved two analytical techniques, X-ray diffraction and Scanning Electron Microscopy (SEM). Sixty-four clay rich samples from the study intervals of the six wells in the two fields have been analysed with the XRD technique. In addition twenty-one mudstone, claystone and sandstone core samples from four wells have been examined by with SEM. Five clay mineral species were identified from the size fraction of less than 2 micron using the procedures of Chamley (1989) and Moore and Reynolds (1997). A quantitative estimate of the clay mineral composition were computed mainly from the ethylene-glycol solvated XRD patterns as suggested by Schwertmann et al. (1993). The results obtained are shown in Appendices 2A and 2B. These results are presented in Figures 7.1, 7.2, 7.3, 7.4, 7.5 and 7.6 in order to reveal the vertical distribution of the clay minerals along each study interval. In addition some XRD graphical charts are shown in Figure 7.7 in order to give a general impression of the degree of crystallinity for these clay minerals. Furthermore, some SEM micrographs are given in Plates 7.1, 7.2, and 7.3.

### 7.1.2 Kaolinite

Kaolinite is identified by its 7.1 Å and 3.58 Å peaks in the air dried X-ray diffraction patterns, wich are unaffected by the ethylene glycol treatment but are destroyed after heating to 550°C (Chamley 1989; Moore and Reynolds 1997). The clay mineral kaolinite was recorded in all of the investigated samples with variable percentages ranging between 8 – 81% (Appendices 2A and 2B). Some of the kaolinite appears in the SEM micographs as pseudohexogonal books arranged face-to-face into an elongated stacked form called "verm" (Plate 7.1 b,c,d,e & f). This vermiform morphology, combined with the typical kaolinite EDX specturm which was observed during the SEM analysis, provide an easy diagnosis for kaolinite (Joann, 1984). However, other SEM micrographs show eroded crystalls of kaolinite (Plate 7.1 a). In some of the SEM micrographs the pseudohexogonal plates or books of the kaolinite fill the pores between the detrital grains (Plate 7.1 d). Some of these books are separated and others are linked by ribbons or sheets of illite, illite/smectite mixed-layer, smectite and chlorite minerals (Plate 7.1 e).

According to Chamley (1989), kaolinite mainly forms in surfacial environments through pedogenetic processes. It may also form in lacustrine environments from the alteration of K-feldspar in acid organic-rich pore waters (Tucker, 1991). Moreover, hydrothermal alteration of alumosilicates, especially of feldspars, may also form kaolinite (Moore & Reynolds, 1989). According to Keller (1956) and Weaver (1989), kaolin minerals require for their formation the efficient removal of the metal cations and presence of $H^+$ ions. These conditions are favoured by strong leaching in the source area, which implies abundant rainfall, permeable rocks and favourable topography, and hence, evacuation of the Ca, Mg, Na and K ions. Climatic conditions favourable for the formation of kaolin minerals are essentially tropical and subtropical.

The vermiform morphology besides the sharp peak patterns of the kaolinite in some of the XRD charts (Fig. 7.7 a) indicate that part of the kaolinite is monocrystalline (Pettijohn, 1975; Weaver, 1989), which means it has authigenically formed. The vermiform morphology was formed due to the complete alteration of the K-feldspar in the organic-rich horizons e.g. noted in the SEM micrographs for the samples from Bentiu Formation in Heglig-2 and Unity-9 wells (Plate 7.1 c & f). However, some of the kaolinites in the studied intervals are detrital, as noted in the SEM micrograph of a sample from Aradeiba Formation in Talih-2 well (Plate 7.1 a). The detrital nature of the kaolinite is supported by the relatively flated kaolinite peaks in some of the XRD charts (Fig.7.7 b).

### 7.1.3  Illite

Illites were identified by their basal diffraction at about 10 Å, which is neither affected by ethylene glycol treatment nor by heating. However, some illite clay minerals may show expandability of approximately up to 5 % (Chamley 1989; Moore and Reynolds 1997). Illite occurs in most of the examined samples throughout the study intervals. Its concentration ranges between 0 – 46 % (Appendices 2A & 2B). These concentrations are higher in the strata of the upper part of Bentiu Formation in Unity-9, Barki-1 and Heglig-2 wells as well as in the strata near the middle part of Aradeiba Formation in Barki-1 and Talih-2 wells (Figs 7.1, 7.2, 7.3 and 7.4). In some SEM micrographs illite appears as irregular flake-like clay platelets forming a "scalloped" habit (Plate 7.2 a & b). The "scalloped" habit and the typical illite EDX specturm provide an easy diagnosis for the illite (Keller et al., 1986). In other SEM micrographs, illite appears as thin filamentous ribbons forming a mat, partially coating detrital

grain surfaces and also bridging the pores and hence creating permeability barriers to fluid flow (Plate 7.2 c & d).

According to Moore & Reynolds (1989) and Chamley (1989), illite is considered to have more Si, Mg and $H_2O$ but less Al-tetrahedal layer and less K-interlayer than muscovite. It is principally formed where the parent rocks are essentially acid igneous or their metamorphic equivalents. Illite is not present in sedimentary rocks derived from basic rock terrain. Rarity of rainfall and hot climate conditions favour the detrital formation of illite. However, the diagenetic replacement of muscovite by illite is favored in clean washed sands but that of feldspar by illite instead of kaolinite appears to be favored by ion-enriched, less acidic pore waters.

The "scalloped" habit of the illite, which was noted in some SEM micrographs of samples from the Aradeiba Formation in Unity-9 well as well as for samples from the Zarga Formation in Talih-2 well indicates, that part of the clay mineral illite in the studied intervals is detrital and formed during intermittent hot dry periods, which had prevailed at the source area (Plate 7.2 a & b). However, part of the illite content was formed authigenically due to the transformation of smectite to illite by burial diagenesis, which resulted in the increase of the illite content in the upper part of Bentiu Formation in Unity-9, Barki-1 and Heglig-2 wells as well as in the strata near the middle part of Aradeiba Formation in Barki-1 and Talih-2 wells (e.g. Plate 7.2 c & d). Also authigenic formation of illite by the alteration of muscovite and feldspar can not be excluded.

### 7.1.4  Smectite

Smectite occurs generally in much lesser amount in comparison to kaolinite. The mineral was determined after the glycolation, when the d-spacing of its basal reflection (001) expands from 15 Å in the normal pattern to 17 Å in the ethylene-glycol solvated pattern (Chamley 1989; Moore & Reynolds 1997). The concentration of smectite in the investigated samples varies between 0 – 50 % (Appendices 2A & 2B). Higher amounts are restricted to the strata near the middle part of Aradeiba Formation in Unity-9 well as well as to the upper part of Aradeiba Formation in Talih-2 and Nabag-1 wells (Figs. 7.1, 7.2 and 7.6). However, its content usually decreases downward with depth.

The morphology of the smectites under the scanning electron microscope resemble "corn-flakes", "maple leafs" or "honeycombs" forming a thin webby crust (Plate 7.3 a). This

webby morphology is distinctive but not unique to smectite (Joann, 1984; Keller et al., 1986). Therefore, the identification of this clay mineral was mainly based on the X-ray diffraction analysis, EDX analysis and then supported by the above habits. The webby crust occurs as a pore-lining mat and sometimes bridges across the pore throats (Plate 7.3 b, c & d), thus reduces the permeability by inhibiting free fluid flow.

According to Weaver (1989) "the climatic and the topographic conditions necessary for the formation of smectite are basically the opposite to those wich favour the formation of kaolinite". Smectite is generally formed in low relief areas where poor drainage prevents the silica and the alkaline earth ions such as $K^+$, $Na^+$, $Ca^{+2}$ and $Mg^{+2}$ from being rapidly removed. Smectite normally develops from the weathering of basic and ultrabasic rocks or their metamorphic equivalents in areas of low rainfall, low water flux and low temperature.

The peaks of the smectite are not sharp as those of the kaolinite, thus this indicates that part of the smectite is polycrystalline (Fig. 7.7 c), which implies a detrital origin. This detrital smectite was formed during intermittent hot dry periods, which had prevailed at the source area. However, other part of the smectite was formed authigenically. The bridging by the smectite webby crust, as seen in the micrographs of samples from the Aradeiba Formation in Talih-2 well and from the Bentiu Formation in Toma-1 well (Plate 7.3 c & d), provides evidence for the authigenic formation of the smectite, sourced by alteration of feldspar and mica. The general decrease of the smectite with increasing depth could be explained by the transformation of smectite to illite.

## 7.1.5  Mixed-Layer Illite/Smectite (I/Sm)

Moore and Reynolds (1997) mentioned three indicators that are crucial for the correct identification and estimation of the mixed-layered illite/smectite: Firstly, the diffraction pattern of the air dried illite/smectite is altered significantly by solvation with ethylene glycol, and such behaviour leads to the provisional identification of illite/smectite. Heating to 350° C for one hour provides confirmation of the identification; the result is a diffraction pattern similar to that of illite. Secondly, the ordering type (Reichweite) is determined by the position of the reflection between 5 and 8.5° 2θ for EG-solvated preparations. Thirdly, the percent of illite can be determined by the position of the reflection near 16 to 17° 2θ, but a better way is to base the estimate on a value for Δ 2θ in the standard Moore and Reynold table.

The mixed-layer illite/smectite clay minerals were encountered in most of the examined samples from the six studied wells and reach a amount of up to 59 % at Aradeiba Formation in Heglig-2 well (Fig. 7.4 & Appendix 2B). Under the scanning electron microscope, the morphology and texture of the illite/smectite mixed layer minerals appear as mixture between a "honeycomb" morphology which is due to the smectite and filamentous ribbons, which is due to the illite. Examples are present in the SEM micrograph of the sample from Aradeiba Formation in Talih-2 well and in the SEM micrograph of the sample from Bentiu Formation in Toma-1 well (Plate 7.2 c & 7.3 d).

The mixed layer I/Sm clay minerals might have formed by the illitization of the smectite layers due to organic acids which had destroyed smectite during burial diagenesis (Chamley, 1989). Several workers have found a close relation between smectite illitization and organic matter maturation (Johns and Shimoyama, 1972; Heroux et al., 1979). The I/Sm transformation has been used as a thermal maturity indicator (Tissot et al., 1987). However, the use of the expandable smectite layers in assessing the thermal maturity of the sediments is a less sensitive method. This is because the smectite transformation during burial diagenesis is controlled by various factors other than temperature and depth of burial (Tissot et al., 1987).

### 7.1.6 Chlorite

The characteristic basal spacing for the clay mineral chlorite is close to 14 Å. Swelling chlorites or pseudo-chlorites expand like smectites when immersed in water or ethylene glycol, but resist heating, where the d-spacings are kept constant at 14 Å and 7 Å for the reflections (001) and (002) respectively.

The concentration of chlorite in the clay mineral fraction of the examined samples ranges between 0 – 18 % (Appendices 2A & 2B). Chlorite appears only in some SEM micrographs, as clusters of "disc-like" chlorite crystals partly filling depressions within detrital grains (Plate 7.4 a & b). Other chloride platelets are stacked face-to-face in a rare beehive-like structure (Plate 7.4 c arrow). Moreover, the SEM analysis has confirmed some chloritization of biotite (Plate 7.4 d ), where the pore-fill consists mostly of individual chlorite flakes oriented face-to-face and aligned parallel to original biotite cleavage planes. Identification of the pore-filling mineral as chlorite was based on the EDX spectrum during the SEM analysis.

Chlorites are considered either as a 2:1 layer group with a hydroxide interlayer, or as a 2:1:1 layer group. Their typical structure shows a regular alternation of negatively charged trioctahedral micaceous layers and of positively charged octahedral sheets. Chlorites are common constituents of low-grade metamorphic rocks. They are less common in igneous rocks, where they occur as hydrothermal alteration products of ferromagnesian minerals. Moreover, they may be formed authigenically as a direct by-product of the smectite to illite transformation, utilizing iron and magnesium released from smectite, diffused at proximity and reprecipitated together with silica supplied from smectite or other detrital silicates (Chamley, 1989).

Part of the chlorite in the studied intervals is detrital, which derived from biotite-rich metamorphic source rocks during periods of a hot and dry palaeoclimate. However, the other part is authigenic formed by the alteration of biotite as has been confirmed in the SEM micrographs from the Aradeiba Formation in Heglig-2 well (Plate 7.4 d). The stacked face-to-face "beehive-like" structure of the chlorite platelets indicates a authigenic formation, e.g noted in the SEM micrograph for the sample from the Aradeiba Formation in Talih-2 well (Plate 7.4 c). However, chlorite was also formed as a direct by-product of the smectite to illite transformation.

## 7.1.7  Distribution of Clay Minerals in the Studied Formations

The clay mineral analysis reveals that the sediments of the upper part of Bentiu, all of Aradeiba and the lower part of Zarga Formation essentially contain five major clay mineral types which are kaolinite, mixed layer illite/smectite, illite, smectite and chlorite. Factors which affect the distribution of clay minerals were studied e.g. by Keller (1956), Wilson et al. (1977), Weaver (1989) and Chamley (1989). All of them agree, that the roles of climate and source area lithology are essential controlling factors in the formation of clay minerals. Furthermore, the geothermal gradient, pressure, permeability, tectonics and pore fluid circulation play important roles in the formation of some clay minerals such as the transformation of smectite to illite or chlorite and the alteration of K-feldspar to kaolinite. Such controlling factors will be discussed later.

## 7.1.8  Vertical Distribution of the Clay Minerals in the Studied Formations

Unity and Heglig Fields are represented by six wells. The samples provide a good vertical and lateral coverage of the different lithostratigraphical units of the study intervals in the two

fields. The distribution of the clay minerals in the wells of the two fields are generally similar. However, the clay minerals assemblages in the wells of the two fields can be classified into two different groups. The first group includes Unity-9 and Talih-2 wells of Unity Field (Figs. 7.1 & 7.2), whereas the second one comprises Heglig-2, Toma-1 and Nabag-1 wells of Heglig Field besides Barki-1 well of Unity Field (Figs.7.3, 7.4, 7.5 & 7.6). Each group of wells is characterized by similar clay minerals assemblages.

### 7.1.8.1  Unity-9 Well

The clay mineral assemblages of the study intervals in Unity-9 well (Fig. 7.1) consist of kaolinite, illite/smectite mixed-layer, illite, smectite and chlorite. Their amounts are given in Appendix 2A. In this well three clay mineral zones could be recognized. Each zone reflects different percentages of the five clay minerals. The lower and the upper boundaries of these zones seem to coincide with the already established lithostratigraphic boundaries as has been determined by lithofacies criteria. The lower zone which extends from the upper part of Bentiu Formation up to a depth of 8420 f, consists of kaolinite (36 – 76 %), I/Sm mixed-layer (8 – 36 %), illite (16 – 32 %), smectite (0 – 7 %) and chlorite (0 – 6 %). The middle zone ranges from a depth of 8420 ft up to 7720 ft . This zone comprises kaolinite (23 – 67 %), smectite (3 – 41 %), I/Sm mixed-layer (9 – 33 %), illite (0 – 20 %) and chlorite (0 – 6 %). The upper clay minerals zone which begins from the depth of 7720 ft up to the lower part of Zarga Formation, consists of kaolinite (25 – 68 %), illite (6 – 26 %), I/Sm mixed-layer (16 – 22 %), chlorite (0 – 9 %) and smectite (0 – 6 %).

### 7.1.8.2  Talih-2 Well

The distribution of the clay mineral assemblages of the study intervals in this well is similar to that of Unity-9 well (Fig. 7.2). These clay minerals are kaolinite, I/Sm mixed-layer, illite, smectite and chlorite. Their occurrences are provided in Appendix 2A. As in the study intervals at Unity-9 well, three clay mineral zones could be established. The lower zone covers the upper part of Bentiu Formation and extends up to a depth of 8450 ft. This zone consists of kaolinite (36 – 77 %), I/Sm mixed-layer (6 – 40 %), illite (5 – 14 %), smectite (0 – 6 %) and 2 – 4 % chlorite clay minerals. The middle zone, which characterizes the middle and the upper part of Aradeiba Formation, was identified within the depth interval of 8450 – 7910 ft. This clay mineral zone contains 0 – 50 % smectite, 8 – 41 % kaolinite, 3 – 39 % I/Sm mixed-layer, 0 – 38 % illite and 0 – 13 % chlorite. The upper zone begins from a depth of

7910 ft and extends upward till the lower part of the Zarga Formation. It contains 32 – 71 % kaolinite, 14 – 28 % I/ Sm mixed-layer, 0 – 32 % smectite, 0 – 15 % illite and 5 – 8 % chlorite.

### 7.1.8.3  Barki-1 Well

The above mentioned five clay minerals are present also in the study intervals at Barki-1 well (Fig.7.3). Their amounts are given in Appendix 2A. According to the vertical distribution of the clay minerals, two clay mineral zones could be recognized. The first zone covers the upper part of Bentiu Formation and extends throughout the lower and the middle part of Aradeiba Formation up to a depth of 4650 ft, whereas the second zone extends from this depth upwards to cover the upper part of Aradeiba and the lower part of Zarga Formation. The differences between the two zones are that: the lower zone contains 23 – 71 % kaolinite, 5 – 46 % illite, 0 – 30 % I/Sm mixed-layer, 0 – 18 % chlorite and 0 – 17 % smectite, whereas the upper zone consists of kaolinite (35 – 55 %), smectite (15 – 28 %), I/ Sm mixed-layer (22 – 23 %), illite (8 – 12 %) and chlorite (0 – 2 %).

### 7.1.8.4  Heglig-2 Well

The clay mineral assemblage of the study intervals in Heglig-2 well (Fig. 7.4) is similar to that of Barki-1 well. These clay mineral assemblages include kaolinite, I/Sm mixed-layer, illite, chlorite and smectite. The clay mineral abundances are shown in Appendix 2B. The study of the clay minerals in this well allows the  recognition of two major clay minerals zones as in Barki-1 well. The first zone, which covers the upper part of the Bentiu Formation and extends throughout the whole of the Aradeiba Formation, contains 22 – 77 % kaolinite, 2 – 59 % I/Sm mixed-layer, 4 – 28 % illite, 2 – 13 % chlorite and 0 – 4 % smectite. The second one characterizes the lower part of the Zarga Formation and contains 36 – 48 % kaolinite, 21 – 30 % smectite, 18 – 26 % I/Sm mixed-layer, 4 – 15 % illite, and 0 – 3 % chlorite.

### 7.1.8.5 Toma-1 Well

The recognized clay minerals in this well (Fig. 7.5) are kaolinite, I/Sm mixed-layer, illite, smectite and chlorite. The percentages of these clay minerals are given in Appendix 2B. Similar as in Barki-1 and Heglig-2 wells, two major clay mineral zones are recognized in this well. The first one covers the upper part of Bentiu Fomation as well as the lower and the middle parts of Aradeiba Formation. This zone comprises 34 – 78 % kaolinite, 15 – 52 % I/

Sm mixed-layer, 4 – 7 % illite, 2 – 8 % chlorite and 0 – 5 % smectite. The second zone covers the upper part of Aradeiba and the lower part of Zarga Formations. This zone contains 24 – 69 % kaolinite, 23 – 27 % I/ Sm mixed-layer, 2 – 30 % smectite, 4 – 13 % illite and 0 – 6 % chlorite.

### 7.1.8.6 Nabag-1 Well

The clay mineral assemblage of the study intervals in Nabag-1 (Fig. 7.6) consists of kaolinite, I/Sm mixed-layer, illite, smectite and chlorite. The percentages of these clay minerals are provided in Appendix 2B. Similar to the above three wells, two clay mineral zones can be recognized. The lower one covers the upper part of the Bentiu Formation and greater part of the Aradeiba Formation up to a depth of 4630 ft . This zone contains 56 – 81 % kaolinite, 11 – 36 % I/Sm mixed layer, 6 – 12 % illite, 0 – 2 % chlorite; it does not contain smectite. The upper zone extends from a depth of 4630 ft upwards to cover the upper part of Aradeiba and the lower part of Zarga Formations. It comprises 19 – 68 % kaolinite, 14 – 37 % smectite, 12 – 29 % I/Sm mixed layer, 6 – 20 % illite and 0 – 4 % chlorite.

**Figure 7.1: Vertical distribution of clay inerals and some major and trace elements in the upper Bentiu, Aradeiba and lower Zarga Formations at well Unity-9, Unity Field, SE Muglad Basin.**



Note: For legend see Fig.(7.1)

**Figure 7.2: Vertical distribution of clay minerals and some major and trace elements in the upper Bentiu, Aradeiba and lower Zarga Formations at well Talih-2, Unity Field, SE Muglad Basin.**

144

**Figure 7.3: Vertical distribution of clay minerals and some major and trace elements in the upper Bentiu, Aradeiba and lower Zarga Formations at well Barki-1, Unity Field, SE Mugald Basin.**



**Figure 7.4: Vertical distribution of clay minerals and some major and trace elements int he upper Bentiu, Aradeiba and lower Zarga Formations at well Heglig-2, Heglig Field SE Muglad Basin.**

**Figure 7.5: Vertical distribution of clay minerals and some major and trace elements int he upper Bentiu, Aradeiba and lower Zarga Formations at well Toma-1, Heglig Field, SE Muglad Basin.**
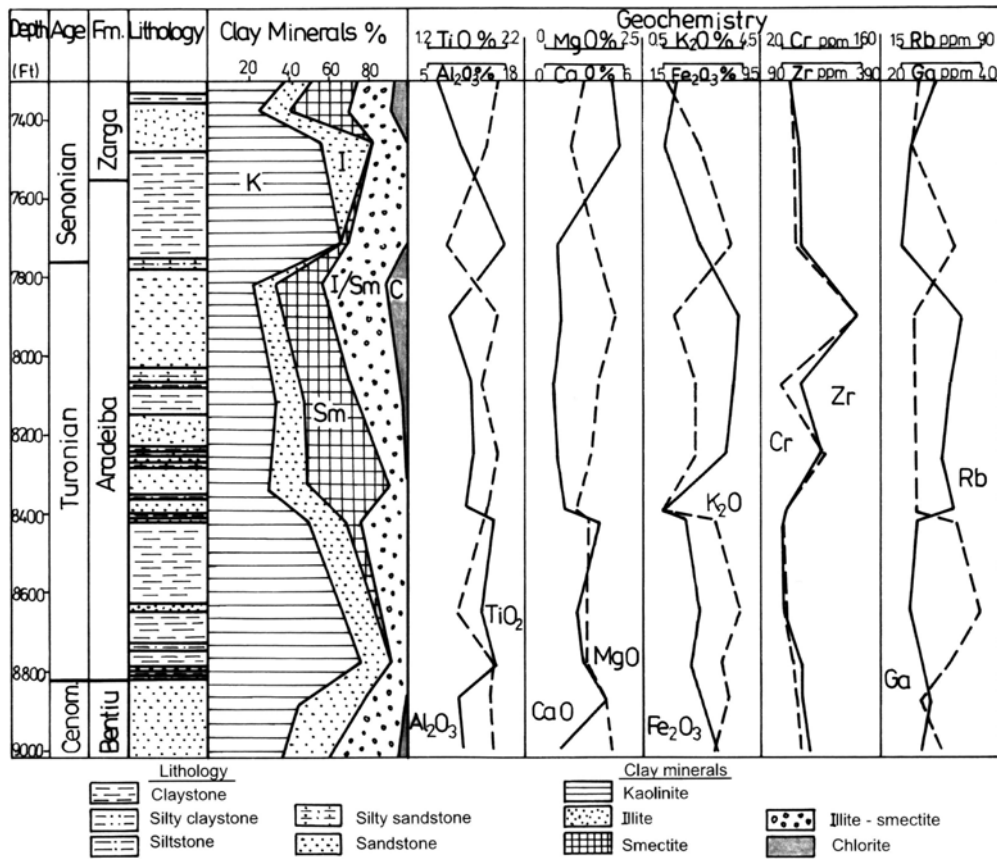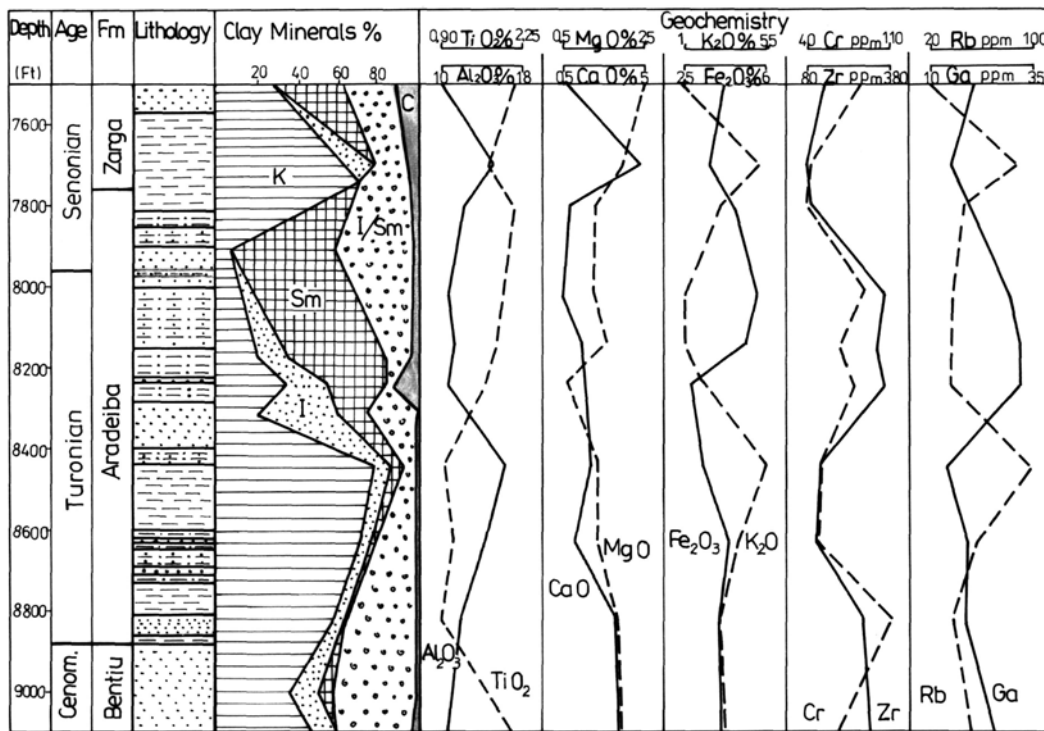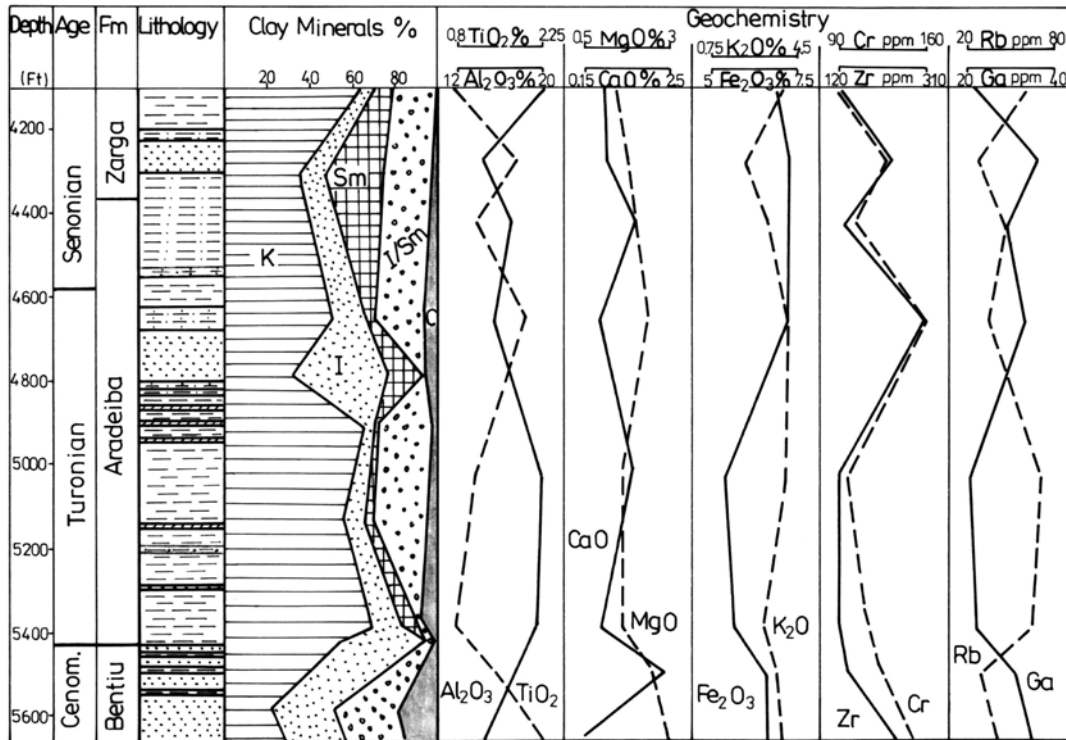


**Figure 7.6: Vertical distribution of clay minerals and some major and trace elements in the upper Bentiu, Aradeiba and lower Zarga Formations at well Nabag-1, Heglig Field, SE Muglad Basin.**
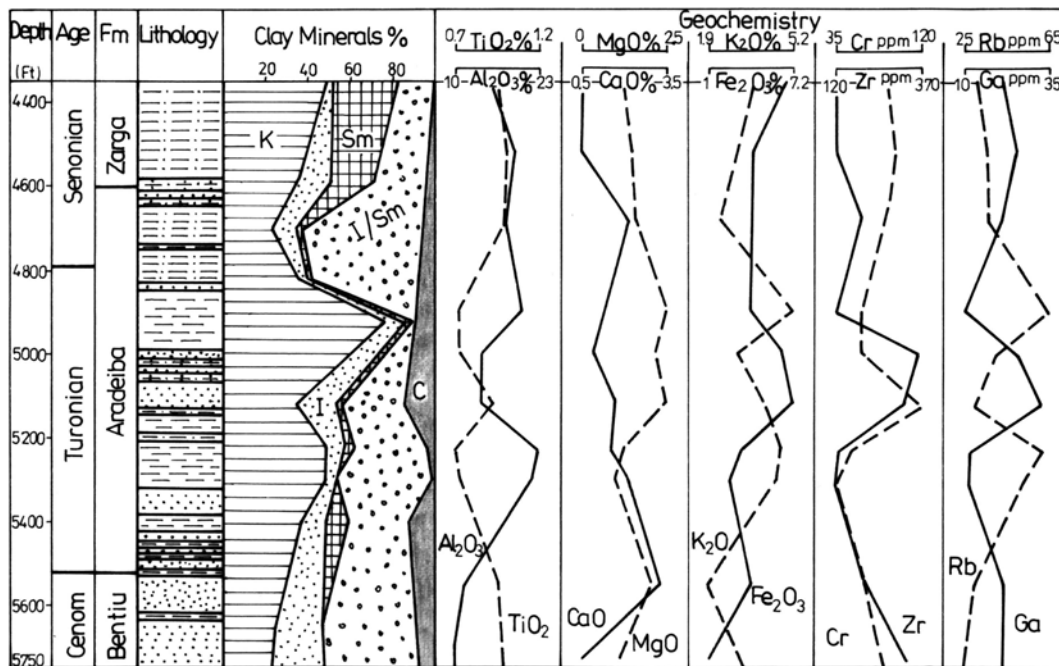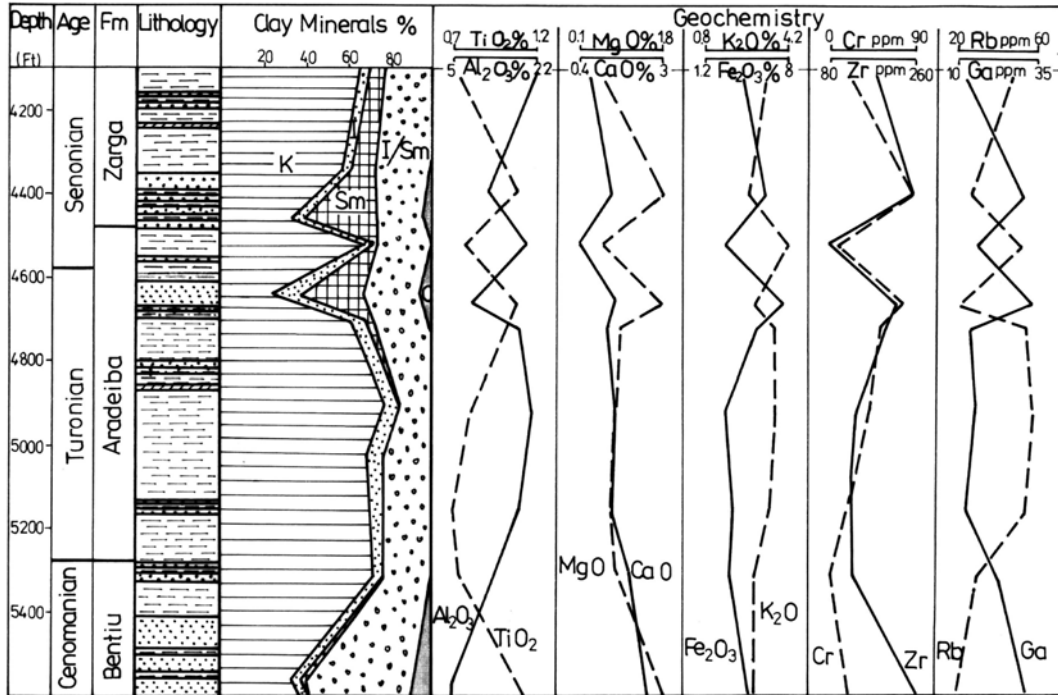
## 7.2 Geochemical Analysis

### 7.2.1 Introduction

Igneous petrographers attach a great deal of significance to the chemical composition of igneous rocks and have used them as the basis of many classifications, but few authors have given attention to chemical composition as a basis for classifying sandstones, e.g. Pettijohn et al. (1987). There are two main reasons for this: the high cost of chemical analyses, and sedimentary petrographers believe that mineralogical and textural distinctions visible in thin section are more fundamental and important than chemical composition (Blatt et al., 1980). However, in fine grained sedimentary rocks such as shale and mudstone, heavy mineral analysis and thin sections are difficult to be made. Therefore, geochemical analysis of characteristic elements can provide excellent indications about weathering processes, petrographic provinces, depositional environments and diagenetic processes (Bjorlykke & Englund, 1979). Moreover, modern techniques have greatly reduced the cost of chemical analysis to a point where it actually costs less for a skilled analyst to make a reliable chemical analysis than it does for a skilled petrographer to make a reliable modal analysis (Blatt et al., 1980). Thus as mentioned earlier, the results of the XRF analysis are used in this chapter for the recognition of the petrographic provinces of the study intervals and to throw light on weathering, depositional environment and diagenetic processes that occured during and after the deposition of the studied sediments.

### 7.2.2 Results

The geochemical data in the present work are presented in Appendices 3A & 3B, which show the concentrations of 20 major and trace elements in the studied intervals of the six studied wells at Unity and Heglig Fields. Ten elements were plotted along the study interval in each of the studied wells combined with the clay minerals in order to show the vertical variations of these elements with depth as well as to throw light on the relation between the distribution of the clay minerals and the concentration of these elements (Figs. 7.1, 7.2, 7.3, 7.4, 7.5 and 7.6).

Two important aspects of the data are considered: the co-variation of elements concentrations relative to each other and the compositional variation of the clay minerals between the studied strata in the two fields. The above two aspects are then used to induce the

factors controlling the chemical composition, depositional environments and the nature of the source rocks for the studied sediments of the two fields.

### 7.2.2.1 Major Elements

Major elements deserve a considerable attention because their study when combined with a careful clay mineralogy, petrography and heavy mineral analyses can be useful for interpreting the history of sedimentary formation (Krauskopf, 1979). The geochemistry of the major elements is discussed below.

The present analysis shows differences in Si-concentration between the studied sediments of the two fields. The average Si concentration of the study intervals in Unity Field wells (Unity-9, Talih-2 and Barki-1 wells) are 62.9 %, 63.3 % and 57.9 % respectively, whereas the average concentration of the study intervals in Heglig Field wells (Heglig -2, Toma -1 and Nabag -1 wells) are 58.3 %, 58.8 % and 53.4 % respectively (Appendices 3A & 3B). According to Hirst (1962), the "free $SiO_2$" is of very fine grain size and thus may represent very fine detrital quartz dust or recrystallized colloidal $SiO_2$. Krauskopf (1979) stated that $SiO_2$ in true solution is more common than colloidal $SiO_2$. On the other hand, Manson (1966) suggested that 95 % of the $SiO_2$ content of the weathering product remains in the solid state. Thus, the relatively higher concentration of $SiO_2$ in the studied sediments of Unity Field at Unity-9 and Talih-2 wells in comparison with the concentration of the $SiO_2$ in the studied sediments of Heglig Field confirms what has been stated before in the clay mineralogy section, about the high occurrence of smectite in the studied sediments of Unity Field at Unity-9 and Talih-2 wells (Figs. 7.1 & 7.2) and these could be interpreted due to the greater amount of deltaic mouth bar sediments in the studied intervals of Unity-9 and Talih-2 wells in comparison with the studied intervals of Heglig Field rather than differences in the source rocks. Moreover, from the facies and the petrographical analyses one can suggest, that the $SiO_2$-content in Unity and Heglig Fields sediments represents mainly detrital quartz dust and to a lesser extent precipitated colloidal silica deposited in fluvial, deltaic and lacustrine environments.

$Al_2O_3$ is concentrated in higher amounts in the studied sediments of Heglig Field at Heglig-2, Toma-1 and Nabag-1 wells (average 16.6 %, 13.1 % and 21 % respectively) (Appendix 3B) compared to the studied sediments of Unity Field at Unity-9, Talih-2 and Barki-1 wells (average 12.3 %, 12.4 % and 16.9 % respectively) (Appendix 3A). This

variation is in agreement with the variation of the clay minerals in the sediments of Unity and Heglig Fields (Figs.7.1, 7.2, 7.3, 7.4 and 7.6). Therefore, it is possible that the type and the amount of the clay minerals deposited, and further, the amount of substitution for Al in the octahedral positions are the most important factors for the final Al content. Hence, the relatively low concentration of Al in Unity Field sediments can be attributed to relatively high amounts of smectite in Unity Field sediments compared to that of the Heglig Field sediments. Smectite is characterized by a low Al/Si ratio and a considerable substitution of $Al^{+3}$ by $Fe^{+3}$ and $Mg^{+2}$ in the octahedral positions (Chamley, 1989).

The element titanium (Ti) was recorded as titanium oxide ($TiO_2$) in low concentrations of not more than 2.5 % (Appendices 3A & 3B). Titanium average contents of the studied sediments in the two fields show two characteristics associated with this element. Firstly, the element generally increases in the studied sediments of the Unity Field wells. Secondly, depletion of Ti in the distal facies environments (lakes or floodplains) in Heglig-2 and Toma-1 wells is strongly noticed (Appendices 3A & 3B and Figs. 7.1, 7.2, 7.3, 7.4 and 7.5). According to Mason (1966), the chemical element Titanium is regarded as having a low mobility during chemical leaching of the source area, hence tending to concentrate preferentially in the proximal facies environments, as it is noticed in the studied sandstone strata of the fluvial channel bars and the deltaic mouth bars in the two fields (Appendices 3A & 3B). These high concentrations in these proximal strata are correlated with the increase of the heavy mineral rutile in the same strata. Therefore, these strata are supposed to be derived mainly from metamorphic rocks, particularly schists and/or gneisses (Mange and Maurer, 1992).

The concentration of $K_2O$ is generally higher compared to that of CaO and $Na_2O$ in most of the analysed samples (Appendices 3A & 3B). Although Potassium has scored some higher concentrations in the studied sediments of Unity Field wells, but its average concentration in these sediments is lower in comparison to its average concentrations in the studied sediments of Heglig Field. The average concentration of $K_2O$ in the studied sediments of Heglig Field is 3.56 % in Heglig-2 well, 3.27 % in Toma-1 well and 2.82 % in Nabag-1 well (Appendices 3B & Figs. 7.4, 7.5 and 7.6), its average concentration in the studied sediments at Unity Field wells is 2.49 % in Unity-9 well and 2.77 % in Talih-2 well. However, in the other Unity Field well, which is Barki-1, a tendency of $K_2O$ enrichment in the studied sediments is observed (average 3.41 %) (Appendices 3A & Figs. 7.1, 7.2 and 7.3).

The responsible factors for these lower values of $K_2O$ could be not only due to the low K-feldspar content in these sediments as revealed in the petrography chapter (Tables 5.1, 5.2 & 5.3), but also the change in the ionic exchange equilbria (Degens et al., 1958). On the other hand, the high increment of $K_2O$ in the studied sediments of Barki-1 well is related to the higher amount of illite in comparison to the sediments of the other study wells. This higher amount of illite is probably due to the smectite – illite transformation.

The chemical element (Fe) was recorded as ferric oxide ($Fe_2O_3$), with concentrations ranging between 1.1 % and 9.3 % in the investigated samples (Appendices 3A & 3B). There is no major change in its concentration between the study intervals in the three studied wells of Heglig Field. The average concentration of Fe in the studied sediments of Heglig-2, Toma-1 and Nabag-1 wells are: 4.38 %, 4.66 % and 4.87 % respectively (Appendix 3B & Figs. 7.4, 7.5 and 7.6). However, the $Fe_2O_3$ concentration is greater in the Aradeiba Formation in Unity-9 well (9.3 %) as well as in the Aradeiba and Zarga Formations, in Barki-1 well (7.2 % and 7.3 %) respectively (Appendix 3A & Figs. 7.1 and 7.3). Apart from the above higher values of the $Fe_2O_3$, its geochemical behaviour does not show obvious lateral or vertical trends. This inconsistent vertical and lateral behaviour of Fe is more likely attributed to the post-depositional concentration of the iron, which is largely depending upon the Eh – pH conditions of the pore water (Mason, 1966; Tucker, 1991).

The MgO concentration in the studied sediments in the two fields varies between 2.04 % (Barki-1 well), 1.72 % (Heglig-2 well), 1.57 % (Talih-2 well), 1.54 % (Unity-9 well) and 1.14 % (Toma-1 well) (Appendices 3A & 3B and Figs. 7.1, 7.2, 7.3,7.4, 7.5 & 7.6). From these percentages it is clear that the MgO concentration is higher in the studied sediments of Barki-1 and Heglig-2 wells relative to that of the other study wells. This is related to the relatively higher amount of chlorite in these sediments at the above two wells (Appendices 2A & 2B and Figs. 7.3 & 7.4). On the other hand, the lower values of MgO in the studied sediments at Toma-1 well can be attributed to relatively small changes in the pH, which could affect the ion exchange capacities of the clays and thus, also help to reduce the MgO values (Grim, 1953).

CaO concentrations are low in the studied sediments in both of the two fields (Appendices 3A & 3B). However, its concentration is relatively high in some horizons at Bentiu and Zarga Formations in Unity-9 and Talih-2 wells. This also has been proven by the presence of carbonate in the thin sections of the core samples from the above mentioned

horizons (Plates 5.1 & 5.3). CaO reaches a value of 4.87 % in Zarga Formation at Unity-9 well, whereas in Bentiu and Zarga Formations at Talih-2 well, the concentration reaches 3.65 % and 4.73 % respectively (Appendix 3A). These relatively high concentrations of CaO can be attributed to the higher amount of smectite in these formations (Figs. 7.1 & 7.2). Accordingly, Ca might have been structurally held in the smectite because the condition of formation of this mineral being suitable for the retention of Ca (Moore & Reynolds, 1997). However, the rarely occurring replacement of feldspar by carbonate could also increase the amount of the CaO (Plate 5.3 f arrow 5).

Sodium (Na) was detected as sodium oxide ($Na_2O$) in all of the examined samples, in concentrations ranging between 0.23 % to 2.83 % (Appendices 3A & 3B). The studied sediments of Heglig Field are characterized by relatively higher amounts of NaO (0.25 – 2.83 %), whereas those of Unity Field are characterized by lower concentrations (0.23 – 1.62 %) (Appendices 3A & 3B). Moreover, a general tendency of downward enrichment in Na is observed at all of the vertical studied profiles in the two fields (Appendices 3A & 3). This lateral and vertical geochemical behaviour of Na is in agreement with the sodic feldspar contents in the studied sediments of the two fields (Tables 5.1, 5.2 & 5.3).

Manganese (Mn) was recorded as MnO in all of the investigated samples with concentration of less than 0.2 % (Appendices 3A & 3B).

Phosphorous (P) was recorded as ($P_2O_5$) in all samples analysed. The concentration of this element ranges between 0.05 % and 0.26 % (Appendices 3A & 3B). The highest concentrations (0.2 – 0.26 % of $P_2O_5$)were observed in horizons of the Bentiu and Aradeiba Formations at Talih-2, Barki-1 and Nabag-1 wells as well as in some horizons of the Aradeiba Formation in Heglig-2 and Toma-1 wells (Appendices 3A & 3B).

Sulphur (S) was often below the detection limit. The highest concentrations (0.21 – 0.37 %) of sulphur are observed in some samples from Bentiu Formation in Talih-2 and Barki-1 wells as well as in some samples from Aradeiba Formation in Unity-9 and Talih-2 wells (Appendices 3A & 3B).

### 7.2.2.2 Trace Elements

Trace elements and the factors affecting their concentration in sediments have been the subject of numerous studies. These studies have tried to assign the various trace elements to particular minerals or organic substances within the sedimentary rocks in order to determine

the provenance and the depositional environment of these rocks. Differences in chemical concentration between Unity Field sediments as well as between Heglig Field sediments are attributed to the role of the factors acting during the sedimentary cycle of weathering, transportation and deposition. These controlling factors will be discussed later.

The concentration of the trace element Barium (Ba) in the studied sediments of the two fields is ranging between 250 ppm and 1294 ppm (Appendices 3A & 3B). Barium generally shows a vertical and lateral behaviour similar to that of Ca throughout the study intervals in the two fields (Appendices 3A & 3B). Low concentrations (250 – 260 ppm) of this element were recorded from the samples of the proximal facies environments in the Aradeiba Formation at Unity-9 and Talih-2 wells. On the other hand, high concentrations (800 – 1294 ppm) of Ba are present in some samples from Bentiu, Aradeiba and Zarga Formations at Unity-9 and Talih-2 wells (Appendices 3A), which were deposited in transitional environmental conditions, at the interface of lacustrine to deltaic or from deltaic to fluvial depositional environments (Fig. 4.17).

Zirconium was recorded in the analysed samples with a concentration of $80 - 381$ ppm (Appendices 3A & 3B). Zirconium generally exhibits vertical and lateral geochemical behaviour similar to the major element titanium throughout the study intervals in the two fields (Figs. 7.1, 7.2, 7.3, 7.4, 7.5 and 7.6). High concentrations (360 – 381 ppm) of Zirconium were recorded in samples of the proximal facies environments in Aradeiba Formation at Unity-9 and Talih-2 wells. In contrast, a low concentration (80 ppm) of Zr is revealed by some samples from lacustrine and floodplains enviroments in Aradeiba Formation at Toma-1 well as well as in Zarga Formation at Talih-2 well (Appendices 3A & 3B).

Chromium (Cr) was recorded from all of the investigated samples. The concentration of this element ranges between 8 ppm and 160 ppm (Appendices 3A & 3B). In general, the vertical and lateral geochemical behaviour of the trace element Cr is resembling that of both Ti and Zr (Figs. 7.1, 7.2 7.3, 7.4, 7.5 and 7.6). The 160 ppm concentration of the Cr was noted in the proximal strata of the Aradeiba Formation at Unity-9 and Barki-1 wells. The 8 ppm concentration was observed in floodplain strata of the Bentiu Formation in Toma-1 well.

Concerning the trace elements Cu and Ni, both of them were recorded in relatively low values in the studied sediments of the two fields (Appendices 3A & 3B). However, the average concencentrations of Cu and Ni are higher in the studied sediments of Heglig Field.

The average concentrations of Cu in Nabag-1, Toma-1 and Heglig-2 wells are: 73 ppm, 43 ppm and 36 ppm respectively. Whereas, the average concentrations of the Ni in the same wells are: 92 ppm, 41 ppm and 56 ppm respectively. In contrast, the average concentrations of the Cu in the studied sediments of the Unity Field wells are: 26 ppm (Unity-9 well), 26 ppm (Talih-2 well) and 56 ppm (Barki-1 well). Whereas, that of the Ni are: 41 ppm, 46 ppm and 86 ppm in the same wells respectively. The concentrations of Cu and Ni mainly depend on the pH – Eh conditions of the media (Mason, 1966). Moreover, primitive planktonic organisms such as algae concentrate Cu and Ni biochemically (Bjorlykke & Englund, 1979). Therefore, the concentration of these elements can be attributed to biochemical reactions and thus the differences in their concentrations from Unity to Heglig Fields may reflect a difference in the biological activity.

The elements Rubidium (Rb) and Gallium (Ga) show low concentration in the studied sediments of the two fields (Appendices 3A & 3B). Generally the two elements show vertical and lateral geochemical behaviour opposite to each other (Figs. 7.1, 7.2, 7.3, 7.4, 7.5 and 7.6). Relative high concentrations of Ga (30 – 38 ppm) were recorded from the proximal fluvial facies in the Bentiu and Aradeiba Formations in Talih-2, Barki-1, Toma-1 and Nabag-1 wells as well as in the Aradeiba Formation in Unity-9 and Heglig-2 wells, and also from the proximal fluvial facies of the Zarga Formation in Unity-9, Barki-1 and Toma-1 wells. In contrast, low concentrations of Rb (20 – 25 ppm) were observed in the same proximal horizons. On the other hand, relatively high concentrations of Rb (65 – 100 ppm) were noticed in the distal facies environments (lacustrine/floodplain) of the Aradeiba Formation at Unity-9, Talih-2, Barki-1, Heglig-2 and Nabag-1 wells as well as in Zarga Formation at Talih-2 well. However, the lower concentrations of Ga (10 – 23 ppm) were encountered in the same above mentioned distal facies.

Vanadium (V) was recorded in all of the analysed samples with very lower concentrations (Apendices 3A & 3B). The concentrations of this element range between 13 and 175 ppm. Relatively high concentrations of 172 and 175 ppm of this element were observed in the upper part of Bentiu, the lower part of Aradeiba and in the lower part of Zarga Formations in Nabag-1 well as well as in the middle part of Aradeiba Formation in Toma-1 well and also at the upper part of Aradeiba Formation in Barki-1 well.

Cobalt (Co) was recorded in most of the analysed samples with very low concentrations ranging between 0 ppm and 40 ppm (Appendices 3A & 3B). There is no significant difference between the study intervals of the two fields in the concentration of Co.
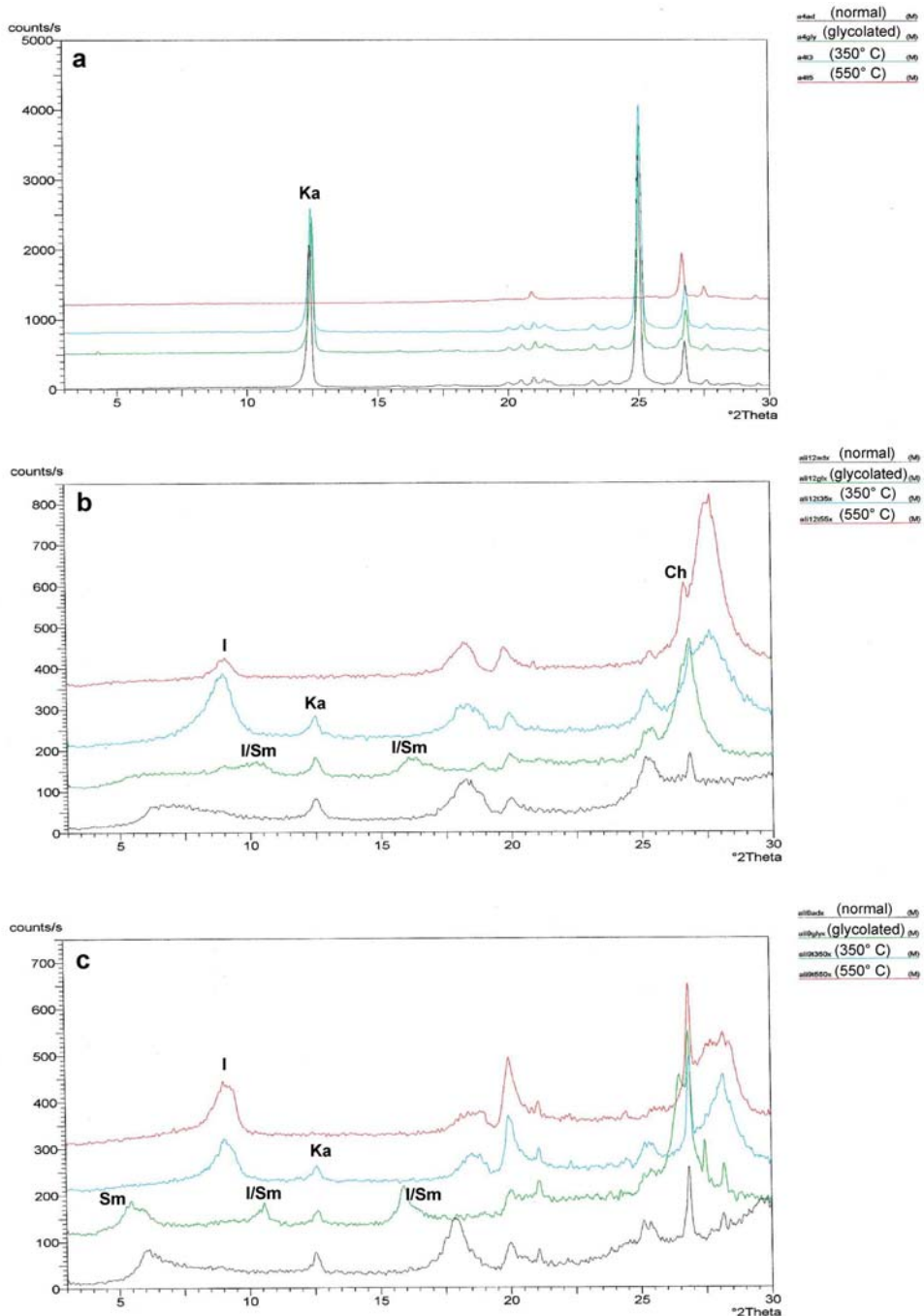


**Figure 7.7: Some XRD graphical charts giving a general impression about the degree of crystallinity of the clay minerals present in the studied formations at the Unity and Heglig Fields.**

### 7.2.3 Processes and Factors Controlling the Clay Minerals and Elements Distribution in the Studied Sediments

Factors controlling the distribution of clay minerals and the concentrations of the elements are difficult to induce because the distribution is frequently the result of non-equilibrium processes. However, the sedimentary cycle of weathering, physical and chemical erosion, transportation, deposition, diagenesis and ultimately lithification involves chemical and physical processes. These processes can be conveniently considered in terms of source rock effects, processes that occur during transport and deposition, and post-depositional processes (Mason, 1966). Moreover, Mason (ibid.) and Chamley (1989) showed that the environmental conditions at both sites of weathering and deposition as well as the nature of the biomass at the site of deposition are effective factors in controlling clay minerals and elements distribution in sedimentary rocks. In addition, tectonic and volcanic events during the weathering and/or transportation and/or deposition and the diagenetic processes after the accumulation of sediments play important roles in controlling the concentration of elements and clay minerals.

According to Keller (1956), Mason (1966), Chamley (1989) and Moore and Reynolds (1997), factors that can control clay minerals and element contents in sedimentary rocks are:

(1) The composition of the source rocks.

(2) The environmental conditions at the sites of weathering and deposition.

(3) The nature of the transpor processes.

(4) The physical and chemical conditions at the site of deposition.

(5) The nature and activity of the biomass at the site of deposition.

(6) Tectonic and volcanic events during weathering, transport and deposition.

(7) Diagenetic processes.

(8) The above factors interact with each other in varying degrees throughout time and so the effect of a single factor is often difficult to isolate.

### 7.2.4 Influence of the Source Rock Composition

As mentioned before, the arrangement of the six study wells allows a good vertical and lateral coverage for the upper part of Bentiu, all of the Aradeiba and the lower part of Zarga Formations in the SE Muglad Basin. The clay mineral associations and element

concentrations show, that the sediments were derived mainly from metamorphic source rocks of acidic nature. The mainly higher amounts of kaolinite in the upper part of Bentiu, lower and middle parts of Aradeiba and lower part of Zarga Formations at Barki-1, Toma-1 and Nabag-1 wells as well as in the lower parts of Aradeiba and Zarga Formations at Unity-9 and Talih-2 wells as well as in the middle part of Bentiu at Talih-2 well and also in the upper part of Aradeiba Formation at Toma-1 well indicate the dominant contribution from a metamorphic acidic rock source. The kaolinite in these strata has mostly formed authigenically as confirmed by the SEM micrographs (Plate 7.1 b – f) and supported by the sharp peaks of the kaolinite in several XRD charts. On the other hand, the relatively low amounts of smectite in the studied intervals of the two fields probably indicate a minor contribution from basic source rocks. However, it is confirmed by the SEM analysis, that part of the smectite was formed authigenically by the complete alteration of feldspar and mica (Plate 7.3 c & d). All of the above assumptions coincide with the results reached by the light and heavy minerals assemblages, which suggest mainly gneisses and to a lesser amount schists of acidic nature as source rocks for the upper part of Bentiu, the whole of Aradeiba and the lower part of Zarga Formations in the two fields.

## 7.2.5  Palaeoenvironmental Influences

The following discussion will outline the role of the palaeoclimate as one of the most important factors that affect the formation and distribution of the minerals. The palaeoclimate in the central and southern Sudan areas during most of the Early Cretaceous to the Early Tertiary, was warm and humid interrupted frequently by dry periods. This is supported by the widespread occurrence of lateritic deposits, kaolins and ironstones (Hallam 1984; Germann et al., 1990). Moreover, the macro- and microflora also indicate a warm palaeoclimate with alternating dry and wet periods (Omer 1983; Awad and Schrank 1990). These prevailing climatic conditions were favourable for widespread hydrolytic processes such as "monosialitization", "bisialtization" and "alitization" (Chamley, 1989). The maximum lacustrine in the central and southern Sudan areas during the Cretaceous time gave rise to the relative increase in the clay mineral kaolinite content in the upper strata of Bentiu Formation in Talih-2 well, in the lower and middle strata of Aradeiba Formation in Barki-1 well, in the lower strata of Aradeiba Formation in Talih-2 well, in the lower and uppermost strata of Aradeiba Formation in Unity-9 well as well as in the lower strata of Zarga Formation in Unity-9 and Talih-2 wells at Unity Field (Appendices 2A & Figs. 7.1, 7.2 and 7.3). Moreover,

this maximum lacustrine stretch also gave rise to the relative increase in the kaolinite content in the upper strata of Bentiu Formation in Toma-1 and Nabag-1 wells, in the lower strata of Aradeiba Formation in Toma-1 and Nabag-1 wells, in the middle strata of Aradeiba Formation in Heglig-2 and Toma-1 wells, in the upper strata of Aradeiba Formation in Toma-1 well, in the lower strata of Zarga Formation in Toma-1 and Nabag-1 wells at Heglig Field (Appendices 2B & Figs. 7.4, 7.5 and 7.6). Whereas, the followed intermittent dry periods gave rise to the increase of the smectite content in the middle strata of the Aradeiba Formation in Unity-9 and Talih-2 wells, in the upper strata of Aradeiba Formation in Talih-2 as well as in the lower strata of Zarga Formation in Unity-9, Talih-2 and Barki-1 wells at Unity Field (Appendices 2A & Figs. 7.1, 7.2 and 7.3) and also they gave rise to the increase of the smectite content in the uppermost strata of Aradeiba Formation and in the lowermost strata of Zarga Formation in Toma-1 and Nabag-1 wells as well as in the lower strata of Zarga Formation in Heglig-2 well at Heglig Field (Figs. 7.4, 7.5 and 7.6 & Appendices 2B). These imply that and as mentioned before, parts of the clay minerals kaolinite and smectite in the Middle – Upper Cretaceous strata at the study area are detrital. The kaolinite part was formed by pedogenic surficial processes in environments characterized by strong leaching, high $H^+$ ions concentration and relatively high topographic relief. Whereas, the smectite part was formed during the intermittent hot dry periods in low relief areas where poor drainage prevents the silica and the alkaline earth ions such as $K^+$, $Na^+$, $Ca^{+2}$ and $Mg^{+2}$ from being rapidly removed.

### 7.2.6  Tectonic Influences

Tectonics have some controls on the development and distribution of clay minerals (Millot, 1970). Tectonic activity modifies the relief, enhances the erosion of parent rocks and hence, consequently impedes pedogenic processes. As a result, the pedogenically derived clay minerals, like kaolinite and smectite, will be reduced in the sedimentary sequences. In contrast, clay minerals directly derived from parent rock or from the lower part of the weathering profiles such as illite and chlorite, will be increased in abundance (Millot, 1970). Three rifting phases have been recognized in the Muglad Basin in Early Cretaceous, Late Cretaceous and Middle Tertiary time. These phases are expressed by three coarsening upward cycles (Schull, 1988). Besides the environmental influences and the diagenetic effects (which will be discussed below), the clay minerals in these cycles must reflect in part, tectonic influences related to rifting. As found in this study, the lower clay minerals zone coincided

with the Late Cretaceous rifting phase sediments. One can suggest that part of the illite and chlorite in the lower clay mineral zone were derived directly by erosion from metamorphic source rocks. However, this suggestion did not exclude a possible diagenetic origin for the illite and the chlorite in this clay mineral zone. The relatively lower amounts of illite and chlorite in the upper clay mineral zone may indicate limited tectonic activity and little burial diagenetic influence.

### 7.2.7 Burial Diagenetic Influences

Dunoyer de Segonzac (1970) characterized the diagenetic domain by the development of illite and chlorite, the absence of true smectite, the instability of kaolinite and the frequent presence of allevardite (the illite/smectite mixed layer). Diagenetic evolution of clay minerals during burial can be identified by the increase of illite, chlorite and illite layers in illite/smectite mixed layers in the upper strata of Bentiu Formation as well as in the middle strata of Aradeiba Formation at Unity Field and also in the upper strata of Bentiu Formation at all of the study wells in Heglig Field, as well as in the lower strata of Aradeiba Formation at Heglig-2 well in Heglig Field (Figs. 7.1, 7.2, 7.3, 7.4, 7.5 and 7.6). Moreover, as mentioned before, the morphological and textural appearance of the illite/smectite mixed layers, which is a mixture between a "honeycomb" morphology (due to the smectite) and filamentous ribbon morphology (due to the illite) in some of the SEM micrographs, provides a good indicatior for burial diagenesis (Plates 7.2 c & 7.3 d). The amount of the illite/smectite mixed layers correlates with an increase of temperature from about 201°F / 94°C to 221°F / 105°C in Unity Field wells as from about 186°F / 86°C to 90°F / 88°C in Heglig Field wells and also an increase of potassium content from 0.5 % to 5.5 % in the studied sediments of Unity Field as well as from 0.8 % to 5.2 % in the studies sediments of Heglig Field (Figs. 7.1, 7.2, 7.3, 7.4, 7.5 and 7.6) and also correlates with an increase of non-volatile organic carbon in the studied sediments of the two fields. Smectite suddenly vanishes or decreases sharply at 4900 ft depth in all of the study intervals except in the study intervals at Unity-9 and Talih-1 wells (Figs. 7.1, 7.2, 7.3, 7.4, 7.5 and 7.6). These exceptional occurrences of smectite could be ascribed to thin sealing beds of shale, which prevent the circulation of pore space fluids, thus lead to the preservation of a certain amount of smectite in these horizons. Chlorite, kaolinite and the irregular mixed layer illite/smectite display noticeable quantitative variations throughout the Middle – Upper Cretaceous studied strata (Figs. 7.1, 7.2, 7.3, 7.4, 7.5 and 7.6), which probably reflect transitional situations between strictly palaeoenvironmental and strictly

diagenetic constraints. Relatively great amount of smectite is considered as being transformed to chlorite as in the upper strata of Bentiu Formation at 5590 ft in Barki-1 well as well as in the lower strata of Aradeiba Formation at 5400 ft in Heglig-2 well and also in the middle strata of Aradeiba Formation at 8238 ft in Talih-2 well (figs. 7.2, 7.3 and 7.4), since the chemical environment is rich in MgO as a result of source rocks rich in biotite (e.g. Plates 5.2 f, 7.4 d). On the other hand, in the upper strata of Bentiu Formation at depths 5750 ft in Heglig-2 well, 5550 ft in Toma-1 well and 9100 ft in Barki-1 well as well as in the middle part of Aradeiba Formation at a depth of 4800 ft in Barki-1 well relative great amount of smectite has been transformed to illite or to illite/smectite mixed layer since the chemical environment is rich in $K_2O$ rather than MgO as a result of rich K-feldspar source rocks origin (Figs. 7.3, 7.4 & 7.5 and e.g. Plates 5.1 d & f).

The geochemistry is closely related to the clay mineralogy. The element geochemistry is highlly affected by the hydrolytic processes, which are in turn controlled by environmental and diagenetic influences. In central and southern Sudan, during the Early Cretaceous to Early Tertiary, a humid warm climate caused intense chemical weathering and widespread lateritisation. This is supported by the increase in kaolinite abundances in these areas (Germann et al., 1990). Moreover, kaolinite signifies strong leaching where the "monosialitization" hydrolytic process has dominated. Intense chemical weathering causes leaching and depletion of mobile cations (Millot, 1970; Keller 1970 & Chamley, 1989). The physiochemical behaviour of the different cations determines the order of leaching and removal. Thus, the most mobile cations are leached first, while the less mobile ones remain behind. Consequently, the most mobile cations will be evacuated downstream distally into "sink" areas like lakes, deltas, floodplains and shoreline environments (Mason, 1966).

The above mentioned relationships may explain, in part, the vertical and lateral distribution of the chemical elements in the study intervals (Figs. 7.1, 7.2, 7.3, 7.4, 7.5 and 7.6). Based on the stage of hydrolysis, preferential leaching and enrichment of elements have happened. For instance, the most mobile elements Mg, Ca, K and Rb had been leached first and transported distally into low relief, poorly drained downstream areas. This may explain, in part, the relatively high abundances of these elements in the floodplain and lacustrine environments at the lower parts of Aradeiba and Zarga Formations in Talih-2, Toma-1 and Nabag-1 Wells as well as at the lower part of Aradeiba Formation in Unity-9 and Barki-1 wells and also at the uppermost of Aradeiba and the lowermost of Zarga Formations in Unity-

9 well (Appendices 3A and 3B & Figs. 4. 16 and 4.17). In contrast, the less mobile elements Ti, Ga, Cr and Zr were been prefentially enriched in the high relief and well drained upstream areas. This may also explain the relatively high abundances of these elements in the braided and meandering sand bars as well as in the deltaic mouth bars environment at the upper part of Bentiu Formation in all of the studied wells as well as at the lower part of Aradeiba Formation in Heglig-2 well as well as at the middle part of Aradeiba Formation in Unity-9, Talih-2 and Barki-1 wells as well as at the upper part of Aradeiba Formation in Talih-2, Toma-1 and Nabag-1 wells and also at the lower part of Zarga Formation in Unity-9, Barki-1 and Toma-1 wells (Appendices 3A and 3B & Figs. 4.16 and 4.17). However, the role of the burial diagenesis, especially in the lower horizons of the above mentioned strata, can not be excluded since diagenesis tends to modify both the clay mineralogy and geochemistry (Hower et al., 1976). The generalized depositional model of the Muglad Basin (Fig. 2.6) can best serve to express the environmental, morphological and transport conditions controls on the hydrolytic processes, and the proximal to distal geochemical differentiation. Moreover, in addition to climate, this shows the close relation between tectonics, sedimentation cycles and geochemical differentiation. That means, a specific geochemical cycle tends to associate with each sedimentation cycle. The variation in the above characteristic geochemical patterns may be due to numbers of factors in addition to the early mentioned ones. For example, the intensity of the hydrolytic processes and their duration are prime factors. Other factors are the variation in humidity, mineral size, activity of organic acids and drainage (Johnsson and Meade, 1991). In summary, the elements geochemical behaviour discussed in this study, which is closely related to the clay mineralogy, reflects the intensity of hydrolysis and other environmental and diagenetic controls.

Moreover, as mentioned before, the present study revealed three clay mineral zones within the studied intervals in Unity-9 and Talih-2 wells at Unity Field. Furthermore, two clay mineral zones are found within the studied intervals in Heglig-2, Toma-1 and Nabag-1 wells at Heglig Field. The lower clay minerals zone in the two wells of Unity Field consists of Kaolinite, illite/smectite mixed layer, illite, smectite and chlorite. Whereas, the middle zone consists of kaolinite, smectite, illite/smectite mixed layer, illite and chlorite. The upper zone comprises kaolinite, illite, illite/smectite mixed layer, chlorite and smectite. The lower and the upper clay mineral zones contain higher values of kaolinite in comparison to the middle clay mineral zone, whereas the middle zone contains a higher value of smectite in comparison to

the lower and the upper clay mineral zones. Furthermore, concerning the clay mineral zones within the studied intervals in the Heglig Field, the lower clay mineral zone consists of kaolinite, illite/smectite mixed layer, illite, chlorite and smectite. The upper zone contains kaolinite, smectite, illite/smectite mixed layer, illite and chlorite. The lower zone contains higher amounts of kaolinite, whereas the upper zone contains a higher amount of smectite in comparison to each other.

As mentioned before, the marked increase of the kaolinite and the distribution of smectite could be attributed to the warm humid climate that was prevailing during the Early Cretaceous to Early Tertiary, which was interrupted frequently by dry seasons. Moreover, the predominance of kaolinite signifies, in part, the reworking of laterites on the rift basin flanks and the adjacent land-masses. These laterites must have been repeatedly reworked, transported and dispersed in the fluvial/deltaic/lacustrine environments. Since the same clay mineral members are present in all of the studied wells at the two fields but with different values and hierarchical arrangement, the absence of the middle clay minerals zone within the studied interval in Barki-1 well (Unity Field) as well as within the studied intervals in Heglig-2, Toma-1 and Nabag-1 wells (Heglig Field) suggests variability in the intensity of the pedogenic weathering processes as controlled by climatic, topographic and transport conditions and variability in burial diagenesis rather than differences in source rocks and tectonic conditions. However, the lower and the upper clay mineral zones indicate environmental, tectonic and burial diagenesis influences. The upper and middle clay mineral zones, which are dominated by kaolinite and smectite, indicate basically environmental influence and minor burial diagenetic effect. They signify also relatively stable tectonic conditions where active pedogenic weathering processes have prevailed. The lower zone, which shows a relative increase of illite, chlorite, mixed layer illite/smectite, a higher illite crystallinity and progressive increase of smectite in the mixed layer illite/smectite, indicates mixed and transitional influences from environmental/ tectonic to burial diagenetic controls.

Within the scope of the previous geochemical studies in the Cretaceous – Tertiary strata of the NW and SE Muglad Basin, Abdullatif (1992) and Bakr (1995) came to similar results. They noted, that the geochemistry along the sedimentary succession shows preferential enrichment and depletion of the more and less mobile elements respectively in the rift basin subenvironments. The more mobile elements (Mg, Ca, K and Rb) enriched distally in the downstream floodplain and lacustrine environments of Sharaf, Abu Gabra, Darfur

Group, and Tendi Formations. In contrast, the less mobile elements (Ti, Cr and Ga) have remained preferably in the proximal high-relief upstream and well-drained environments, such as the sand rich Bentiu, Darfur Group, Amal and Adok Formations.

# Plate 7.1
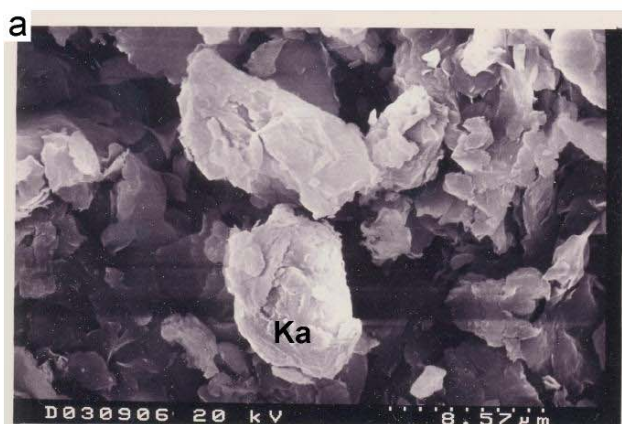
Micrograph (a) shows detrital kaolinite in a sample from the Aradeiba Formation at Talih-2 well in Unity Field.
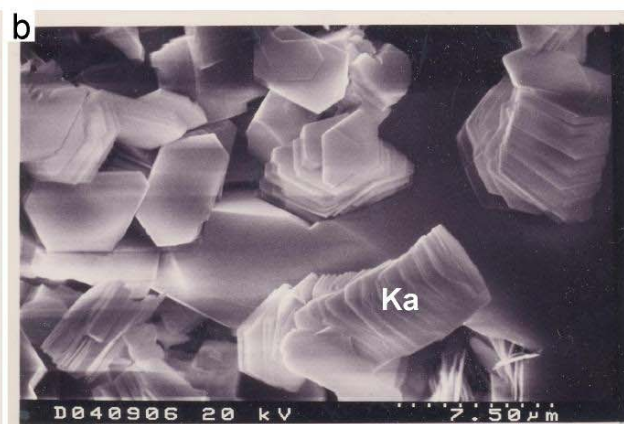
Micrograph (b) shows pseudohexogonal books arranged face-to-face into an elongated form called "verm" in a sample from the Zarga Formation at Talih-2 well in Unity Field.
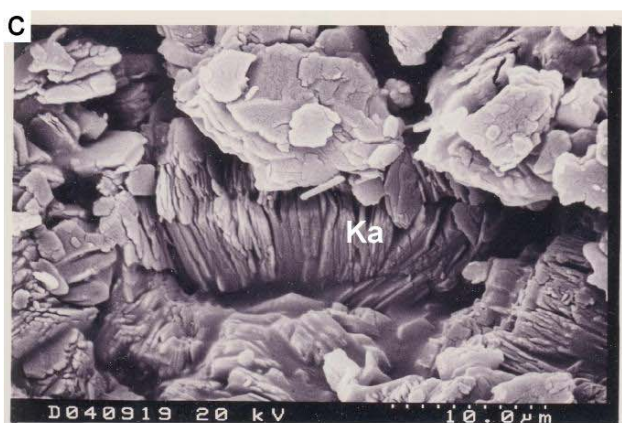
Micrograph (c) shows pseudohexogonal books arranged face-to-face into an elongated form called "verm" in a sample from the Bentiu Formation at Heglig-2 well in Heglig Field.
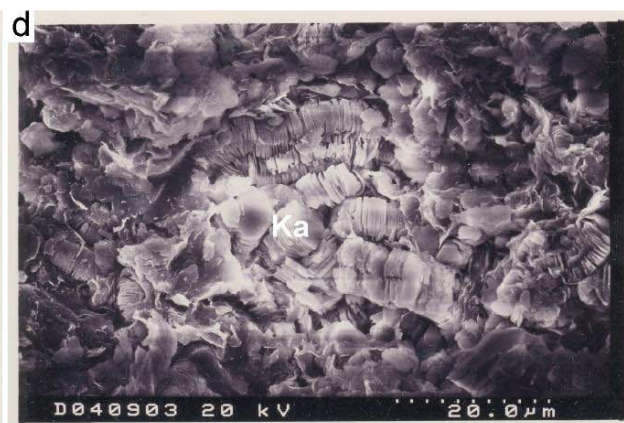
Micrograph (d) shows pseudohexogonal books of kaolinite filling a pore between detrital grains in a sample from the Aradeiba Formation at Talih-2 well in Unity Field.
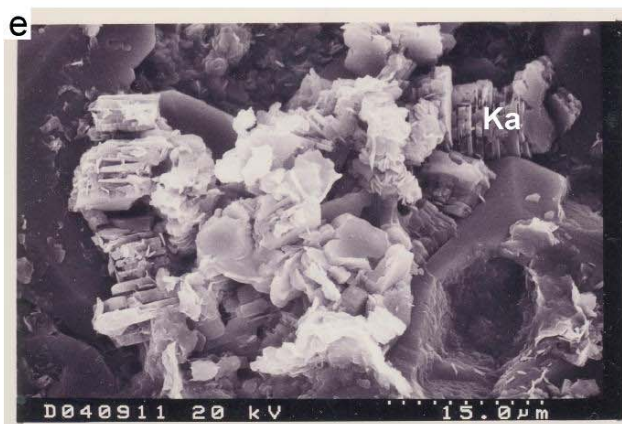
Micrograph (e) shows pseudohexogonal books of kaolinite. Some books are separated and others are linked by ribbons or sheets of illite, illite/ smectite mixed-layer, smectite and chlorite clay minerals in a sample from the Aradeiba Formation at Heglig-2 well in Heglig Field.
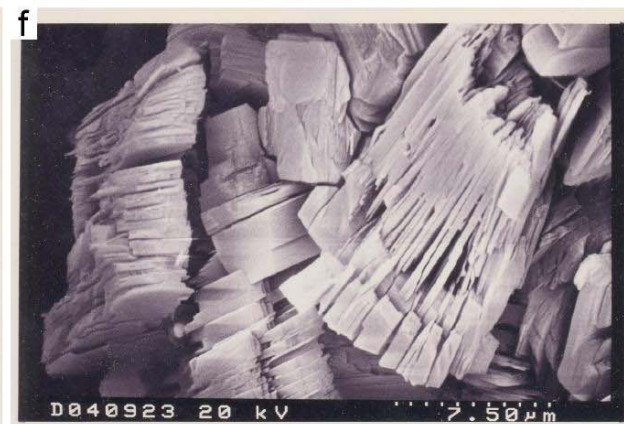
Micrograph (f) shows formation of kaolinite by complete alteration of K-feldspar in a sample from the Bentiu Formation at Unity-9 well in Unity Field.

# Plate 7.2



Micrograph (a) shows irregular flake-like clay platelets of illite forming a "scalloped" habit in a sample from the Zarga Formation at Talih-2 well in Unity Field.



Micrograph (b) shows irregular flake-like clay platelets of illite forming a "scalloped" habit in a sample from the Aradeiba Formation at Unity-9 well in Unity Field.



Micrograph (c) shows development of illite due to the transformation of the smectite to illite by burial diagenesis in a sample from the Aradeiba Formation at Talih-2 well in Unity Field.



Micrograph (d) shows thin filamentous ribbons of illite forming a mat, partially coating some detrital grains and also bridging the pores, thus forming permeability barriers to fluid flow in a sample from the Bentiu Formation at Unity-9 well in Unity Field.

# Plate 7.3
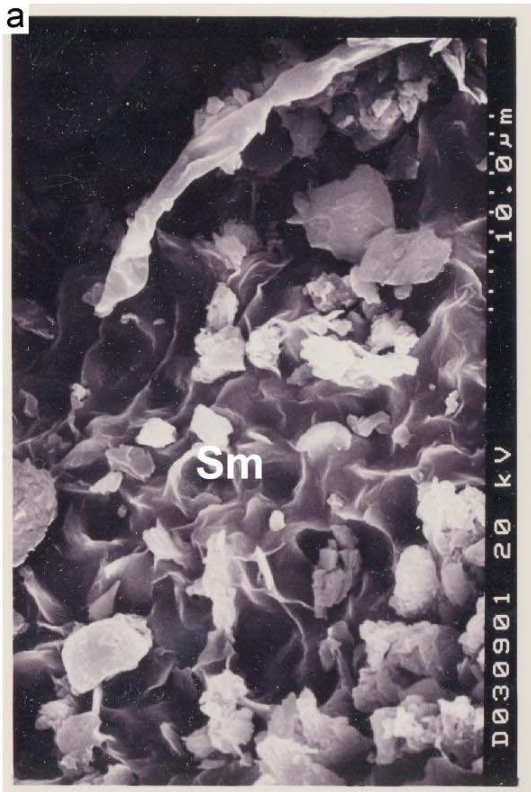


Micrograph (a) shows "maple leaf" or "honeycomb" of smectite forming a webby crust covering some detrital grains in a sample from the Zarga Formation at Unity-9 well in Unity Field.
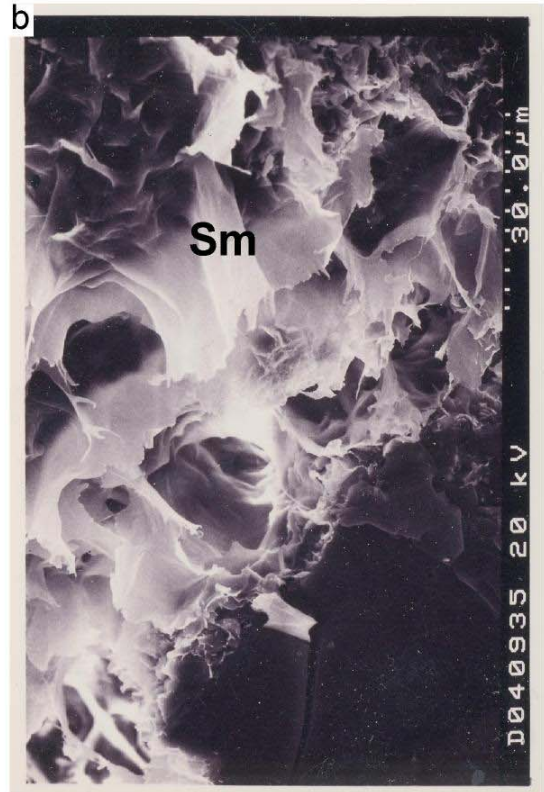


Micrograph (b) shows a webby crust of smectite occurs as a pore-lining mat in a sample from the Aradeiba Formation at Heglig-2 well in Heglig Field.
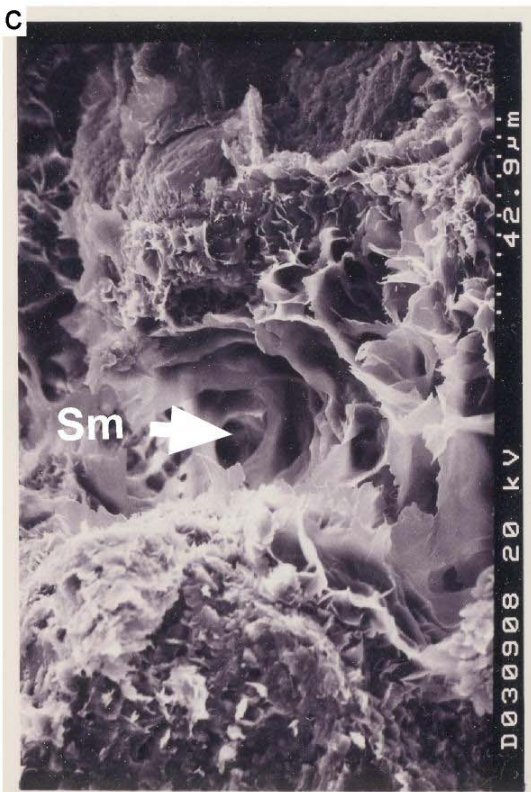


Micrograph (c) shows a webby crust of smectite bridging across a pore throat in a sample from the Aradeiba Formation at Talih-2 well in Unity Field.
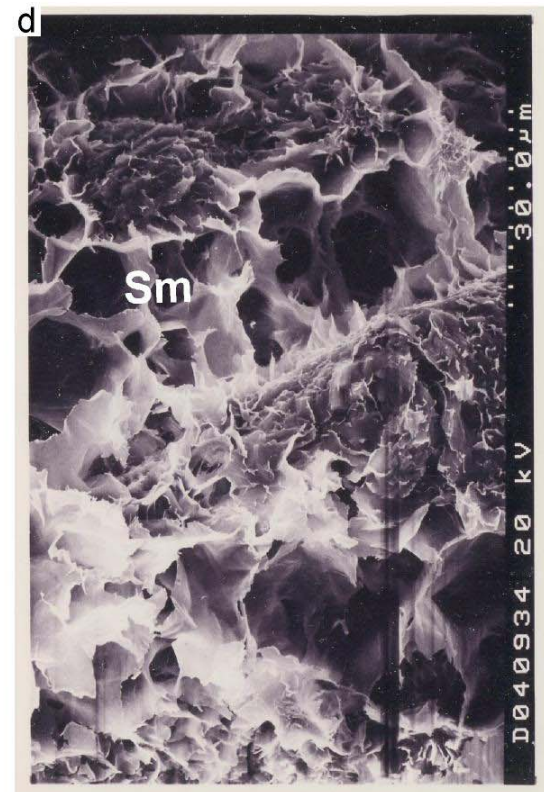


Micrograph (c) shows a webby crust of illite/ smectite bridging across a pore in a sample from the Bentiu Formation at Toma-1 well in Heglig Field.

# Plate 7.4



Micrograph (a) shows some clusters of "disc-like" chlorite crystals partly filling a depression within detrital grains in a sample from the Bentiu Formation at Heglig-2 well in Heglig Field.
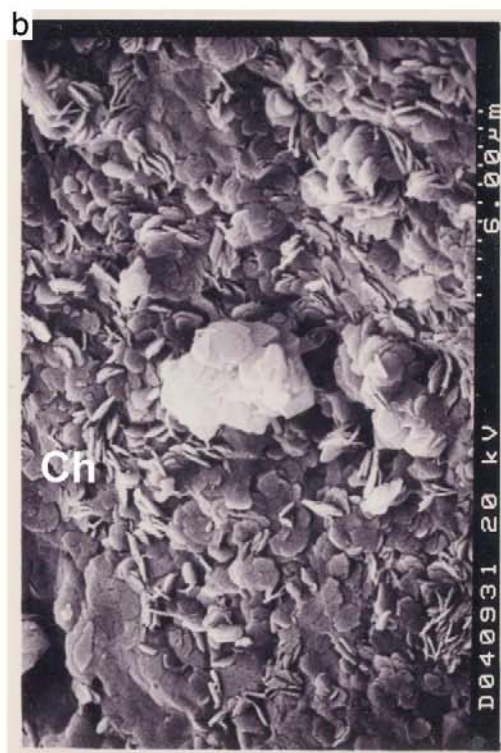
Micrograph (b) shows separated and clustered "disc-like" chlorite crystals filling some depressions between detrital grains in a sample from Aradeiba Formation at Talih-2 well in Unity Field.

Micrograph (c) shows platelets of chlorite stacked face-to-face in a "beehive-like" structure in a sample from the Aradeiba Formation at Talih-2 well in Unity Field.

Micrograph (d) shows chloritization of biotite grain. the chlorite flackes were oriented face-to-face and aligned parallel to original biotite cleavage planes in a sample from the Aradeiba Formation at Heglig-2 well in Heglig Field.

# 8 Summary and Conclusion

1. The study area lies in the south-eastern part of the Muglad Rift Basin, which is the largest and most important oil-producing basin of the Sudan. In the Sudan, the Central and Southern Sudan Interior Rift Basins evolved during Late Jurassic? to Early Tertiary time in response to rifting processes. Similar processes were active in other parts of Central Africa as well as along the eastern and western continental margins of Africa, and caused the formation of major rift basins.

2. The tectonic development of the Muglad Rift Basin passed through a pre-rifting phase, three rifting phases and a sag phase. These phases resulted in the deposition of three major depositional cycles with a total thickness of up to 13 km of non-marine siliciclastic sediments.

3. The large-scale facies variations in the basin are primarily controlled by tectonic processes and structures. In sub-basins with high rates of subsidence, such as the Kaikang Trough, and in times of overall intensified subsidence, relatively deep lacustrine conditions prevailed in the centre of the basin. Consequently, thick sequences of lacustrine sediments were deposited there. Tectonics seem to have influenced also the facies distribution and architectural style of the fluvial sediments. In contrast, cyclical lake-level fluctuations were probably caused by palaeoclimatic changes.

4. The facies description and the analysis of conventional cores from the Bentiu, Aradeiba and Zarga Formations in the Unity and Heglig oil fields revealed the presence of nine major lithofacies types, all of them are siliciclastic sediments. They can be interpreted as deposits of fluvial, deltaic and lacustrine environments. Moreover, based on wire line logs, cores and cutting samples description and analyses and also on seismic sections analysis, the Middle – Upper Cretaceous strata in Unity and Heglig Fields can be classified into three different units of first-order sequences that represent: fluvial-dominated unit, lacustrine-dominated unit and deltaic-dominated unit. The fluvial-dominated sequence unit characterizes the whole of the Bentiu Formation as well as the lowermost part of the Aradeiba Formation in Unity Field, the middle part of the Aradeiba Formation in Unity-9 well and the upper part of Aradeiba Formation as well as the middle part of Zarga Formation in Unity Field (Fig 4.17). Fluvial sequences unit is also found throughout the Bentiu Formation in Heglig Field, in the lower and middle parts of Aradeiba Formation in Heglig-2 well as well as in the lower and the

middle parts of Zarga Formation in Toma-1 and Nabag-1 wells in Heglig Field (Fig 4.16). Whereas, the lacustrine-dominated sequences unit occurs in the lower and upper parts of the Aradeiba Formation in Unity-9 well, in the lower part of the Aradeiba Formation in Talih-2 and Barki-1 wells as well as in the lower and upper parts of the Zarga Formation in Unity-9 and Talih-2 wells (Unity Field). Moreover, this sequences unit characterizes the lower part of the Aradeiba Formation in Toma-1 and Nabag-1 wells. Also some lacustrine sequences occur in the strata near the middle part of the Aradeiba Formation in Heglig-2 well. Furthermore, the lacustrine sequences unit characterizes the middle part of the Zarga Formation in Heglig-2 and Nabag-1 wells as well as the upper part of the Zarga Formation in Toma-1 well (Heglig Field). However, the deltaic-dominated sequences unit occurs near the middle and near the upper parts of the Aradeiba Formation in Unity-9 well, in the middle part and near the upper part of the Aradeiba Formation in Talih-2 well, in the lower part of the Zarga Formation in Unity-9 well as well as in the lower and middle parts of the Zarga Formation in Talih-2 well (Unity Field). Moreover, this sequences unit characterizes the middle part and the strata near the upper horizons of the Aradeiba Formation in Toma-1 well, the top of the Aradeiba Formation in Heglig-2 well and the top horizons of the Zarga Formation in Heglig-2 and Nabag-1 wells (Heglig Field).

5. The seismic analysis revealed, that the maximum thickness of the Cretaceous sediments in the southern part of the Heglig Field and in the Unity Field is about 2550 m and 3190 m respectively, whereas the maximum sediment thickness in the NE part of the Heglig Field reaches about 2500 m. Generally, the thickness of the sediment in the study area increases in the western flank towards the Kaikang Trough (Fig. 4.22), which represents the deepest subbasin of the Muglad Rift Basin. The maximum thickness of the Cretaceous sediments in the NW part of the Heglig Field is about 6000 m. The seismic interpretation has revealed three seismic facies reflection patterns: parallel and subparallel reflection patterns, divergent reflection pattern and hummocky clinoform pattern. The parallel and subparallel reflection patterns, which indicate uniform rates of deposition, characterize the Amal, Nayil, Tendi and Adok Formations in the Unity Field as well as the Amal and Nayil Formations in the Heglig Field (Figs. 4.18 & 4.20). The divergent reflection pattern resulted from differential subsidence rates in the half-graben of the SE Muglad Basin. It is present on the seismic line gn 98-010, which extends from the NE of the study area and runs across the Heglig Field to Kaikang Trough in the West of the study area (Fig. 4.22). The hummocky clinoform pattern,

which is a pattern of prograding reflection, indicates small clinoform lobes of a delta, that had undergone distributary switching. This type of reflection pattern characterizes the Aradeiba, Zarga, Ghazal and Baraka Formations in Unity-9 and Khairat-NE-4 wells in Unity Field (Fig. 4.18). Moreover, this pattern of progradational deltaic reflection was confirmed by the dominant coarsening upward funnel shape patterns of the gamma-ray and the spontaneous potential wire line logs at the above mentioned strata in the unity-9 well (Figs. 4.9, 4.11 & 4.15). The interpretation of the seismic sections of lines sd 81-013 and gn 98-010, which trend NE-SW across the study area, indicate several structural oil traps (Figs. 4.21 and 4.23). This is because these seismic sections cross major fault planes. In contrast, the interpreted seismic section of line sd 82-202, which trends NW-SE and runs parallel to the major faults shows very few structural traps (Fig. 4.19).

6. The lithofacies association and the depositional patterns of the Muglad Basin were controlled by allocyclic and autocyclic processes, which include tectonic, palaeoclimatic as well as depositional mechanisms.

7. Thin section investigations and scanning electron microscope analysis of core samples from the Bentiu, Aradeiba and Zarga Formations in Unity and Heglig Fields revealed that feldspar accounts for 13.5 – 22 %, that of the quartz and the lithic fragments are ranging between 75.7 – 85.2 % and 0.0 – 7.3 % respectively (Table 5.4). Consequently the sandstones are classified as subarkoses. Besides quartz and feldspar, detrital micas are present and also some fine-grained matrix. The feldspars are usually altered. The cementing material of the sandstones in Bentiu, Aradeiba and Zarga Formations is rather similar. The sandstones of the Bentiu Formation are cemented by quartz with 1.2 – 6 % carbonates and 1.3 – 2 % iron oxides. Moreover, they contain some matrix (usually illite/smectite mixed-layer, kaolinite and illite) (Table 5.1 and Plate 5.1). However, the sandstones of the Aradeiba Formation are cemented by quartz and 0.5 – 3.8 % iron oxides with 0.0 – 3 % carbonates; they also contain some matrix (usually kaolinite, smectite, illite, illite/smectite mixed-layer) (Table 5.2 and Plate 5.2). The sandstones of the Zarga Formation are cemented by quartz and 4 – 8 % carbonates with 0.0 – 0.5 % iron oxides; they contain higher amounts of more matrix (usually kaolinite, smectite, illite, few illite/smectite mixed-layer) than the former formations (Table 5.3 and Plate 5.3). In all of the examined samples, polycrystalline quartz occurs in higher percentages than monocrystalline quartz. These higher rations of polycrystalline to monocrystalline quartz indicate a metamorphic source region. However, the studied

sandstones of Unity Field in Unity-9 and Talih-2 wells (Tables 5.1, 5.2 and 5.3) have lower percentages of polycrystalline quartz, potassic and sodic feldspars than the examined samples of the Heglig Field. e.g. in Heglig-2 and Toma-1 wells (Tables 5.1 and 5.2). Moreover, the monocrystalline quartz grains in the studied sandstones of Heglig Field are subangular to subrounded and are poorly to moderately sorted, whereas in the studied sandstones of Unity Field, the monocrystalline quartz grains are subrounded to rounded and are moderately to well sorted (Plates 5.1, 5.2 & 5.3). These differences could be attributed to a longer distance of transportation and to a prolonged abrasion of the Unity Field sediments.

8. The modal analysis of the sandstones revealed, that they stem generally from a continental provenance, transitional between the stable interior of a craton and a basement uplift, which is a basement area of relatively high relief along rifts. This allows the detrital components to be recycled and transported for rather long distances and to be deposited in extensional and pull-apart basins. The lack of appreciable amounts of siderite, calcite and iron oxide cements besides their co-existence suggests that the lake system was hydrologically open and maximum lake level was imposed by an outlet, so it had a relatively stable water level and shoreline.

9. Thin section investigations and the scanning electron microscope (SEM) analysis for the sandstones of the Bentiu, Aradeiba and Zarga Formations have revealed, that their reservoir quality was affected positively and negatively by several diagenetic processes. These processes include: mechanical compaction factors (grain slippage and crushing of the ductile grains), quartz overgrowths, precipitation of siderite and calcite, feldspar and clay minerals authigenesis, dissolution of carbonate and of the labile detrital grains and clay infiltration. The reservoir quality of the study intervals was not only affected by the above mentioned diagenetic processes, but also in a large-scale by the type of depositional environment (lacustrine, fluvial and deltaic environments), which controlled the distribution of the facies types within the basin as well as by the subsidence of the basin besides the structural relief variations that had happened during the initiation of the second rifting phase, which led to the fast transportation and rapid burial of the sediments. Furthermore, the reservoir quality was influenced by the detrital composition of the sandstones, by their textures and the grain-size distribution.

10. The reservoir quality of the Bentiu and Aradeiba Formations in general is better than that of the Zarga Formation. The porosity of the Bentiu and Aradeiba Formations ranges between

16.7 – 30.0 % and 18.6 – 25.3 % respectively, whereas the porosity of the Zarga Formation ranges between 16.3 – 23.7 %. Since the sandstones of the Bentiu and Zarga Formations are mainly cemented with quartz, these two formations had suffered less from compation. The sandstones of the Zarga Formation contain higher amounts of phyllosilicate grains and carbonate authigenic cement, hence the formation had lost part of its porosity through the compative deformation of the ductile grains and the cements, which was followed by authigenic precipitation of clays within the pore spaces, which in turn reduced the porosity of this formation. However, the dissolution of carbonate cement in the sandstones of the Zarga and Bentiu Formations led to the development of secondary porosity. In the deeper horizons of the Bentiu and Aradeiba Formations, the transformation of smectite clay to illite and to illite/smectite mixed layer led to the reduction of the porosity (Plates 7.1 – 7.4).

11. The study of the heavy minerals revealed, that the amounts of the heavy minerals kyanite and garnet supersede those of zircon, tourmaline and rutile. This indicates a metamorphic source rock of originally granitic and/or granodioritic composition for the sediments of the study area. Three heavy mineral assemblage zones with obvious lateral and vertical continuity were identified: a zircon-rutile zone (ZR), a sillimanite-epidote-hornblende zone (SEH) and a kyanite-staurolite-andalusite-garnet zone (KStAnG). The ZR zone defines the upper part of Bentiu and Aradeiba Formations in almost all of the study intervals except at Heglig-2, where it covers the upper part of Bentiu Formation, as well as the lowermost part and the middle part of Aradeiba Formation. However, the SEH zone characterizes the uppermost horizons of Bentiu, the lower as well as the uppermost part of Aradeiba and the lower part of Zarga Formations in Barki-1, Toma-1 and Nabag-1 wells. It also covers the lower part of Aradeiba Formation in Heglig-2 well and the uppermost of Aradeiba, as well the lower part of Zarga Formations in Unity-9 and Talih-2 wells. The KStAnG zone encompasses the lower and the middle part of Aradeiba Formation in the Unity Field except at Barki well, where it is represented by the middle part of the Aradeiba Formation. In the Heglig Field the zone is not clearly present.

12. On the basis of the ZTR (zircon-tourmaline-rutile) index as well as on the SEH (sillimanite-epidote-hornblende) index, four major maturation levels were constructed: immature, moderately mature, mature and overmature (Figs. 6.7 & 6.8). The evolutionary trends in these maturation levels show clearly the weathering and reworking history, through which these sedimentary rocks were significantly modified.

13. The clay mineral analysis revealed, that the studied strata are essentially composed of kaolinite, illite, smectite, illite/smectite mixed layer and chlorite. The vermiform morphology besides the sharp peak pattern of the kaolinite in some of the XRD charts indicate that part of the kaolinite is monocrystalline, which means it has authigenically formed. However, some of the kaolinite are detrital. Moreover, part of the illite, smectite, illite/smectite mixed layer and chlorite contents are detrital in origin, whereas the other parts were authigenically formed.

14. In these strata, three to two clay mineral zones, which reflect mainly different environmental and diagenetic conditions were established. The lower clay mineral zone consists of kaolinite, illite/smectite mixed layer, illite, smectite and chlorite. Whereas, the middle zone consists of kaolinite, smectite, illite/smectite mixed layer, illite and chlorite. The upper zone comprises kaolinite, illite, illite/smectite mixed layer, chlorite and smectite. The lower and the upper clay mineral zones contain higher values of kaolinite in comparison to the middle clay mineral zone, whereas the middle zone contains a higher value of smectite in comparison to the lower and the upper clay mineral zones. The higher amount of the kaolinite in the lower and in the upper zones suggest most probably the intensity of chemical weathering and leaching processes under warm humid climate. The marked presence of smectite in the middle zone suggest that the warm humid climate was interrupted by dry seasons. Moreover, the lower clay mineral zone, which shows an increase of illite, chlorite, mixed layer illite/smectite and a higher illite crystallinity, indicates mixed and transitional influences from environmental/ tectonic to burial diagenetic controls.

15. The geochemical investigation shows enrichment and depletion of certain chemical elements in the study area. For example, the more mobile elements Mg, Ca, K and Rb occur in higher percentages in the distal facies types (i.e. in the lacustrine deposits, deltaic distal bar deposits and floodplain sediments), as in the lower parts of Aradeiba and Zarga Formation in Talih-2, Toma-1 and Nabag-1 wells, as well as in the lower part of Aradeiba Formation in Unity-9 and Barki-1 wells and also in the uppermost of Aradeiba and the lowermost of Zarga Formations in Unity-9 well. In contrast, the less mobile elements Ti, Ga, Cr and Zr remained in higher amounts in the proximal facies types (i.e. in the fluvial channel bars deposits and deltaic mouth bar deposits), as in the upper part of Bentiu Formation in all of the studied area, as well as in the lower part of Aradeiba Formation in Heglig-2 well, as well as in the middle part of Aradeiba Formation in Unity-9,Talih-2 and Barki-1 wells, as well as in the upper part

of Aradeiba Formation in Talih-2, Toma-1 and Nabag-1 wells and also in the lower part of Zarga Formation in Unity, Barki-1 and Toma-1 wells.

16. The distribution of the clay minerals and the concentrations of the elements throughout the study area were controlled by several processes and factors, which include: composition of the source rock, the environmental conditions at the site of weathering and deposition, the nature of transport, the physical and chemical conditions at the site of deposition, tectonic event and diagenetic processes.

# 9 Ackowledgements

Also, I wish to express my sincere appreciation to Dr. Jonckheere for his valuable assistance in processing the seismic lines.

Finally, this work could not be possible without the support and encouragement of my family. Their financial support, assistance and patience are greatly appreciated.

# 10 References

A'amir, A. O. (2000) Sedimentology of Cretaceous outcropping strata at the NE margin of the Muglad Rift Basin Western Kordofan State, Sudan. M.Sc. thesis, University of Khartoum, 150 p., Khartoum, Sudan.

Abdullatif, O. M. (1989) Channel-fill and sheet-flood facies sequences in the ephemeral terminal River Gash, Kassala, Sudan. Sedimentary Geology, **63**, pp. 171-184, Amsterdam.

Abdullatif, O. M. (1992) Sedimentology of the late Jurassic/Cretaceous-tertiary strata of the NW Muglad and the Nile rift basins, Sudan. Ph.D. Thesis, University of Khartoum, 231 p.,  Khartoum, Sudan.

Abdullatif, O. M. and Barazi, N. (1992) Clay sedimentology, burial diagenesis and organic maturation of the Muglad rift Basin, Sudan. The 29th International Geological Congress, abstract, Kyoto, Japan.

Adams, A. E., Mackenzie, W. S. and Guilford, C. (1995) Atlas of sedimentary rocks under the microscope. 104 p., Longman, Harlow.

Ahmed, A. S. (1983) Geology of south central Sudan basin, lithostratigraphy and sedimentary evolution. M. Sc. Thesis, University of Khartoum, Khartoum, Sudan.

Ahmed, Y. M. (1993) Depositional models and diagenetic events of the Sudan interior rift basins with special reference to Abu Gabra Formation, Muglad rift basin, Sudan. M.Sc. Thesis, 130 p., University of Tokyo, Japan.

Ahmed, Y. M. (1996) Organic matter characterization and environmental control on organic facies and lithofacies of early Cretaceous Lake Assalam, NW Muglad Basin, Sudan. Ph.D. Thesis, University of Tokyo, 110 p., Tokyo, Japan.

Allen, P. A. and Allen, J. R. (1990) Basin Analysis: Principles and Applications, 451 p., Blackwell Scientific Publications, Oxford.

Anadon, P., Cabrera, L., Julia, R., and Marzo, M. (1991) Sequential arrangement and asymmetrical fill in the Miocene Ubielos de Mora Basin (northeast Spain). In: Lacustrine facies analysis (Ed. by Andon, P., Cabrera, L. and Kelts, K.). Special Publication int. Ass. Sediment., **13**, pp. 257-275.

Awad, M. Z. (1994) Stratigraphic, palynological and paleoecological studies in the east-central Sudan (Khartoum and Kosti Basins), late Jurassic to middle Tertiary. Berliner geowissenschaftliche Abhandlungen, A, **161**, 163 p., Berlin.

Awad, M. Z. and Schrank, E. (1990) Macrofloral and palaeoecological study of the Albian-Cenomanian Omdurman Formation, Sudan. 15th Colloquium on African Geology, Nancy, France.

Bakr, M. (1995) Mesozoic and Cenozoic sedimentary facies of Muglad, Melut and Blue Nile rift basins, Sudan. Ph.D. Thesis, University of Khartoum, Khartoum, Sudan.

Barazi, N. (1985) Sedimentologie und Stratigraphie des Abyad-Beckens (NW-Sudan). Berliner geowissenschaftliche Abhandlungen, A, **64**, 85 p., Berlin.

Basu, A., Young, S. W., Suttner, L. J., James, W. C. and Mack, G. H. (1975) Re-evaluation of the use of undulatory extinction and polycrystallinity in detrital quartz for provenance interpretation. Journal of Sedimentary Petrology, **45**, pp. 873-882.

Beauchamp, J. Omer, M. K. and periaux, J. (1990) Province and dispersial pattern of the Cretaceous clastics in north east Africa: Climate and structural setting. Journal of African Earth Science, **10**, 172, pp. 243-253.

Bermingham, P. M., Fairhead, J. D. and Stuart, G. W. (1983) Gravity study of the Central African Rift system: A model of continental disruption 2. The Darfur domal uplift and associated Cainozoic volcanism. Tectonophysics, **94**, pp. 205-222, Amsterdam.

Bjorlykke, K. and England, J. O. (1979) Geochemical response to Upper Precambrian rift basin sedimentation and Lower Palaeozoic epicontinental sedimentation in South Norway. Chemical Geology, **27**, pp. 271-295.

Blatt, H., Middleton, G. V. and Murray, R. C. (1980) Origin of sedimentary rocks. Prentice Hall, 634 p., New Jersey.

Boles, J. R. (1982) Active albitization of plagioclase, Gulf Coast Tertiary. American Journal of Science, **282**, pp. 165-180.

Bosellini, A. Russo, A. and Assefa, G. (2001) The Mesozoic succession od Dire Dawa, Harar Province, Ethiopia. Journal of African Earth Science, **32**, 3, pp. 403-417, Oxford.

Bosworth, W. (1992) Mesozoic and early Tertiary rift tectonics in east Africa. Tectonophysics, **209**, pp. 115-137.

Bringley, G. W. and Brown, G. (1984) Crystal structures of the clay minerals and their X-ray identification. Mineralogical Society, pp. 495, London.

Browne, S. E. and Fairhead, J. D. (1983) Gravity study of the central African rift system, a model of continental disruption.1. The Ngaoundere and Abu Gabra rifts. Tectonophysics, **94**, pp. 187-203, Amsterdam.

Browne, S. E., Fairhead, J. D. and Mohamed, I. I. (1985) Gravity study of the White Nile rift, Sudan, and its regional tectonic setting. Tectonophysics, **113**, 123-137, Amsterdam.

Bussert, R. (2002a) The structural and sedimentological evolution of Cretaceous intracratonal basins in central northern Sudan (submitted to Journal of African Earth Sciences).

Bussert, R. and Vrbka, P. (2002b) Groundwater Resources of Mesozoic Sedimentary Basins in northern Sudan, between Khartoum and Ed Debba (submitted to Zentral Blatt für Geologie und Paläontologie).

Cant, D. J. (1984) Subsurface facies analysis. In Facies Models (Ed. by R. G. Walker). Geoscience, pp. 299-308, Canada.

Carver, R. E. (1971) Procedures in sedimentary petrology. John Wiley, 653 p., New York.

Chamley, H. (1989) Clay sedimentology. Springer-Verlag, 623 p., Berlin, Heidelberg.

Coleman, R. L. and Prior, D. B. (1982) Deltaic environments. In: Sandstone depositional environments (Ed. by Scholle, P. and Spearing, D.). Memoir American Association of Petroleum Geologists, **31,** pp. 139-178.

Degens, E. T., Williams, E. G. and Keith, M. C. (1985) Environmental studies of carboniferous sediments part II: Application of geochemical criteria. American Association of Petroleum Geologists Bulletin, **42,** (5), pp. 981-997, Tulsa.

Desio, A. (1935) Studi geologici sulla Cirenaica, sul deserto libico, Sulla Tripolitana et sul Fezzan Orientale. R. Accad. d., It Cufra, **1**, 464 p.

Dickinson, W. R. (1985) Interpreting provenance relations from detrital modes of sandstones. In: Provenance of Arenites (Ed. by Zuffa, G. G.), pp. 333-361, Reidel, Dordrecht.

Dualeh, A. H., Reuther, C. and Scheck, P. (1990) Basement structure and sedimentology cover of Somalia. Berliner geowissenschaftliche Abhandlungen, A, **120**, 2, pp. 505-518, Berlin.

Dunoyer de Segonzac, G. (1970) The transformation of clay minerals during diagnesis and low-grade metamorphism : a review. Sedimentology, **15**, pp. 281-346.

El Amin, M. B. (1993) Basin evolution and sedimentary facies with special reference to oil production in Muglad, Sudan. M.Sc. Thesis, University of Portsmouth, England.

El Badi, S. (1995) Sudanese ribes. M.Ar. Thesis, University of Khartoum, 121 p., Khartoum, Sudan.

El Shafie, A. A. (1975) Lithology of the Umm Rawaba Formation and its paleageography in connection with water problems, Sudan. Ph.D. Thesis, 130 p., geological Exploration Institute, Moscow.

Emery, D. and Myers, K. (1996) Sequence stratigraphy, 297 p. Blackwell Science Ltd., Oxford.

Eslinger, E. and Prear, D. R. (1988) Clay minerals for petroleum geologists and engineers: SEPM Short Course Notes, No. 22, Society of Economic Paleontologists and Mineralogists, Tulsa, Oklahoma.

Ethridge, F. G., Flores, R. M. and Harvey, M. D. (1987) Recent developments in fluvial sedimentology. Society of Economic Paleont. Mineral. Special Publication.

Ethridge, F. G., Jackson, T. J. and Youngbergh, A. D. (1981) Floodbasin sequence of a fine-grained meander belt subsystem; The coal-bearing lower Wasatch and upper Fort Union Formations, southern Powder River Basin, Wyoming. In: Recent and ancient non-marine depositional environments (Ed. by Ethridge, F. G. and Flores, R. M). Society of Economic Paleont. Mineral. Special Publication, **31**, pp. 191-209, Tulsa.

Fairhead, J. D. (1988) Mesozoic plate tectonic reconstruction of the central south Atlantic Ocean: The role of the west and central African rift system. Tectonophysics, **155**, pp. 181-195.

Fairhead, J. D. and Green, C. M. (1989) Controls on rifting in Africa and the regional tectonic model for the Nigeria and east Niger rift basins. Journal of African Earth Science, **8**, (2-4), pp. 231-249, Oxford.

Folk, R. L. (1974) Petrology of sedimentary rocks. Hemphill, 159 p., Austin, Texas.

Franz, G., Breitkreuz, C., Coyle, D. A., El Hur, B., Heinrich, W., Paulick, H., Pudlo, D., Steiner, G. and Smith, R. (1997). Geology of the alkaline Meidob Volcanic Field, late Cenozoic, in Sudan. Journal of African Earth Science, **25**, pp. 1-29.

Franz, G., Pudlo, D. Urlacher, G. Haußman, U., Boven, A. and Wemmer, K. (1994) The Darfur Dome, western Sudan: The product of a subcontinental mantle plume. Geologische Rundschau, **83**, pp. 614-623.

Frostick, L.E. and Reid, I. (1989) Climatic versus tectonic controls on fan sequences: Lessons from the Dead Sea, Israel. Journal geol. Soc., **146**, pp. 527-538, London.

Gawthorpe,R. L. and Colella, A. (1990) Tectonic controls on coarse-grained delta depositional system in rift basins. In: Coarse-grained deltas (Ed. by Colella, A. and Proir, D.). Special Publication int. Ass. Sediment, **10**, pp. 113-127.

Germann, K., Fischer, K. and Schwarz, T. (1990) accumulation of lateritic weathering products (kaolins, bauxitic laterites, ironstones) in sedimentary basins of northern Sudan. Berliner geowissenschaftliche Abhandlungen, A, **120**, Berlin.

Germann, K., Kuche; A., Doering, T. and Fischer, K. (1987) Late Cretaceous laterite-derived sedimentary deposits (oolitic ironstones, kaolin, bauxites) in upper Egypt. Berliner geowissenschaftliche Abhandlungen, A, **75**, 3, pp. 727-758, Berlin.

Getaneh, A. (1981) Gohatsion Formation: A new Lias-Malm lithostratigraphic unit from the Abbay River Basin, Ethiopia. Geoscience Journal, **2**, 1, pp. 63-88.

Getaneh, A. (1988) Potential hydrocarbon-generating rock units within the Phanerozoic sequence of the Ogaden Basin, Ethiopia. A preliminary assessment using the Lopatin model. Journal of Petroleoum Geology, **11**, 4, pp. 461-472.

Godin, P. D. (1991) Fining-upward cycles in the sandy braided-river deposits of the Westwater Canyon member (upper Jurassic), Morrison Formation, New Mexico. Sedimentary Geology, **70**, pp. 61-82.

GRAS (Geological Research Authority of the Sudan) (1981) Geological map for the south western part of the Sudan. Scale 1:100.000.

Grim, R. E. (1953) Clay mineralogy. McGraw-Hill, 384 p., New York.

Gumati, Y. D. and Narin, A. E. M. (1991) Tectonic subsidence of the Shire basin, Libya. Journal of Petroleum Geology, **14**, pp. 93-102.

Hallam, A. (1984) Continental humid and arid zones during the Jurassic and Cretaceous, Palaegeo., Palaeoclimat. Palaeoecology, **47**, pp. 195-223.

Harrison, M. N. and Jackson, J. K. (1958) Ecological classification of the vegetation of the Sudan. Forests Bulletin, **2**, pp. 19-23.

Heroux, Y., Chagnon, A. and Bertrand, R. (1979) compilation and correlation of major thermal maturation indicators. Bulletin American Association of Petroleum Geologists, **63**, 12, pp. 2128-2144.

Hirst, D. M. (1962) The geochemistry of modern sediments from the Gulf of Paria-1. The relationship between the mineralogy and the distribution of major elements. Geochemica et Cosmochimica, **26**, pp. 309-334.

Hower, J., Elsinger, E. V., Hower, M. E. and Perry, E. A. (1976) Mechanism of burial metamorphism of argillaceous sediments: 1, mineralogical and chemical evidence. Bulletin Geological Society of America, **87**, pp. 725-737.

Hubert, J. F. (1962) A zirkon-tourmaline-rutil maturity index and the interdepence of the composition of heavy mineral assemblages with the gross composition and texture of sandstones. Journal of Sedimentary Petrology, **32**, pp. 440-450.

Hubert, J. F. (1971) Analysis of heavy minerals assemblages. In: Procedure in sedimentary petrology (Ed. by Carter, R. E. ), pp. 453-478, New York.

Hussien, H. A. (1097) Sedimentology and basin analysis with emphasis on lithofacies and reservoir quality of Bentiu Formation, Sudan. M.Sc. thesis, University of Khartoum, 152 p., Khartoum, Sudan.

Idriss, A. M. (2001) Depositional environment and reservoir geology of the late Albian-Cenomanian Bentiu formation in Heglig and Unity Fields, Muglad Basin, Sudan. M.Sc. Thesis, University of Khartoum, Khartoum, Sudan.

Joann, E. W. (1984) SEM Petrology Atlas. American Association of Petroleum Geologists, Tulsa.

Johns, W. D. and Shimoyama, A. (1972) Clay minerals and petroleum-forming reactions during burial and diagenesis. Bulletin American Association of Petroleum Geologists, **56**, pp. 2160-2167.

Johnsson, M. and Meade, R. (1991) Chemical weathering of fluvial sediments during alluvial storage: The Macuapanim Island point bar, Solomoes river, Brazil. Jornal of Sedimentary Petrology, **60**, 6, pp. 827-842.

Kaska, H. V. (1989) A spore and pollen zonation of Early Cretaceous to Tertiary non-marine sediments of central Sudan. Palynology, **13**, pp. 79-90.

Keller, W. D. (1956) Clay minerals a sinfluenced by environments of their formation. Bulletin American Association of Petroleum Geologists, **40**, pp. 2689-2710.

Keller, W. D. (1970) environmental aspects of clay minerals. Journal of sedimentary Petrology, **40**, pp. 788-813.

Keller, W. D. Reynolds, R.C. Inoue, A. (1986) Morphology of clay minerals in the smectite-to-illite conversion series by scanning electron microscopy. Clays clay Min., 34, pp. 187-197.

Kerr, P. F. (1977) Optical Mineralogy. Mc Graw-Hill Book Company.

Kheiralla, M. K. (1966) A study of the Nubian sandstone formation of the Nile Valley between 12°N and 17°42'N with reference to the groundwater geology. M.Sc. Thesis, University of Khartoum, Khartoum, Sudan.

Klitzsch, E. (1983) Geological research in and around Nubia. Episodes, **3**, pp. 15-19, Ottawa.

Klitzsch, E. (1984) Northwestern Sudan and bordering areas: geological development since Cambrian time. Berliner geowissenschaftliche Abhandlungen, A, **50**, pp. 15-19, Berlin.

Klitzsch, E. (1986) Plate tectonics and cratonal geology in northeast Africa (Egypt/Sudan). Geologische Rundschau, **75**, 3, pp. 753-768, Stuttgard.

Klitzsch, E. (1989) Zur Stratigraphie Nubiens. Das Ende des Nubischen Sandsteines als stratigraphischer Begriff. Zeitschrift der deutschen geologischen Gesellschaft, 140, pp. 151-160, Hannover.

Klitzsch, E. (1990) Paleogeographical development and correlation of continental strata (former Nubian Sandstones) in northeast Africa. Journal of African Earth Science, **10**, 1/2., pp. 1203-1211, Oxford.

Klitzsch, E. and Lejal-Nicol (1984) Flora and fauna from strata in Southern Egypt and Northern Sudan. Berliner geowissenschaftliche Abhandlungen, A, **50**, pp. 47-79, Berlin.

Klitzsch, E. and Sguyres, H.-C. (1990) Paleozoic and Mesozoic geological history of northeastern Africa based upon new interpretation of Nubian strata. AAPG Bulletin, **74**, 8, pp. 1203-1211.

Klitzsch, E. and Wycisk, P. (1987) Geology of the sedimentary basin of northern Sudan and bordering areas. Berliner geowissenschaftliche Abhandlungen, A, **75**, 1, pp. 97-136, Berlin.

Kogbe, C. A. (1980) The trans-Saharan seaway during the cretaceous. In: Geology of Libya (Ed. by Salem and Busrevil ). proceedings of the second symposium of the geology of Libya, pp. 91-96,. Academic Press, London.

Kogbe, C. A. and Burollet, P. F. (1990) A review of the continental sediments in Africa. Journal of African Earth Science, **10**, ½, pp. 1-27.

Krauskopf, K. B. (1979) Introduction to geochemistry. McGraw-Hill, 617 p., New York.

Krumbein, W. C. and Rasmussen (1941) The problem error in sampling beach sand for heavy mineral analysis. Journal of Sedimentary Petrology, **11**, pp. 10-20.

Le franc, J. and Guiraud, R. (1990) The intercontinental intercalaire of north western Sahara and its equivalents in neighbouring regions. Journal of African Earth Science, **10**, 1/2., pp. 27-79, Oxford.

Lejal-Nicol, A. (1990) Paleofloristic evolution of Angiosperms during the Cretaceous and early Tertiary in Egypt and northern Sudan. Berliner geowissenschaftliche Abhandlungen, A, **120**, Berlin.

Lowell, J. D. and Henik, G. J. (1972) Sea-floor spreading and structural evolution of southern red Sea. American Association of Petroleum Geologists Bulletin, **56**, pp. 247-259, Tulsa.

Maarouf, S. T. (1998) Sedimentology and basin analysis with emphasis on the lithofacies and reservoir quality of Darfur Group and Amal Formation, NW Muglad Basin, Sudan. M.Sc. Thesis, University of Khartoum, Khartoum, Sudan.

Mange, M. A. and Maurer, H. F. (1992) Heavy Minerals in Colour, Champan and Hall. 147 p., London.

Mansour, N. (1990) Geochemisch-sedimentologische und tektonische Untersuchungen am Uweinat-Safsaf-Aswan-Schwellensystem (Südägypten/Nordsudan). Berliner Geowissenschaftliche Abhandlungen, A, **122**, 115 p., Berlin.

Mason, B. (1966) Principles of geochemistry (third edition). John Wiley & Sons Inc., pp. 149-191, New York.

Mbede, E. I. (1987) A review of the hydrocarbon potential of Kenya. Journal of African Earth Science, **6**, 3, pp. 313-322, Oxford.

McDonald, P. (2000) Outlook for oil and gas in an area of deregulation. The middle east and north Africa (special report). Petroleum Economist Ltd, 65 p., London.

McHarque, T. R., Heidrick, T. L. and Livingston, J. E. (1992) Tectonostratigraphic development of the interior Sudan rifts, central Africa. In: geodynamics of Rifting, Volume II. Case history studies on rifts: north and south America and Africa (Ed. by Ziegler, P. A.) Tectonophysics, **213**, pp. 187-202.

Mermingham, P. M., Fairhead, J. D. and Stuart, G. W. (1983) Gravity study of the central African rift system: A model of continental disruption 2. The Darfur domal uplift and associated Cainozoic volcanism. Tectonophysics, **94**, pp. 205-222.

Miall, A. D. (1978) Lithofacies types and vertical profile models in braided river deposits: a summery. In: Fluvial sedimentology (Ed. by Miall, A. D.). Memoir, **5**, pp. 597-604, Ottawa.

Miall, A. D. (1984) Principles of sedimentary basin Analyses, 490 p., Springer-Verlag, new York.

Miall, A. D. (1988) reservoir heterogeneities in fluvial sandstones: Lessons from outcrop studies. American Association of Petroleum Geologists Bulletin, **72,** pp. 682-697, Tulsa.

Milliken, K. L. (1989) Petrography and composition of authigenic feldspars, Oligocene Frio Formation, South Texas. Journal of Sedimentary Petrology, **59**, pp. 361-374.

Millot, G. (1970) Geology of clays. Springer-Verlag, 425 p., Paris.

Mohamed, A. Y., Pearson, M. J., Ashcroft, W. A., Illiffe, J. E. and Whiteman, A. J. (1999) Modeling petroleum generation in the southern Muglad Basin, Sudan. American Association of Petroleum Geologists Bulletin, **83**, pp. 1943-1964, Tulsa.

Mohamed, A. Y., Pearson, M. J., Ashcroft, W. A., Illiffe, J. E. and Whiteman, A. J. (2002) Petroleum maturation modelling, Abu Gabra-Sharaf area, Muglad Basin, Sudan. Journal of African Earth Science, **35**, pp. 331-344, Oxford.

Mohammed, A. S. (1997) The sedimentology of the lacustrin-fluvial Sharaf and Abu Gabra Formations (lower Cretaceous) NW Muglad Rift Basin, Sudan. M.Sc. Thesis, 154 p., University of Khartoum, Khartoum, Sudan.

Moore, D. M. and Reynolds, R. C. (1997) X-ray diffraction and the identification and analysis of clay minerals (second edition). Oxford University Press, Inc., 371 p., Oxford.

Morton, A. C. (1979) Depth control of intrastratal solution of heavy minerals from the Palaeocene of the North Sea. Journal of Sedimentary Petrology, **49**, 1, pp. 281-286.

Morton, A. C. (1985) Heavy minerals in provenance studies. In: Provenance of Arenites (Ed. by G. G. Zuffa), pp. 249-277, Reidel. Dordrecht.

Morton, A. C. and Hallsworth, C. R. (1994) Identifying provenance-specific features of detrital heavy mineral assemblages in sandstone. Sedimentary Geology, **90**, pp. 241-256.

Nahon, D. (1986) Evolution of iron crusts in tropical landscapes. In: Rates of chemical weathering of rocks and minerals (Steven et al.). pp. 169-191, Orlando.

Omer, M. K. (1983) The geology of the Nubian Sandstone Formation in Sudan. Stratigraphy, sedimentary dynamics, diagenesis. 227 p., Khartoum (Geological and Mineral Resources Department, Ministry of energy and Mining), Sudan.

Peterson, J. A. (1986) Geology and petroleum resources of central and east-central Africa. Modern Geology, **10**, pp. 329-364.

Pettijohn, F. J. (1975) Sedimentary rocks. Harper & Row. 628 p., New York.

Pettijohn, F. J., Potter, P. E. and Siever, R. (1987) Sand and sandstone. Springer Verlag, 553 p., New York.

Pomeyrol, R. (1968) Nubian Sandstone. American Association of Petroleum Geologists Bulletin, **52**, pp. 584-600, Tulsa.

Prasad, G. (1971) Nubian Sandstone paleoenvironment in Sudan. American Association of Petroleum Geologists Bulletin, **55**, 883 p., Tulsa.

Prasad, G., Lejal-icol and Vandois-Mieja, N. (1986) A tertiary age for upper Nubian sandstone Formation, central Sudan. American Association of Petroleum Geologists Bulletin, **70**, 2, pp. 138-142, Tulsa.

Reading, H. G. and Levell, B. K. (1996) Controls on the sedimentary rock record. In: Sedimentary environments: Processes, facies and stratigraphy (Ed. by reading, H. G.). Blackwell Scientific Publications, pp. 171-184, Amsterdam.

Reeves, C. V., Karanja, F. M. and Macleod, J. N. (1987) geophysical evidence for a failed Jurassic rift and triple junction in Kenya. Earth Planatary Science Letters, **81**, pp. 299-311, Amsterdam.

RRI (Robertson Research International PLC) (1991) Appraisal of the hydrocarbon bearing reservoirs. Unity Area, **1**, Sudan. Unpublished.

Rüssegger, J. (1837) Kreide und Sandstein, Einfluss von Graniten und letztren Porphyren, Grünsteine etc. in Ägypten und Nubian bis nach Sennar. Neues Jahrbuch der Mineralogie, Geognosie und Petrologie und Petrefacten Kunde (Jahrgang 1837), pp. 665-669.

Saigal, G. C., Morad, S., Bj✶rlykke, K., Egeberg, P. K. and Aagaard, P. (1988) Diagenetic albitization of detrital K-feldspar in Jurassic, Lower Cretaceous and Tertiary clastic reservoir rocks from offshore Norway, I. textures and origin. Journal of Sedimentary Petrology, **58**, pp. 1003-1013.

Sandford, K. S. (1935) Geological observation on the southerwestern frontiers of the Anglo-Egyptian Sudan and the adjoining part of the southern Libyan desert. Quarterly Journal Geological Society London, **80**, pp. 323-381.

Schandelmeier, H. and Puddlo, D. (1990) The Central African Fault Zone (CAFZ) in Sudan-a possible continental transform fault. Berliner geowissenschaftliche Abhandlungen, A, **120**, pp. 31-44, Berlin.

Schandelmeier, H. and Reynolds, P.O. 1997. (Eds). Palaeogeographic-Palaeotectonic Atlas of North-eastern Africa and adjacent areas. A.A. Balkema, Rotterdam: 168 pp (Explanatory Notes) and 17 Maps.

Schandelmeier, H., Klitzsch, E., Hendriks, F. and Wycisk, P. (1987) Structural developments of north-east Africa since Precambrian times. Berliner geowissenschaftliche Abhandlungen, A, **75**, pp. 5-24, Berlin.

Schandelmeier, H., Reynolds, P. O. and Küster, D. (1993) Spatial and temporal relationship between alkaline magmatism and early rifting in north/central Sudan. In: Geoscientific research in northeast Africa (Ed. by Thorweihe, U. and Schandelmeier, H.). pp. 221-225, A. A. Balkema, Rotterdam.

Schull, T. J. (1988) Rift basins of interior Sudan: Petroleum exploration and discovery. American Association of Petroleum Geologists Bulletin, **72**, pp. 1128-1142, Tulsa.

Schwertmann, U. and Niederbudde, E. (1993) Tonminerale in Böden. In: Tonminerale und Tone (Ed. by Lagaly, G.). 490 p., Steinkopff Verlag, Darmstadt.

Selley, R. C. (1985) Ancient sedimentary environments. Chapman Hall, 317 p., London.

Smith, J. (1949) Distribution of the tree species in the Sudan in relation to rainfall and soil texture. Sudan Mini. Agric. Bulletin, **4**, pp. 48-53.

Sturm, M. (1979) Origin and composition of clastic varves. In: Moraines and varves (Ed. by Schlüchter, C.). pp. 281-285, Balkema, Rotterdam.

Surdan, R. C. and Crossey, L. J. (1985) Organic-inorganic reactions during progressive burial: key to porosity and permeability enhancement and preservation. Phil. Trans. Roy. Soc. Lond., **A315**, pp. 135-136.

Talbot, M. R. (1988) he origins of lacustrine oil source rocks: evidence from the lakes of tropical Africa. In: Lacustrine petroleum source rocks (Ed. by Fleet, A. J., Kelts, K. and Talbot, M. R.). Special Publication Geological Society London, **40**, pp. 29-43, Bristol.

Tang, Z., Parnell, J. and Longstaffe, F. J. (1997) Diagenesis and reservoir potential of Permian-Triassic fluvial/lacustrine sandstones in the southern Junggar Basin, NW China. Bulletin American Association of Petroleum Geologists, **18**, 11, pp. 1843-1865.

Teggart, J. E., Linsay, J. R., Scott, B. A., Vivit, D. V., Bartel, A. J. and Stewart, K. C. (1987) Analysis of geological materials by X-ray flouresence spectrometry. In: Methods for geochemical analysis (Ed. by Baedecher, P. A.). U.S.A. Geological Survey Bulletin, **1770**.

Tissot, B. P., Pelet, R. and Urgerer, Ph. (1987) Thermal history of sedimentary basins, maturation indices and kinetics of oil generation. Bulletin American Association of Petroleum Geologists, 7**1**, 12, pp. 1445-1467.

Tucker, M. E. (1988) Techniques in sedimentology. Blackwells, 394 p., Oxford.

Tucker, M. E. (1991) Sedimentary petrology: An introduction to the origin of sedimentary rocks(second edition). Blackwell Scientific Publications, 260 p., Oxford.

Vail, J .R. and Rex, D. C. (1971) Potassium-Argon measurement on Pre-Nubian basement rocks from Sudan. Proc. Geol. Soc., **1664**, pp. 205-214, London.

Vail, J. R. (1978) Outline of the geology and mineral deposits of the Democratic Republic of Sudan and adjacent areas. Overseas Geol. Miner. Resour., **49**, 67 p., London.

Vail, J. R. (1985) Alkaline ring complexes in Sudan. Journal of African Earth Science, **3**, (1-2), pp. 51-59.

Van Houten, F. B. (1980) Latest Jurassic early Cretaceous regressive facies, northeast Africa craton. American Association of Petroleum geologists Bulletin, **64**, 5, pp. 857-867.

Walker, T. R., Waugh, B. and Crone, A. J. (1978) Diagenesis in first-cycle desert alluvium of Cenozoic age, southwestern United States and northwestern Mexico. Bulletin geological Society of America, **89**, pp. 19-32.

Walters, L. J., Owen, D. E., Henley A. L., Winsten M. S. and Valek, K. W. (1987) Depositional environments of the Dakota Sandstone and adjacent units in the San Juan Basin utilizing discriminant analysis of trace elements in shales. Journal of Sedimentary Petrology, **57**, 2, pp. 565-277.

Wanli, Y. (1985) Daging Oil Field, Peopleis Republic of China: A giant field with oil of non-marine origin. American Association of Petroleum Geologists, **69,** pp. 1101-1111, Tulsa.

Weaver, C. E. (1989) Clays, muds and shales. Elsevier, 820 p., Amsterdam.

Wilson, M. D. and Pittman, E. D. (1977) Authigenic clays in sandstones: recognition and influence on reservoir properties and paleoenvironmental analysis. Journal of Sedimentary Petrology, **47**, pp. 3-31.

Witheman, A. J. (1971) The geology of the Sudan Republic. Clarendon Press, Oxford.

Wycisk, P., Klitzsch, E., Jas, C. and Reynolds, O. (1990) Intracratonal sequence development and structural control of Phanerozoic strata in Sudan. Berliner geowissenschaftliche Abhandlungen, A, **120**, pp. 45-86, Berlin.

Wycisk, P., Klitzsch, E., Jas, C. and Reynolds, O. (1990) Intracratonal sequence development and structural control of Phanerozoic strata in Sudan. Berliner geowissenschaftliche Abhandlungen, A, **75**, pp. 249-310, Berlin.

Zussman, J. (1977) Physical method in determinative mineralogy (second edition). Academic press INC., pp. 201-273 and 371-391, London.

# 11 Appendices

**Appendix 1 (A): Percetanges of the major heavy minerals in the study intervals at Unity-9, Talih-2 and Barki- 1 wells in Unity Field, SE Muglad Basin.**

| Well | Fm. | Sample Depth (ft) | Zr | T | R | K | St | An | Sill | E | G | H | ZTR % | SEH % |
|------|-----|------|-----|-----|-----|-----|-----|-----|------|-----|-----|-----|------|------|
| Unity-9 | Zarga | 7310 | 7.9 | 4.0 | 15.0 | 32.0 | 5.0 | 8.5 | 2.0 | 2.0 | 20.8 | 2.8 | 26.9 | 6.8 |
| | | 7400 | 9.0 | 3.2 | 14.9 | 30.0 | 5.2 | 7.6 | 3.2 | 2.6 | 22.1 | 2.6 | 27.1 | 8.4 |
| | Aradeiba | 7590 | 12.5 | 0.0 | 13.4 | 30.3 | 2.6 | 4.4 | 3.0 | 3.8 | 27.6 | 2.4 | 25.9 | 9.2 |
| | | 7680 | 8.1 | 2.7 | 10.8 | 29.0 | 3.6 | 6.6 | 2.2 | 3.2 | 32.4 | 1.4 | 21.6 | 6.8 |
| | | 7780 | 17.1 | 2.8 | 9.6 | 24.0 | 2.4 | 5.4 | 0.0 | 2.4 | 36.4 | 0.0 | 29.5 | 2.4 |
| | | 7880 | 25.0 | 0.0 | 12.5 | 17.0 | 1.3 | 2.0 | 0.0 | 0.0 | 42.2 | 0.0 | 37.5 | 0.0 |
| | | 7970 | 19.0 | 1.9 | 11.6 | 22.0 | 2.0 | 4.8 | 0.0 | 0.0 | 38.7 | 0.0 | 32.5 | 0.0 |
| | | 8050 | 9.1 | 3.4 | 11.5 | 28.0 | 3.0 | 6.5 | 0.0 | 0.0 | 38.5 | 0.0 | 24.0 | 0.0 |
| | | 8130 | 6.2 | 0.0 | 9.3 | 31.0 | 3.6 | 7.5 | 0.0 | 0.0 | 42.4 | 0.0 | 15.5 | 0.0 |
| | | 8220 | 13.5 | 3.3 | 7.9 | 27.0 | 3.0 | 7.2 | 0.0 | 0.0 | 38.0 | 0.0 | 24.7 | 0.0 |
| | | 8310 | 11.3 | 0.0 | 14.0 | 26.0 | 2.4 | 6.6 | 0.0 | 0.0 | 39.7 | 0.0 | 25.3 | 0.0 |
| | | 8390 | 4.0 | 2.0 | 9.0 | 29.0 | 2.7 | 6.0 | 0.0 | 0.0 | 43.3 | 0.0 | 15.0 | 4.0 |
| | | 8480 | 3.8 | 2.8 | 8.5 | 29.0 | 3.4 | 6.0 | 0.0 | 0.0 | 46.5 | 0.0 | 15.1 | 0.0 |
| | | 8590 | 3.9 | 0.0 | 8.0 | 28.0 | 3.0 | 4.0 | 0.0 | 0.0 | 53.1 | 0.0 | 11.9 | 0.0 |
| | | 8730 | 14.0 | 3.3 | 12.7 | 17.0 | 0.0 | 0.0 | 0.0 | 0.0 | 53.0 | 0.0 | 30.0 | 0.0 |
| | Bentiu | 8890 | 14.3 | 2.6 | 12.0 | 19.8 | 0.0 | 0.0 | 0.0 | 0.0 | 51.3 | 0.0 | 28.9 | 0.0 |
| | | 9000 | 14.5 | 2.0 | 13.2 | 17.0 | 0.0 | 0.0 | 0.0 | 0.0 | 53.3 | 0.0 | 29.7 | 0.0 |
| Talih-2 | Zarga | 7490 | 5.6 | 0.7 | 19.0 | 31.3 | 3.0 | 10.0 | 3.0 | 4.0 | 20.0 | 3.3 | 25.3 | 10.3 |
| | | 7650 | 6.0 | 1.0 | 13.0 | 33.0 | 4.0 | 11.0 | 4.0 | 4.0 | 20.5 | 3.5 | 20.0 | 11.5 |
| | Aradeiba | 7860 | 8.7 | 3.9 | 17.2 | 31.0 | 0.0 | 7.4 | 1,6 | 2.7 | 23.9 | 3.6 | 29.8 | 7.9 |
| | | 7960 | 13.2 | 1.0 | 16.1 | 27.0 | 2.0 | 7.0 | 0.0 | 0.0 | 33.7 | 0.0 | 30.3 | 0.0 |
| | | 8080 | 8.5 | 3.7 | 15.6 | 29.0 | 1.0 | 9.0 | 0.0 | 0.0 | 33.2 | 0.0 | 27.8 | 0.0 |
| | | 8160 | 8.0 | 3.2 | 14.4 | 30.0 | 3.0 | 8.0 | 2.0 | 0.0 | 31.4 | 0.0 | 25.6 | 2.0 |
| | | 8230 | 9.4 | 3.4 | 12.0 | 28.0 | 0.0 | 6.0 | 0.0 | 0.0 | 41.2 | 0.0 | 24.8 | 0.0 |
| | | 8260 | 10.8 | 0.0 | 13.8 | 27.0 | 1.5 | 8.0 | 0.0 | 0.0 | 38.8 | 0.0 | 24.6 | 0.0 |
| | | 8350 | 10.7 | 2.3 | 13.4 | 30.0 | 1.0 | 3.0 | 0.0 | 0.0 | 39.6 | 0.0 | 26.4 | 0.0 |
| | | 8480 | 4.3 | 1.8 | 9.3 | 31.0 | 2.0 | 7.0 | 0.0 | 2.0 | 42.6 | 0.0 | 15.4 | 2.0 |
| | | 8540 | 5.7 | 1.9 | 9.0 | 31.0 | 1.0 | 9.0 | 0.0 | 2.0 | 39.4 | 2.0 | 16.6 | 4.0 |
| | | 8680 | 12.0 | 4.2 | 8.3 | 30.0 | 0.0 | 6.0 | 0.0 | 0.0 | 39.5 | 0.0 | 24.5 | 0.0 |
| | | 8780 | 8.0 | 0.3 | 8.0 | 28.0 | 1.0 | 6.0 | 0.0 | 2.0 | 46.7 | 0.0 | 16.3 | 2.0 |
| | Bentiu | 8860 | 17.3 | 1.5 | 7.7 | 24.0 | 0.0 | 4.0 | 0.0 | 0.0 | 45.5 | 0.0 | 26.5 | 0.0 |
| | | 9100 | 7.5 | 2.0 | 18.0 | 22.5 | 1.0 | 2.0 | 0.0 | 0.0 | 47.0 | 0.0 | 27.5 | 0.0 |
| Barki-1 | Zarga | 4100 | 7.0 | 2.3 | 10.0 | 33.0 | 2.0 | 9.0 | 3.6 | 2.2 | 27.9 | 3.0 | 19.3 | 8.8 |
| | | 4250 | 12.0 | 3.6 | 14.3 | 29.0 | 2.0 | 9.3 | 3.6 | 2.0 | 21.9 | 2.3 | 29.9 | 7.9 |
| | Aradeiba | 4400 | 8.0 | 2.0 | 14.0 | 27.0 | 1.7 | 10.0 | 3.0 | 2.4 | 28.2 | 3.7 | 24.0 | 9.1 |
| | | 4520 | 8.3 | 0.4 | 13.3 | 30.0 | 2.7 | 7.0 | 1.0 | 1.0 | 36.3 | 0.0 | 22.0 | 2.0 |
| | | 4600 | 12.6 | 2.4 | 9.2 | 33.7 | 3.1 | 6.0 | 1.0 | 1.0 | 31.0 | 0.0 | 24.0 | 2.0 |
| | | 4700 | 19.0 | 2.1 | 15.0 | 25.0 | 0.0 | 8.0 | 0.0 | 0.0 | 30.9 | 0.0 | 36.1 | 0.0 |
| | | 4820 | 10.1 | 1.7 | 13.5 | 28.7 | 1.8 | 8.0 | 0.0 | 0.0 | 36.2 | 0.0 | 25.3 | 0.0 |
| | | 4940 | 8.8 | 2.2 | 13.5 | 27.9 | 3.0 | 8.0 | 2.0 | 1.5 | 33.1 | 0.0 | 24.5 | 3.5 |
| | | 5030 | 6.0 | 2.7 | 12.2 | 32.0 | 3.9 | 8.9 | 0.0 | 0.0 | 36.3 | 0.0 | 20.9 | 0.0 |
| | | 5150 | 7.2 | 2.5 | 12.2 | 30.0 | 3.0 | 7.0 | 0.0 | 0.0 | 38.0 | 0.0 | 21.9 | 0.0 |
| | | 5360 | 8.2 | 1.4 | 10.0 | 28.0 | 0.0 | 3.6 | 2.0 | 2.8 | 42.0 | 2.0 | 9.6 | 6.8 |
| | Bentiu | 5500 | 11.7 | 2.0 | 13.0 | 26.0 | 0.0 | 2.6 | 1.3 | 1.9 | 39.6 | 1.9 | 26.7 | 5.1 |
| | | 5650 | 15.0 | 2.0 | 18.0 | 23.0 | 0.0 | 0.0 | 0.0 | 0.0 | 42.0 | 0.0 | 35.0 | 0.0 |

**Appendix 1 (B): Percentages of the major heavy minerals in the study intervals at Nabag-1, Toma-1 and Heglig-2 wells Heglig Field, SE Muglad Basin.**

| Well | Fm. | Sample Depth (ft) | Zr | T | R | K | St | An | Sill | E | G | H | Gl-r | ZTR % | SEH % |
|------|-----|-------------------|-----|-----|------|------|-----|------|------|-----|------|-----|------|-------|-------|
| Nabag-1 | Zarga | 3810 | 8.0 | 2.0 | 13.0 | 42.0 | 2.0 | 9.0 | 7.0 | 3.0 | 6.0 | 5.0 | 3.0 | 23.0 | 15.0 |
| | | 3960 | 9.0 | 2.0 | 12.0 | 38.0 | 3.0 | 8.0 | 5.0 | 2.0 | 16.0 | 3.0 | 2.0 | 23.0 | 10.0 |
| | Aradeiba | 4200 | 12.0 | 3.0 | 15.0 | 37.0 | 1.0 | 8.0 | 0.0 | 1.0 | 22.0 | 0.0 | 0.0 | 30.0 | 1.0 |
| | | 4400 | 16.0 | 2.0 | 11.0 | 32.0 | 0.0 | 0.0 | 0.0 | 2.0 | 36.0 | 0.0 | 0.0 | 30.0 | 2.0 |
| | | 4600 | 12.0 | 2.0 | 11.0 | 33.0 | 2.0 | 6.0 | 3.0 | 0.0 | 28.0 | 3.0 | 0.0 | 25.0 | 6.0 |
| | | 4880 | 7.0 | 1.0 | 10.0 | 34.0 | 2.0 | 6.0 | 6.0 | 2.0 | 26.0 | 6.0 | 0.0 | 18.0 | 14.0 |
| | Bentiu | 5220 | 9.0 | 1.0 | 12.0 | 32.0 | 2.0 | 5.0 | 2.0 | 2.0 | 35.0 | 0.0 | 0.0 | 22.0 | 4.0 |
| | | 5450 | 13.0 | 2.0 | 15.0 | 29.0 | 1.0 | 3.0 | 0.0 | 0.0 | 37.0 | 0.0 | 0.0 | 30.0 | 0.0 |
| Toma-1 | Zarga | 4110 | 8.0 | 2.0 | 9.0 | 40.0 | 2.0 | 11.0 | 2.0 | 2.0 | 21.0 | 3.0 | 0.0 | 19.0 | 7.0 |
| | | 4440 | 13.0 | 3.0 | 12.0 | 38.0 | 1.0 | 5.0 | 0.0 | 2.0 | 26.0 | 0.0 | 0.0 | 28.0 | 2.0 |
| | Aradeiba | 4520 | 5.5 | 1.0 | 10.0 | 37.0 | 2.9 | 10.0 | 6.3 | 3.7 | 18.6 | 5.0 | 0.0 | 16.5 | 15.0 |
| | | 4580 | 9.5 | 2.5 | 11.0 | 37.0 | 1.1 | 6.0 | 0.0 | 0.0 | 32.7 | 0.0 | 0.0 | 23.0 | 0.0 |
| | | 4640 | 12.2 | 2.6 | 14.8 | 30.0 | 3.0 | 5.0 | 0.0 | 0.0 | 32.4 | 0.0 | 0.0 | 29.6 | 0.0 |
| | | 4760 | 7.0 | 1.2 | 11.6 | 34.0 | 2.6 | 9.0 | 0.0 | 0.0 | 34.6 | 0.0 | 0.0 | 19.8 | 0.0 |
| | | 4800 | 13.0 | 1.0 | 15.6 | 29.0 | 2.6 | 4.0 | 0.0 | 0.0 | 34.8 | 0.0 | 0.0 | 29.6 | 0.0 |
| | | 4860 | 6.0 | 0.0 | 11.0 | 34.0 | 0.0 | 12.0 | 0.0 | 0.0 | 37.0 | 0.0 | 0.0 | 17.0 | 0.0 |
| | | 5040 | 3.4 | 1.3 | 10.2 | 36.0 | 3.0 | 12.0 | 4.4 | 2.7 | 24.0 | 3.0 | 0.0 | 14.9 | 10.1 |
| | | 5130 | 8.8 | 1.1 | 9.6 | 34.0 | 2.8 | 10.0 | 2.7 | 2.0 | 27.0 | 2.0 | 0.0 | 19.5 | 6.7 |
| | | 5210 | 7.5 | 2.2 | 9.3 | 32.0 | 2.0 | 8.0 | 2.0 | 1.0 | 35.0 | 1.0 | 0.0 | 18.9 | 4.0 |
| | | 5280 | 9.6 | 2.6 | 8.5 | 30.0 | 1.5 | 6.0 | 1.8 | 0.0 | 38.0 | 2.0 | 0.0 | 20.7 | 3.8 |
| | Bentiu | 5430 | 12.0 | 2.0 | 13.0 | 29.0 | 1.0 | 3.0 | 1.0 | 2.0 | 37.0 | 0.0 | 0.0 | 27.0 | 3.0 |
| | | 5600 | 15.0 | 2.0 | 13.0 | 26.0 | 1.0 | 4.0 | 0.0 | 0.0 | 39.0 | 0.0 | 0.0 | 30.0 | 0.0 |
| Heglig-2 | Zarga | 4380 | 9.0 | 1.0 | 14.0 | 37.0 | 0.0 | 12.0 | 3.0 | 3.0 | 18.0 | 3.0 | 0.0 | 24.0 | 9.0 |
| | | 4500 | 11.7 | 2.3 | 13.0 | 36.0 | 0.0 | 9.2 | 1.3 | 1.9 | 23.3 | 1.3 | 0.0 | 27.0 | 4.5 |
| | Aradeiba | 4620 | 13.5 | 2.0 | 14.0 | 33.0 | 0.3 | 6.0 | 0.0 | 0.0 | 30.3 | 0.0 | 0.0 | 29.5 | 0.0 |
| | | 4740 | 6.0 | 2.5 | 12.0 | 39.0 | 2.0 | 9.7 | 3.7 | 2.6 | 17.7 | 4.8 | 0.0 | 20.5 | 11.1 |
| | | 4840 | 13.7 | 1.3 | 15.0 | 31.0 | 0.0 | 6.0 | 0.0 | 0.0 | 33.0 | 0.0 | 0.0 | 30.0 | 0.0 |
| | | 4940 | 6.8 | 1.4 | 10.4 | 35.0 | 2.0 | 9.5 | 4.1 | 1.2 | 27.6 | 2.0 | 0.0 | 18.6 | 7.3 |
| | | 5040 | 16.5 | 3.4 | 9.6 | 29.0 | 0.7 | 5.0 | 0.0 | 0.0 | 35.7 | 0.0 | 0.0 | 29.4 | 0.0 |
| | | 5140 | 14.0 | 2.8 | 13.2 | 32.0 | 1.0 | 4.0 | 0.0 | 0.0 | 32.9 | 0.0 | 0.0 | 30.0 | 0.0 |
| | | 5240 | 6.8 | 1.2 | 8.0 | 30.0 | 1.8 | 9.0 | 1.6 | 1.2 | 37.2 | 3.2 | 0.0 | 16.0 | 6.0 |
| | | 5300 | 6.1 | 1.0 | 7.6 | 30.0 | 1.5 | 7.0 | 1.2 | 1.0 | 40.0 | 4.6 | 0.0 | 14.7 | 6.8 |
| | | 5380 | 9.5 | 6.0 | 7.3 | 28.2 | 0.0 | 7.0 | 0.0 | 0.0 | 40.0 | 2.0 | 0.0 | 22.8 | 2.0 |
| | | 5550 | 12.3 | 3.9 | 9.8 | 26.3 | 0.0 | 5.8 | 0.0 | 1.3 | 39.3 | 1.3 | 0.0 | 26.0 | 2.6 |
| | Bentiu | 5750 | 16.2 | 2.0 | 11.9 | 25.0 | 0.0 | 4.0 | 0.0 | 2.0 | 37.9 | 0.0 | 0.0 | 30.1 | 2.0 |

Note: Fm. = Formation, Zr = Zircon, T = Tourmaline, R = Rutile, Kyanite, St = Staurolite, An = Andalusite, Sill = Sillimanite, E = Epidote, G = Garnet, H = Hornblende, Gl- r = Glaucophane – riebeckite, ZTR = Zircon – Tourmaline – Rutile index

**Appendix 2 (A): Percentages of clay minerals in the study intervals at Unity-9, Talih-2 and Barki-1 wells in Unity Field, SE Muglad Basin.**

| Well | Formation | Sample Depth (ft) | Clay minerals | | | | |
|---|---|---|---|---|---|---|---|
| | | | Kaolinite % | Illite % | Smectite % | Illite/Smectite % | Chlorite % |
| Unity-9 | Zarga | 7253 | 68 | 6 | 6 | 16 | 3 |
| | | 7380 | 25 | 14 | 30 | 22 | 9 |
| | | 7463 | 56 | 26 | 0 | 18 | 0 |
| | Aradeiba | 7720 | 67 | 0 | 3 | 30 | 0 |
| | | 7820 | 23 | 10 | 23 | 33 | 11 |
| | | 8120 | 35 | 15 | 25 | 23 | 2 |
| | | 8330 | 31 | 20 | 41 | 9 | 0 |
| | | 8414 | 50 | 19 | 7 | 24 | 0 |
| | | 8780 | 76 | 16 | 0 | 8 | 0 |
| | Bentiu | 8887 | 44 | 32 | 0 | 24 | 0 |
| | | 9050 | 36 | 22 | 0 | 36 | 6 |
| Talih-2 | Zarga | 7517 | 32 | 0 | 32 | 28 | 8 |
| | | 7702 | 63 | 15 | 0 | 14 | 8 |
| | | 7733 | 71 | 0 | 0 | 23 | 5 |
| | Aradeiba | 7910 | 8 | 0 | 50 | 39 | 3 |
| | | 8155 | 41 | 22 | 0 | 36 | 0 |
| | | 8174 | 22 | 14 | 47 | 11 | 3 |
| | | 8238 | 34 | 20 | 30 | 3 | 13 |
| | | 8310 | 21 | 38 | 14 | 26 | 0 |
| | | 8440 | 77 | 8 | 6 | 6 | 2 |
| | | 8640 | 70 | 5 | 3 | 20 | 2 |
| | | 8830 | 53 | 6 | 1 | 37 | 2 |
| | Bentiu | 9000 | 36 | 14 | 7 | 40 | 3 |
| | | 9210 | 61 | 10 | 0 | 24 | 4 |
| Barki-1 | Zarga | 4150 | 55 | 8 | 15 | 22 | 0 |
| | | 4310 | 35 | 12 | 28 | 23 | 2 |
| | Aradeiba | 4660 | 52 | 16 | 4 | 22 | 5 |
| | | 4790 | 32 | 46 | 17 | 0 | 6 |
| | | 4910 | 66 | 5 | 1 | 26 | 2 |
| | | 5120 | 57 | 10 | 3 | 26 | 4 |
| | | 5390 | 71 | 13 | 8 | 2 | 6 |
| | Bentiu | 5427 | 55 | 41 | 4 | 0 | 0 |
| | | 5590 | 23 | 29 | 0 | 30 | 18 |

**Appendix 2 (B): Percentages of clay minerals in the study intervals at Heglig-2, Toma-1 and Nabag-1 wells in Heglig Field, SE Muglad Basin.**

| Well | Formation | Sample Depth (ft) | Clay minerals | | | | |
|------|-----------|-------------------|---------------|---|---|---|---|
| | | | Kaolinite % | Illite % | Smectite % | Illite/Smectite % | Chlorite % |
| Heglig-2 | Zarga | 4380 | 48 | 4 | 30 | 18 | 0 |
| | | 4590 | 36 | 15 | 21 | 26 | 3 |
| | Aradeiba | 4700 | 24 | 12 | 2 | 59 | 3 |
| | | 4820 | 36 | 4 | 2 | 50 | 7 |
| | | 4920 | 77 | 9 | 3 | 2 | 8 |
| | | 5120 | 35 | 18 | 2 | 32 | 13 |
| | | 5220 | 49 | 9 | 4 | 35 | 3 |
| | | 5300 | 50 | 5 | 0 | 44 | 2 |
| | | 5400 | 37 | 11 | 10 | 30 | 12 |
| | Bentiu | 5660 | 27 | 22 | 0 | 44 | 7 |
| | | 5850 | 22 | 28 | 0 | 46 | 4 |
| Toma-1 | Zarga | 4180 | 62 | 6 | 8 | 24 | 0 |
| | | 4340 | 57 | 5 | 11 | 26 | 1 |
| | | 4460 | 34 | 6 | 35 | 23 | 2 |
| | Aradeiba | 4520 | 69 | 4 | 2 | 24 | 0 |
| | | 4640 | 24 | 13 | 30 | 27 | 6 |
| | | 4700 | 61 | 7 | 5 | 25 | 2 |
| | | 4900 | 78 | 7 | 0 | 15 | 0 |
| | | 5230 | 69 | 7 | 0 | 23 | 0 |
| | Bentiu | 5313 | 73 | 4 | 0 | 23 | 0 |
| | | 5560 | 34 | 4 | 3 | 52 | 8 |
| Nabag-1 | Zarga | 3850 | 68 | 6 | 14 | 12 | 0 |
| | | 4100 | 39 | 11 | 24 | 24 | 2 |
| | Aradeiba | 4230 | 19 | 18 | 37 | 22 | 4 |
| | | 4400 | 20 | 20 | 30 | 26 | 4 |
| | | 4520 | 30 | 16 | 23 | 29 | 2 |
| | | 4630 | 56 | 8 | 0 | 36 | 0 |
| | | 4820 | 75 | 6 | 0 | 19 | 0 |
| | | 5020 | 81 | 8 | 0 | 11 | 0 |
| | Bentiu | 5200 | 66 | 13 | 0 | 19 | 2 |
| | | 5320 | 67 | 12 | 0 | 21 | 0 |

**Appendix 3 (A): XRF analysis results of the upper Bentiu, all Aradeiba and lower Zarga Formations at the studied wells in Unity Field, SE Muglad Basin.**

| Well | Formation | Sample Depth (ft) | SiO$_2$ % | Al$_2$O$_3$% | Fe$_2$O$_3$% | MnO % | MgO % | CaO % | Na$_2$O% | K$_2$O % | TiO$_2$ % | P$_2$O$_5$ % | SO$_3$ % |
|------|-----------|-------------------|-----------|--------------|--------------|-------|-------|-------|----------|----------|-----------|--------------|----------|
| Unity-9 | Zarga | 7241 | 72.01 | 5.96 | 2.94 | 0.197 | 1.26 | 4.83 | 1.05 | 0.56 | 2.13 | 0.050 | 0.000 |
| | | 7470 | 67.49 | 10.46 | 1.74 | 0.052 | 0.83 | 5.70 | 1.59 | 2.35 | 1.94 | 0.075 | 0.018 |
| | Aradeiba | 7720 | 53.87 | 17.82 | 5.21 | 0.13 | 1.67 | 0.97 | 0.33 | 3.84 | 1.45 | 0.152 | 0.044 |
| | | 7900 | 68.05 | 8.77 | 9.29 | 0.129 | 2.27 | 1.19 | 1.61 | 1.04 | 2.12 | 0.084 | 0.00 |
| | | 8070 | 61.83 | 12.28 | 8.60 | 0.10 | 1.70 | 0.70 | 0.47 | 2.13 | 1.96 | 0.140 | 0.00 |
| | | 8250 | 59.19 | 12.92 | 8.09 | 0.10 | 1.59 | 0.82 | 0.54 | 2.05 | 2.09 | 0.152 | 0.255 |
| | | 8393 | 73.31 | 11.59 | 1.52 | 0.058 | 0.94 | 1.46 | 1.40 | 0.50 | 1.98 | 0.050 | 0.00 |
| | | 8417 | 54.12 | 16.09 | 4.08 | 0.094 | 1.41 | 4.32 | 0.65 | 3.08 | 1.96 | 0.096 | 0.030 |
| | | 8650 | 58.24 | 14.27 | 4.99 | 0.12 | 1.37 | 2.45 | 0.68 | 4.40 | 1.62 | 0.187 | 0.159 |
| | | 8780 | 55.52 | 16.20 | 3.97 | 0.13 | 1.30 | 2.58 | 1.18 | 3.26 | 2.03 | 0.166 | 0.172 |
| | Bentiu | 8871 | 63.87 | 10.37 | 5.37 | 0.043 | 1.97 | 4.87 | 1.18 | 3.62 | 2.02 | 0.057 | 0.038 |
| | | 9000 | 67.55 | 10.89 | 6.99 | 0.080 | 2.17 | 1.27 | 1.23 | 3.13 | 2.07 | 0.122 | 0.00 |
| Talih-2 | Zarga | 7500 | 68.27 | 10.04 | 4.11 | 0.054 | 2.47 | 0.85 | 1.51 | 1.02 | 2.14 | 0.068 | 0.00 |
| | | 7702 | 50.98 | 15.23 | 3.5 | 0.038 | 1.96 | 4.73 | 0.86 | 3.86 | 1.69 | 0.068 | 0.00 |
| | Aradeiba | 7800 | 58.51 | 12.39 | 4.68 | 0.10 | 1.33 | 0.98 | 0.51 | 2.97 | 2.12 | 0.19 | 0.00 |
| | | 8020 | 67.58 | 10.90 | 5.64 | 0.10 | 1.25 | 0.61 | 0.32 | 1.11 | 1.88 | 0.167 | 0.0 |
| | | 8137 | 64.82 | 11.45 | 5.03 | 0.077 | 1.64 | 1.53 | 1.25 | 1.06 | 1.84 | 0.266 | 0.0 |
| | | 8239 | 71.65 | 10.73 | 2.87 | 0.116 | 0.63 | 1.65 | 1.96 | 2.09 | 1.65 | 0.143 | 0.0 |
| | | 8440 | 58.95 | 16.40 | 3.25 | 0.11 | 1.36 | 2.03 | 0.44 | 5.48 | 1.00 | 0.202 | 0.372 |
| | | 8632 | 62.56 | 14.48 | 4.57 | 0.071 | 1.35 | 1.20 | 0.89 | 3.93 | 1.12 | 0.050 | 0.00 |
| | Bentiu | 8820 | 64.35 | 12.13 | 3.92 | 0.16 | 1.85 | 3.40 | 1.55 | 2.94 | 0.94 | 0.169 | 0.112 |
| | | 9100 | 65.37 | 10.89 | 4.06 | 0.101 | 1.92 | 3.65 | 1.61 | 3.28 | 2.10 | 0.207 | 0.211 |
| Barki-1 | Zarga | 4120 | 50.80 | 19.90 | 6.93 | 0.07 | 1.46 | 0.77 | 0.25 | 3.70 | 0.80 | 0.13 | 0.075 |
| | | 4280 | 64.10 | 14.38 | 7.30 | 0.07 | 1.80 | 0.80 | 0.24 | 2.22 | 1.79 | 0.112 | 0.088 |
| | Aradeiba | 4430 | 59.61 | 17.39 | 7.20 | 0.082 | 1.99 | 1.65 | 0.49 | 3.17 | 1.13 | 0.178 | 0.00 |
| | | 4660 | 60.53 | 15.73 | 7.22 | 0.05 | 2.43 | 0.65 | 0.30 | 3.97 | 1.97 | 0.128 | 0.00 |
| | | 5030 | 50.87 | 20.00 | 5.43 | 0.154 | 1.61 | 1.57 | 0.23 | 4.00 | 1.12 | 0.241 | 0.00 |
| | | 5390 | 52.02 | 19.48 | 5.62 | 0.03 | 1.60 | 0.68 | 0.28 | 3.00 | 0.80 | 0.154 | 0.114 |
| | Bentiu | 5500 | 60.81 | 15.57 | 6.35 | 0.07 | 2.50 | 2.37 | 1.60 | 3.50 | 1.44 | 0.223 | 0.214 |
| | | 5650 | 64.88 | 12.76 | 6.6 | 0.01 | 2.95 | 0.27 | 1.62 | 3.78 | 2.21 | 0.179 | 0.220 |

| Well | Formation | Sample Depth (ft) | Ba ppm | Co ppm | Cr ppm | Cu ppm | Ga ppm | Ni ppm | Rb ppm | V ppm | Zr ppm |
|------|-----------|-------------------|--------|--------|--------|--------|--------|--------|--------|-------|--------|
| Unity-9 | Zarga | 7241 | 579 | 20 | 33 | 20 | 30 | 20 | 30 | 34 | 109 |
|  |  | 7470 | 820 | 13 | 41 | 19 | 21 | 21 | 28 | 61 | 149 |
|  | Aradeiba | 7720 | 430 | 23 | 50 | 43 | 20 | 60 | 60 | 36 | 160 |
|  |  | 7900 | 250 | 20 | 160 | 20 | 35 | 32 | 25 | 89 | 381 |
|  |  | 8070 | 489 | 10 | 20 | 14 | 32 | 100 | 25 | 62 | 158 |
|  |  | 8250 | 552 | 18 | 100 | 18 | 30 | 50 | 27 | 40 | 262 |
|  |  | 8393 | 294 | 20 | 30 | 20 | 33 | 20 | 30 | 33 | 93 |
|  |  | 8417 | 1294 | 23 | 21 | 31 | 24 | 41 | 67 | 120 | 97 |
|  |  | 8650 | 566 | 17 | 30 | 32 | 22 | 50 | 87 | 69 | 100 |
|  |  | 8780 | 472 | 20 | 40 | 36 | 25 | 40 | 60 | 56 | 170 |
|  | Bentiu | 8871 | 1110 | 11 | 47 | 26 | 27 | 28 | 39 | 67 | 168 |
|  |  | 9000 | 321 | 20 | 57 | 31 | 25 | 28 | 55 | 89 | 193 |
| Talih-2 | Zarga | 7500 | 516 | 20 | 83 | 23 | 23 | 32 | 23 | 132 | 140 |
|  |  | 7702 | 885 | 11 | 42 | 15 | 16 | 23 | 83 | 67 | 80 |
|  | Aradeiba | 7800 | 580 | 22 | 40 | 32 | 23 | 50 | 51 | 39 | 100 |
|  |  | 8020 | 260 | 20 | 90 | 30 | 28 | 100 | 40 | 71 | 360 |
|  |  | 8137 | 774 | 25 | 67 | 40 | 31 | 38 | 40 | 94 | 339 |
|  |  | 8239 | 361 | 20 | 80 | 0.0 | 31 | 20 | 30 | 48 | 371 |
|  |  | 8440 | 520 | 14 | 50 | 46 | 15 | 60 | 100 | 34 | 122 |
|  |  | 8632 | 1240 | 30 | 50.5 | 32 | 21 | 51 | 45 | 142 | 111 |
|  | Bentiu | 8820 | 880 | 13 | 110 | 22 | 20 | 50 | 40 | 72 | 300 |
|  |  | 9100 | 310 | 21 | 68 | 24 | 30 | 33 | 60 | 124 | 320 |
| Barki-1 | Zarga | 4120 | 762 | 21 | 90 | 38 | 22 | 80 | 60 | 36 | 130 |
|  |  | 4280 | 311 | 18 | 130 | 36 | 36 | 156 | 25 | 54 | 240 |
|  | Aradeiba | 4430 | 392 | 29 | 105 | 37 | 29 | 48 | 46 | 173 | 130 |
|  |  | 4660 | 343 | 16 | 160 | 20 | 33 | 11 | 35 | 61 | 310 |
|  |  | 5030 | 405 | 25 | 96 | 23 | 20 | 50 | 72 | 142 | 122 |
|  |  | 5390 | 398 | 20 | 115 | 38 | 22 | 70 | 65 | 43 | 120 |
|  | Bentiu | 5500 | 458 | 36 | 126 | 199 | 31 | 135 | 30 | 96 | 143 |
|  |  | 5650 | 522 | 14 | 150 | 61 | 35 | 138 | 40 | 132 | 240 |

**Appendix 3 (B): XRF analysis results of the upper Bentiu, all Aradeiba and lower Zarga Formations at the studied wells in Heglig Field, SE Muglad Basin.**

| Well | Formation | Sample Depth (ft) | $SiO_2$ % | $Al_2O_3$ % | $Fe_2O_3$ % | MnO % | MgO % | CaO % | $Na_2O$% | $K_2O$ % | $TiO_2$ % | $P_2O_5$ % | $SO_3$ % |
|---|---|---|---|---|---|---|---|---|---|---|---|---|---|
| Heglig-2 | Zarga | 4340 | 56.94 | 15.69 | 6.53 | 0.07 | 1.30 | 0.54 | 0.25 | 3.59 | 0.96 | 0.10 | 0.00 |
| | | 4520 | 55.63 | 19.13 | 4.30 | 0.07 | 1.54 | 0.57 | 0.49 | 2.98 | 1.01 | 0.13 | 0.00 |
| | Aradeiba | 4680 | 58.27 | 17.58 | 4.28 | 0.11 | 1.62 | 2.20 | 0.97 | 2.33 | 1.01 | 0.12 | 0.00 |
| | | 4900 | 49.04 | 20.10 | 4.20 | 0.05 | 2.50 | 1.25 | 1.13 | 5.20 | 0.73 | 0.13 | 0.08 |
| | | 5000 | 63.14 | 14.33 | 6.24 | 0.13 | 2.20 | 0.93 | 0.72 | 3.03 | 0.73 | 0.14 | 0.00 |
| | | 5120 | 63.27 | 13.69 | 7.20 | 0.06 | 2.48 | 1.69 | 0.39 | 4.04 | 0.93 | 0.10 | 0.00 |
| | | 5230 | 48.61 | 22.76 | 3.34 | 0.07 | 1.30 | 1.52 | 0.29 | 4.72 | 0.70 | 0.21 | 0.11 |
| | | 5300 | 49.54 | 21.70 | 2.48 | 0.05 | 1.05 | 2.15 | 1.90 | 4.56 | 0.72 | 0.12 | 0.16 |
| | Bentiu | 5550 | 66.89 | 11.68 | 4.13 | 0.08 | 2.10 | 3.30 | 2.13 | 1.93 | 0.96 | 0.05 | 0.00 |
| | | 5723 | 72.41 | 10.00 | 1.10 | 0.02 | 1.18 | 0.50 | 2.16 | 3.23 | 0.98 | 0.05 | 0.00 |
| Toma-1 | Zarga | 4160 | 49.85 | 21.42 | 4.56 | 0.10 | 0.80 | 0.86 | 1.21 | 3.25 | 0.80 | 0.12 | 0.08 |
| | | 4400 | 59.82 | 12.33 | 6.24 | 0.09 | 1.80 | 1.46 | 1.25 | 2.71 | 1.09 | 0.09 | 0.00 |
| | Aradeiba | 4520 | 50.75 | 20.68 | 3.09 | 0.07 | 0.64 | 0.65 | 1.27 | 4.16 | 0.87 | 0.08 | 0.14 |
| | | 4660 | 65.47 | 8.79 | 7.85 | 0.06 | 1.80 | 1.53 | 0.41 | 2.89 | 1.08 | 0.11 | 0.00 |
| | | 4720 | 50.89 | 18.34 | 5.49 | 0.08 | 0.93 | 1.30 | 1.20 | 3.62 | 1.02 | 0.16 | 0.00 |
| | | 4920 | 51.08 | 21.41 | 3.02 | 0.12 | 0.86 | 1.55 | 1.28 | 3.74 | 0.81 | 0.22 | 0.00 |
| | | 5150 | 58.92 | 18.34 | 3.66 | 0.12 | 0.78 | 1.47 | 0.96 | 3.44 | 0.72 | 0.14 | 0.14 |
| | Bentiu | 5313 | 70.26 | 13.36 | 3.20 | 0.02 | 0.90 | 2.00 | 2.18 | 2.82 | 0.74 | 0.05 | 0.00 |
| | | 5580 | 72.44 | 5.00 | 4.83 | 0.02 | 1.80 | 2.58 | 2.20 | 2.83 | 1.01 | 0.05 | 0.00 |
| Nabag-1 | Zarga | 3850 | 46.74 | 22.89 | 5.82 | 0.13 | 1.63 | 1.05 | 0.28 | 2.99 | 0.66 | 0.08 | 0.10 |
| | | 4100 | 51.72 | 20.34 | 6.16 | 0.07 | 2.22 | 0.85 | 0.25 | 1.78 | 0.93 | 0.08 | 0.09 |
| | Aradeiba | 4295 | 60.56 | 16.70 | 6.31 | 0.09 | 2.25 | 1.02 | 1.25 | 2.27 | 1.50 | 0.09 | 0.10 |
| | | 4580 | 54.04 | 20.10 | 5.66 | 0.05 | 1.54 | 1.25 | 1.33 | 2.17 | 0.93 | 0.13 | 0.08 |
| | | 4680 | 51.57 | 21.53 | 5.30 | 0.04 | 0.90 | 0.79 | 1.35 | 3.08 | 1.00 | 0.13 | 0.12 |
| | | 4880 | 50.96 | 24.09 | 4.31 | 0.04 | 0.95 | 0.64 | 1.25 | 3.30 | 0.85 | 0.15 | 0.14 |
| | | 5050 | 49.99 | 25.96 | 2.95 | 0.04 | 0.98 | 0.66 | 2.16 | 3.20 | 0.93 | 0.21 | 0.17 |
| | Bentiu | 5250 | 51.65 | 22.58 | 4.66 | 0.08 | 1.47 | 0.95 | 2.21 | 3.10 | 1.10 | 0.24 | 0.18 |
| | | 5450 | 63.40 | 15.37 | 2.68 | 0.04 | 1.41 | 0.72 | 2.83 | 3.50 | 1.97 | 0.11 | 0.16 |

| Well | Formation | Sample Depth (ft) | Ba ppm | Co ppm | Cr ppm | Cu ppm | Ga ppm | Ni ppm | Rb ppm | V ppm | Zr ppm |
|---|---|---|---|---|---|---|---|---|---|---|---|
| Heglig-2 | Zarga | 4340 | 438 | 21 | 88 | 30 | 21 | 60 | 30 | 108 | 120 |
| | | 4520 | 467 | 20 | 93 | 28 | 25 | 120 | 35 | 107 | 120 |
| | Aradeiba | 4680 | 736 | 23 | 84 | 21 | 21 | 42 | 36 | 54 | 193 |
| | | 4900 | 740 | 34 | 60 | 70 | 10 | 140 | 65 | 16 | 120 |
| | | 5000 | 579 | 20 | 60 | 20 | 25 | 36 | 40 | 14 | 364 |
| | | 5120 | 365 | 11 | 120 | 18 | 33 | 30 | 30 | 17 | 320 |
| | | 5230 | 793 | 18 | 50 | 66 | 12 | 40 | 62 | 18 | 130 |
| | | 5300 | 788 | 12 | 35 | 68 | 11 | 50 | 53 | 17 | 120 |
| | Bentiu | 5550 | 344 | 20 | 64 | 20 | 22 | 20 | 27 | 18 | 220 |
| | | 5723 | 329 | 20 | 81 | 20 | 22 | 20 | 25 | 13 | 331 |
| Toma-1 | Zarga | 4160 | 473 | 14 | 30 | 62 | 15 | 60 | 43 | 14 | 190 |
| | | 4400 | 365 | 11 | 90 | 54 | 30 | 50 | 27 | 18 | 260 |
| | Aradeiba | 4520 | 737 | 15 | 10 | 62 | 16 | 80 | 50 | 103 | 80 |
| | | 4660 | 422 | 10 | 80 | 20 | 33 | 30 | 22 | 175 | 230 |
| | | 4720 | 429 | 20 | 55 | 60 | 14 | 33 | 51 | 28 | 199 |
| | | 4920 | 539 | 29 | 42 | 38 | 15 | 47 | 56 | 13 | 133 |
| | | 5150 | 560 | 8 | 20 | 52 | 12 | 30 | 52 | 17 | 125 |
| | Bentiu | 5313 | 309 | 0.0 | 8 | 20 | 22 | 20 | 30 | 149 | 130 |
| | | 5580 | 369 | 20 | 20 | 20 | 30 | 20 | 21 | 175 | 260 |
| Nabag-1 | Zarga | 3850 | 619 | 34 | 70 | 85 | 20 | 61 | 45 | 144 | 79 |
| | | 4100 | 559 | 40 | 82 | 41 | 28 | 77 | 38 | 154 | 92 |
| | Aradeiba | 4295 | 373 | 30 | 120 | 29 | 38 | 52 | 20 | 147 | 169 |
| | | 4580 | 440 | 34 | 128 | 42 | 27 | 140 | 40 | 175 | 140 |
| | | 4680 | 474 | 29 | 99 | 64 | 22 | 152 | 80 | 154 | 119 |
| | | 4880 | 576 | 34 | 77 | 72 | 22 | 107 | 100 | 151 | 80 |
| | | 5050 | 531 | 37 | 78 | 151 | 23 | 116 | 96 | 172 | 84 |
| | Bentiu | 5250 | 725 | 30 | 80 | 100 | 29 | 64 | 38 | 151 | 89 |
| | | 5450 | 487 | 32 | 90 | 79 | 31 | 64 | 22 | 172 | 93 |